Rhodium- und Platinkomplexe mit schwefelfunktionalisierten Phosphanliganden – Neuartige Organometallverbindungen und Metallacyclen

Dissertation

zur Erlangung des akademischen Grades
doctor rerum naturalium (Dr. rer. nat.)

vorgelegt der

Naturwissenschaftlichen Fakultät II – Chemie, Physik und Mathematik
der Martin-Luther-Universität Halle-Wittenberg

von Herrn Dipl.-Chem. Michael Block

geb. am 12.04.1981 in Bernburg (Saale)

Gutachter:

1. Prof. Dr. Dirk Steinborn

2. Prof. Dr. Berthold Kersting

Datum der Verteidigung: 03.02.2011

Halle (Saale), den 12.11.2010

Inhaltsverzeichnis

[1] Siehe Nummerierung.

Abkürzungsverzeichnis

Ant	Anthracyl
Ar	Aryl
Biph	Biphenyl
n-Bu	*n*-Butyl
*t*Bu	*tert*-Butyl
cod	Cycloocta-1,5-dien
Cy	Cyclohexyl
dmpe	Bis(dimethylphosphino)ethan
dppe	Bis(diphenylphosphino)ethan
dppm	Bis(diphenylphosphino)methan
dppp	Bis(diphenylphosphino)propan
Et	Ethyl
LDA	Lithium(diisopropyl)amid
Me	Methyl
Naph	Naphthyl
Ph	Phenyl
P^P	Diphosphan(e)
i-Pr	Isopropyl
n-Pr	*n*-Propyl
P^SO$_x$Ph	ω-phosphinofunktionalisiertes Alkylphenylsulfid, -sulfoxid, -sulfon
Pyr	Pyridyl
R	organischer Rest
RT	Raumtemperatur
THF	Tetrahydrofuran
TMEDA	*N*,*N*,*N'*,*N'*-Tetramethylethylendiamin
Y	Heteroatom

Nummerierung

Die Nummerierung aller Liganden und Komplexe wird aus den Publikationen übernommen. Zusätzlich erfolgt unter Angabe der Großbuchstaben [**A]** – [**D]** der Verweis auf die entsprechende Publikation.

Nummerierung der Komplexe

Folgende Komplexe kommen in mehreren Veröffentlichungen vor und besitzen daher eine Doppelnummerierung, die im Folgenden wiedergegeben ist:

[RhCl($Ph_2PCH_2CH_2CH_2SPh$-κ*P*)(dppe)]	[**5bB**/**11aC**]
[RhCl($Ph_2PCH_2CH_2CH_2SPh$-κ*P*)(cod)]	[**6B**/**10aC**]
[Rh{CH(SPh)$CH_2CH_2PPh_2$-κ*C*,κ*P*}(dppe)]	[**13bB**/**23aC**]
[Rh{CH(SPh)$CH_2CH_2PPh_2$-κ*C*,κ*P*}(cod)]	[**14B**/**22aC**]
[RhCl($Ph_2PCH_2CH_2CH_2SO_2Ph$-κ*P*)(dppe)]	[**10cA**/**11cC**]
[RhCl($Ph_2PCH_2CH_2CH_2SO_2Ph$-κ*P*)(cod)]	[**13A**/**10cC**]
[Rh{CH(SO_2Ph)$CH_2CH_2PPh_2$-κ*C*,κ*P*}(dppe)]	[**8cA**/**23cC**]
[Rh{CH(SO_2Ph)$CH_2CH_2PPh_2$-κ*C*,κ*P*}(cod)]	[**11A**/**22cC**]

Häufig verwendete Rhodium(I)- und Platin(II)-Precursorkomplexe sowie Liganden sind mit Ziffern nummeriert. In eckigen Klammern ist nachfolgend die Nummerierung in den jeweiligen Publikationen angegeben.

(**3**)	[{Rh(cod)}$_2$(μ-Cl)$_2$]	[**5A**, **3B**, **4C**]
(**4**)	[{Rh(dppm)}$_2$(μ-Cl)$_2$]	[**7bA**, **4aB**]
(**5**)	[{Rh(dppe)}$_2$(μ-Cl)$_2$]	[**7cA**, **4bB**, **5C**]
(**6**)	[{Rh(dppp)}$_2$(μ-Cl)$_2$]	[**7dA**, **4cB**]
(**7**)	[{Rh(dmpe)}$_2$(μ-Cl)$_2$]	[**7aA**, **4dB**]
(**8**)	[Pt_2{$(COMe)_2H$}$_2$(μ-Cl)$_2$]	[**1D**]
(**9**)	$Ph_2PCH_2CH_2CH_2SPh$	[**1B**, **3aC**, **2D]**
(**10**)	$Ph_2PCH_2CH_2CH_2SO_2Ph$	[**1A**, **3cC**, **3D]**

1. Einleitung und Problemstellung

Platinmetalle (Ru, Rh, Pd, Os, Ir, Pt) besitzen eine breite industrielle Anwendung in der Werkstoffentwicklung sowie in der Katalyse [1]. Neben einer Reihe von heterogen katalysierten Reaktionen, wie der Ammoniakoxidation an Platin (OSTWALD-Verfahren), der Verwendung von Platin in Abgaskatalysatoren von Automobilen bzw. von Palladium und Platin als Hydrierkatalysatoren, spielen Platinmetalle auch eine herausragende Rolle in der homogenen Katalyse. Als Beispiel hierfür seien die (enantioselektive) Hydrierung von Olefinen mit Hilfe von Rhodiumkomplexen (WILKINSON) [2], palladiumkatalysierte C–C-Knüpfungsreaktionen (KUMADA, SUZUKI, STILLE) [3] sowie rutheniumkatalysierte Olefinmetathesereaktionen (GRUBBS) [4,5] genannt. Gerade bei letzteren spielen Metallacyclen in Form von Metallacyclobutanen eine entscheidende Rolle.

Ausgehend von Cycloalkanen gelangt man durch formale Substitution einer CH_2-Gruppe durch ein Metallfragment zu Metallacycloalkanen des Typs **I** (Schema 1). Weitere (formale) Substitutionen durch neutrale Heteroatomgruppen YR_n führen zur Entstehung von metallorganischen Innerkomplexen (Typ **II**) bzw. Metallacyclen, bei denen das Metall an zwei Heteroatome koordiniert ist (Typ **III**).

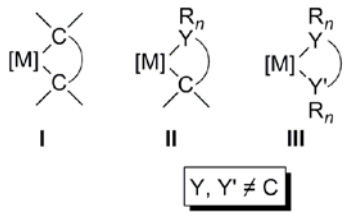

Schema 1.

Organometallkomplexe vom Typ **I** sind neben ihrer Bedeutung in der Synthesechemie [6–8] auch als Modellverbindungen bei Untersuchungen von metallorganischen Elementarreaktionen von Interesse [9,10]. Innerkomplexe, die auch als "metallorganische intramolekulare Koordinationsverbindungen" bezeichnet werden (Typ **II**), sind durch eine Bindung des Metalls zum Kohlenstoff sowie zu einem LEWIS-basischen Heteroatomzentrum YR_n (YR_n = NR_2, PR_2, OR, SR, ...) charakterisiert. Seit der Synthese und Charakterisierung der aluminiumorganischen Innerkomplexe [$AlEt_2(CH_2CH_2CH_2CH_2OEt$-κ*C*,κ*O*)] und [$AlEt_2$-($CH_2CH_2CH_2NEt_2$-κ*C*,κ*N*)] durch BÄHR und MÜLLER im Jahr 1955 [11] und einem durch Cyclometallierung hergestellten *o*-(Phenylazo)phenyl-Nickelkomplex durch KLEIMANN and

DUBECK [12], ist die Synthese von metallorganischen Innerkomplexen Gegenstand von vielen Untersuchungen gewesen [13–18], so dass gegenwärtig von nahezu allen Metallen des Periodensystems derartige Komplexe bekannt sind. Innerkomplexe bilden bevorzugt thermodynamisch begünstigte Fünfringe aus, deren hohe Stabilität bereits 1966 durch Untersuchungen von zinnorganischen Innerkomplexen mit *O*- und *N*-funktionalisierten Liganden nachgewiesen wurde [19]. Ihre Darstellung erfolgt im Allgemeinen durch Cyclometallierung, die unter oxidativer Addition der C–H Bindung (welcher oft eine agostische C–H···M-Wechselwirkung vorausgeht) oder unter Abspaltung eines anionischen Liganden X^- mit Hilfe einer Base abläuft (Schema 2).

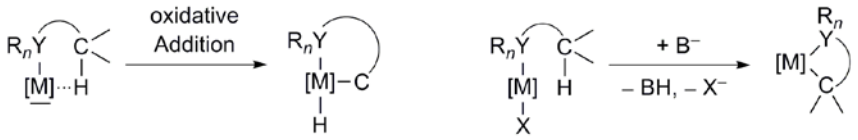

Schema 2.

Cyclometallierungen sind eine sehr effiziente Form der C–H-Aktivierung, da es sich hierbei um intramolekulare Reaktionen handelt, die durch eine Präkoordination des LEWIS-basischen Zentrums YR_n eingeleitet werden.

Allgemein lassen sich die Anwendungen der metallorganischen Innerkomplexe in der Synthesechemie unter Berücksichtigung ihrer Stabilität/Reaktivität in drei Gruppen unterteilen [16]:

Innerkomplexe hoher Stabilität. Diese werden als Edukte für die Synthese und Funktionalisierung verschiedener organischer Verbindungen verwendet und finden z. B. bei Carbonylierungs-, Alkenylierungs- oder Acylierungsreaktionen Anwendung [20–22].

Intermediär gebildete Innerkomplexe von hoher Reaktivität. Sie treten als hochreaktive Zwischenverbindungen z. B. in Carbonylierungs- oder Kreuzkupplungsreaktionen auf [23,24] und reagieren mit Substraten zu den entsprechenden Produkten weiter.

Katalytisch aktive Innerkomplexe. Derartige Innerkomplexe stellen gängige Katalysatorsysteme z. B. bei Kreuzkupplungen [25–27], Umlagerungen [28] oder Metathesereaktionen [29–31] dar. Da diese Reaktionen unter Einbeziehung des am Metall gebundenen Kohlenstoffatoms ablaufen, sind sie oftmals regio- und stereoselektiv [16].

Metallkomplexe mit homobidentaten Liganden, wie z. B. Diphosphanen oder Diaminen (Typ **III**), sind seit Jahrzehnten Gegenstand der klassischen Koordinationschemie und finden eine breite industrielle Anwendung. Jedoch besitzen heterobidentate Liganden (P^S, P^O) zwei entscheidende Vorteile: Zum einen erzeugen sie aufgrund der zwei unterschiedlichen Donoratome eine sterische und elektronische Asymmetrie am Metallzentrum und zum anderen, als Konsequenz der verschiedenen Donorstärken, können sie als hemilabile Liganden fungieren. Das bedeutet, dass der Ligand durch Dissoziation bzw. Rekoordination des schwächeren Donors (Y') eine vakante Koordinationsstelle am Metallzentrum erzeugen (**IIIa**) bzw. wieder schließen (**IIIb**) kann [32].

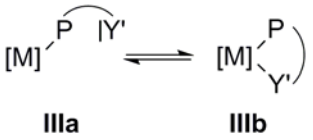

IIIa **IIIb**

Ein bekannter großtechnischer Prozess, bei dem Nickelkomplexe mit P^O-Chelatliganden (**IIIc**) als Katalysatoren Anwendung finden, ist der Shell Higher Olefin Process (*SHOP*) zur Herstellung von linearen α-Olefinen (C_{12}–C_{18}) durch Oligomerisation von Ethen. Neben den beim *SHOP* verwendeten Metallkomplexen mit P^O-Chelatliganden sind entsprechende Komplexe mit P^S-Liganden ebenfalls von großem Interesse. Da auch diese über einen starken (*P*) und einen schwächeren (*S*) Donor verfügen, spielen die daraus resultierenden elektronischen Effekte (z. B. *trans*-Einfluss, *trans*-Effekt) eine wichtige Rolle beim Design von Metallkomplexen [33]. Dementsprechend finden Komplexe mit derartigen Liganden bei einer Reihe von homogenkatalysierten Reaktionen Anwendung [34–37].

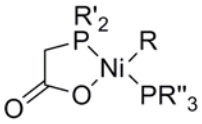

IIIc

Von den in Schema 1 beschriebenen Komplextypen, ist eine Vielzahl mit Rhodium als Zentralatom bekannt und sie stehen auch gegenwärtig im Fokus vieler Untersuchungen. So finden rhodacyclische Komplexe vom Typ **I**–**III** (Schema 1) unter anderem Anwendung bei C–C- und C–H-Bindungsaktivierungen [38,39], Cycloisomerisierungen [40] oder Alkin-Oligomerisationen [41].

Die Innerkomplexbildung spielt auch bei Hauptgruppenmetallen eine wichtge Rolle. In der eigenen Arbeitsgruppe [42–44] wurde die Regioselektivität bei Lithiierungen von γ-funktionalisierten Propylphenylsulfiden $PhSCH_2CH_2CH_2YR_n$ (YR_n = NR_2, OR) untersucht, wobei gefunden wurde, dass die Lithiierung der CH_2-Gruppe in Nachbarschaft zum Schwefelatom (α-CH_2-Gruppe) gegenüber einer *ortho*-Lithiierung des Phenylrings deutlich bevorzugt ist.

Als Ursache hierfür ist eine Präkoordination der Organolithiumverbindung R'Li an die funktionelle Gruppe YR_n zu sehen. Da sich diese in einer Chelat begünstigenden Position befindet, kommt es zur Ausbildung eines lithiumorganischen Innerkomplexes (α-Lithiierung, Schema 3) [43].

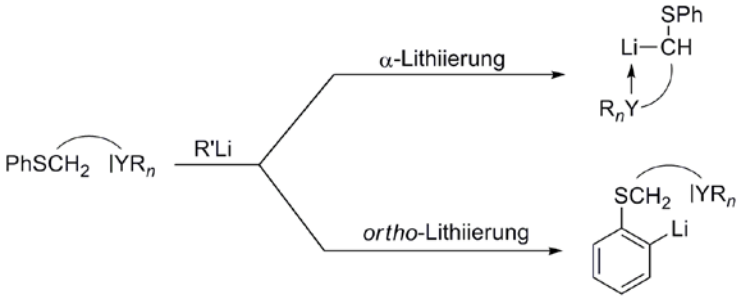

Schema 3.

Darüber hinaus übt die Donorfunktion YR_n einen maßgeblichen Einfluss auf den Aggregationsgrad von Organolithiumverbindungen und, als Konsequenz daraus, auf die Reaktivität der lithiierten Verbindungen aus, welche sich unter anderem in deren Organylierungstendenz [45] oder einer carbenoiden Zersetzung widerspiegeln kann [46].

Zielstellung der Arbeit

Das Ziel der vorliegenden Arbeit kann in zwei Schwerpunkte unterteilt werden: In Fortführung vorangegangener Untersuchungen [47] sollte ermittellt werden, welchen Einfluss eine Variation des Arylsystems in γ-alkoxyfunktionalisierten Propylarylsulfiden auf die Regioselektivität der Lithiierung hat, nachdem bereits der sterische und elektronische Einfluss der OR-Funktion untersucht worden war [44]. Dabei sollte ein tieferer Einblick in die Synthese und die Reaktivität von Organolithiumverbindungen gewonnen werden, da diese gängige Synthone in der organischen Synthesechemie darstellen.

Den zweiten Schwerpunkt stellte die Synthese und Charakterisierung von Rhodium(I)- und Platin(II)-Komplexen mit den in Schema 4 gezeigten ω-phosphinofunktionalisierten Alkylphenylsulfid- (**I**), -sulfoxid- (**II**) und -sulfonliganden (**III**) dar.

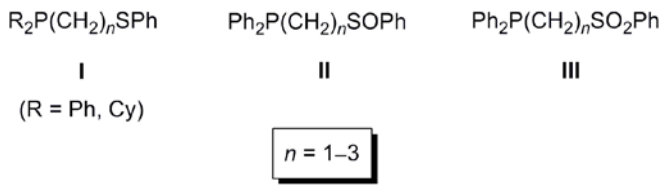

Schema 4.

Aufgrund ihres vielfältigen Koordinationspotentials stellen Verbindungen vom Typ **I**–**III** eine besonders interessante Klasse von Liganden dar. So sollte untersucht werden, welchen Einfluss die Spacerlänge *n* und die daraus resultierende Ringgröße auf eine bidentate Koordination (κ*P*,κ*S*/*O*) dieser Liganden hat. Im Fall der flexidentaten, funktionalisierten Sulfoxidliganden **II** galt es zudem zu klären, welche Faktoren den Koordinationsmodus der Sulfinylfunktion (κ*P*,κ*S vs.* κ*P*,κ*O*) beeinflussen.

Darüber hinaus sollte durch Reaktivitätsuntersuchungen von kationischen Rhodiumkomplexen gegenüber CO festgestellt werden, ob κ*P*,κ*S*-koordinierte Liganden vom Typ **I** (*n* = 3) hemilabile Eigenschaften besitzen.

Eine Deprotonierung der Liganden **I**–**III** in α-Position sollte einen neuen Zugang zu metallorganischen Rhodiumkomplexen eröffnen, wobei zu untersuchen war, inwieweit Stabilität und Reaktivität von der Spacerlänge *n* sowie der Basizität des Carbanions, die durch die benachbarte Schwefelfunktionalität SO_x (*x* = 0–2) gesteuert werden kann, abhängen.

2. Ergebnisse und Diskussion

2.1. Synthese und Metallierung von γ-alkoxyfunktionalisierten Propylarylsulfiden[1]

2.1.1. Synthese und Charakterisierung

Zur Darstellung der γ-alkoxyfunktionalisierten Propylarylsulfide (**1a–l/a'–j'**, Schema 5) wurden die kommerziell nicht erhältlichen Arylthiole ausgehend von den entsprechenden Arylbromiden synthetisiert, welche dabei mit zwei Äquivalenten Natriumethanthiolat umgesetzt wurden. Die in Schema 6 gezeigten der γ-alkoxyfunktionalisierten Propylarylsulfide wurden im Sinne einer WILLIAMSON-Ethersynthese durch Umsetzung von ArSK mit $BrCH_2CH_2CH_2OR$ erhalten [48]. Die Konstitution der Verbindungen wurde NMR-spektroskopisch (^1H, ^{13}C) sichergestellt. Ausgewählte ^1H- und ^{13}C-NMR-spektroskopische Daten von in der Literatur noch nicht beschriebenen Verbindungen des Typs $ArSCH_2CH_2$-CH_2OR sind in Tabelle 1 wiedergegeben.

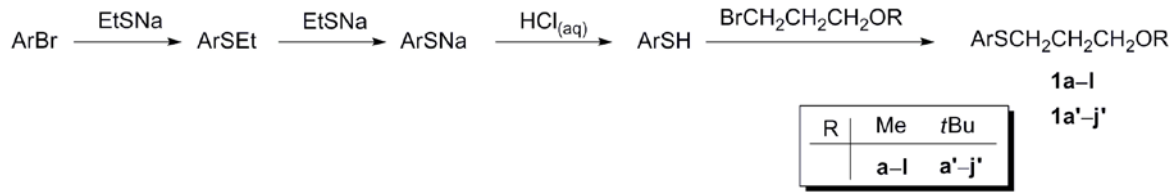

Schema 5.

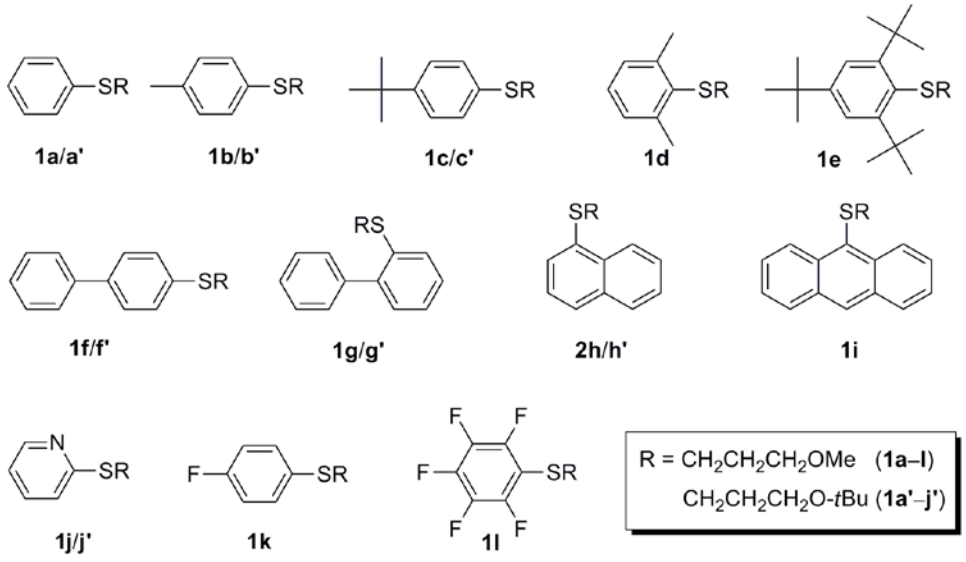

Schema 6.

[1] Die hier aufgeführten Untersuchungen sind zum Teil in Kooperation mit Herrn Dipl.-Chem. G. Ludwig entstanden [49].

Tabelle 1. Ausgewählte ^{1}H- und ^{13}C-NMR-spektroskopische Parameter (δ, ppm) von γ-alkoxyfunktionalisierten Propylarylsulfiden $ArSC_{\alpha}H_2C_{\beta}H_2C_{\gamma}H_2OR$ (**1c–l**).

	Ar/R	$\delta_{H\text{-}\alpha}$	$\delta_{H\text{-}\beta}$	$\delta_{H\text{-}\gamma}$	$\delta_{C\text{-}\alpha}$	$\delta_{C\text{-}\gamma}$
1c	4-(*t*Bu)C_6H_4/Me	2.96	1.87	3.45	31.2	71.0
1d	2,6-$(Me_3)_2C_6H_3$/Me	2.70.	1.76	3.42	32.0	71.3
1e	2,4,6-$(t$Bu$)_3C_6H_2$/Me	2.51	1.82	2.70	38.6	71.6
1f	4-Biph/Me	3.03	1.92	3.48	30.4	70.9
1f'	4-Biph/*t*Bu	3.03	1.87	3.46	59.7	72.7
1g	2-BiPh/Me	2.86	1.82	3.35	30.2	71.0
1g'	2-BiPh/*t*Bu	2.83	1.74	3.31	30.4	72.6
1h	1-Naph/Me	3.09	1.93	3.49	30.9	70.9
1h'	1-Naph/*t*Bu	3.08	1.88	3.47	31.0	72.6
1i	Ant/Me	2.94	1.73	3.39	34.0	71.1
1j	2-Pyr/Me	3.21	1.96	3.48	26.9	71.2
1k	4-FC_6H_4/Me	2.92	1.82	3.43	31.5	70.7
1l	C_6F_5/Me	2.93	1.75	3.44	31.9	70.2

2.1.2. Zur Regioselektivität der Metallierung

Die Lithiierung der Sulfide erfolgte bei −78 °C in Toluol mit *n*-BuLi/TMEDA. Aufgrund der Bildung von mehreren Regioisomeren und der damit verbundenen großen Anzahl von Signalen in den ^{1}H- und ^{13}C-NMR-Spektren sowie der teilweisen Überlagerung von Signalmustern, wurde auf eine direkte NMR-spektroskopische Charakterisierung der erhaltenen Organolithiumverbindungen verzichtet. Vielmehr wurden die entsprechenden zinnorganischen Verbindungen herangezogen, welche im Sinne einer Transmetallierungsreaktion erhalten wurden.

Dazu wurde zu den Reaktionslösungen Trimethylzinnchlorid gegeben, wodurch die stannylierten Sulfide **2a–h'** als luft- und hydrolysestabile, farblose bis gelbe Öle erhalten wurden. Mit Hilfe der ^{119}Sn-NMR-Spektroskopie erfolgte daraufhin die Bestimmung der Produktverteilung (Regioselektivität). Dabei stellte sich heraus, dass neben der erwarteten α- und *ortho*-Metallierung mitunter auch eine Metallierung der Alkylsubstituenten des Arylsystems oder der OR-Funktion (*alkyl*/*alkyl'*-Metallierung) stattgefunden hat (Schema 7).

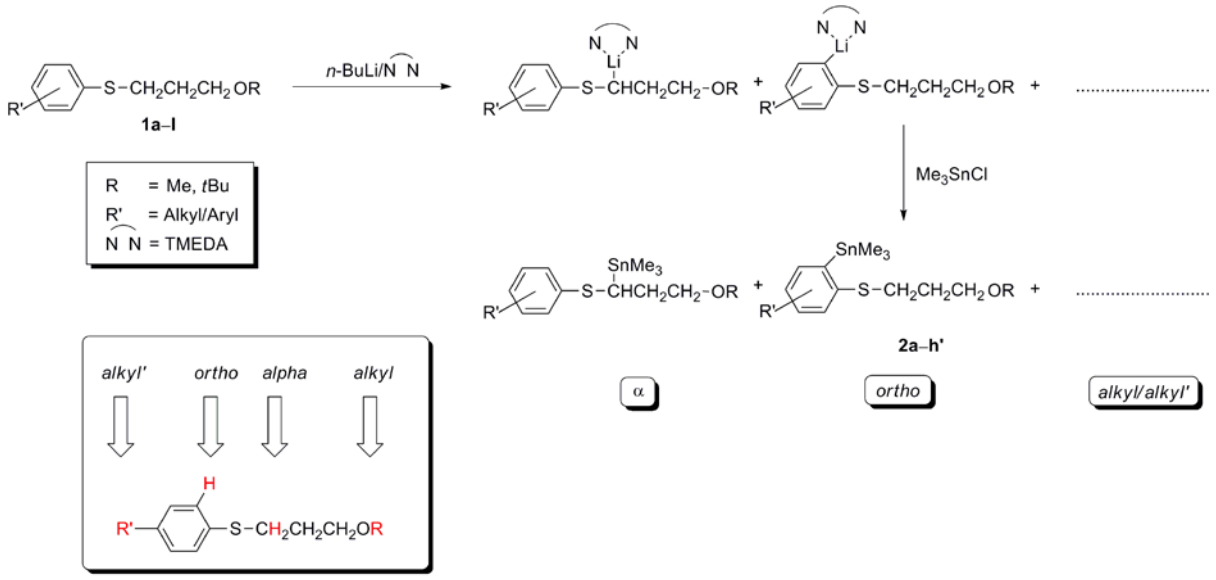

Schema 7.

Die Zuordnung der Signale in den ^{119}Sn-NMR-Spektren der Organozinnverbindungen **2a**–**h'** erfolgte auf nachstehender Grundlage:

- Die in der α-Position stannylierten Sulfide zeigen eine typische Verschiebung δ_{Sn} von 5 bis 9 ppm und weisen $^{1}J_{Sn,C}$-Kopplungskonstanten von 339–344 Hz auf.
- Die in der *ortho*-Position stannylierten Sulfide weisen eine charakteristische Verschiebung δ_{Sn} von –28 bis –31 ppm auf.
- Die in der a*lkyl/alkyl'*-Position stannylierten Sulfide besitzen eine typische Verschiebung δ_{Sn} von 3.0 bis 3.3 ppm und $^{1}J_{Sn,C}$-Kopplungskonstanten von 328–329 Hz.

Die ^{119}Sn-Verschiebungen der Regioisomere der stannylierten Sulfide **2a**–**h'** sowie deren prozentuale Verteilung sind in Tabelle 2 zusammengestellt. Während die Zuordnung der einzelnen Regioisomere gelang, gestaltete sich deren Trennung schwierig. Auf chromatographischem Weg konnten lediglich die α-stannylierten Verbindungen von **2c**, **2c'**, **2f** und **2h** in Substanz isoliert werden. Versuche, die Isomere destillativ zu trennen, führten nicht zum gewünschten Erfolg. Die in Tabelle 2 nicht aufgeführten Sulfide (**1e**, **1i**–**l**) konnten unter den angegebenen Bedingungen nicht mit *n*-BuLi(TMEDA)/Me_3SnCl metalliert werden.

Tabelle. 2. Übersicht zur Regioselektivität der Metallierung in der α-, *ortho*-, *alkyl*/*alkyl'*-Position (%) der γ-alkoxyfunktionalisierten Propylarylsulfide **1a–h'** sowie ausgewählte ^{119}Sn-NMR-spektroskopische Daten (δ, ppm) und $^{1}J_{Sn,C}$-Kopplungskonstanten (in Hz) in Klammern der entsprechenden stannylierten Verbindungen.

Sulfid[a)]		Produktverteilung (δ_{Sn}/$^{1}J_{Sn,C}$)[b)]			
		α	*ortho*	*alkyl*	*alkyl'*
2a	**1a**	100 (6.7/–)	–	–	–
2a'	**1a'**	64 (8.9)	33 (–29.1)	3 (3.2)	–
2b	**1b**	89 (5.9/343.9)	11 (–29.0/–)	–	–
2b'	**1b'**	–	13 (–29.4/–)	–	87 (3.2/328.7)
2c	**1c**	78 (5.7/343.6)	–	–	22 (3.2/328.7)
2c'	**1c'**	16 (7.7/339.3)	5 (–28.9/–)	–	79 (3.3/329.2)
2d	**1d**	–	–	–	100 (3.3/328.9)
2f	**1f**	70 (7.4/–)	–	30 (3.3/–)	–
2f'	**1f'**	16 (8.6/–)	5 (–29.7/–)	79 (3.0/328.7)	–
2g	**1g**	100 (7.1/–)	–	–	–
2g'	**1g'**	–	5 (–29.5/–)	92 (3.1/328.7)	–
2h	**1h**	100 (7.1/344.2)	–	–	–
2h'	**1h'**	54 (8.8/340.1)	5 (–30.9/–)	41 (3.2/–)	–

a) Siehe Schema 6, Seite 9. b) Aufgrund von zu schwachen Signalintensitäten konnten nicht alle $^{1}J_{Sn,C}$-Kopplungskonstanten eindeutig ermittelt werden.

Die Werte in Tabelle 2 zeigen, dass sich neben der bereits beschriebenen Abhängigkeit vom sterischen Anspruch der Alkoxyfunktion [44] eine Variation des Arylsystems ebenfalls auf die Regioselektivität auswirkt. Aus den bislang vorliegenden Ergebnissen lassen sich folgende, vorläufige Schlussfolgerungen ziehen:

- Eine Modifikation des Arylsystems bei den *tert*-butoxyfunktionalisierten Verbindungen führt zu einem deutlichen Rückgang der α-Metallierung, jedoch nicht zugunsten der *ortho*-Metallierung. Statt dessen erfolgt eine Metallierung der O-*t*Bu-Funktion (*alkyl*-Metallierung) bzw. der Alkylgruppen am Aromatensystem (*alkyl'*-Metallierung), die mit Ausnahme von **2h'** sogar die Hauptprodukte darstellen.
- Die Verbindungen mit der sterisch wenig anspruchsvollen Methoxyfunktionalisierung reagieren weniger empfindlich auf eine Variation des Arylsystems. Die zuvor beschriebene *alkyl*/*alkyl'*-Metallierung tritt – mit Ausnahme von **2d** – nur in untergeordnetem Maße auf.

- Bei den mit Alkylgruppen (+I-Effekt) substituierten Phenylsystemen (**1b**–**d**) führt die Umsetzung mit *n*-BuLi(TMEDA)/Me_3SnCl als Konkurrenz zur α-Produktbildung zur *alkyl'*-Metallierung, welche im Fall des *m*-Xylylsystems (**1d**) sogar selektiv ist. Eine Metallierung der Alkoxyfunktion (*alkyl*-Metallierung) wurde hier nicht beobachtet.
- Bei den mit aromatischen Gruppen (–I-Effekt) substituierten Phenylsystemen (**1f**–**h'**) ist das Entgegengesetzte der Fall, da hier als dominierende Konkurrenzreaktion die Metallierung der Alkoxyfunktionalisierung gefunden wurde. Eine *alkyl'*-Metallierung ist hier naturgemäß nicht möglich.
- Derivate mit stark elektronenziehenden Fluorsubstituenten (**1k**, **1l**) sowie mit einem sterisch stark abgeschirmten *S*-Atom (**1e**) setzen sich unter den angegebenen Bedingungen überhaupt nicht mit *n*-BuLi(TMEDA)/Me_3SnCl um.

Auf Grundlage der bisherigen Untersuchungen scheint die Regioselektivität sowohl vom sterischen, als auch vom elektronischen Einfluss der funktionellen Gruppen am Arylsystem abzuhängen. Weiterführende Untersuchungen müssen zudem klären, welche Rolle die Natur des Elektrophils (Me_3SnCl *vs.* Me_3SiCl *vs.* MeOD) in den Reaktionen (Schema 7) spielt.

2.2. Rhodiumorganische Innerkomplexe mit *P*,*S*- und *N*,*S*-funktionalisierten Propylliganden [A, B, C]

2.2.1. Synthese und Charakterisierung

Die Synthese von rhodiumorganischen Innerkomplexen mit *P*,*S*-funktionalisierten Propylliganden erfolgt in zwei Stufen (Route **a**/**d**, **b**/**e**, **c**/**f**, Schema 8). In einem ersten Schritt werden die P^SO_xPh-Liganden ($R_2PCH_2CH_2CH_2SPh$, R = Ph, Cy; $PPh_2CH_2CH_2CH_2SO_xPh$, *x* = 1, 2) mit dinuklearen, chloridoverbrückten Rhodium(I)-komplexen vom Typ $[(RhL_2)_2(\mu\text{-}Cl)_2]$ (L_2 = cod, P^P) unter Spaltung der Rh–Cl–Rh-Brücken zu mononuklearen Komplexen des Typs $[RhCl(R_2PCH_2CH_2CH_2SO_xPh\text{-}\kappa P)L_2]$ umgesetzt, in denen die P^SO_xPh-Liganden monodentat (κ*P*) koordiniert sind (Route **a**, **b**, **c**).

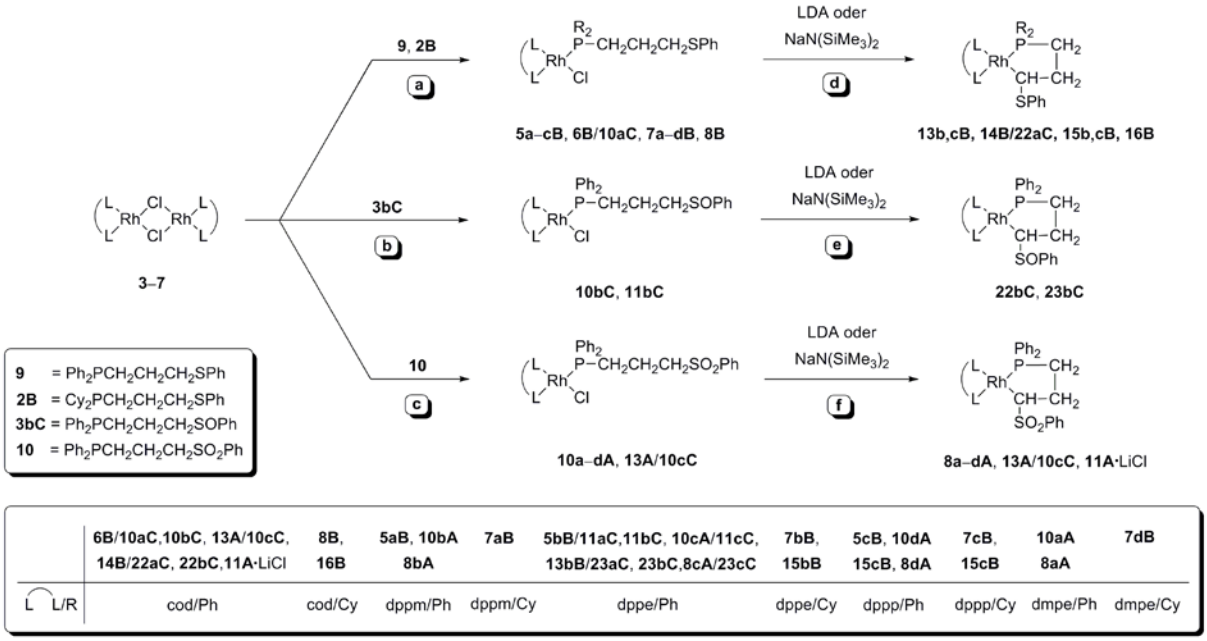

	6B/10aC,10bC, 13A/10cC, 14B/22aC, 22bC,11A·LiCl	8B, 16B	5aB, 10bA 8bA	7aB	5bB/11aC,11bC, 10cA/11cC, 13bB/23aC, 23bC,8cA/23cC	7bB, 15bB	5cB, 10dA 15cB, 8dA	7cB, 15cB	10aA 8aA	7dB
L L/R	cod/Ph	cod/Cy	dppm/Ph	dppm/Cy	dppe/Ph	dppe/Cy	dppp/Ph	dppp/Cy	dmpe/Ph	dmpe/Cy

Schema 8.

Die Komplexe wurden als gelbe bis orangefarbene, luftempfindliche (Ausnahme: **6B**/**10aC**, **13A**/**10cC**) Feststoffe in Ausbeuten von 48–90 % erhalten und ^{1}H-, ^{13}C-, ^{31}P-NMR-spektroskopisch, elementaranalytisch, durch hochauflösende Massenspektrometrie (HRMS-ESI) (**10bC**, **11bC**) sowie durch Röntgeneinkristallstrukturanalyse (**7bB**·C_6H_6, **10cA**) charakterisiert. Die ^{31}P-NMR-Spektren aller cod-Komplexe treten als AX-Spinsysteme, die der Diphosphankomplexe als AEMX- sowie als ABMX-Spinsysteme auf (A, B, E, M = ^{31}P; X = ^{103}Rh). Unabhängig von der Natur der Schwefelfunktionalisierung zeigen alle P^SO$_x$Ph-Liganden ähnliche Verschiebungen in den ^{31}P-NMR-Spektren ($\delta_P \approx 25$ ppm), welche im Vergleich zu den freien Liganden um 20–30 ppm zu tieferem Feld verschoben sind. Der große *trans*-Einfluss von Phosphanliganden wird durch einen Vergleich der Rh-P-Kopplungskonstanten deutlich. Die $^{1}J_{Rh,P}$-Kopplungen der P^SO$_x$Ph-Liganden in den Diphosphankomplexen sind im Vergleich zu den analogen cod-Komplexen (P ist *trans* zu P' bzw. C=C) um ca. 20 Hz kleiner. Innerhalb der Diphosphankomplexe wird gefunden, dass die $^{1}J_{Rh,P''}$-Kopplungen (P'' ist *trans* zu Cl) ca. 50 Hz größer als die entsprechenden $^{1}J_{Rh,P'}$-Kopplungen (P' ist *trans* zu P) sind, wodurch der abnehmende *trans*-Einfluss in der Reihenfolge PR_3 > Olefin > Cl bestätigt wird. Die quadratisch-planare Geometrie derartiger Rh(I)-Komplexe wird anhand der Festkörperstrukturen von zwei Komplexen (**7bB**·C_6H_6, **10cA**) belegt.

Der zweite Schritt zur Darstellung von rhodiumorganischen Innerkomplexen [Rh{CH-(SO_xPh)$CH_2CH_2PR_2$-κ*C*,κ*P*}L_2] ist die Reaktion der soeben beschriebenen Komplexe mit Stickstoffbasen wie LDA oder $NaN(SiMe_3)_2$, wobei eine selektive Deprotonierung der α-CH_2-Gruppe eintritt (Schema 8, Route **d**, **e**, **f**). Die beiden rhodiumorganischen Innerkomplexe mit dem γ-phosphinofunktionalisierten Sulfoxidliganden $^{\ominus}$C*H(S*OPh)$CH_2CH_2PPh_2$-κ*C*,κ*P* (**22bC**, **23bC**) besitzen zwei Chiralitätszentren, die voranstehend durch „*" markiert sind. Während im ^{31}P-NMR-Spektrum der Reaktionslösung des dppe-Komplexes **23bC** nur ein Diastereomer gefunden wird, zeigen sich beim cod-Komplex **22bC** zunächst zwei Diastereomere in einem Verhältnis von ca. 1:1. Jedoch findet innerhalb von zwei Stunden eine Isomerisierung statt, die selektiv zur Bildung eines der beiden Diastereomere führt. Die Diastereoselektivität der Cyclometallierung ist darüber hinaus durch die Tatsache belegt, dass in den ^{1}H- und ^{13}C-NMR-Spektren der isolierten Komplexe nur ein Satz von Signalen gefunden wird.

Ein alternativer Syntheseweg für die Darstellung von rhodiumorganischen Innerkomplexen mit deprotonierten γ-funktionalisierten Propylphenylsulfonen ist in Schema 9 beschrieben.

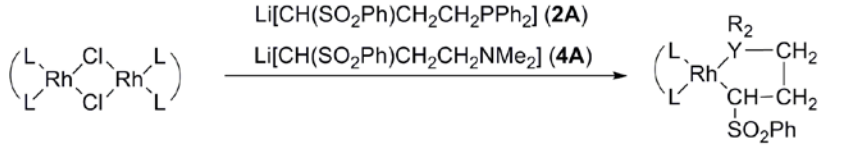

	3, 11A·LiCl, 12A·LiCl	4, 8bA, 9bA	5, 8cA/23cC, 9cA	6, 8dA, 9dA	7, 8aA, 9aA
L L	cod	dppm	dppe	dppp	dmpe

	8A	9A
	11A·LiCl	12A·LiCl
YR_2	PPh_2	NMe_2

Schema 9.

Im Gegensatz zu den sulfanylfunktionalisierten Phosphanen Ph_2P^SPh führt die Reaktion von $Ph_2PCH_2CH_2CH_2SO_2Ph$ (**11**) und $Me_2NCH_2CH_2CH_2SO_2Ph$ (**3A**) mit *n*-BuLi selektiv zur Deprotonierung der α-CH_2-Gruppe und damit zu den entsprechenden Verbindungen Li[$CH(SO_2Ph)CH_2CH_2PPh_2$] (**2A**) und Li[$CH(SO_2Ph)CH_2CH_2NMe_2$] (**4A**).

Diese können, ohne in Substanz isoliert zu werden, mit den dinuklearen, chloridoverbrückten Rhodium(I)-Komplexen **3**–**7** zu den entsprechenden Innerkomplexen [Rh{CH(SO_2Ph)-$CH_2CH_2YR_2$-κ*C*,κ*Y*}L_2] (YR_2 = PPh_2, NMe_2) umgesetzt werden.

Versuche, die rhodiumorganischen Innerkomplexe mit NMe_2-funktionalisierten Sulfonliganden auf dem in Schema 8 beschriebenen Weg zu erhalten, misslangen, da die Umsetzungen von $Me_2NCH_2CH_2CH_2SO_2Ph$ mit den dinuklearen Rhodiumkomplexen keine Reaktion zeigten. Dies ist vermutlich auf ein geringeres Donorvermögen der Aminogruppe NMe_2 im Vergleich zur Phosphinogruppe PR_2 zurückzuführen. In der Literatur sind Reaktionen beschrieben, bei denen der Komplex [{Rh(cod)}$_2$(μ-Cl)$_2$] mit Pyridinen, sekundären Aminen L und Diaminen L^L zu Komplexen des Typs [RhCl(cod)L] bzw. [Rh(cod)L^L]$^+$ reagiert, wogegen das tertiäre Triethylamin keine Reaktion zeigt [50]. Somit beschränkt sich die Synthese von Komplexen des Typs **9A** auf die in Schema 9 beschriebene Variante. In Analogie zu den funktionalierten Sulfonen führt die Reaktion des funktionalisierten Sulfoxids $Ph_2PCH_2CH_2$-CH_2SOPh mit *n*-BuLi ebenfalls unter selektiver Deprotonierung der α-CH_2-Gruppe zur Bildung von Li[CH(SOPh)$CH_2CH_2PPh_2$]. Allerdings wurden im Rahmen der vorliegenden Arbeit keine Versuche unternommen, die Innerkomplexe **22bC** und **23bC** auf dem in Schema 9 beschriebenen Weg zu erhalten.

Wie in Schema 10 gezeigt, gelingt darüber hinaus die Synthese von Innerkomplexen vom Typ **III** durch Ligandsubstitution (cod → P^P), was durch Zugabe der entsprechenden Diphosphane zu Komplexen des Typs **I** und anschließender Deprotonierung (Route **a**) oder durch Umsetzung der jeweiligen Diphosphane mit den cod-Innerkomplexen vom Typ **II** (Route **b**) geschieht.

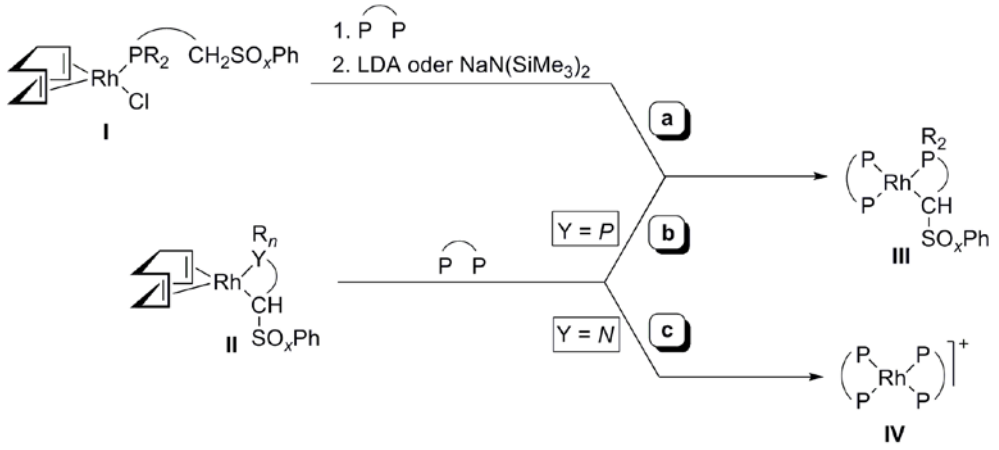

Schema 10.

Diese einfach verlaufenden Ligandsubstitutionsreaktionen verdeutlichen das stärkere Donorvermögen von Diphosphanen im Vergleich zu Olefinen. Wie anhand von Route **c** zu erkennen ist, führen die Reaktionen von Diphosphanen (P^P) mit [Rh{CH(SO_2Ph)$CH_2CH_2NMe_2$-κ*C*,κ*N*}(cod)]·LiCl (Typ **II**, Y = *N*, *x* = 2) nicht zu den entsprechenden Innerkomplexen, sondern weitestgehend (> 90 %), unter Abspaltung beider Liganden zur Bildung der homoleptischen, kationischen Komplexe $[Rh(P\text{^}P)_2]^+$ (Typ **IV**).

Alle erhaltenen rhodiumorganischen Innerkomplexe (Schemata 8–10) fielen als gelbe bis braune, hydrolyse- und luftempfindliche Feststoffe an und konnten in Ausbeuten von bis zu 91 % isoliert werden. Die Innerkomplexe mit dicyclohexylphosphinofunktionalisierten Liganden zeigen selbst bei –78 °C eine auffallend hohe Löslichkeit in unpolaren Lösungsmitteln wie *n*-Pentan, was deren niedrige Ausbeuten (31–35 %) erklärt. Die beiden cod-Komplexe **11A**·LiCl und **12A**·LiCl können durch Umkristallisation aus THF/*n*-Pentan bzw. THF als LiCl-freie Verbindungen gewonnen und röntgeneinkristallographisch charakterisiert werden. Die Charakterisierung der erhaltenen rhodiumorganischen Innerkomplexe erfolgte NMR-spektroskopisch (^{1}H, ^{13}C, ^{31}P), elementaranalytisch, durch hochauflösende Massenspektrometrie (**22bC**, **23bC**) sowie durch Röntgeneinkristallstrukturanalyse (**9cA**·THF, **11A/22cC**, **12A**). Die ^{31}P-NMR-Spektren der Innerkomplexe mit cod-Liganden zeigen AX-Spinsysteme, die mit dppm-, dppp- und dmpe-Coliganden AMX, AEMX sowie ABMX Spinsysteme. Sämtliche dppe-Komplexe vom Typ [Rh{CH(SO_xPh)$CH_2CH_2PR_2$-κ*C*,κ*P*}-(dppe)] zeigen komplizierte ABCX Spinsysteme (A, B, C, E, M = ^{31}P; X = ^{103}Rh) höherer Ordnung, was auf die nahezu identischen chemischen Umgebungen der drei Phosphoratome sowie auf die ähnlich großen $^1J_{Rh,P}$- und $^2J_{P,P}$-Kopplungskonstanten zurückzuführen ist. Im Vergleich zu den entsprechenden Komplexen mit monodentat koordinierten P^SO_xPh-κ*P*-Liganden sind vor allem die um ca. 35 ppm tieffeldverschobenen ^{31}P-Resonanzen ihrer deprotonierten Kongenere sowie die Vergrößerung der $^1J_{Rh,P}$-Kopplungskonstanten von ca. 130 Hz auf ca. 150 Hz auffällig. Der zunehmende *trans*-Einfluss in der Reihe $NR_3 < PR_3 < CR_3$ wird an den entsprechenden $^1J_{Rh,P}$-Kopplungskonstanten (P ist *trans* zu NR_3, PR_3 bzw. CR_3) deutlich, welche sich von ca. 180 Hz (NR_3) über ca. 150 Hz (PR_3) auf etwa 125 Hz (CR_3) verkleinern. In den ^{13}C-NMR-Spektren führt die Innerkomplexbildung zu einer mäßigen Tieffeldverschiebung der α-Kohlenstoffatome, deren Koordination am Rhodium in sämtlichen cod-Komplexen sowie in den Komplexen mit dem NMe_2-funktionalisierten Liganden zusätzlich durch die $^1J_{Rh,C}$-Kopplungskonstanten (16.4–30.4 Hz) bewiesen ist.

Damit wurde eine einfache Synthese von rhodiumorganischen Innerkomplexen gefunden. Zwar können die im ersten Schritt entstehenden Rh(I)-Komplexe, welche die P^SO_xPh-Liganden κ*P*-koordiniert haben, in Substanz isoliert werden, zur Darstellung der entsprechenden Innerkomplexe ist das jedoch nicht nötig. Die selektive Deprotonierung der α-CH_2-Gruppe ist vor allem bei den Komplexen mit koordinierten γ-phosphinofunktionalisierten Sulfiden (x = 0) interessant, da die Deprotonierung der freien Liganden mit *n*-BuLi/TMEDA unselektiv erfolgt und zu einem Gemisch von Regioisomeren (α, *ortho*, Aryl) führt [43,51]. Über die diastereoselektive Bildung von Metallacyclen, wie sie bei den Innerkomplexen mit sulfinylfunktionalisierten Liganden beobachtet wird, sowie über deren Verwendung als Katalysatorsysteme ist in der Literatur bereits berichtet worden [52–56]. Das relativ geringe Donorvermögen von Aminen des Typs NR_3 (R = Alkyl), welches unter anderem von Reaktivitätsuntersuchungen von Iminophosphoranliganden bekannt ist [57,58] sowie die leichte Spaltbarkeit von Rh–N-Bindungen, die eingehend bei Raktionen von Komplexen des Typs [RhCl(olefin)(*i*-$Pr_2PCH_2CH_2NMe_2$-κ*P*,κ*N*)] mit CO, C_2H_4 and H_2 untersucht wurde [59], kann ebenfalls bestätigt werden. Darüber hinaus wird durch Umsetzung der lithiierten Sulfone Li[$CH(SO_2Ph)CH_2CH_2YR_2$] (YR_2 = PPh_2, **2A**; NMe_2, **4A**) mit Rhodium(I)-Precursorkomplexen ein alternativer Syntheseweg zur Darstellung von metallorganischen Innerkomplexen aufgezeigt. Die selektive Deprotonierung von funktionalisierten Sulfonen ist auf die deutlich erhöhte Acidität der α-CH_2-Protonen im Vergleich zu entsprechenden Sulfiden [60–62] zurückzuführen.

2.2.2. Strukturelle Aspekte von rhodiumorganischen Innerkomplexen

Die beiden Komplexe **9cA**·THF und **12A** (Abbildung 2) stellen zwei Vertreter der relativ kleinen Gruppe von strukturell charakterisierten Rh(I)-Innerkomplexen dar, die Liganden mit einer κ*C*,κ*N*-Koordination aufweisen. Darüber hinaus gelang die röntgeneinkristallographische Charakterisierung des Innerkomplexes [Rh{$CH(SO_2Ph)CH_2CH_2PPh_2$-κ*C*,κ*P*}(cod)] (**12A**), dessen Molekülstruktur ebenfalls in Abbildung 1 wiedergegeben ist.

Erwartungsgemäß sind die Rhodiumatome in allen drei Komplexen quadratisch-planar koordiniert, wobei vor allem die entsprechenden C1–Rh–Y-Winkel (Y = N, P) mit 81.3(7)–82.1(1)° vom Idealwert (90°) abweichen, was auf einen relativ kleinen Biss der Chelatliganden hindeutet.

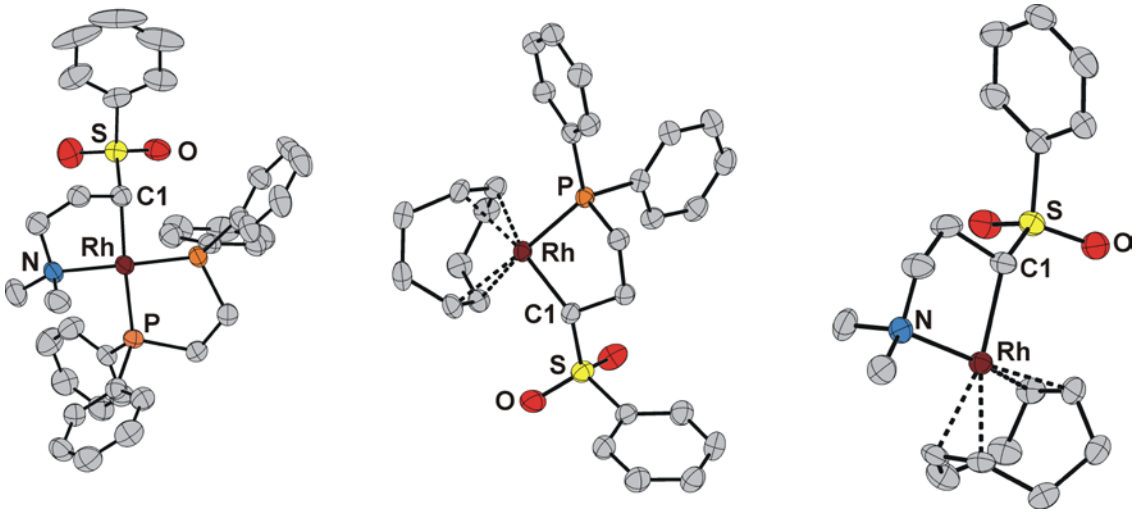

Abbildung 1. Molekülstrukturen von [Rh{CH(SO_2Ph)$CH_2CH_2NMe_2$-κ*C*,κ*N*}(dppe)] (links), [Rh{CH(SO_2Ph)-$CH_2CH_2PPh_2$-κ*C*,κ*P*}(cod)] (Mitte) und [Rh{CH(SO_2Ph)$CH_2CH_2NMe_2$-κ*C*,κ*N*}(cod)] (rechts) in Kristallen von **9cA**·THF, **11A** bzw **12A**. Die Ellipsoide sind mit einer Wahrscheinlichkeit von 50 % dargestellt. Die H-Atome sind aus Gründen der Übersichtlichkeit nicht abgebildet. Ausgewählte strukturelle Parameter (Abstände in Å, Winkel in °), **9cA**·THF: Rh–N 2.222(4), Rh–C1 2.161(4), N–Rh–C1 82.1(1); **11A**: Rh–P 2.264(8), Rh–C1 2.181(3), Rh–C22/23_{cg} 2.142(4), P–Rh–C1 81.3(7), **12A**: Rh–N 2.175(3), Rh–C1 2.149(3), Rh–C22/23_{cg} 2.011(2), N–Rh–C1 81.6(1).

Der bereits diskutierte unterschiedlich starke *trans*-Einfluss der Liganden spiegelt sich in den entsprechenden Bindungslängen wider. So ist z. B. die Bindung Rh–C22/23_{cg} in **11A** (*trans* zu P; cg = Schwerpunkt) mit 2.142(4) Å erheblich länger als die analoge Bindung in **12A** (2.011(2) Å, *trans* zu N). Der größere *trans*-Einfluss von Phosphanen im Vergleich zu Olefinen wird bei einem Vergleich der Rh–N-Bindungslängen von **9cA** und **12A** deutlich (2.222(4) Å *vs.* 2.175(3) Å). Darüber hinaus bestätigen die unterschiedlichen Rh–P-Bindungslängen in **9cA** (2.258(1)/2.191(1) Å, P ist *trans* zu C bzw. N) letztendlich die bereits anhand der $^1J_{Rh,P}$-Kopplungen gefundene Abstufung des *trans*-Einflusses in der Reihenfolge NR_3 ≈ Olefine < PR_3 < CR_3. Die unterschiedlichen Rh–C1-Bindungslängen in **11A** (2.181(3) Å) und **12A** (2.149(3) Å) sind vermutlich auf die Größenunterschiede des N- bzw. P-Atoms zurückzuführen, da in beiden Komplexen derselbe *trans*-ständige Coligand (cod) koordiniert ist.

2.3. Rhodacyclische Komplexe mit ω-*P*-funktionalisierten Alkylphenylsulfiden, -sulfoxiden und -sulfonen [B, C]

2.3.1. Synthese und Charakterisierung von kationischen Rhodiumkomplexen

Komplexe des in 2.2.1. ausführlich beschriebenen Typs [RhCl($R_2PCH_2CH_2CH_2SO_xPh$-κ*P*)L_2] können nicht nur als Precursoren für rhodiumorganische Innerkomplexe fungieren, sondern auch Reaktionen mit Chloridionenakzeptoren, wie Tl[PF_6] oder Ag[BF_4], eingehen. Unter Abspaltung des Chloridoliganden in Form der schwerlöslichen Salze TlCl bzw. AgCl wird die nun vakante vierte Koordinationsstelle am Rhodium durch ein weiteres Heteroatom (S bzw. O) der P^SO_xPh-Liganden besetzt, was die Bildung von kationischen Komplexen des Typs [Rh($R_2PCH_2CH_2CH_2SPh$-κ*P*,κ*S*)L_2][PF_6] (R = Ph, Cy; L_2 = cod, P^P; Schema 11) und [Rh{$Ph_2P(CH_2)_nSO_xPh$-κ*P*,κ*O*/*S*}L_2][BF_4] (L_2 = cod, dppe; *n* = 1–3, *x* = 0–2; Schema 12) zur Folge hat.

Die erhaltenen kationischen Rhodiumkomplexe wurden in Ausbeuten von 71–91 % als gelbe bis orangefarbene, mäßig luft- und hydrolyseempfindliche Feststoffe isoliert und NMR-spektroskopisch (^{1}H, ^{13}C, ^{31}P), durch hochauflösende Massenspektrometrie sowie durch Röntgendiffraktometrie (**10B**, **15bC**, **15cC**) charakterisiert.

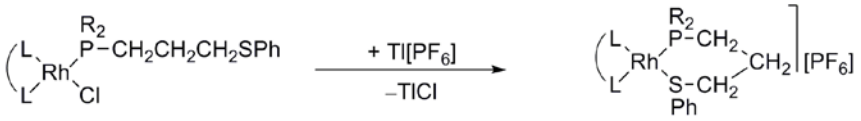

5a–cB, 6B/10aC, 7a–dB, 8B → **9a–cB, 10B, 11a–dB, 12B**

R = Ph; **5B, 6B/10aC, 9B, 10B**
R = Cy; **7B, 8B, 11B, 12B**

	5aB, 7aB 9aB, 11aB	**5bB/11aC, 7bB, 9bB, 11bB**	**5cB, 7cB 9cB, 11cB**	**7dB, 11dB**	**6B/10aC, 8B, 10B, 12B**
L L	dppm	dppe	dppp	dmpe	cod

Schema 11.

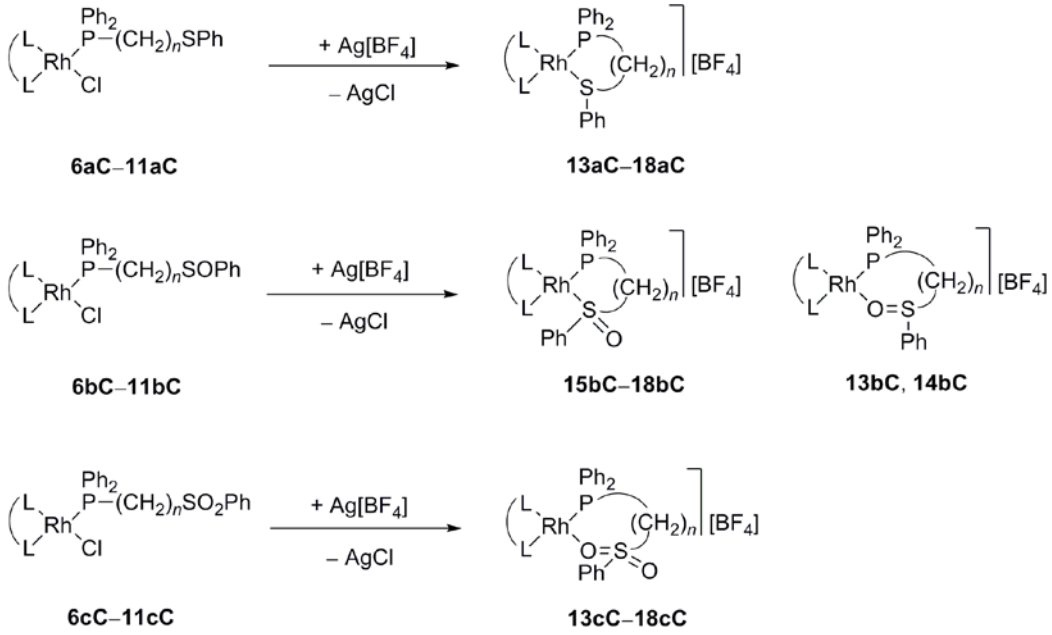

	6C	7C	8C	9C	10C	11C	13C	14C	15C	16C	17C	18C
n	1	1	2	2	3	3	1	1	2	2	3	3
L L	cod	dppe	cod	dppe	cod	dppe	cod	dppe	cod	dppe	cod	dppe

Schema 12.

ω-Phosphinofunktionalisierte Sulfoxidliganden können aufgrund ihrer flexidentaten Natur pinzipiell zwei Koordinationsmodi ausbilden: κ*P*,κ*S* und κ*P*,κ*O*. Diese können experimentell durch den unterschiedlichen *trans*-Einfluss von S bzw. O unterschieden werden. Dazu werden die entsprechenden $^{1}J_{Rh,Y}$-Kopplungskonstanten (Y= C, P'; *trans* zu S bzw. O) der Komplexe $[Rh\{R_2P(CH_2)_nSOPh\text{-}\kappa P,\kappa S/O\}L_2][BF_4]$ mit denen der analogen Komplexe, bei denen sulfanyl- (P^SPh-κ*P*κ*S*) und sulfonylfunktionalisierte Liganden (P^SO_2Ph-κ*P*κ*O*) am Rhodium koordiniert sind, verglichen. Das Ergebnis ist in Abbildung 2 graphisch dargestellt.

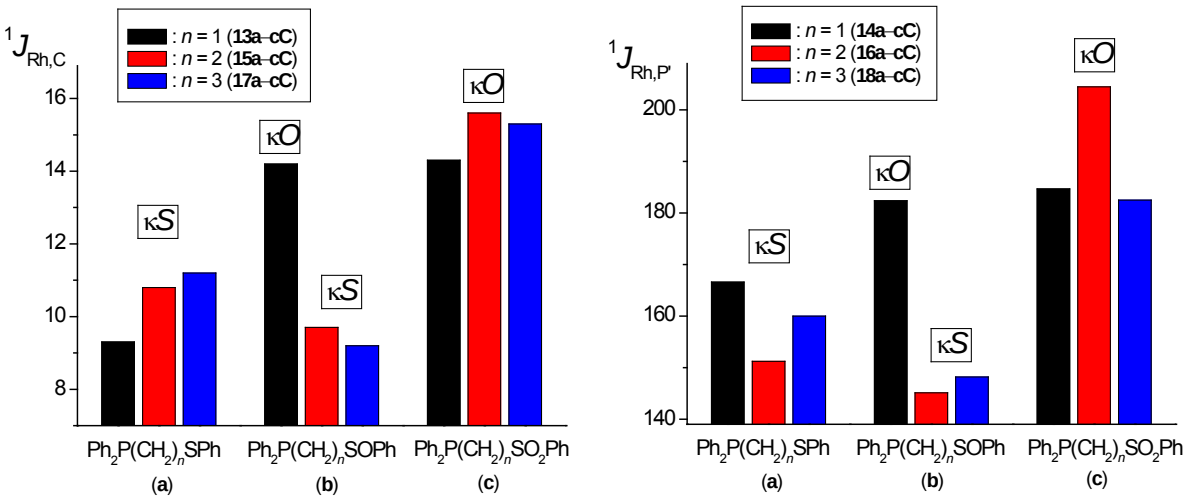

Abbildung 2. Graphische Darstellung der $^1J_{Rh,C}$-Kopplungskonstanten in den Komplexen **13C**, **15C**, **17C** (links) und der $^1J_{Rh,P'}$-Kopplungskonstanten in den Komplexen **14C**, **16C**, **18C** (rechts). C und P' sind *trans* zu S bzw. O.

Anhand der Abbildung wird deutlich, dass in den beiden Komplexen mit dem Ph_2PCH_2SOPh-Liganden (**13bC**, **14bC**) eine κ*P*,κ*O*-Koordination vorliegt, wogegen die beiden β- bzw. γ-diphenylphosphinofunktionalisierten Sulfoxidliganden $Ph_2P(CH_2)_nSOPh$ mit einem Dimethylen- (*n* = 2; **15bC**, **16bC**) und Trimethylenspacer (*n* = 3; **17bC**, **18bC**) κ*P*,κ*S*-koordiniert sind (Schema 12), was im Fall des Komplexes $[Rh(Ph_2PCH_2CH_2SOPh\text{-}\kappa P,\kappa S)(cod)][BF_4]$ (**15bC**) durch eine Festkörperstruktur bestätigt ist. Damit führt die entsprechende Koordination der Sulfoxidliganden in allen Komplexen ausschließlich zur Bildung von thermodynamisch stabilen fünf- und sechsgliedrigen Rhodacyclen.

Im Fall der in Schema 13 gezeigten Kompexe mit κ*P*,κ*S*-koordinierten ω-funktionalisierten Sulfid- (**I**) und κ*P*,κ*O*-koordinierten Sulfonliganden (**II**) ist der Koordinationsmodus durch die Ligandstruktur festgelegt, so dass neben fünf- und sechsgliedrigen Ringen auch thermodynamisch weniger stabile vier- (**I**, *n* = 1) und siebengliedrige Ringe (**II**, *n* = 3) gebildet werden.

Die ^{31}P-NMR-Spektren sämtlicher cod-Komplexe liegen als AX-Spinsysteme, die der Diphosphankomplexe als AEMX-, ABMX- bzw. ABCX-Spinsysteme vor. Das schwach-koordinierende Anion ($[PF_6]^-$ bzw. $[BF_4]^-$) hat erwartungsgemäß keinen messbaren Einfluss auf die NMR-spektroskopischen Daten, was durch einen Vergleich der entsprechenden Komplexe deutlich wird; eine Variation der Phosphinofunktion PR_2 in den Komplexen des Typs $[Rh(R_2PCH_2CH_2CH_2SPh\text{-}\kappa P,\kappa S)L_2][PF_6]$ (R = Ph, Cy) wirkt sich dagegen lediglich auf die chemischen Verschiebungen und Kopplungskonstanten der γ-C-Atome bzw. der P-Atome der P^SPh-Liganden aus.

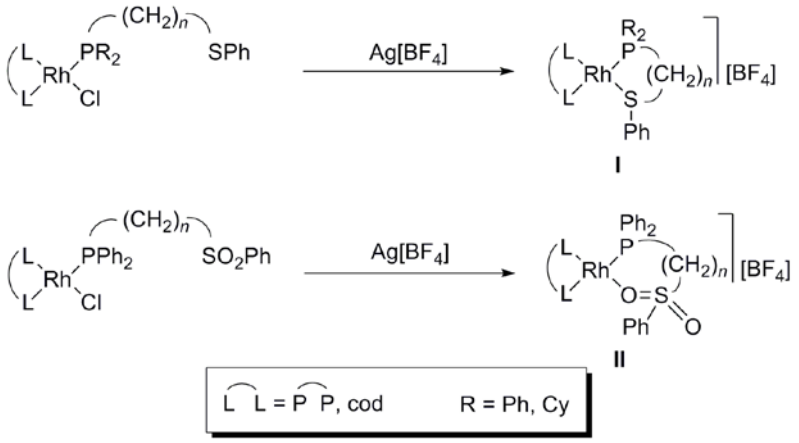

Schema 13.

Im Gegensatz dazu haben sowohl die Spacerlänge $(CH_2)_n$ (n = 1–3), als auch die Natur der Schwefelfunktionalisierung SO_x (x = 0–2) in Komplexen des Typs [Rh{$Ph_2P(CH_2)_nSO_x$Ph-κ*P*,κ*O*/*S*}L_2][BF_4] einen sehr großen Einfluss auf die chemischen Verschiebungen bzw. die Kopplungskonstanten. Stellvertretend dafür sind in Tabelle 3 ausgewählte NMR-spektroskopische Daten von kationischen Rhodium(I)-Komplexen aufgelistet.

Tabelle 3. Ausgewählte NMR-spektroskopische Daten (δ, ppm; J in Hz) der Komplexe [Rh{$Ph_2P(CH_2)_{n-1}C_\alpha H_2$-$SO_x$Ph-κ*P*,κ*O*/*S*}$L_2$][$BF_4$].

		L_2 = cod					L_2 = dppe		
	n/x	$\delta_{\alpha\text{-}C}$ ($^mJ_{P,C}$)	δ_P ($^1J_{Rh,P}$)	$\delta_{C=C}$[a] ($^1J_{Rh,C}$)		n/x	$\delta_{\alpha\text{-}C}$ ($^mJ_{P,C}$)	δ_P ($^1J_{Rh,P}$)	$\delta_{P'}$[b] ($^1J_{Rh,P'}$)
13aC	1/0	107.7	–31.1	86.5	**14aC**	1/0	60.3	–22.8	69.1
		(7.3)[c]	(119.5)	(9.3)			(19.3)[c]	(111.1)	(166.6)
15bC	2/1	52.9	52.7	78.0/78.3	**16bC**	2/1	60.3	57.8	60.1
		(s)	(135.8)	(8.1/11.3)			(9.5)[d]	(136.4)	(145.1)
17cC	3/2	57.0	24.2	71.6	**18cC**	3/2	–	21.2	70.5
		(3.8)[e]	(147.8)	(15.3)				(127.0)	(182.5)

a) Vom cod-Liganden, *trans* zu S bzw. O. b) Vom dppe-Liganden, *trans* zu S bzw. O. c) m = 1. d) m = 2. e) m = 3.

Der oben beschriebene Einfluss wird vor allem bei den Komplexen **13aC** und **14aC** in Form der stark hochfeldverschobenen Phosphorresonanzen (δ_P –31.1/–22.8 ppm) bzw. tieffeld-verschobenen α-C-Resonanzen (δ_C 107.7/60.3 ppm) des Ph_2PCH_2SPh-κ*P*,κ*S*-Liganden sehr deutlich, was vermutlich auf die Ausbildung eines gespannten RhPCS-Vierrings zurück-zuführen ist, da in strukturell ähnlichen Rhodiumkomplexen mit einem κ^2*P*,*P'*-koordinierten dppm-Liganden (RhPCP-Vierring) vergleichbare Verschiebungen gefunden werden [63–65].
Während bei der Reaktion des Komplexes [RhCl(Ph_2PCH_2SPh-κ*P*)(cod)] (**6aC**) mit Ag[BF_4] in CH_2Cl_2 ein in Schema 13 beschriebener kationischer Komplex vom Typ **I** erhalten wird, führt die analoge Umsetzung in THF unerwartet zur Bildung des trimeren Rhodiumkom-plexes [Rh_3(μ-Cl)(μ-Ph_2PCH_2SPh-κ*P*:κ*S*)$_4$][BF_4]$_2$ (**12C**), welcher innerhalb einiger Stunden als THF-Addukt **12C**·4THF auskristallisiert. Der Komplex wurde spektroskopisch, elementar-analytisch sowie röntgeneinkristallographisch charakterisiert. Anhand der Festkörperstruktur (Abbildung 3) wird deutlich, dass das Kation durch einen nahezu planaren Rh_3Cl-Vierring mit vier verbrückenden μ-Ph_2PCH_2SPh-κ*P*:κ*S*-Liganden aufgebaut ist. Dabei weist es eine ungefähre C_2-Symmetrie auf, wobei die Drehachse durch das zentrale Rhodium- und das Chloratom verläuft.

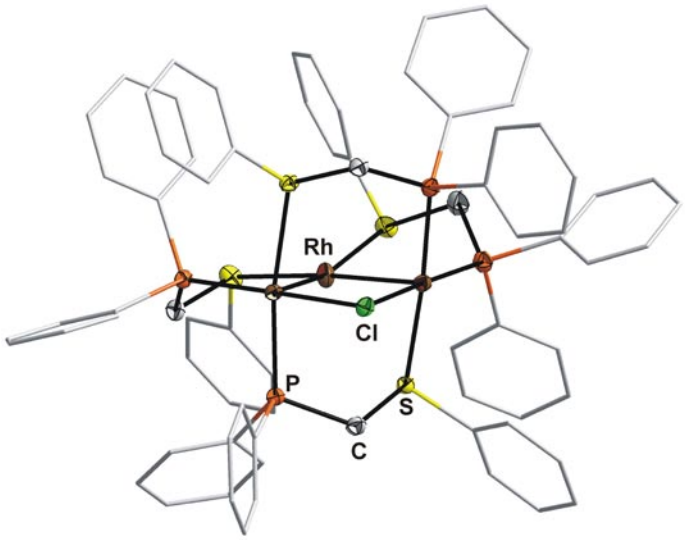

Abbildung 3. Molekülstruktur des Kations in Kristallen von [Rh_3(μ-Cl)(μ-Ph_2PCH_2SPh-κ*P*:κ*S*)$_4$][BF_4]$_2$·4THF (**12C**·4THF). Die Ellipsoide sind mit einer Wahrscheinlichkeit von 30 % dargestellt. Aus Gründen der Über-sichtlichkeit sind keine H-Atome und die Phenylringe als Stabmodell abgebildet.

Damit gelingt eine einfache Synthese von kationischen Rh(I)-Komplexen mit bidentaten P^S- und P^O-Liganden, die interessant für verschiedene homogenkatalysierte Reaktionen sein können [66–69]. Die flexidentaten Eigenschaften von Sulfoxidliganden spiegeln sich in den unterschiedlichen Koordinationsmodi (κ*P*,κ*S* und κ*P*,κ*O*) wider, wobei diese ausschließlich von der Spacerlänge und damit von der gebildeten Ringgröße abhängen. Eine Abhängigkeit von der LEWIS-Basizität der Coliganden, wie sie für nicht-funktionalisierte Sulfoxide [70] bzw. für *N*-Phosphinosulfinamid-Liganden (PNSO-Liganden) [71] beschrieben ist, wird nicht gefunden. Der trinukleare Rh(I)-Komplex **12C**·4THF ähnelt in seiner Struktur einem A-Frame-Komplex, wie er für eine Vielzahl von Komplexen mit dppm-Liganden gefunden wird [72,73].

2.3.2. Zur Reaktivität von kationischen Rhodiumkomplexen gegenüber CO

Während die Reaktion der kationischen Rhodiumkomplexe mit Diphosphanen als Coliganden [Rh($R_2PCH_2CH_2CH_2SPh$-κ*P*,κ*S*)(P^P)][PF_6] (R = Ph, Cy) mit Kohlenmonoxid bereits bei –78 °C zur Bildung von Carbonylkomplexen des Typs [Rh(CO)($R_2PCH_2CH_2CH_2SPh$)(P^P)]$^+$ führt, zeigen die analogen cod-Komplexe keine Reaktion – auch nicht bei Raumtemperatur. Die ^{31}P-NMR-Spektren der Reaktionslösungen der Carbonylkomplexe weisen breite Signale auf, was auf eine Moleküldynamik bzw. ein Gleichgewicht in Lösung hindeutet. Am Beispiel des Carbonylkomplexes [Rh(CO)($Ph_2PCH_2CH_2CH_2SPh$)(dppe)]$^+$ kann gezeigt werden, dass das Gleichgewicht bei –80 °C eingefroren ist. Im ^{31}P-NMR-Spektrum werden die Resonanzen von zwei Rhodiumkomplexen in einem Verhältnis von 3:1 gefunden, welche jeweils drei chemisch inequivalente Phosphoratome aufweisen. Die Koordination von CO wurde ^{13}C-NMR- (δ_C 189.8–192.8 ppm) sowie IR-spektroskopisch belegt. In den IR-Spektren zeigen sich jeweils zwei Banden bei ca. 1990 und 2022 cm^{-1}, was im Schwingungsbereich von terminal gebundenem CO liegt. Dagegen werden in den HRMS-ESI-Spektren mit einer Ausnahme lediglich die decarbonylierten Kationen [M–CO]$^+$ als Basispeaks detektiert, was vermutlich auf Zersetzung der Komplexe während des Ionisationsprozesses zurückzuführen ist. Alle Versuche, die erhaltenen Carbonylkomplexe durch Verdampfung des Lösungsmittels oder durch Ausfällen und anschließendes Trocknen in Substanz zu isolieren, führten zur Zersetzung mit einer partiellen Rückbildung der Ausgangskomplexe [Rh($R_2PCH_2CH_2CH_2$-SPh-κ*P*,κ*S*)(P^P)][PF_6].

Quantenchemische Rechnungen auf DFT-Niveau geben einen Einblick in die Bildung der Carbonylkomplexe.[1] Um den Rechenaufwand zu reduzieren, wurden die Phenyl- und Cyclohexylgruppen durch Methylgruppen ersetzt, woraus sich der berechnete Komplex $[Rh(CO)(Me_2PCH_2CH_2CH_2SMe)(dmpe)]^+$ (**21**$_{calc}$**B**) ergab, für den drei Gleichgewichtsstrukturen ermittelt wurden (Abbildung 4).

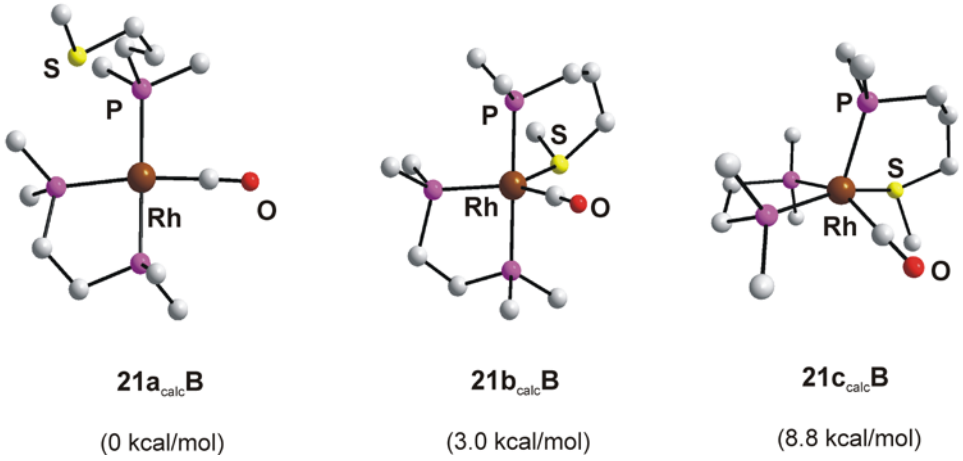

Abbildung 4. Berechnete Gleichgewichtsstrukturen von $[Rh(CO)(Me_2PCH_2CH_2CH_2SMe)(dmpe)]^+$, welche den $Me_2PCH_2CH_2CH_2SMe$-Liganden κ*P*- (**21a**$_{calc}$**B**) bzw. κ*P*,κ*S*- (**21b**$_{calc}$**B**, **21c**$_{calc}$**B**) koordiniert haben. Aus Gründen der Übersichtlichkeit sind die H-Atome nicht abgebildet. Die Energien sind relativ zum thermodynamisch stabilsten Isomer **21a**$_{calc}$**B**.

Dabei ist das Rhodiumatom im thermodynamisch stabilsten Isomer **21a**$_{calc}$**B** quadratisch-planar koordiniert, wogegen die Rhodiumatome in den beiden anderen Komplexen eine verzerrt trigonal-bipyramidale (**21b**$_{calc}$**B**) bzw. quadratisch-pyramidale (**21c**$_{calc}$**B**) Koordinationsgeometrie aufweisen. Während die zwei Isomere **21a**$_{calc}$**B** und **21b**$_{calc}$**B** von ähnlicher Energie sind ($\Delta\Delta G^{\ominus}$ = 3.0 kcal/mol), erweist sich **21c**$_{calc}$**B** als das thermodynamisch ungünstigste Isomer ($\Delta\Delta G^{\ominus}$ = 8.8 kcal/mol). Die Carbonylkomplexbildung gemäß Gleichung 1 ist sowohl exotherm (ΔE = –16.1 kcal/mol, 0 K), als auch unter Berücksichtigung von Lösungsmitteleffekten (CH_2Cl_2) exergonisch ($\Delta G^{\ominus}$ = –7.7 kcal/mol).

[1] Die quantenchemischen Rechnungen wurden von Herrn Dipl.-Chem. T. Kluge angefertigt.

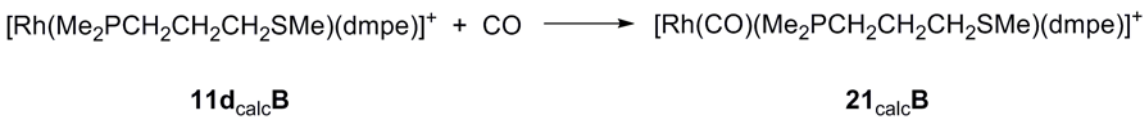

Gleichung 1.

Wenn man nun die Ergebnisse der quantenchemischen Rechnungen auf die experimentellen Befunde überträgt, ist die beobachtete Moleküldynamik in den Reaktionslösungen der Carbonylkomplexe auf ein Gleichgewicht zwischen einem vier- und einem fünffach koordinierten Rhodiumatom zurückzuführen, wobei die P^SPh-Liganden κ*P*- bzw. κ*P*,κ*S*-koordiniert sind (Schema 14). Damit kann die Koordination der P^SPh-Liganden als hemilabil beschrieben werden. Über ein ähnliches Koordinationsverhalten von P^S-Liganden wurde bereits berichtet [74].

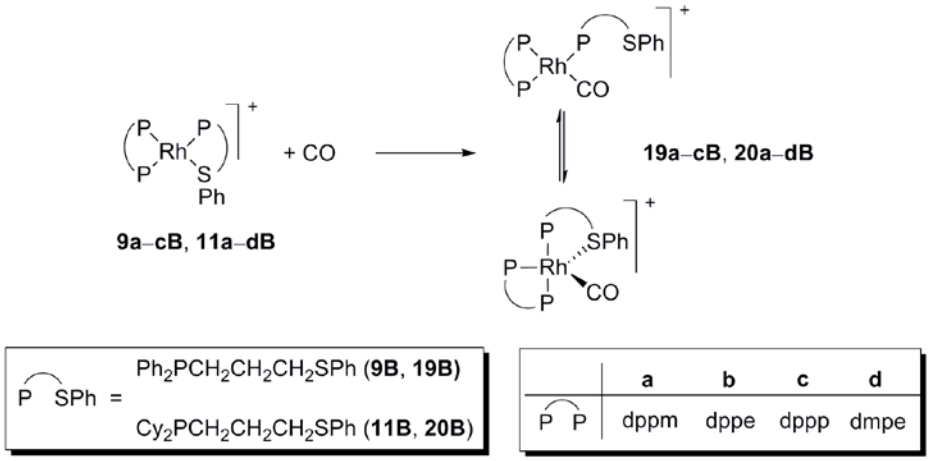

Schema 14.

Interessant sind derartige Liganden für die homogene Katalyse, da die Dissoziation des labileren Donors temporär eine vakante Koordinationsstelle am Metallzentrum schaffen kann, an der ein Substrat koordinieren kann. Die Rekoordination des Donors an das potentiell koordinativ ungesättigte Metallzentrum in einem Folgeschritt trägt wiederum zur Stabilisierung der katalytisch aktiven Spezies bei [75]. Des Weiteren lassen Komplexe mit hemilabilen Liganden eine Aktivierung von kleinen Molekülen, wie CO oder O_2 zu [76–78].

2.3.3. Synthese und Charakterisierung von zwitterionischen Rhodiumkomplexen

Neutrale Komplexe, die innerhalb des Moleküls eine formale Ladungstrennung zwischen einem kationischen Metallzentrum und einem negativ geladenen Liganden aufweisen, werden als zwitterionisch (oder Betain-artig) bezeichnet [79].

So führt die Reaktion der Komplexe [RhCl($R_2PCH_2CH_2CH_2SPh$-κ*P*)(dppm)] (R = Ph, **9aB**; Cy, **11aB**) mit LDA nicht wie zunächst erwartet zur Bildung der entsprechenden Innerkomplexe (Kapitel 2.2.1., S. 13). Vielmehr werden unter Deprotonierung der CH_2-Gruppe des dppm-Liganden die zwitterionischen Komplexen [Rh($dppm_{-H}$-κ^2*P*,*P*′)($R_2PCH_2CH_2CH_2SPh$-κ*P*,κ*S*)] (**17B**, **18B**) erhalten. Diese fielen in Ausbeuten von etwa 72 % als orangefarbene bzw. braune Feststoffe an und NMR-spektroskopisch (^1H, ^{13}C, ^{31}P) sowie durch hochauflösende Massenspektrometrie charakterisiert (Schema 15).

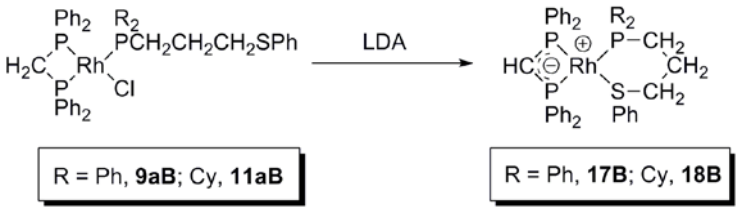

Schema 15.

Ein Vergleich der NMR-spektroskopischen Daten von **17B** und **18B** mit denen der analogen kationischen Komplexe [Rh($R_2PCH_2CH_2CH_2SPh$-κ*P*,κ*S*)(dppm)][PF_6] (**9aB**, **11aB**) zeigt, dass die Deprotonierung des dppm-Liganden zu einer deutlichen Hochfeldverschiebung (^1H, ^{13}C) der Methingruppe führt. Darüber hinaus gelang die röntgeneinkristallographische Charakterisierung von Komplex **18B**·THF. Deren Ergebnisse zeigen, dass die Deprotonierung der CH_2-Gruppe mit einer deutlichen Verkürzung der P–C-Bindungen und einer Verlängerung der Rh–P-Bindungen (im Vergleich zu analogen Rhodiumkomplexen mit nichtdeprotonierten dppm-Liganden) einhergeht, was mit einer Ylid-artigen Struktur in Übereinstimmung steht [80]. Des Weiteren wird durch quantenchemische Rechnungen auf DFT-Niveau am Beispiel von Komplex **17B** gezeigt, dass die Bildung des zwitterionischen Komplexes unter kinetischer Kontrolle steht; die Bildung des entsprechenden rhodiumorganischen Innerkomplexes [Rh{CH(SPh)$CH_2CH_2PPh_2$-κ*C*,κ*P*}(dppm)] ist thermodynamisch um mehr als 21 kcal/mol günstiger.

Darüber hinaus werden zwitterionische Komplexe des Typs [Rh(Ph_2PCHSO_xPh-κ*P*,κ*S*/*O*)L_2] (L_2 = cod, dppe; *x* = 0–2) gemäß Schema 16 durch Umsetzung der entsprechenden Komplexe [RhCl($Ph_2PCH_2SO_x$Ph-κ*P*)L_2] mit $NaN(SiMe_3)_2$ unter Deprotonierung der α-CH_2-Gruppen erhalten.

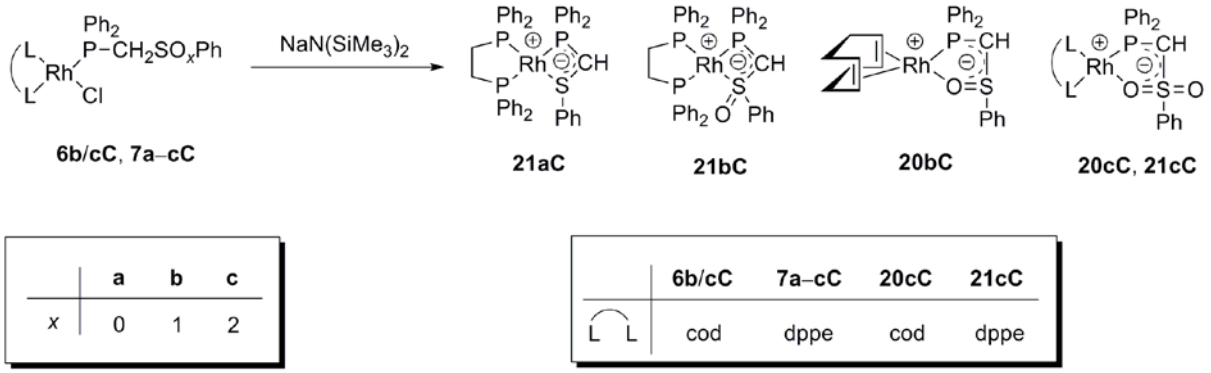

	a	b	c
x	0	1	2

	6b/cC	7a–cC	20cC	21cC
L L	cod	dppe	cod	dppe

Schema 16.

Im Gegensatz zu den oben beschriebenen zwitterionischen Komplexen mit einem $dppm_{-H}$-Liganden zeigen die Komplexe **20C** und **21C** eine deutliche geringere Stabilität in Lösung. Die auffallend gute Löslichkeit dieser Komplexe in unpolaren Lösungsmitteln erschwert zudem deren Isolierung, was nur mäßige Ausbeuten zur Folge hat (52–61 %). Der deprotonierte, funktionalisierte Sulfoxidligand ist, wie sein protoniertes Kongener, ebenfalls von flexidentater Natur, so dass im Fall des cod-Komplexes **20bC** eine κ*P*,κ*O*- und im Fall des dppe-Komplexes **21bC** eine κ*P*,κ*S*-Koordination vorliegt. Der Koordinationsmodus kann auch hier NMR-spektroskopisch ermittelt werden (vgl. Kapitel 2.3.1., S. 21).

In einem Fall ([RhCl(Ph_2PCH_2SPh-κ*P*)(cod)], **6aC**) führt die Deprotonierung mit $NaN(SiMe_3)_2$ nicht zur Bildung des entsprechenden zwitterionischen Komplexes, sondern zu dem dinuklearen Komplex [{Rh{μ-CH(SPh)PPh_2-κ*C*:κ*P*}(cod)}$_2$] (**19C**), welcher innerhalb von 24 Stunden als THF-Addukt (**19C**·THF) auskristallisiert und röntgeneinkristallographisch charakterisiert werden kann. Die Festkörperstuktur zeigt, dass die beiden Rhodiumatome jeweils von einem cod-Liganden sowie von zwei verbrückenden μ-CH(SPh)PPh_2-κ*C*:κ*P*-Liganden koordiniert sind (Abbildung 5). Jedoch weisen die Rhodiumatome, bedingt durch einen relativ kurzen apikalen Rh–S-Abstand (2.5449(8) Å), eine Pseudopentakoordination auf.

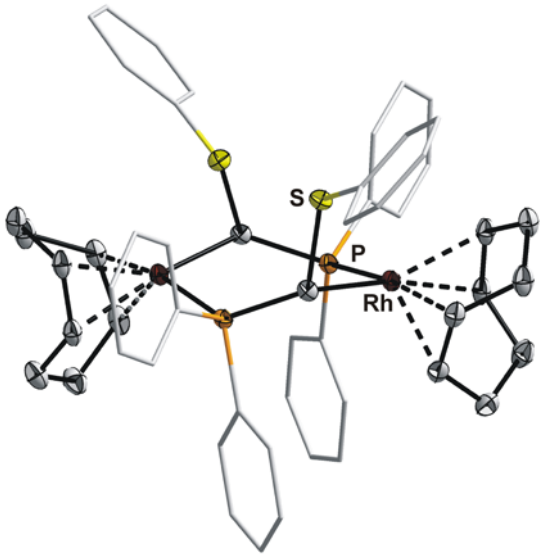

Abbildung 5. Molekülstruktur von [{Rh{μ-CH(SPh)PPh_2-κ*C*:κ*P*}(cod)}$_2$] (**19C**) in Kristallen von **19C**·THF. Die Ellipsoide sind mit einer Wahrscheinlichkeit von 30 % dargestellt. Aus Gründen der Übersichtlichkeit sind keine H-Atome und die Phenylringe als Stabmodell abgebildet.

Zwitterionische Komplexe vereinigen die erstrebenswerten Reaktivitäten von kationischen mit der erwünschten Löslichkeit und der Lösungsmitteltoleranz von neutralen Komplexen, was sie für die Anwendung in verschiedenen homogenkatalysierten Reaktionen interessant macht [81–83].

Die Bildung der zwitterionischen Komplexe, die durch Deprotonierung der $Ph_2PCH_2SO_xPh$-Liganden entstehen, ist darauf zurückzuführen, dass eine κ*C*,κ*P*-Koordination (Innerkomplexbildung), wie sie bei den analogen Liganden mit einem Trimethylen-Spacer gefunden wird (Kapitel 2.2.1., S. 13), die Ausbildung eines hochgespannten RhPC-Dreirings zur Folge hätte. Interessanterweise sind in der Literatur bisher nur zwitterionische Komplexe mit *P*,*S*-Liganden beschrieben, bei denen das Carbanion Teil eines Carborans oder eines aromatischen Ringsystems ist [84,85]. Weiterhin wird deutlich, dass der Koordinationsmodus des sulfinylfunktionalisierten Liganden vom Coliganden abhängt: Beim starken Donor dppe wird eine κ*P*,κ*S*- und beim schwächeren Donor cod eine κ*P*,κ*O*-Koordination gefunden. Eine derartige Abhängigkeit des Koordinationsmodus von Sulfoxiden vom Coliganden ist auf Grundlage des HSAB-Konzepts diskutiert worden [86].

Die Festkörperstruktur von Komplex [Rh(dppm$_{-H}$-κ^2*P*,*P*′)($Cy_2PCH_2CH_2CH_2SPh$-κ*P*,κ*S*)] (**17B**) ist neben [Rh(dppm$_{-H}$-κ^2*P*,*P*′)(dppm-κ^2*P*,*P*′)] [63] erst die zweite Rhodiumverbindung in der vergleichsweise kleinen Gruppe von strukturell charakterisierten Komplexen mit dppm$_{-H}$-Liganden.

2.4. Zur Reaktivität von Platina-β-diketonen gegenüber $Ph_2PCH_2CH_2CH_2SO_xPh$ (x = 0, 2) [D]

2.4.1. Synthese und Charakterisierung von Acetyl(chlorido)platin(II)-Komplexen

Das dinukleare Platina-β-diketon $[Pt_2\{(COMe)_2H\}_2(\mu\text{-}Cl)_2]$ (**8**) reagiert gemäß Schema 17 mit zwei Äquivalenten $Ph_2PCH_2CH_2CH_2SPh$ (**9**) bzw. vier Äquivalenten $Ph_2PCH_2CH_2CH_2SO_2Ph$ (**10**) zu den entsprechenden mononuklearen Acetyl(chlorido)platin(II)-Komplexen. Beide Komplexe wurden als luftstabile, weiße Feststoffe in Ausbeuten von > 70 % erhalten und vollständig spektroskopisch, elementaranalytisch und durch Röntgeneinkristalldiffraktometrie (**4D**) charakterisiert. Die *trans*-Anordnung der beiden Phosphanliganden in **5D** wird unter anderem durch die Größe der $^1J_{Pt,P}$-Kopplungskonstante (3366 Hz) belegt.

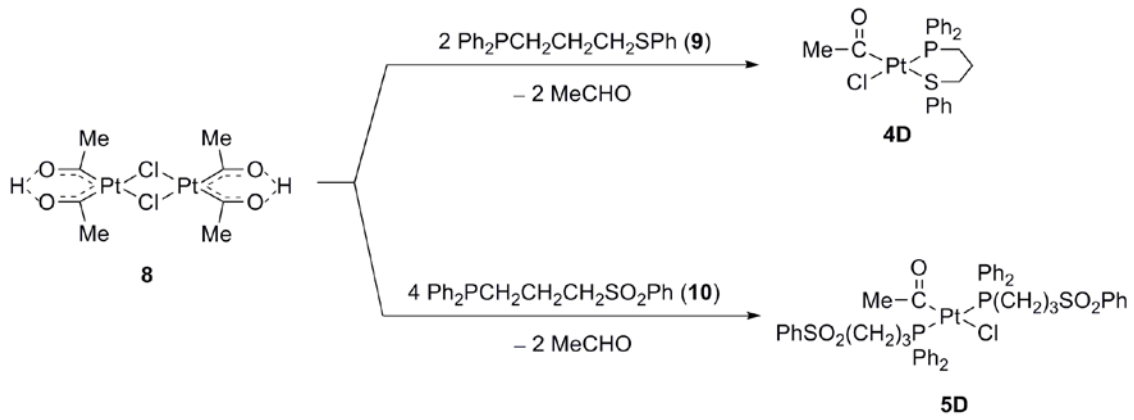

Schema 17.

Während das phosphinofunktionalisierte Sulfid **9** als Chelatligand fungiert (κ*P*,κ*S*) und damit in seiner Reaktivität bidentaten P^P- und N^S-Donoren entspricht [87,88], koordiniert das analoge Sulfon **10** lediglich monodentat (κ*P*) an das Platin, wie es bei nicht-funktionalisierten Phosphanen PR_3 beobachtet wird [89]. Letzteres ist auf das schwache Donorvermögen der Sulfonylfunktion zurückzuführen.

Reaktionen von Platina-β-diketonen mit mono- und bidentaten Liganden zu Acetyl–(chlorido)platin(II)-Komplexen laufen über einen nicht beobachteten intermediären Acetyl-(hydrido)platin(IV)-Komplex ab, dem eine reduktive C–H-Eliminierung von Acetaldehyd folgt [90]. Bei der Verwendung von N^N-Donoren sind diese Platin(IV)-Spezies außerordentlich stabil und können daher in Substanz isoliert werden [87,91].

2.4.2. Zur Reaktivität von Acetyl(chlorido)platin(II)-Komplexen

Beim Erwärmen der Acetyl(chlorido)platin(II)-Komplexe **4D** und **5D** in benzolischer Lösung kommt es gemäß Route **a/b** (Schema 18) zu einer CO-Extrusion, was die Bildung der entsprechenden Methyl(chlorido)platin(II)-Komplexe zur Folge hat.

Durch die Zugabe von $Ag[BF_4]$ zu Komplex **5D** gelingt gemäß Route **c** unter Abspaltung des Chloridoliganden in Form von AgCl die Bildung eines Methyl(carbonyl)platin(II)-Komplexes (**9D**). Wird die in Schema 17 beschriebene Reaktion von Platina-β-diketon (**8**) mit dem funktionalisierten Sulfon **10** in einem molaren Verhältnis von 1:2 durchgeführt, so ist das erhaltene Gemisch von **5D** und **8** in Lösung nicht stabil und reagiert innerhalb von zwei Tagen bei Raumtemperatur gemäß Route **d** zum Methyl(chlorido)carbonylplatin(II)-Komplex **7D**. In siedendem Benzol läuft diese Reaktion innerhalb von zwei Stunden ab.

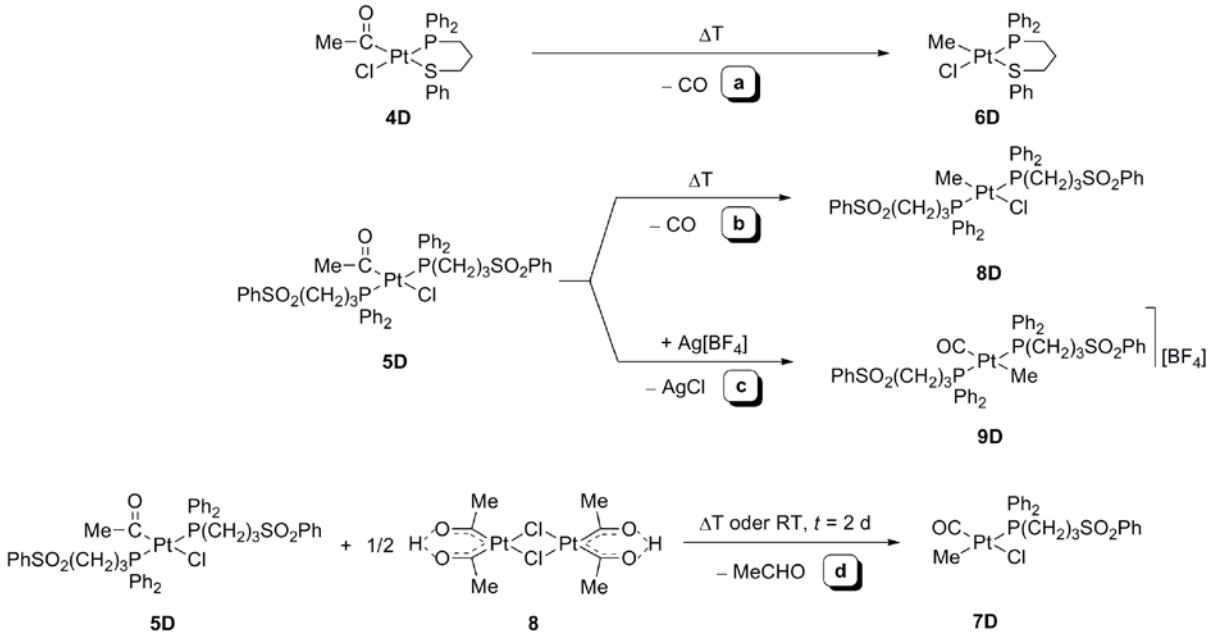

Schema 18.

Die Komplexe **6D**–**9D** wurden in Ausbeuten von ca. 75 % als luftstabile, weiße Feststoffe erhalten und vollständig spektroskopisch, elementaranalytisch sowie durch Röntgeneinkristalldiffraktometrie (**6D**) charakterisiert. Die $^1J_{Pt,P}$-Kopplungskonstanten in den Komplexen **6D**–**9D** spiegeln den abnehmenden *trans*-Einfluss in der Reihenfolge Me > PR_3 > Cl wider, da sie sich von ca. 1450 Hz (**7D**) über ca. 3050 bzw. 2500 Hz (**8D**, **9D**) auf etwa 4400 Hz (**6D**) verkleinern.

Die Resonanzen der Methyl-C-Atome in den ^{13}C-NMR-Spektren der Komplexe **6D**–**9D** sind im Vergleich zu denen der Acetylkomplexe (**4D**, **5D**) um mehr als 40 ppm zu höherem Feld verschoben. Darüber hinaus belegt die Größe der $^{1}J_{Pt,C}$-Kopplungskonstanten in **6D**–**9D** (480–660 Hz) zweifelsfrei die Koordination der Methylgruppe an das Platin.
Damit kann gezeigt werden, dass Methylplatin(II)-Komplexe über Decarbonylierung der entsprechenden Acetylkomplexe zugänglich sind, was in Übereinstimmung mit in der Literatur beschriebenen Reaktionen steht [89,92]. Darüber hinaus wird gefunden, dass die hier beschriebenen Decarbonylierungen bereits bei Raumtemperatur ablaufen, wenn am Platin eine vakante Koordinationsstelle geschaffen wird, was im Fall von **9D** durch Zugabe von Ag[BF_4] und am Beispiel von **7D** durch überschüssiges Platina-β-diketon erreicht wird. Über derartige Decabonylierungen wurde auch bei α-Ketoacyl- und Formyl-Platin(II)-Komplexen berichtet [93,94]. Weiterhin ist anzumerken, dass die Bildung des Methyl(chlorido)carbonylplatin(II)-Komplexes **7D** diastereoselektiv abläuft, wogegen bei analogen Untersuchungen von Pt(II)-Komplexen mit dem nicht-funktionalisierten PPh_3-Liganden (anstelle von Ligand **10**) die Bildung von zwei Diastereomeren beobachtet wird [95].

Bifunktionelle α,ω-heteroatomfunktionalisierte Verbindungen sind in der Koordinationschemie und in der Organometallchemie wegen ihres vielfältigen Koordinationspotentials und ihrer vielseitigen Reaktionsmöglichkeiten von besonderer Bedeutung. Die im Rahmen der vorliegenden Arbeit erzielten Ergebnisse liefern neue Erkenntnisse über die Abhängigkeit der Regioselektivität vom Arylsystem bei der Metallierung von Verbindungen des Typs $ArSCH_2CH_2CH_2OR$ sowie zum Koordinationsverhalten von bifunktionaliserten Liganden des Typs $Ph_2P(CH_2)_nSO_xPh$ bzw. der durch Deprotonierung erhaltenen Alkylliganden. Dabei konnte gezeigt werden, dass durch die Wahl geeigneter Rhodium(I)- und Platin(II)-Precursorkomplexe, die eine mono- oder eine bidentate Koordination dieser Liganden zulassen, gezielt verschiedenartige Koordinationsmodi realisiert werden können. Der Koordinationsmodus hängt ausgeprägt von der Spacerlänge *n* sowie der Natur der Schwefelfunktionalisierung (S *vs*. SO *vs*. SO_2) ab und kann darüber hinaus durch die Coliganden gesteuert werden. Daraus resultiert ein breites Spektrum an Reaktionsmöglichkeiten, welches sich unter anderem in der Ausbildung von metallorganischen Innerkomplexen, zwitterionischen Komplexen und Komplexen mit hemilabilen Liganden widerspiegelt.

3. Zusammenfassung

Aufgrund ihres vielseitigen Koordinationspotentials stellen heterobidentate Liganden eine besonders interessante Substanzklasse dar. Im Gegensatz zu konventionellen, homobidentaten Liganden wie Diphosphanen oder Diaminen erzeugen sie am Metallzentrum eine sterische und elektronische Asymmetrie und können darüber hinaus als hemilabile Liganden agieren, was sie für eine Vielzahl von homogenkatalysierten Reaktion interessant macht. Der Koordinationsmodus derartiger Liganden und damit die Struktur bzw. Reaktivität der erhaltenen Komplexe kann dabei durch eine Reihe von Faktoren gesteuert werden. In der Literatur sind vorwiegend Komplexe mit bifunktionellen P^S- und P^O-Liganden beschrieben, während vergleichsweise wenig über P^SO-Liganden, die beide Koordinationsmodi auf sich vereinigen, berichtet wird.

Im Rahmen dieser Arbeit steht die Synthese und Charakterisierung von rhoda- und platinacyclischen Komplexen mit Liganden des Typs $R_2P(CH_2)_nSO_xPh$ sowie deren deprotonierte Kongenere im Fokus. In Fortführung vorangegangener Untersuchungen wird darüber hinaus über die Abhängigkeit der Regioselektivität bei der Metallierung von γ-alkoxyfunktionalisierten Propylarylsulfiden berichtet.

Zur Regioselektivität der Metallierung von γ-alkoxyfunktionalisierten Propylarylsulfiden

1. Bei der Metallierung von γ-alkoxyfunktionalisierten Propylarylsulfiden vom Typ **I** durch Lithiierung mit *n*-BuLi/TMEDA und nachfolgender Umsetzung mit Me_3SnCl wurde gefunden, dass neben der erwarteten α- und *ortho*-Metallierung auch eine Metallierung der OR-Gruppe (R = Me, *t*Bu; *alkyl*-Metallierung) bzw. eine Metallierung der Alkylfunktionalisierungen am Arylsystem (*alkyl*'-Metallierung) auftritt. Der Vergleich von OMe- und O-*t*Bu-funktionalisierten Sulfiden zeigt, dass letztere erheblich empfindlicher auf eine Variation des Arylsystems reagieren, da hier die α-Metallierung stärker zurückgedrängt wird. Generell scheint eine *alkyl'*- gegenüber einer *alkyl*-Metallierung bevorzugt abzulaufen, da bei Derivaten, die beiden Reaktionen zugänglich sind, nur erstere beobachtet wird.

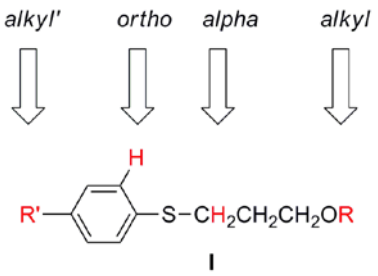

I

Zur Synthese und Charakterisierung von metallorganischen Innerkomplexen und zwitterionischen Komplexen

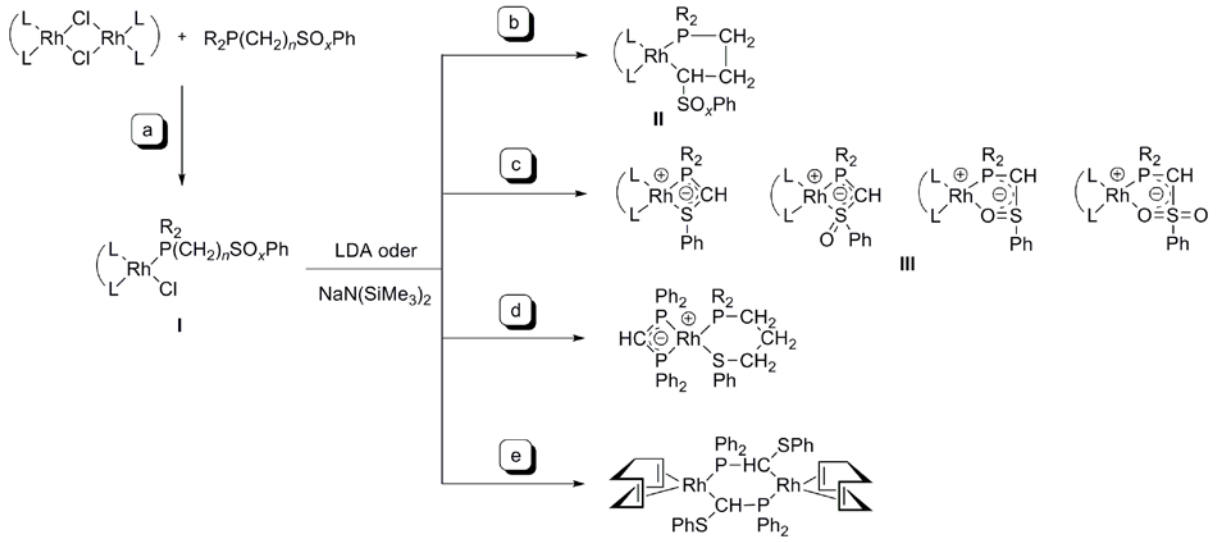

2. Die Umsetzung von dinuklearen Rh(I)-Komplexen $[(RhL_2)_2(\mu\text{-}Cl)_2]$ (L = cod, dppm, dppe, dppp, dmpe) mit ω-phosphinofunktionalisierten Alkylphenylsulfiden, -sulfoxiden und -sulfonen $Ph_2P(CH_2)_nSO_xPh$ (n = 1–3, x = 0–2) führt gemäß Route **a** zu mononuklearen Rh(I)-Komplexen des Typs $[RhCl(R_2P(CH_2)_nSO_xPh\text{-}\kappa P)L_2]$ (**I**), in denen die bifunk–tionellen Liganden κ*P*-koordiniert sind. Die Konstitution dieser Komplexe wurde spektroskopisch, elementaranalytisch und röntgeneinkristallographisch belegt. Im Gegensatz dazu zeigte das *N*-funktionalisierte Sulfon $Me_2NCH_2CH_2CH_2SO_2Ph$ keine Reaktion.

3. Die Umsetzung von Komplexen des Typs **I** mit Stickstoffbasen, wie LDA oder Natriumbis(trimethylsilyl)amid, führt zu einer selektiven Deprotonierung der α-CH_2-Gruppe. Bei den Kompexen, die einen bifunktionalisierten Liganden mit einem Trimethylenspacer (n = 3) koordiniert haben, kommt es dabei gemäß Route **b** unter Abspaltung des Chloridoliganden zu einer κ*C*,κ*P*-Koordination der deprotonierten Liganden, das heißt zur Ausbildung von metallorganischen Innerkomplexen (Typ **II**). Im Fall der sulfinylfunktionalisierten Liganden (x = 1) verläuft die Innerkomplexbildung diastereoselektiv. Die Komplexe vom Typ **II** wurden vollständig spektroskopisch, elementaranalytisch und teilweise durch Röntgeneinkristalldiffraktometrie charakterisiert. Die ^{31}P-NMR-Spektren zeigen teilweise Spinsysteme höherer Ordnung (ABMX, ABCX), welche mithilfe eines Spektrensimulations- und Iterationsprogramms vollständig gelöst werden konnten.

4. Die Deprotonierung von Komplexen des Typs **I**, in denen der Ligand eine P–CH_2–S-Baueinheit aufweist (*n* = 1), führt gemäß Route **c** zur Bildung von zwitterionischen Rhodiumkomplexen. Diese besitzen ein „freies" carbanionisches Kohlenstoffatom und der Ligand ist demzufolge κ*P*,κ*S*- bzw. κ*P*,κ*O*-koordiniert. Der Koordinationsmodus der flexidentaten sulfinylfunktionalisierten Liganden (*x* = 1) wird dabei vom Coliganden (cod *vs.* dppe) gesteuert.

5. Die Reaktion von LDA mit Komplexen des Typs **I**, die einen sulfanylfunktionalisierten Liganden und dppm als Coliganden koordiniert haben (L^L = dppm, *n* = 3, *x* = 0), führt nicht zur Innerkomplexbildung (Typ **II**), sondern gemäß Route **d** zur Deprotonierung der Methylengruppe des dppm-Liganden, was die Enstehung der zwitterionischen Komplexe [Rh(dppm$_{-H}$-κ^2*P*,*P'*)($R_2PCH_2CH_2CH_2SPh$-κ*P*,κ*S*)] (R = Ph, Cy) zur Folge hat, deren Konstitution unter anderem durch eine Röntgeneinkristallstrukturanalyse des Cyclohexylderivates belegt ist. Quantenchemische Rechnungen zeigen, dass die Bildung der zwitterionischen Komplexe unter kinetischer Kontrolle steht, da die Bildung der entsprechenden Innerkomplexe vom Typ **II** thermodynamisch um mehr als 20 kcal/mol günstiger ist.

6. Gemäß Route **e** führt die Deprotonierung in einem Fall (*n* = 1, *x* = 0) zur Bildung des dinuklearen rhodiumorganischen Komplexes [{Rh(μ-$Ph_2PCHSPh$-κ*C*:κ*P*)(cod)}$_2$]·THF, dessen Konstitution durch eine Röntgeneinkristallstrukturanalyse sichergestellt wurde. Dabei weisen die beiden Rhodiumatome eine *pseudo*-Pentakoordination auf, was durch einen relativ kurzen apikalen Rh–S-Abstand (2.5449(8) Å) belegt ist.

7. Komplexe vom Typ **I**, die einen bifunktionalisierten Liganden mit einem Dimethylenspacer (*n* = 2) koordiniert haben, zersetzen sich bei Reaktionen mit LDA bzw. $NaN(SiMe_3)_2$. Der *N*-funktionalisierte Ligand $Me_2NCH_2CH_2CH_2SO_2Ph$ kann nicht mit [$(RhL_2)_2$(μ-Cl)$_2$] zu Komplexen vom Typ **I**, in denen der Ligand κ*N*-koordiniert ist, umgesetzt werden. Zur Darstellung der entsprechenden Innerkomplexe muss daher der freie Ligand zunächst mit *n*-BuLi deprotoniert und anschließend mit dinuklearen Rh(I)-Komplexen zu den Innerkomplexen [Rh{$CH(SO_2Ph)CH_2CH_2NMe_2$-κ*C*,κ*N*}L_2] umgesetzt werden.

Zur Synthese und Reaktivität von kationischen rhodacyclischen Komplexen

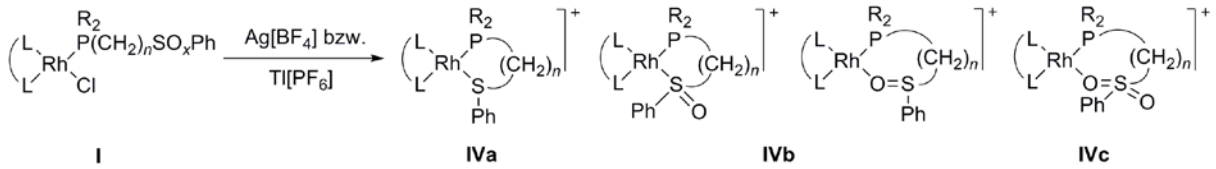

8. Die Umsetzung von Komplexen des Typs **I** mit Chloridionenakzeptoren wie $Ag[BF_4]$ oder $Tl[PF_6]$ führt unter Abspaltung von AgCl bzw. TlCl zur Bildung der kationischen rhodacyclischen Komplexe **IVa**–**c**, in denen die Liganden κ*P*,κ*S*- bzw. κ*P*,κ*O*-koordiniert sind.

9. Der Koordinationsmodus der flexidentaten sulfinylfunktionalisierten Liganden (x = 1) in Komplexen des Typs **IVb** hängt von der gebildeten Ringgröße und damit von der Spacerlänge n ab. Mit einem Di- und Trimethylenspacer (n = 2, 3) wird eine κ*P*,κ*S*- und mit einem Methylenspacer (n = 1) eine κ*P*,κ*O*-Koordination gefunden, so dass in allen Fällen ausnahmslos thermodynamisch stabile Fünf- und Sechsringe gebildet werden. In den Komplexen **IVa** und **IVc** sind die sulfanyl- (x = 0) bzw. sulfonylfunktionalisierten Liganden (x = 2) nicht flexidentat, so dass hier neben Fünf- und Sechsringen auch die Bildung von thermodynamisch weniger günstigen vier- und siebengliedrigen Ringen beobachtet wird.

10. Durch eine Lösungsmittelvariation (CH_2Cl_2 → THF) wird bei der Umsetzung von $Ag[BF_4]$ mit einem Komplexes vom Typ **I** (L^L = cod, n = 1, x = 0) die Bildung des trinuklearen kationischen Rhodium(I)-Komplexes $[Rh_3(\mu\text{-}Cl)(\mu\text{-}Ph_2PCH_2SPh\text{-}\kappa P{:}\kappa S)_4][BF_4]_2 \cdot 4THF$ beobachtet, dessen Grundgerüst von einem viergliedrigen Rh_3Cl-Ring und vier μ-Ph_2PCH_2SPh-Liganden gebildet wird und der in seiner Struktur einem A-Frame-Komplex ähnelt. Dabei besitzen zwei Rhodiumatome eine trigonal-bipyramidale und das zentrale Rhodiumatom eine quadratisch-planare Konfiguration. Das Kation weist eine angenäherte C_2-Symmetrie auf, wobei die Drehachse durch das Chlor- und das zentrale Rhodiumatom verläuft.

11. Die Umsetzung der kationischen Komplexe vom Typ **IVa** (L^L = P^P, *n* = 3) mit CO führt zur Bildung von kationischen Rhodiumcarbonylkomplexen des Typs **V**, die sich bei Raumtemperatur in einem dynamischen Gleichgewicht befinden. Quantenchemische Rechnungen zeigen, dass diese Moleküldynamik auf ein Gleichgewicht zwischen einem vier- und einem fünfach koordinierten Rh(I)-Komplex, in dem die *P*,*S*-Liganden κ*P*- bzw. κ*P*,κ*S*-koordiniert sind, zurückzuführen ist. Daher kann die Koordination der phosphinofunktionalisierten Sulfidliganden als hemilabil beschrieben werden. Komplexe vom Typ **IVa** mit einem cod-Coliganden zeigen keine Reaktivität gegenüber CO.

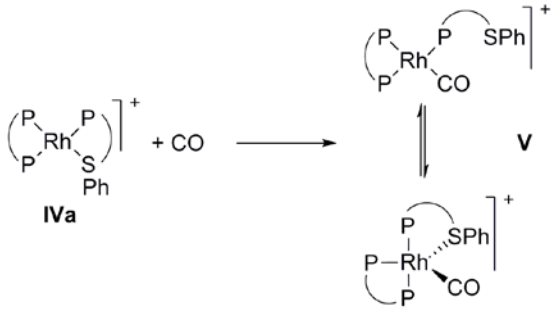

Zur Reaktivität von Platina-β-diketonen gegenüber $Ph_2PCH_2CH_2CH_2SO_xPh$ (x = 0, 2)

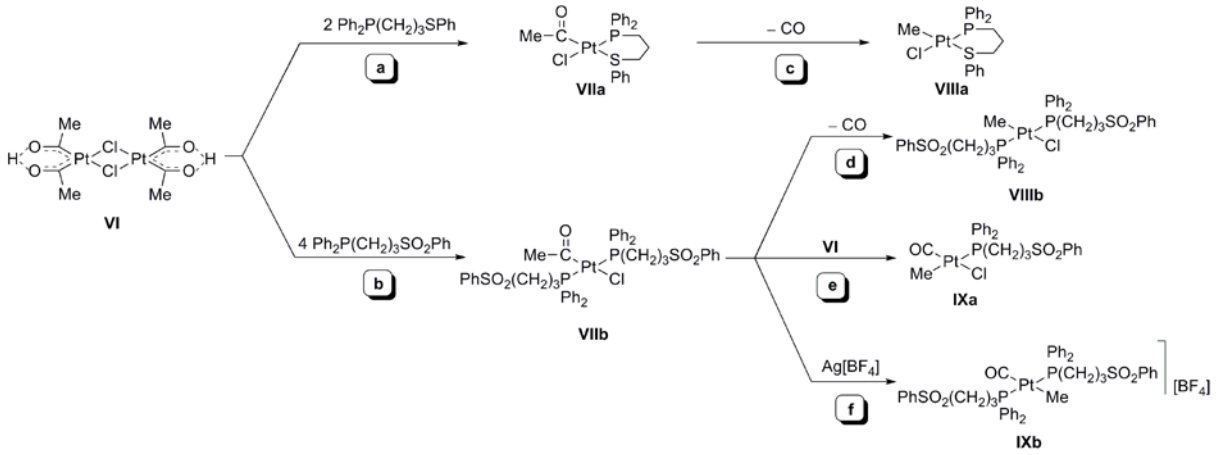

12. Die Umsetzungen der beiden Liganden $Ph_2PCH_2CH_2CH_2SPh$ und $Ph_2PCH_2CH_2CH_2$-SO_2Ph mit dem elektronisch ungesättigten Platina-β-diketon $[Pt_2\{(COMe)_2H\}_2(\mu\text{-}Cl)_2]$ (**VI**) führen nach Route **a**/**b** zur Bildung der Acetyl(chlorido)platin(II)-Komplexe **VIIa**,**b**. Während das funktionalisierte Sulfid in **VIIa** eine κ*P*,κ*S*-Koordination aufweist, ist das entsprechende Sulfon in **VIIb** lediglich κ*P*-koordiniert.

13. In der Wärme unterliegen Acetyl(chlorido)platin(II)-Komplexe **VIIa**,**b** gemäß Route **c**/**d** einer CO-Extrusion, wobei es zur Bildung der entsprechenden Methyl(chlorido)platin(II)-Komplexe **VIIIa**,**b** kommt. Durch Zugabe von $Ag[BF_4]$ (Route **f**) oder durch die Gegenwart von nicht umgesetztem Platina-β-diketon (**VI**, Route **e**) wird am Platin eine freie Koordinationsstelle erzeugt, wobei Komplex **VIIb** zu den Platin(methyl)carbonylkomplexen **IXa**,**b** weiterreagiert. Die Bildung von Komplex **IXa** verläuft dabei diastereoselektiv.

Die Ergebnisse der vorliegenden Arbeit belegen das vielfältige Koordinationspotential von bifunktionellen P^SO_xPh-Liganden, das sich unter anderem in der Bildung von metallorganischen Innerkomplexen, zwitterionischen Komplexen oder Komplexen mit hemilabilen Liganden widerspiegelt. In Rhodium- und Platinkomplexen mit *P*,*S*-funktionalisierten Liganden des Typs $R_2P(CH_2)_nSO_xPh$ und ihren in α-Position deprotonierten Kongeneren hat die Spacerlänge $(CH_2)_n$ (n = 1–3) sowie die Basizität des carbanionischen α-Kohlenstoffs, welche über die benachbarte Schwefelfunktionalisierung SO_x (x = 0–2) gesteuert werden kann, einen maßgeblichen Einfluss auf den Koordinationsmodus und damit auf die Reaktivität der erhaltenen Komplexe. Darüber hinaus besteht die Möglichkeit die Struktur der Komplexe durch Variation des Coliganden zu beeinflussen. Die vorliegenden Ergebnisse erweitern damit die Kenntnisse auf dem Gebiet der Koordinationschemie und Organometallchemie von Platinmetallen mit α,ω-heteroatomfunktionalisierten Liganden.

4. Literaturverzeichnis

[1] A. F. Hollemann, E. Wiberg, *Lehrbuch der Anorganischen Chemie*, 102, Gruyter Berlin, 2007.

[2] J. A. Osborn, F. H. Jardine, J. F. Young, G. Wilkinson, *J. Chem. Soc. A* **1966**, 1711.

[3] F. Diedrich, P. J. Stang, *Metal-Catalyzed Cross-Coupling Reactions*, Wiley-VCH, Weinheim 1998.

[4] R. H. Grubbs, W. Tumas, *Science* **1989**, *243*, 907.

[5] R. H. Grubbs, *Tetrahedron* **2004**, *60*, 7117.

[6] F. Zheng, A. Sivaramakrishna, J. R. Moss, *Coord. Chem. Rev.* **2007**, *251*, 2056.

[7] H. Harada, R. K. Thalji, R. G. Bergman, J. A. Ellman, *J. Org. Chem*. **2008**, *73*, 6772.

[8] B. Blom, H. Clayton, M. Kilkenny, J. R. Moss, *Adv. Organomet. Chem.* **2006**, *54*, 149.

[9] C. Elschenbroich, *Organometallchemie*, 6. Aufl., Vieweg + Teubner, Wiesbaden 2008.

[10] D. Steinborn, *Grundlagen der metallorganischen Komplexkatalyse*, 2. Aufl., Vieweg + Teubner, Wiesbaden 2010.

[11] G. Bähr, G. E. Müller, *Chem. Ber*. **1955**, *88*, 251.

[12] J. P. Kleiman, M. Dubeck, *J. Am. Chem. Soc.* **1963**, *85*, 1544.

[13] M. Nolte, E. Singleton, E. van der Stok, *J. Organomet. Chem.* **1977**, *142*, 387.

[14] E. Klei, J. H. Teuben, *J. Organomet. Chem.*, **1981**, *214*, 53.

[15] T. A. K. Al-Allaf, *Asian J. Chem.* **2000**, *12*, 869.

[16] I. Omae, *J. Organomet. Chem.* **2007**, *692*, 2608.

[17] R. Beck, M. Frey, S. Camadanli, H.-F. Klein, *Dalton Trans*. **2008**, *37*, 4981.

[18] J. Campos, A. C. Esqueda, E. Carmona, *Chem. Eur. J*. **2010**, *16*, 419.

[19] S. Matsuda, S. Kikkawa, I. Omae, *Kogyo Kagaku Zasshi* **1966**, *69*, 646.

[20] J. M. Thompson, R. F. Heck, *J. Org. Chem.* **1975**, *40*, 2667.

[21] R. A. Holton, *Tetrahedron Lett.* **1977**, *18*, 355.

[22] R .A. Holton, K. J. Natalie Jr., *Tetrahedron Lett.* **1981**, *22*, 267.

[23] H.-F. Klein, M. Helwig, U. Koch, U. Flörke, H.-J. Haupt, *Z. Naturforsch.* **1993**, *48b*, 778.

[24] F. Kakiuchi, M. Matsumoto, K. Tsuchiya, K. Igi, T. Hayamizu, N. Chatani, S. Murai, *J. Organomet. Chem.* **2003**, *686*, 134.

[25] J. K. Stille, *Angew. Chem. Int. Ed. Engl.* **1986**, *25*, 508.

[26] N. Miyaura, A. Suzuki, *Chem. Rev.* **1995**, *95*, 2457.

[27] W. A. Herrmann, V. P. W. Böhm, C.-P. Reisinger, *J. Organomet. Chem.* **1999**, *576*, 23.

[28] T. K. Hollis, L. E. Overman, *J. Organomet. Chem.* **1999**, *576*, 290.

[29] Q. Yao, Y. Zhang, *Angew. Chem. Int. Ed.* **2003**, *42*, 3395.

[30] H. Clavier, N. Audic, J.-C. Guillemin, M. Mauduit, *J. Organomet. Chem.* **2005**, *690*, 3585.

[31] M. Arisawa, Y. Terada, C. Theeraladanon, K. Takahashi, M. Nakagawa, A. Nishida, *J. Organomet. Chem.* **2005**, *690*, 5398.

[32] M. Bassetti, *Eur. J. Inorg. Chem.* **2006**, 4473.

[33] H. Pellisier, *Tetrahedron* **2007**, *63*, 1297.

[34] E. Guimet, M. Diéguez, A. Ruiz, C. Claver, *J. Chem. Soc., Dalton Trans*. **2005**, 2557.

[35] X. Caldentey, M. A. Pericàs, *J. Org. Chem*. **2010**, *75*, 2628.

[36] X. Verdaguer, M. A. Pericàs, A. Riera, M. A. Maestro, J. Mahía, *Organometallics* **2003**, *22*, 1868.

[37] E. Hauptmann, P. J. Fagan, W. Marshall, *Organometallics* **1999**, *18*, 2061.

[38] A. B. Chaplin, A. S. Weller, *Organometallics* **2010**, *29*, 2332.

[39] T. K. Hyster, T. Rovis, *J. Am. Chem. Soc*. **2010**, *132*, 10565.

[40] H. Kim, C. Lee, *J. Am. Chem. Soc*. **2005**, *127*, 10181.

[41] P. Xue, H. S. Y. Sung, I. D. Williams, G. Jia, *J. Organomet. Chem*. **2006**, *691*, 1945.

[42] M. Linnert, C. Bruhn, T. Rüffer, H. Schmidt, D. Steinborn, *Organometallics* **2004**, *23*, 3668.

[43] M. Linnert, C. Bruhn, C. Wagner, M. Block, T. Rüffer, H. Schmidt, D. Steinborn, *Advances in Coordination, Bioinorganic and Inorganic Chemistry* (Eds.: M. Melnik, J. Sima, M. Tatarko), STU Press Bratislava, 2005, S. 170.

[44] M. Block, M. Linnert, S. Gómez-Ruiz, D. Steinborn, *J. Organomet. Chem.* **2009**, *694*, 3353.

[45] V. H. Gessner, C. Däschlein, C. Strohmann, *Chem. Eur. J.* **2009**, *15*, 3320.

[46] T. Rüffer, C. Bruhn, A. H. Maulitz, D. Ströhl, D. Steinborn, *Organometallics* **2000**, *19*, 2829.

[47] M. Block, *Diplomarbeit*, Martin-Luther-Universität Halle-Wittenberg, 2006.

[48] H. Meerwein in *Houben-Weyl – Methoden der Organischen Chemie*, Vol. XI/3, Thieme Stuttgart, 1965, S. 1.

[49] G. Ludwig, *Diplomarbeit*, Martin-Luther-Universität Halle-Wittenberg, 2010.

[50] M. P. Li, R. S. Drago, *J. Am. Chem. Soc.* **1976**, *98*, 5129.

[51] M. Linnert, C. Bruhn, T. Rüffer, H. Schmidt, D. Steinborn, *Organometallics* **2004**, *23*, 3668.

[52] C. Schaffner-Hamann, A. von Zelewsky, A. Barbieri, F. Barigelletti, G. Muller, J. P. Riehl, A. Neels, *J. Am. Chem. Soc*. **2004**, *126*, 9339.

[53] M.-C. P Yeh, L.-W. Chuang, C.-C. Hwu, J.-M. Sheu, L.-C. Row, *Organometallics* **1995**, *14*, 3396.

[54] P. Alvarez, E. Lastra, J. Gimeno, P. Bran, J. A. Sordo, J. Gomez, L. R. Falvello, M. Bassetti, *Organometallics* **2004**, *23*, 2956.

[55] S. B. Han, X. Gao, M. J. Krische, *J. Am. Chem. Soc*. **2010**, *132*, 9153.

[56] I. S. Kim, S. B. Han, M. J. Krische, *J. Am. Chem. Soc*. **2009**, *131*, 2514.

[57] P. Imhoff, S. C. A. Nefkens, C. J. Elsevier, K. Goubitz, C. H. Stam, *Organometallics* **1991**, *10*, 1421.

[58] P. Imhoff, C. J. Elsevier, C. H. Stam, *Inorg. Chim. Acta* **1990**, *175*, 209.

[59] H. Werner, A. Hampp, B. Windmüller, *J. Organomet. Chem.* **1992**, *435*, 169.

[60] G. L. Edwards in *Comprehensive Organic Functional Groups Transformations 1*, (Eds. A. R. Katritzky, O. Meth-Cohn, C.W. Rees), Elsevier Oxford, 1995, S. 105.

[61] F. G. Bordwell, J. C. Branca, C. R. Johnson, N. R. Vanier, *J. Org. Chem.* **1980**, *45*, 3884.

[62] W. Ando, A. Sekiguchi, T. Migita, *J. Am. Chem. Soc.* **1975**, *97*, 7160.

[63] D. E. Chebi, P. E. Fanwick, I. P. Rothwell, *Organometallic* **1990**, *9*, 2948.

[64] R. Fornika, C. Six, H. Görls, M. Kessler, C. Krüger, W. Leitner, *Can. J. Chem*. **2001**, *79*, 642.

[65] M. Block, C. Wagner, S. Gómez-Ruiz, D. Steinborn, *Dalton Trans*. **2010**, *39*, 4336.

[66] J. W. Faller, B. J. Grimmond, D. G. D`Alliessi, *J. Am. Chem. Soc*. **2001**, *123*, 2525.

[67] J. W. Faller, B. J. Grimmond, M. Curtis, *Organometallics* **2000**, *195*, 174.

[68] J. W. Faller, J. C. Wilt, *Tetrahedron Lett.* **2005**, *45*, 7613.

[69] E. Guimet, M. Diéguez, A. Ruiz, C. Claver, *J. Chem. Soc., Dalton Trans.* **2005**, 2557.

[70] R. Dorta, H. Rozenberg, L. J. W. Shimon, D. Milstein, *Chem. Eur. J*. **2003**, *95*, 237.

[71] T. Achard, J. Benet-Buchholz, A. Riera, X. Verdaguer, *Organometallics* **2009**, *28*, 480.

[72] T. A. Ryan, *Coord. Chem. Rev.* **1984**, *57*, 75.

[73] F. Shafiq, K. W. Kramarz, R. Eisenberg, *Inorg. Chim. Acta* **1993**, *213*, 111.

[74] A. M. Brown, M. V. Ovchinnikov, C. A. Mirkin, *Angew. Chem. Int. Ed.* **2005**, *44*, 4207.

[75] J. W. Faller, S. C. Milheiro, J. Parr, *J. Organomet. Chem*. **2008**, *693*, 1478.

[76] M. Bressan, F. Morandini, *J. Organomet. Chem*. **1983**, *247*, C8.

[77] M. Bressan, F. Morandini, A. Morvillo, *J. Organomet. Chem*. **1985**, *280*, 139.

[78] J. R. Dilworth, J. R. Miller, N. Wheatley, M. J. Baker, J. G. Sunley, *J. Chem.Soc., Chem. Commun.* **1995**, 1579.

[79] M. Stradiotto, K. D. Hesp, R. J. Lundgren, *Angew. Chem. Int. Ed.* **2010**, *49***,** 494.

[80] H. H. Karsch, M. Reisky, Eur. *J. Inorg. Chem*. **1998**, 905.

[81] J. Cipot, R. McDonald, M. Stradiotto, *Chem. Commun*. **2005**, 4932.

[82] R. J. Lundgren, M. Stradiotto, *Chem. Eur. J.* **2008**, *14*, 10388.

[83] J. Cipot, C. M. Vogels, R. McDonald, S. A. Westcott, M. Stradiotto, *Organometallics* **2006**, *25*, 5965.

[84] X.-K. Huo, G. Su, G.-X. Jin, *Dalton Trans*. **2010**, *39*, 1954.

[85] K. D. Hesp, R. McDonald, M. J. Ferguson, M. Stradiotto, *J. Am. Chem. Soc*., **2008**, *130*, 16394.

[86] M. Calligaris, O. Carugo, *Coord. Chem. Rev*., **1996**, *153*, 83.

[87] D. E. Chebi, P. E. Fanwick, I. P. Rothwell, *Organometallics* **1990**, *9*, 2948.

[88] M. Gerisch, C. Bruhn, A. Vyater, J. A. Davies, D. Steinborn, *Organometallics* **1998**, *17*, 3101

[89] T. Gosavi, E. Rusanov, H. Schmidt, D. Steinborn, *Inorg. Chim. Acta* **2004**, 357.

[90] C. Albrecht, C. Wagner, D. Steinborn, *Z. Anorg. Allg. Chem*. **2008**, *334*, 2858.

[91] D. Steinborn, *Dalton Trans*. **2005**, 2664.

[92] A. Vyater, C. Wagner, K. Merzweiler, D. Steinborn, *Organometallics* **2002**, *21*, 4369.

[93] C. Albrecht, C. Wagner, K. Merzweiler, T. Lis, D. Steinborn, *Appl. Organomet. Chem*. **2005**, *19*, 1155.

[94] J-T. Chen, Y.-S. Yeh, C.-S. Yang, F.-Y. Tsai, G.-L. Huang, B.-C. Shu, T.-M. Huang, Y.-S. Chen, G.-H. Lee, M.-C. Cheng, C.-C. Wang, Y. Wang, *Organometallics* **1994**, *13*, 4804.

[95] D. Vuzman, E. Poverenov, Y. Diskin-Posner, G. Leitus, L. J. W. Shimon, D. Milstein, *Dalton Trans*. **2007**, 5692.

[96] M. Gerisch, F. W. Heinemann, C. Bruhn, J. Scholz, D. Steinborn, *Organometallics* **1999**, *18*, 564.

Danksagung

An meinen sehr verehrten Hochschullehrer, Herrn Prof. Dr. D. Steinborn, möchte ich an dieser Stelle ein besonderes Wort des Dankes richten, da er durch die Überlassung des außerordentlich interessanten und ergiebigen Themas, dessen freier Gestaltung sowie durch wertvolle Anregungen, Hinweisen und Diskussionen, zum Gelingen der Arbeit beigetragen hat.

Herrn Dr. H. Schmidt danke ich für die Hilfe bei der Auswertung von NMR-Spektren sowie für die immer gewährte Diskussions- und Gesprächsbereitschaft, die mitunter über das Spektrum der Chemie hinausging.

Herrn Dipl.-Chem. M. Bette, Herrn Dr. C. Wagner, Herrn S. Gómez-Ruiz und Herrn Prof. Dr. K. Merzweiler schulde ich für die Anfertigung von Röntgeneinkristallstrukturanalysen und der immer gewährten Hilfe bei deren Auswertung ebenfalls Dank.

Mein besonderer Dank gilt Herrn Dipl.-Chem. G. Ludwig, der im Rahmen seiner Diplomarbeit mit viel Geduld und Sorgfalt Teile des hier vorgestellten Themas bearbeitet hat und somit zum Gelingen der Arbeit beigetragen hat.

Für die Anfertigung von NMR-Spektren bedanke ich mich bei Herrn Dr. D. Ströhl, Frau R. Flächsenhaar sowie Frau Y. Schiller.

Für die Aufnahme von zahlreichen ESI-Massenspektren möchte ich mich bei Herrn Dr. J. Schmidt bedanken.

Für das sehr angenehme Arbeitsklima und die interessanten Diskussionen und Gespräche, möchte an dieser Stelle bei allen Mitgliedern und ehemaligen Mitgliedern der Arbeitsgruppe um Prof. Dr. Steinborn bedanken. Außerdem danke ich allen Angehörigen des Institutes, die zum Gelingen dieser Arbeit beigetragen haben.

Nicht zuletzt gilt mein besonderer Dank meiner Familie und insbesondere meiner Freundin Stephanie, die mir stets ein Rückhalt waren, Unterstützung geboten haben und viel Verständnis aufgebracht haben. Ohne sie wäre die Anfertigung der Arbeit nicht möglich gewesen.

Lebenslauf

Name	Michael Block
Geburtsdatum	12.04.1981
Geburtsort	Bernburg
Nationalität	deutsch
Familienstand	ledig
Anschrift	Bernhardystraße 26, 06110 Halle

09/2006 – 10/2010	Wissenschaftlicher Mitarbeiter (Promotionsstudium) an der Martin-Luther-Universität Halle-Wittenberg im Arbeitskreis von Prof. Dr. Steinborn
10/2005 – 06/2006	Diplomarbeit: "*Untersuchungen zur regioselektiven Metallierung von O-funktionalisierten Alkylphenylsulfiden und -sulfonen*"
10/2001 – 06/2006	Studium der Chemie an der Martin-Luther Universität Halle-Wittenberg Abschluss: Diplom-Chemiker
06/2000 – 04/2001	Grundwehrdienst
08/1991 – 06/2000	Hermann-Hellriegel-Gymnasium Bernburg Abschluss: Abitur
08/1997 – 06/1998	Morley-Stanwood High School, Morley MI, USA
08/1987 – 06/1991	Grundschule

Eidesstattliche Erklärung

Hiermit erkläre ich an Eides statt, dass ich die vorliegende Arbeit selbstständig und nur unter Verwendung der angegebenen Quellen und Hilfsmittel angefertigt habe.
Diese Arbeit wurde bisher an keiner anderen Universität oder Hochschule vorgelegt.

Halle (Saale), den 12.11.2010

Anhang

Publikationen zur Arbeit

[A] M. Block, C. Wagner, S. Gómez-Ruiz, D. Steinborn, *Dalton Trans*. **2010**, *39*, 4636. (Seite A1)

[B] M. Block, T. Kluge, M. Bette, J. Schmidt, D. Steinborn, *Organometallics* **2010**, *29*, 6749. (Seite A12)

[C] M. Block, M. Bette, C. Wagner, J. Schmidt, D. Steinborn, *J. Organomet. Chem*. im Druck. (Seite A26)

[D] M. Block, M. Bette, C. Wagner, D. Steinborn, *Z. Anorg. Allg. Chem*. im Druck. (Seite A40)

Synthesis, characterization and structures of cyclic organorhodium complexes of the type [Rh{CH(SO_2Ph)$CH_2CH_2YR_2$-κ*C*,κ*Y*}L_2] (YR_2 = PPh_2, NMe_2; L_2 = diphosphine, cyclooctadiene)‡†

Michael Block,[a] Christoph Wagner,[a] Santiago Gómez-Ruiz[b] and Dirk Steinborn*[a]

Received 22nd January 2010, Accepted 25th March 2010
First published as an Advance Article on the web 23rd April 2010
DOI: 10.1039/c001452d

Reactions of dinuclear chloridorhodium(I) complexes [(RhL_2)$_2$(μ-Cl)$_2$] (L_2 = P⌒P: $Me_2P(CH_2)_2PMe_2$, dmpe, **7a**; $Ph_2PCH_2PPh_2$, dppm, **7b**; $Ph_2P(CH_2)_2PPh_2$, dppe, **7c**; $Ph_2P(CH_2)_3PPh_2$, dppp, **7d**; L_2 = cycloocta-1,5-diene, cod, **5**) with lithiated γ-phosphino- and γ-aminofunctionalized propyl phenyl sulfones (Li[CH(SO_2Ph)$CH_2CH_2PPh_2$], **2**; Li[CH(SO_2Ph)$CH_2CH_2NMe_2$], **4**) led to the formation of organorhodium inner complexes of the type [Rh{CH(SO_2Ph)$CH_2CH_2PPh_2$-κ*C*,κ*P*}(P⌒P)] (**8a–d**), [Rh{CH(SO_2Ph)$CH_2CH_2NMe_2$-κ*C*,κ*N*}(P⌒P)] (**9a–d**), [Rh{CH(SO_2Ph)$CH_2CH_2PPh_2$-κ*C*,κ*P*}(cod)]·LiCl (**11**·LiCl) and [Rh{CH(SO_2Ph)$CH_2CH_2NMe_2$-κ*C*,κ*N*}(cod)]·LiCl (**12**·LiCl), respectively. Single-crystal X-ray diffraction analysis of **9c**·THF, **11** and **12** exhibited in all three compounds a distorted square planar coordination of the rhodium atoms having bidentately coordinated neutral co-ligands (cod, **11**, **12**; dppe, **9c**) and anionic α-phenylsulfonyl γ-phosphinopropyl (κ*C*,κ*P*; **11**) and γ-aminopropyl ligands (κ*C*,κ*N*; **12**, **9c**), thus being typical organorhodium inner complexes. Furthermore, organorhodium inner complexes of type **8** were obtained in reactions of the dinuclear chloridobridged rhodium complexes [(RhL_2)$_2$(μ-Cl)$_2$] (L_2 = P⌒P, **7a–d**; cod, **5**; $(C_2H_4)_2$, **6**) with the (non-lithiated) γ-phosphinofunctionalized propyl phenyl sulfone $PhSO_2CH_2CH_2CH_2PPh_2$ (**1**) resulting in the formation of complexes having the sulfone κ*P* coordinated ([$RhClL_2$-($Ph_2PCH_2CH_2CH_2SO_2$Ph-κ*P*)] (L_2 = P⌒P, **10a–d**; cod, **13**; $(C_2H_4)_2$, **14**) which were deprotonated (**10a–d**, **13**) at the α-C atom with lithium diisopropyl amide (LDA) in a subsequent reaction. Single-crystal X-ray diffraction analysis of **10c** (P⌒P = dppe) revealed the expected square-planar coordination geometry of Rh. The identities of all rhodium complexes have been unambiguously proved by microanalyses and NMR spectroscopy (^{1}H, ^{13}C, ^{31}P).

1. Introduction

Metallacycles are cyclic compounds having at least one metal–carbon bond where both the carbon and the metal atom are part of a ring system. In general, they are more stable than their open-chain analogues because hydride elimination reactions are hampered for stereoelectronic reasons. Metallacycles play an important role as model compounds for investigations of organometallic elementary steps.[1,2] Furthermore, they are intermediates in transition metal catalyzed reactions such as oxidative coupling reactions,[3,4] activation of C–H bonds[5–8] and olefin metathesis reactions.[9,10] In 1955, Bähr and Müller described the two complexes [$AlEt_2$($CH_2CH_2CH_2CH_2$OEt-κ*C*,κ*O*)] and [$AlEt_2$($CH_2CH_2CH_2NEt_2$-κ*C*,κ*N*)] and introduced the term "organometallic inner complexes" (also named as organometallic intramolecular-coordination compounds) for metallacycles which are characterized by a M–C bond and a bond of the metal to a neutral Lewis-basic heteroatom group like NR_2, PR_2, OR or SR being also part of the cycle.[11] In 1966 investigations of organotin inner complexes having a coordinated oxygen or nitrogen atom exhibited a very high stability of five-membered metallacycles.[12] Organotransition metal inner complexes were broadly prepared by cyclometallation (especially orthometallation) reactions resulting in five-membered metallacycles in most cases. A prerequisite for such metallations is that the C–H bonds to be activated are brought in close vicinity to the metal centers mostly by pre-coordination of the organic moiety onto a Lewis-basic heteroatom group YR_n.[13] The first report, the synthesis of an *o*-(phenylazo)phenyl nickel complex, dated from 1963.[14]

Generally, such inner complexes are of importance in three types of applications in organic syntheses:[15] the first application is to utilize the ease of synthesis of these compounds and the chelate ring stability. These cyclometallation products are then further used for the synthesis of organic derivatives by manifold reactions such as insertion, substitution or rearrangement – for example carbonylation,[16] alkenylation,[17] acylation[18] or Diels-Alder reactions.[19] If the cyclometallation products are less stable the five-membered ring intermediates easily can react with substrates in substitution reactions which represents the second type of application. Such reactions are regiospecific since

[a]*Institut für Chemie, Martin-Luther-Universität Halle-Wittenberg, Kurt-Mothes-Straße 2, D-06120, Halle, Germany. E-mail: dirk.steinborn@chemie.uni-halle.de*
[b]*Departamento de Química Inorgánica y Analítica, E.S.C.E.T., Universidad Rey Juan Carlos, 28933, Móstoles, Madrid, Spain*

† Electronic supplementary information (ESI) available: Preparation and NMR spectroscopic data of starting materials. CCDC reference numbers 759014–759017. For ESI and crystallographic data in CIF or other electronic format see DOI: 10.1039/c001452d

‡ Dedicated to Professor Uwe Rosenthal on the occasion of his 60th birthday.

they proceed at the metal bound carbon atom and they have been reported on carbonylations,[20] cross-coupling reactions,[21] ring expansions[22] or carbocyclizations.[23] The third kind of application are metal-catalyzed reactions where inner complexes are involved. These reactions include, in organic chemistry widely used, cross-coupling reactions like the Stille, Suzuki or Heck reactions,[24–26] rearrangements,[27] metatheses,[28–30] reductions[31] and other reactions.

We are interested in α-sulfur functionalized propyl ligands having an additional Lewis-basic heteroatom group ($YR_2 = PPh_2$, NMe_2) in γ-position, being favorable for the formation of five-membered MC_3Y cycles. In the case of lithiated γ-functionalized propyl phenyl sulfides of the type [Li{CH(SPh)CH_2-CH_2YR_n}(tmeda)] (YR_n = NMe_2, O*t*-Bu) the formation of organolithium inner complexes by coordination of the YR_n group could be unambiguously proved by single-crystal X-ray diffraction analysis.[32,33] However, lithiated alkyl phenyl sulfones, regardless whether they bear a Lewis-basic heteroatom group YR_n in γ-position or not, are typically dimeric molecules in the solid state having no metal–carbon bonds but "free" α-carbanionic centers[34] and only few examples with a lithium–carbon bond could be structurally characterized.[35–37] Here we report on the formation of five-membered rhodacycles with the general formula [Rh{CH(SO_2Ph)$CH_2CH_2YR_2$-κ*C*,κ*Y*}L_2] ($YR_2 = PPh_2$, NMe_2; L_2 = diphosphine, cyclooctadiene), thus being cyclic organorhodium complexes.

2. Results and discussion

2.1. Synthesis

The reactions of dinuclear diphosphine-chloridorhodium complexes **7a–d** with lithiated γ-phosphino- and γ-aminofunctionalized propyl phenyl sulfones **2** and **4** resulted in the formation of organorhodium inner complexes of the type [Rh{CH(SO_2Ph)-$CH_2CH_2PPh_2$-κ*C*,κ*P*}(P⌒P)] (**8a–d**) and [Rh{CH(SO_2Ph)-$CH_2CH_2NMe_2$-κ*C*,κ*N*}(P⌒P)] (**9a–d**), respectively (Scheme 1). In the sense of one-pot reactions, at first the requisite sulfones $PhSO_2CH_2CH_2CH_2PPh_2$ (**1**) and $PhSO_2CH_2CH_2CH_2NMe_2$ (**3**) were lithiated with *n*-BuLi in toluene followed by the reaction with the rhodium complexes **7a–d** at −78 °C. The same reactions were found to proceed in THF as solvent but difficulties encountered to obtain the complexes free of LiCl in this way. The yellowish to orange air-sensitive complexes **8a–d**/**9a–d** were obtained in yields between 48 and 91%. All complexes were found to decompose in methylene chloride and chloroform at room temperature and, additionally, complex **9d** also in THF.

Another route to obtain the organometallic inner complexes of type **8** were the reactions of the dimeric diphosphine-chloridorhodium complexes **7a–d** with the (non-lithiated) γ-phosphinofunctionalized propyl phenyl sulfone $PhSO_2CH_2CH_2CH_2PPh_2$ (**1**) resulting in the formation of type **10** complexes [RhCl(P⌒P)($Ph_2PCH_2CH_2CH_2SO_2$Ph-κ*P*)] that contain the sulfone in a κ*P* coordination mode (Scheme 1). These chloridorhodium complexes with $PhSO_2CH_2CH_2CH_2PPh_2$-κ*P* ligands were isolated in 65–88% yield and proved to be air-sensitive, too. In contrast to **10a** and **10d**, the complexes **10b** and **10c** were found to be stable in methylene chloride. Type **10** complexes reacted with lithium diisopropylamide (LDA) in toluene/THF under deprotonation neighboured to the sulfur center (α-CH_2 group) of the phosphinofunctionalized sulfone ligand resulting in the formation of the inner complexes **8a–d**. Using MeLi or *n*-BuLi as deprotonating agent led to decomposition which might be caused by the stronger nucleophilic character of these bases. In contrast, the γ-aminofunctionalized sulfone $PhSO_2CH_2CH_2CH_2NMe_2$ (**3**) did not react with type **7** complexes at all (Scheme 1).

As the diphosphine complexes [{Rh(P⌒P)}$_2$(μ-Cl)$_2$] (**7a–d**), the respective cyclooctadiene complex [{Rh(cod)}$_2$(μ-Cl)$_2$] (**5**) was found to react with the lithiated γ-phosphino and γ-aminofunctionalized propyl phenyl sulfones **2** and **4** as well, yielding the organorhodium inner complexes **11** and **12** (Scheme 2). Precipitation from the reaction mixtures (toluene solutions) with *n*-pentane resulted in the formation of the LiCl adducts ([Rh{CH(SO_2Ph)$CH_2CH_2PPh_2$-κ*C*,κ*P*}(cod)]·LiCl, **11**·LiCl; [Rh{CH(SO_2Ph)$CH_2CH_2NMe_2$-κ*C*,κ*N*}(cod)]·LiCl, **12**·LiCl) as yellow powders. Recrystallisation from THF/*n*-pentane and THF, respectively, gave well shaped crystals of complexes **11** and **12** which were shown to be free of LiCl by X-ray diffraction analyses.

The analogous reactions of the ethylene complex [{Rh(C_2H_4)$_2$}$_2$(μ-Cl)$_2$] (**6**) with **2** and **4** led to decomposition. On

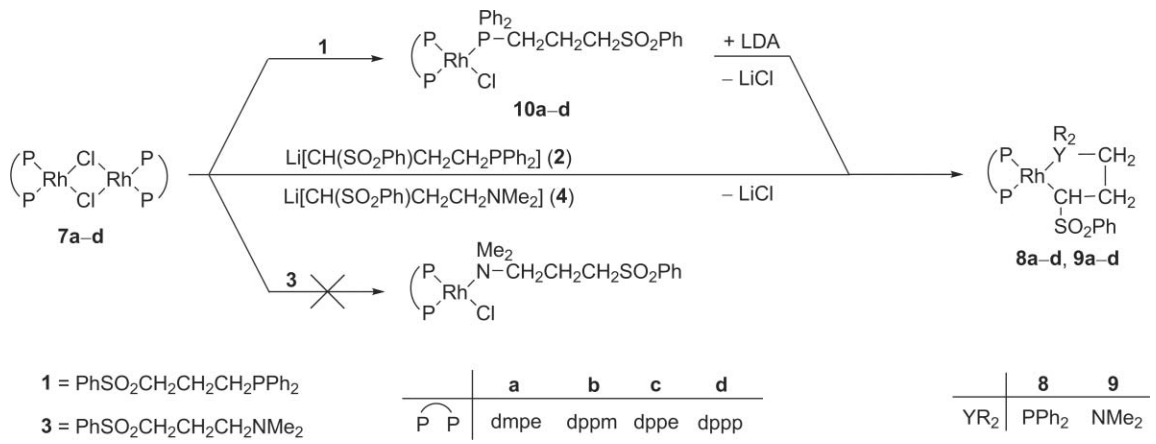

Scheme 1 Synthesis of organorhodium inner complexes **8a–d** and **9a–d**.

Table 1 Selected NMR spectroscopic data (δ in ppm, J in Hz) of [$RhClL_2(Ph_2PCH_2CH_2CH_2SO_2Ph$-κ*P*)] (**10a–d**, **13**, **14**). The values for $PhSO_2CH_2CH_2CH_2PPh_2$ (**1**) are given for comparison

		$PhSO_2C_\alpha H_2–C_\beta H_2–C_\gamma H_2–PPh_2$				Co-ligand L_2	
	L_2	$\delta_{\alpha\text{-}C}$ ($^3J_{P,C}$)	$\delta_{\beta\text{-}C}$ ($^2J_{P,C}$)	$\delta_{\gamma\text{-}C}$ ($^1J_{P,C}$)	δ_P ($^1J_{Rh,P}$)	δ_P ($^1J_{Rh,P}$)[a]	$\delta_{P'}$ ($^1J_{Rh,P'}$)[a]
10a	dmpe	58.2 (10.3)	20.7 (5.2)	27.6 (20.9)	23.7 (133.1)	45.8 (137.7)	43.3 (166.4)
10b	dppm	56.8 (12.7)	19.7 (5.2)	26.3 (22.3)	23.3 (134.2)	–41.5 (118.5)	–15.5 (156.0)
10c	dppe	57.6 (13.6)	20.1 (5.1)	26.9 (22.5)	23.7 (131.6)	58.9 (140.2)	73.9 (184.7)
10d	dppp	58.2 (13.0)	21.3 (7.1)	28.0 (24.0)	25.6 (132.9)	12.9 (132.5)	34.0 (174.9)
13	cod	57.1 (13.8)	20.0 (2.7)	26.6 (25.2)	27.8 (149.2)	—	—
14	$(C_2H_4)_2$	56.7 (14.0)	19.9 (s, br)	27.9 (31.0)	48.7 (186.1)	—	—
1	—	56.7 (13.6)	19.5 (18.8)	26.7 (12.5)	–16.4	—	—

[a] P and P′ are *trans* to P of the $PhSO_2CH_2CH_2CH_2PPh_2$ ligand and Cl, respectively.

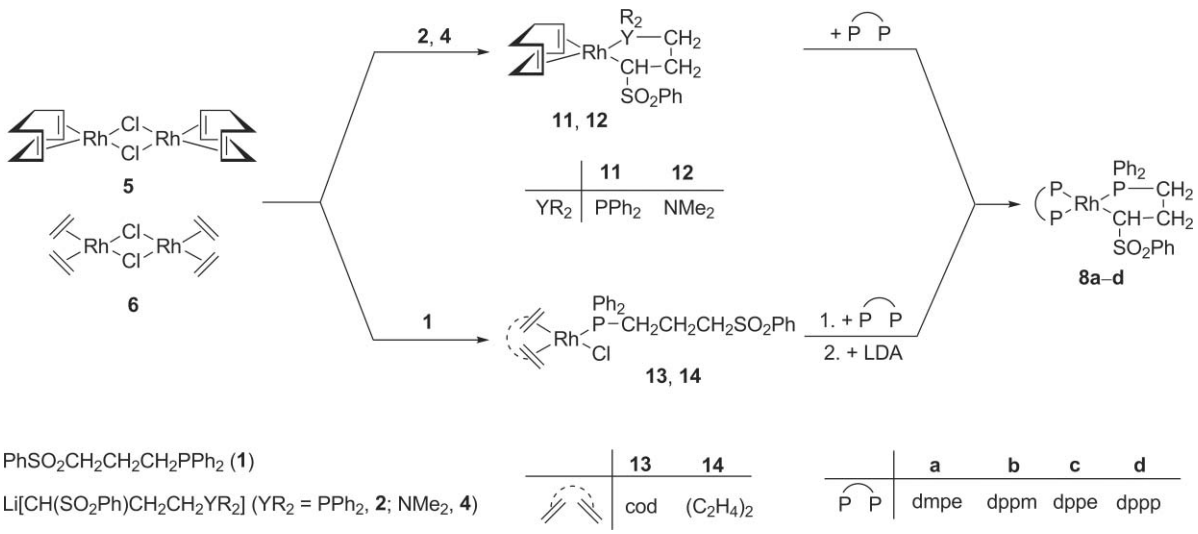

Scheme 2 Synthesis of organorhodium inner complexes **8a–d**, **11**, **12** and chloridorhodium phosphine complexes **13** and **14**.

the other hand, the olefin complexes **5** and **6** reacted with the non-lithiated γ-phosphinofunctionalized propyl phenyl sulfone **1** yielding the chloridorhodium complexes **13** and **14** with $PhSO_2CH_2CH_2CH_2PPh_2$-κ*P* ligands (Scheme 2). As for **7a–d**, neither **5** nor **6** was found to react with the γ-aminofunctionalized propyl phenyl sulfone **3**.

Complexes **11**·LiCl, **12**·LiCl, **13** and **14** were isolated with yields between 66 and 83% as yellow to orange solids. While [RhCl(cod)($Ph_2PCH_2CH_2CH_2SO_2Ph$-κ*P*)] (**13**) was air-stable and stable in chloroform as well as in methylene chloride, the complexes **11**·LiCl, **12**·LiCl and **14** were sensitive against air and moisture and decomposed in halogenated solvents. The identities of all complexes have been confirmed by elemental analyses, NMR (^{1}H, ^{13}C, ^{31}P) spectroscopic investigations and single-crystal X-ray diffraction analyses (**9c**·THF, **10c**, **11**, **12**). Complex **11** could also be obtained by deprotonation of the cyclooctadiene-chloridorhodium complex **13** with LDA. Complexes **11** and **13**/**14** opened up another route for the synthesis of the organorhodium inner complexes **8a–d** *via* ligand substitution (cod by P⌒P) and *via* ligand substitution (cod/C_2H_4 by P⌒P) followed by reaction with LDA, respectively (Scheme 2). Unexpectedly, addition of diphosphines to the γ-aminofunctionalized propyl inner complex [Rh(cod){$CH(SO_2Ph)CH_2CH_2NMe_2$-κ*C*,κ*N*}] (**12**) did not lead to the formation of the respective inner rhodium complexes **9a–d** but to the predominant formation (> 90%) of the cationic bis(diphosphine)rhodium(I) complexes $[Rh(P⌒P)_2]^+$ which have been prepared by an alternative method before.[38,39]

2.2. Spectroscopic characterization

2.2.1. Rhodium complexes with $PhSO_2CH_2CH_2CH_2PPh_2$-κ*P* ligands. Selected NMR spectroscopic parameters of the chloridorhodium complexes with $PhSO_2CH_2CH_2CH_2PPh_2$-κ*P* ligands (**10a–d**, **13** and **14**) are given in Table 1. The ^{31}P NMR spectra of complexes **10b–d** are of first order with an AEMX spin system (A, E, M = ^{31}P; X = ^{103}Rh) whereas that of **10a** is of higher order (ABMX spin system) which was analyzed by using the PERCH software package.[40] Although in **10a** the ^{13}C atoms of the propyl chain are part of a higher order spin systems, simulations with the PERCH software exhibited that they can be treated as first order. In type **10** complexes the differences in the two $^1J_{Rh,P}$ coupling constants of the P⌒P co-ligand between $\Delta J = 12.7$ Hz (**10a**) and $\Delta J = 44.5$ Hz (**10c**) allowed the assignment of the P atoms *trans* to the $PhSO_2CH_2CH_2CH_2PPh_2$ ($^1J_{Rh,P} = 118.5$–141.4 Hz) and *trans* to the chlorido ligand ($^1J_{Rh,P} = 154.1$–184.7 Hz), respectively, as given in Table 1. The κ*P* coordination of the γ-phosphinopropyl phenyl sulfone ligand is clearly shown by the lowfield shift of the ^{31}P nucleus by about 40 ppm for type **10** complexes. The

Table 2 Selected NMR spectroscopic data (δ in ppm, J in Hz) of organorhodium inner complexes [Rh{CH(SO_2Ph)$CH_2CH_2YR_2$-κC,κY}L_2] (**8a–d**, **9a–d**, **11**, **12**). The values for $PhSO_2CH_2CH_2CH_2PPh_2$ (**1**) and $PhSO_2CH_2CH_2CH_2NMe_2$ (**3**) are given for comparison

		$PhSO_2C_\alpha H–C_\beta H_2–C_\gamma H_2–YR_2$				Co-ligand L_2	
	L_2/YR_2	$\delta_{\alpha\text{-}C}$	$\delta_{\beta\text{-}C}$ ($^2J_{P,C}$)	$\delta_{\gamma\text{-}C}$ ($^1J_{P,C}$)	δ_P ($^1J_{Rh,P}$)	δ_P ($^1J_{Rh,P}$)	$\delta_{P'}$ ($^1J_{Rh,P'}$)
8a	dmpe/PPh_2	61.0–61.8 (m)	30.3 (19.5)	36.5 (22.9)	58.0 (144.3)	35.8 (128.8)[a]	35.5 (144.8)[a]
8b	dppm/PPh_2	61.6–62.6 (m)	28.5 (17.3)	34.2 (23.3)	57.9 (154.8)	13.7 (113.5)[a]	–21.0 (133.7)[a]
8c	dppe/PPh_2	61.1–63.0 (m)	29.5 (24.0)	35.0 (22.2)	55.5 (153.1)	59.3 (133.0)[a]	61.1 (155.5)[a]
8d	dppp/PPh_2	66.1–67.0 (m)	29.5 (14.4)	37.5 (23.8)	55.6 (156.0)	16.3 (127.1)[a]	19.5 (150.1)[a]
9a	dmpe/NMe_2	57.0 (9.1/69.2)[b]	30.6	66.3	—	28.3 (148.2)[c]	47.1 (175.9)[c]
9b	dppm/NMe_2	57.1 (7.0/68.8)[b]	30.4	65.8	—	–17.2 (125.0)[c]	–1.7 (165.5)[c]
9c	dppe/NMe_2	60.9 (7.9/67.9)[b]	30.4	66.3	—	58.2 (150.5)[c]	76.0 (188.1)[c]
9d	dppp/NMe_2	61.4 (8.9/67.0)[b]	29.8	66.4	—	14.2 (141.3)[c]	37.8 (187.8)[c]
11	cod/PPh_2	63.0 (4.6)[d]	29.7 (13.3)	33.0 (26.9)	52.0 (172.0)	—	—
12	cod/NMe_2	54.9	30.6	66.5	—	—	—
1	—	56.7 (13.6)[e]	19.5 (18.8)	26.7 (12.5)	–16.4	—	—
3	—	54.0	20.7	57.2	—	—	—

[a] P and P′ are *trans* to *C* and to *P* of the P⌒CHSO_2Ph ligand, respectively. [b] $^2J_{P,C}$ coupling constants to the P atoms (*cis*/*trans*) of the P⌒P co-ligand L_2. [c] P and P′ are *trans* to *C* and to *N* of the $PhSO_2CHCH_2CH_2NMe_2$ ligand, respectively. [d] $^2J_{P,C}$. [e] $^3J_{P,C}$.

$^1J_{Rh,P}$ couplings between 131.6 and 134.2 Hz are typical for phosphorus atoms having another *P* atom in *trans* position.[41–43] The coordination induced shifts of the aliphatic carbon atoms of the $PhSO_2CH_2CH_2CH_2PPh_2$ ligand proved to be small (up to 1.8 ppm) but considerably large for the respective proton shifts (up to 0.68 ppm). The $^1J_{Rh,P}$ couplings in complexes **13** (149.2 Hz) and **14** (186.1 Hz) are as expected for ^{31}P atoms having an olefin ligand in the *trans* position.[44–47] The downfield shift of the ^{31}P nucleus in **14** (δ 48.7 ppm) is even larger than in **10a–d** and **13** (δ 23.3–27.8 ppm) but still in the usual region.[48,49] Compared to [{Rh(cod)}$_2$(μ-Cl)$_2$] (**5**; –CH=CH–: δ_C 78.7 ppm, δ_H 4.18 ppm) and [{Rh(C_2H_4)$_2$}$_2$(μ-Cl)$_2$] (**6**; CH_2=CH_2: δ_C 60.7 ppm, δ_H 3.10 ppm), in the olefin complexes **13** and **14** the olefin carbon atoms and protons are no longer chemically equivalent and were found at δ_C 70.6/105.3 ppm δ_H 2.96/5.40 ppm (**13**) and at δ_C 48.2 (br) ppm δ_H 2.05/2.90 ppm (br/br) (**14**). The broadening of these signals in complex **14** and of the aliphatic protons of the phosphino ligand may indicate molecular dynamics possibly an exchange of the ethylene ligand by solvent molecules (THF).

2.2.2. Organorhodium inner complexes. Selected NMR spectroscopic parameters of the organorhodium inner complexes (**8a–d**, **9a–d**, **11**, **12**) are given in Table 2. The ^{31}P NMR spectra of complexes **8b**, **9a–d** and **11** are of first order with AEMX (A, E, M = ^{31}P; X = ^{103}Rh) (**8b**), AMX (**9a–d**) and AX spin systems (**11**). The ^{31}P nuclei in complexes **8a** and **8d** are part of ABMX spin systems (A, B, M = ^{31}P; X = ^{103}Rh) (Fig. 1) and those of **8c** of an ABCX system (Fig. 2). In complexes **8a–d** the signals of the α-C atoms proved to be of too high multiplicity to be analyzed whereas, as for **10a**, the signals of the β- and γ-C atoms in **8a** and **8d** could be analyzed as first order spectra. For complex **8c** the $^nJ_{P,C}$ coupling constants (n = 1, 2, Table 2) were obtained by simulation the ABCMX spin systems (A, B, C = ^{31}P; M = ^{13}C; X = ^{103}Rh) using the PERCH software. Due to the less multiplicity in complexes **9a–d** all coupling constants were obtained directly from the spectra, among them the $^1J_{Rh,C}$ couplings (25.5–27.1 Hz).

In the organorhodium inner complexes **8a–d** the differences between the two $^1J_{Rh,P}$ coupling constants of the co-ligand P⌒P from ΔJ = 16.0 Hz (**8a**) to ΔJ = 23.0 Hz (**8d**) allowed the assignment of the P atoms *trans* to the P ($^1J_{Rh,P}$ = 133.7–155.5 Hz) and the C atom ($^1J_{Rh,P}$ = 113.5–133.0 Hz) of the P⌒CHSO_2Ph ligand, respectively. In complexes **9a–d** the differences between the two $^1J_{Rh,P}$ coupling constants (ΔJ = 27.7–46.5 Hz) are greater due to the smaller *trans* influence of the NMe_2 compared to the

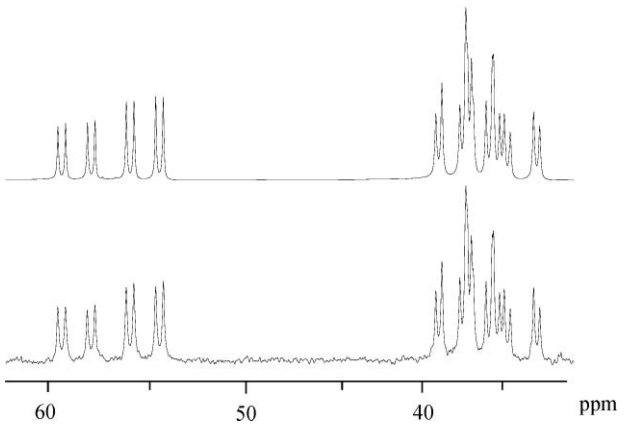

Fig. 1 Simulated (above) and measured (81 MHz, below) ^{31}P NMR spectrum of [Rh{CH(SO_2Ph)$CH_2CH_2PPh_2$-κC,κP}(dmpe)] (**8a**). The ABM part of the ABMX spin system is shown (A, B, M = ^{31}P; X = ^{103}Rh).

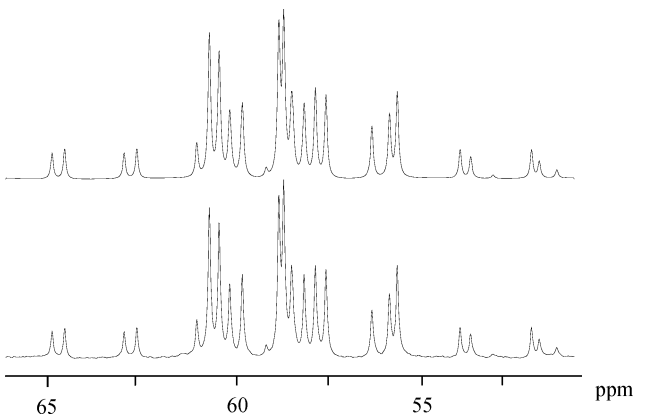

Fig. 2 Simulated (above) and measured (81 MHz, below) ^{31}P NMR spectrum of [Rh{CH(SO_2Ph)$CH_2CH_2PPh_2$-κC,κP}(dppe)] (**8c**). The ABC part of the ABCX (A, B, C = ^{31}P, X = ^{103}Rh) spin system is shown.

PPh_2 group.[50,51] In the case of complexes **8** these assignments were further confirmed by the magnitudes of the $^2J_{P,P}$ coupling constants: the P atoms of the P⌒P ligands *trans* to C have two *cis*-couplings whereas the P′ atoms (*trans* to P of the P⌒$CHSO_2Ph$ ligand) have one *trans*- and one *cis*-coupling. Both, the *cis* ($^2J_{P,P\,cis}$ = 25.8–67.7 Hz) as well as the *trans* coupling constants ($^2J_{P,P\,trans}$ = 310.8–340.5 Hz) are in the expected range[52,53] Deprotonation of **1**/**3** and the κ*C*,κ*P*/κ*C*,κ*N* coordination of the resulting anions to Rh gives rise to lowfield shifts of the α-C atoms by 5–10 ppm and of the P atoms (**8a–d**) by about 70 ppm. The greater *trans* influence of the PPh_2 group in complexes **8a–d** compared to the NMe_2 group in complexes **9a–d** is reflected in markedly smaller (by 31–38 Hz) coupling constants between Rh and the P atom in *trans* position. In the inner complex **11** having a cod co-ligand the $^1J_{Rh,P}$ coupling constant was found to be greater by about 20 Hz compared to **8a–d** reflecting the order of the *trans* influence cod < diphosphines.

2.3. Structural investigations

2.3.1. Structure of [RhCl(dppe)($Ph_2PCH_2CH_2CH_2SO_2Ph$-κ*P*)] (10c). Crystals of **10c** suitable for X-ray diffraction analysis were obtained from THF/*n*-pentane at room temperature. The compound crystallized in isolated monomeric molecules without unusual intermolecular interactions (shortest distance between non-hydrogen atoms: 3.240(5) Å, O2···C46′). The molecular structure is shown in Fig. 3, selected structural parameters are given in the figure caption. The rhodium atom is square-planar coordinated by the two phosphorus atoms of the dppe ligand, by the phosphorus atom of the phosphinofunctionalized sulfone as well as by a chlorido ligand. Due to the bite of the dppe ligand the P1–Rh–P2 angle (85.2(4)°) is slightly diminished. The five-membered rhodacycle (RhP_2C_2) adopts a half-chair conformation, twisted on the two C atoms. The Rh–P3 and Rh–P2 bonds (2.320(1)/2.263(1) Å) are in the expected range for P atoms having another phosphorus atom in *trans* position.[54–56] As expected, the Rh–P1 bond (2.179(1) Å) is shorter than the other two Rh–P bonds due to the smaller *trans* influence of the chlorido ligand.[57–59]

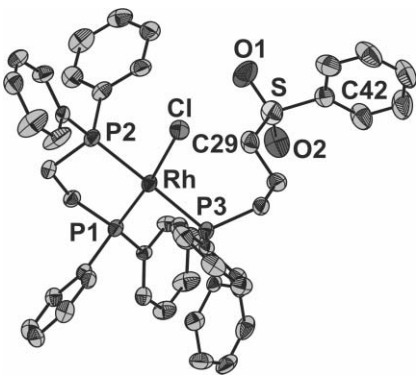

Fig. 3 Molecular structure of [RhCl(dppe)($Ph_2PCH_2CH_2CH_2SO_2Ph$-κ*P*)] in crystals of **10c**. The ellipsoides are shown with a probability of 50%. H atoms have been omitted for clarity. Selected structural parameters (distances in Å, angles in °): Rh–Cl 2.391(1), Rh–P1 2.179(1), Rh–P2 2.263(1), Rh–P3 2.320(1), Cl–Rh–P2 89.0(3), Cl–Rh–P3 89.9(3), P1–Rh–P2 85.2(4), P1–Rh–P3 95.8(3), Cl–Rh–P1 174.1(3), P2–Rh–P3 176.6(4), C29–S–C42 103.9(2), O1–S–O2 118.4(2).

The O1–S–O2 (118.4(2)°) and C29–S–C42 (103.9(2)°) angles were found to be as those in sulfones (median O–S–O: 118.6°, lower/higher quartile: 117.9/119.3° n = 2490; median C–S–C: 105.0°, lower/higher quartile: 103.6/103.4° n = 2490; n–number of observations[60]).

2.3.2. Structures of organorhodium inner complexes. Crystals of [Rh{$CH(SO_2Ph)CH_2CH_2NMe_2$-κ*C*,κ*N*}(dppe)]·THF (**9c**·THF), [Rh{$CH(SO_2Ph)CH_2CH_2PPh_2$-κ*C*,κ*P*}(cod)] (**11**) and [Rh{$CH(SO_2Ph)CH_2CH_2NMe_2$-κ*C*,κ*N*}(cod)] (**12**) suitable for X-ray diffraction analyses were obtained from THF/*n*-pentane (**9c**·THF, **12**) and THF (**11**), respectively, at room temperature. All compounds crystallized in isolated molecules without unusual intermolecular interactions (shortest distance between non-hydrogen atoms: 3.722(7) Å, C19···C4′, **9c**·THF; 3.183(6) Å, O1···C12′, **11**; 3.285(5) Å, C4···C4′, **12**). The molecular structures are shown in Fig. 4–6. Selected structural parameters are given in the figure captions. In all three complexes the rhodium atoms are located in the center of a distorted square planar environment. The primary donor sets of the rhodium atoms are built up by a bidentate neutral ligand (1,5-cyclooctadiene, **11**, **12**; dppe, **9c**·THF) and by a bidentate anionic α-phenylsulfonyl γ-phosphinopropyl (**11**) and γ-aminopropyl ligand (**12**, **9c**·THF) with a κ*C*,κ*P* and a κ*C*,κ*N* coordination, respectively. In all three complexes the five-membered rhodacycles $RhYC_3$ reveal quite small C1–Rh–Y angles (81.3(7)–82.1(1)°) pointing to a relatively small bite of the chelate ligand. While the two nitrogen containing rhodacycles $RhNC_3$ in **9c**·THF and **12** adopt a half-chair configuration twisted on C2 and C3 the metallacycle $RhPC_3$ in **11** adopts an envelope configuration on C3.

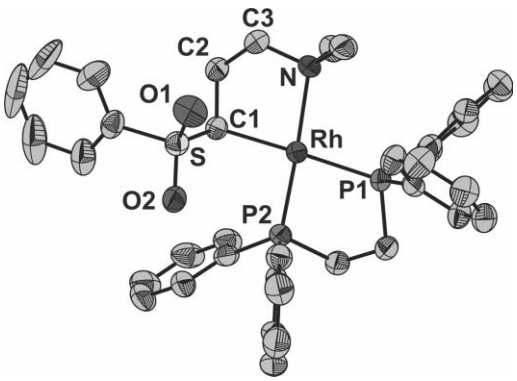

Fig. 4 Molecular structure of [Rh{$CH(SO_2Ph)CH_2CH_2NMe_2$-κ*C*,κ*N*}-(dppe)] in crystals of **9c**·THF. The ellipsoides are shown with a probability of 50%. H atoms have been omitted for clarity. Selected structural parameters (distances in Å, angles in °): Rh–P1 2.258(1), Rh–P2 2.191(1), Rh–C1 2.161(4), Rh–N 2.222(4), P1–Rh–P2 83.5(4), P1–Rh–N 99.8(9), P2–Rh–C1 94.1(1), N–Rh–C1 82.1(1), P1–Rh–C1 175.1(1), P2–Rh–N 172.6(1).

Obviously due to the greater size of the *P* atom (compared to the *N* atom) the Rh–C1 bond in **11** is longer (2.181(3) Å) than in complexes **9c**·THF (2.161(4) Å) and **12** (2.149(3) Å). On the other hand, the Rh–P bond in **11** (2.264(8) Å) is slightly shorter than those in other rhodium(I) complexes with P ligands having an olefin ligand in *trans* and a carbanion in *cis* position (median: 2.298 Å, lower/higher quartile: 2.278/2.325 Å, n = 15[60]). The bidentate binding of the co-ligands L_2 (dppe, **9c**·THF; cod, **11**, **12**)

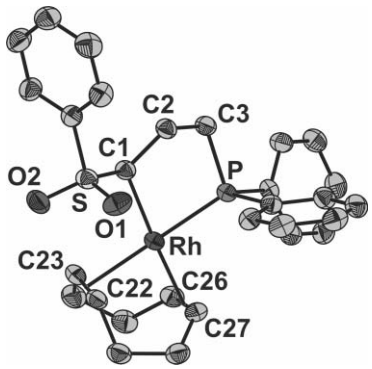

Fig. 5 Molecular structure of [Rh{CH(SO$_2$Ph)CH$_2$CH$_2$PPh$_2$-κ*C*,κ*P*}(cod)] in crystals of **11**. The ellipsoids are shown with a probability of 50%. H atoms have been omitted for clarity. Selected structural parameters (distances in Å, angles in °): Rh–P 2.264(8), Rh–C22/23$_{cg}$ (cg = center of gravity) 2.142(4), Rh–C1 2.181(3), Rh–C26/27$_{cg}$ 2.057(3), P–Rh–C26/27$_{cg}$ 95.3(2), C26/27$_{cg}$–Rh–C22/23$_{cg}$ 85.4(9), P–Rh–C1 81.3(7), C22/23$_{cg}$–Rh–C1 98.1(1), P–Rh–C22/23$_{cg}$ 177.8(2), C1–Rh–C26/27$_{cg}$ 175.4(7).

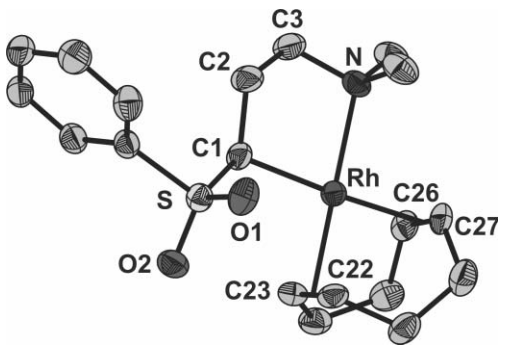

Fig. 6 Molecular structure of [Rh{CH(SO$_2$Ph)CH$_2$CH$_2$NMe$_2$-κ*C*,κ*N*}(cod)] in crystals of **12**. The ellipsoids are shown with a probability of 50%. H atoms have been omitted for clarity. Selected structural parameters (distances in Å, angles in °): Rh–N 2.175(3), Rh–C22/23$_{cg}$ 2.011(2), Rh–C1 2.149(3), Rh–C26/27$_{cg}$ 2.061(2), N–Rh–C26/27$_{cg}$ 94.6(7), C26/27$_{cg}$–Rh–C22/23$_{cg}$ 87.0(9), N–Rh–C1 81.6(1), C22/23$_{cg}$–Rh–C1 97.1(8), N–Rh–C22/23$_{cg}$ 176.5(7), C1–Rh–C26/27$_{cg}$ 174.0(8).

gives rise to slightly diminished P1–Rh–P2 (83.5(4)°, **9c**·THF) and C22/23$_{cg}$–Rh–C26/27$_{cg}$ (85.4(9)°, **11**; 87.0(9)°, **12**; cg = center of gravity) angles. The difference in the Rh–P bond lengths by 0.067 Å in **9c**·THF can be attributed to the difference in the *trans* influence of a neutral N and an anionic C ligand and is in the usual range.[61–63]

2.4 Conclusion

To summarize (Scheme 3), organorhodium inner complexes of the type [Rh{CH(SO$_2$Ph)CH$_2$CH$_2$YR$_2$-κ*C*,κ*Y*}L$_2$] (**III**, **IV**; YR$_2$ = PPh$_2$, NMe$_2$; L$_2$ = P⁀P, cod) were prepared by reactions of lithiated γ-phosphino- and γ-aminofunctionalized propyl phenyl sulfones with the requisite dinuclear complexes [(RhL$_2$)$_2$(μ-Cl)$_2$] (**I** → **III**, **II** → **IV**; Scheme 3). While in the case of the rhodaphosphacyclic complexes cod could be substituted by diphosphines (**III** → **IV**), the respective reactions of the azarhodacyclic complexes resulted with cleavage of both the organo ligands and the cod co-ligand only in the formation of cationic bis(diphosphine) complexes (**III** → **V**). Furthermore, chloridorhodium complexes with neutral PhSO$_2$CH$_2$CH$_2$CH$_2$PPh$_2$-κ*P* ligands were obtained in reactions of [(RhL$_2$)$_2$(μ-Cl)$_2$] (L$_2$ = P⁀P, cod, (C$_2$H$_4$)$_2$) with the phosphinofunctionalized sulfones (**I**/**II** → **VI**) whereas the aminofunctionalized sulfones did not react at all. Syntheses of type **VI** complexes opened up a way to prepare the inner complexes **III**/**IV** by deprotonation the *P* coordinated sulfone with LDA (**VI** → **III**/**IV**).

As shown here (**I**/**II** → **VI**) and as well known from numerous reactions described in literature[64] the cleavage of Rh–Cl–Rh bridges by phosphines proceeds smoothly under formation of phosphine rhodium complexes irrespective of the type of the phosphine. Although analogous reactions of [{Rh(cod)}$_2$(μ-Cl)$_2$] with pyridines, secondary amines and diamines have been described to proceed in most cases either with the formation of type [RhCl(cod)L] or [Rh(cod)L$_2$]$^+$ complexes, the tertiary aliphatic amine NEt$_3$ was found not to react at all.[65] Moreover, in analogous reactions of iminophosphoranes with dinuclear rhodium complexes [(RhL$_2$)$_2$(μ-Cl)$_2$] (L$_2$ = cod, (CO)$_2$) it was shown that the reactivity of these ligands strongly depends on the nucleophilicity of the *N* atom.[66,67] Furthermore, the ease

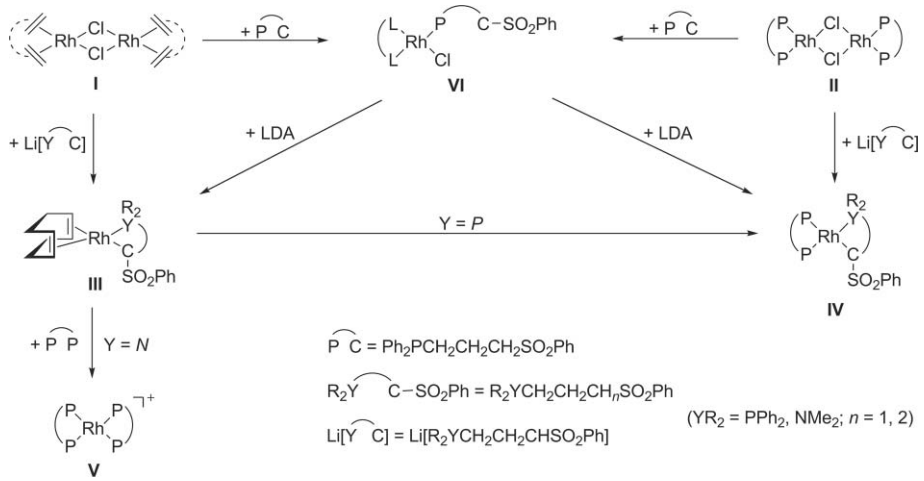

Scheme 3 Different routes to organorhodium inner complexes.

of cleaving Rh–N bonds as found in the reactions **III** → **V** (Scheme 3) was demonstrated on similar complexes by reaction of [RhCl(olefin)(*i*-PrPCH$_2$CH$_2$NMe$_2$-κ*P*,κ*N*)] with CO, C_2H_4 and H_2.[46] On the basis of all these findings the different reactivity of γ-phosphinopropyl and γ-aminopropyl phenyl sulfones towards dinuclear chloridobridged rhodium complexes can be understood. Thus, an easy access to a series of new organorhodium inner complexes bearing α-deprotonated sulfone ligands having an additional *P* or *N* donor site was found.

3. Experimental

3.1. General comments

All reactions and manipulations were carried out under argon using standard Schlenk techniques. Diethyl ether, toluene, *n*-pentane, and THF were dried over Na/benzophenone and freshly distilled prior to use. NMR spectra (^{1}H, ^{7}Li, ^{13}C, ^{31}P) were recorded at 27 °C on Varian Gemini 200, VXR 400, and Unity 500 spectrometers. Chemical shifts are relative to solvent signals ($CDCl_3$, δ_H 7.24, δ_C 77.0; CD_2Cl_2, δ_H 5.32, δ_C 53.8; C_6D_6, δ_H 7.15, δ_C 128.0; THF-d_8, δ_H 1.73/3.58, δ_C 25.4/67.6; CD_3NO_2, δ_H 4.33, δ_C 62.8) as internal references; δ(^{7}Li) is relative to external LiCl (1 M in H_2O); δ(^{31}P) is relative to external H_3PO_4 (85%). Multiplets in NMR spectra of higher order resulting in pseudo doublets and triplets are denoted by "d" and "t", respectively; the distance between the outer lines is given as *N*. Coupling constants $J_{P,P}$ and $J_{P,Rh}$ from higher order multiplets ("m") were obtained by using the PERCH NMR software package.[40] For couplings in ring systems only the shortest coupling path is given. Microanalyses (C, H, N) were performed in the Microanalytical Laboratory of the University of Halle using a CHNS-932 (LECO) as well as a VARIO EL elemental analyzer. [{Rh(cod)}$_2$(μ-Cl)$_2$] (**5**), [{Rh(C_2H_4)$_2$}$_2$(μ-Cl)$_2$] (**6**) and [{Rh(P⌒P)}$_2$(μ-Cl)$_2$] (**7a–d**) were prepared according to literature procedures.[68,45,69] Details of the preparation of starting compounds and a complete set of their NMR spectroscopic data are given in the ESI.† Li[CH(SO$_2$Ph)CH$_2$CH$_2$PPh$_2$] (**2**) and Li[CH(SO$_2$Ph)CH$_2$CH$_2$NMe$_2$] (**4**) were obtained by addition of *n*-BuLi (0.31 ml, 0.50 mmol, 1.6 M in *n*-hexane) at −78 °C to a solution of PhSO$_2$CHCH$_2$CH$_2$YR$_2$ (YR$_2$ = PPh$_2$, **1**; NMe$_2$, **3**; 0.50 mmol) in toluene (5 mL). Compounds **2** and **4** were used as obtained after stirring the reaction mixtures for 4 h at room temperature.

3.2. Preparation of [Rh{CH(SO$_2$Ph)CH$_2$CH$_2$PPh$_2$-κ*C*,κ*P*}(P⌒P)] (8a–d)

Route A. Li[CH(SO$_2$Ph)CH$_2$CH$_2$PPh$_2$] (**2**) (0.50 mmol) dissolved in toluene (5 mL) was added slowly *via* a syringe to a suspension of the respective rhodium complex [{Rh (μ-Cl)(P⌒P)}$_2$] (**7a–d**) (0.25 mmol) in toluene (5 mL) at −78 °C. After warming to room temperature the mixture was stirred overnight and filtered to separate the precipitated LiCl. The filtrate was reduced to half of its volume and *n*-pentane was added (5 mL). The resulted precipitate was filtered, washed with *n*-pentane (3 × 5 mL) and dried *in vacuo*.

Route B:. At −78 °C to a stirred suspension of the respective rhodium complex [{Rh(P⌒P)}$_2$(μ-Cl)$_2$] (**7a–d**) (0.25 mmol) in toluene (5 mL) PhSO$_2$CH$_2$CH$_2$CH$_2$PPh$_2$ (**1**) (184.2 mg, 0.50 mmol) in toluene (5 mL) was added *via* a syringe. Then the reaction mixture was stirred for 1 h at room temperature, cooled to −78 °C again and LDA (0.55 ml, 0.50 mmol, 0.91 M in THF) was slowly added. After warming to room temperature the mixture was stirred for 30 min. The precipitated LiCl was filtered, the filtrate was reduced to half of its volume and *n*-pentane (5 mL) was added. The precipitated compound was filtered, washed with *n*-pentane (3 × 5 mL) and dried *in vacuo*.

Route C. At room temperature to a stirred suspension of [{RhL$_2$}$_2$(μ-Cl)$_2$] (L$_2$ = cod, **5**; (C_2H_4)$_2$, **6**; 0.25 mmol) in toluene (5 mL) PhSO$_2$CH$_2$CH$_2$CH$_2$PPh$_2$ (**1**) (168.2 mg, 0.50 mmol) dissolved in toluene (10 mL) was added slowly. After stirring for 3 h the respective diphosphine P⌒P (0.50 mmol) dissolved in toluene (5 mL) was added. The reaction mixture was stirred for 3 h, at −78 °C LDA (0.55 mL, 0.50 mmol, 0.91 M in THF) was slowly added and stirred for further 30 min at room temperature. The precipitated LiCl was filtered, the filtrate was reduced to half of its volume and *n*-pentane (5 mL) was added. The precipitated compound was filtered, washed with *n*-pentane (3 × 5 mL) and dried *in vacuo*.

P⌒P = dmpe (**8a**). Yield: 229 mg (74%, route A). Found: C, 52.41; H, 5.73; Calcd. for $C_{46}H_{41}P_3SO_2Rh$ (620.48): C, 52.27; H, 5.85. ^{1}H NMR (400 MHz, THF-d_8): δ 0.79/0.91/1.65/1.69 (d/d/d/d, ^2J(^{1}H,^{31}P) = 7.5/7.5/8.3/8.3 Hz, 3H/3H/3H/3H, P(C*H*$_3$)$_2$), 1.18–1.44 (m, 2H, CHC*H*$_2$CH$_2$), 1.35–1.39/1.57–1.82 (m/m, 2H/2H, Me$_2$PC*H*$_2$C*H*$_2$PMe$_2$), 3.55 (s, br, 1H, C*H*SO$_2$Ph), 7.28–7.38 (m, 10H, *m*-, *p*-, *o*-H P*Ph*$_2$), 7.69–7.82 (m, 5H, *m*-, *p*-, *o*-*H* SO$_2$*Ph*). ^{13}C NMR (100 MHz, THF-d_8): δ 15.4/15.7/17.8/18.1 (d/d/d/d, ^1J(^{13}C,^{31}P) = 20.6/19.3/21.8/22.1 Hz, P*C*H$_3$), 30.3 (d, ^2J(^{13}C,^{31}P) = 19.5 Hz, CH*C*H$_2$CH$_2$), 31.5/31.7 ("d"/"d", *N* = 23.1/22.2 Hz Me$_2$P*C*H$_2$*C*H$_2$PMe$_2$), 36.5 (dd, ^1J(^{13}C,^{31}P) = 22.9 Hz, ^3J(^{13}C,^{31}P$_{trans}$) = 7.1 Hz, CHCH$_2$*C*H$_2$), 61.0–61.8 (m, *C*HSO$_2$Ph), 128.3–146.9 (C_{Ar}). ^{31}P NMR (81 MHz, THF-d_8): δ 35.5 (m, ^2J(^{31}P,^{31}P) = 34.9 Hz, ^2J(^{31}P,^{31}P) = 332.9 Hz, ^1J(^{31}P,^{103}Rh) = 144.8 Hz, *P* (dmpe) *trans* to P), 35.8 (m, ^2J(^{31}P,^{31}P) = 34.9 Hz, ^2J(^{31}P,^{31}P) = 29.9 Hz, ^1J(^{31}P,^{103}Rh) = 128.8 Hz, *P* (dmpe) *trans* to *C*), 58.0 (ddd, ^2J(^{31}P,^{31}P) = 29.9 Hz, ^2J(^{31}P,^{31}P) = 332.9, ^1J(^{31}P,^{103}Rh) = 144.3 Hz, CHCH$_2$CH$_2$*P*Ph$_2$).

P⌒P = dppm (**8b**). Yield: 377 mg (88%, route A). Found: C, 64.74; H, 5.09; Calcd for $C_{46}H_{42}P_3SO_2Rh$ (854.73): C, 64.64; H, 4.95. ^{1}H NMR (400 MHz, THF-d_8): δ 1.27–1.36/1.51–1.69 (m/m, 1H/1H, CHC*H*$_2$CH$_2$), 2.11/2.76 (m/m, 1H/1H, CHCH$_2$C*H*$_2$), 3.68 (m, 1H, C*H*SO$_2$Ph), 3.91–3.99/4.29–4.37, (m/m, 1H/1H, Ph$_2$PC*H*$_2$PPh$_2$), 6.94–8.06 (m, 35H, H_{Ar}).

^{13}C NMR (100 MHz, THF-d_8): δ 28.5 (d, ^2J(^{13}C,^{31}P) = 17.3 Hz, CH*C*H$_2$CH$_2$), 34.2 (dd, ^1J(^{13}C,^{31}P) = 23.3 Hz, ^3J(^{13}C,^{31}P$_{trans}$) = 4.7 Hz, CHCH$_2$*C*H$_2$), 48.6 ("t", *N* = 35.2 Hz, Ph$_2$P*C*H$_2$PPh$_2$), 61.6–62.6 (m, *C*HSO$_2$Ph), 125.0–145.2 (m, C_{Ar}). ^{31}P NMR (81 MHz, THF-d_8): δ–21.0 (ddd, ^2J(^{31}P,^{31}P) = 67.7 Hz, ^2J(^{31}P,^{31}P) = 340.5 Hz, ^1J(^{31}P,^{103}Rh) = 133.7 Hz, *P*(dppm) *trans* to P), 13.7 (ddd, ^2J(^{31}P,^{31}P) = 67.7 Hz, ^2J(^{31}P,^{31}P) = 32.1 Hz, ^1J(^{31}P,^{103}Rh) = 113.5 Hz, *P*(dppm) *trans* to *C*), 57.9 (ddd, ^2J(^{31}P,^{31}P) = 32.1 Hz, ^2J(^{31}P,^{31}P) = 340.58, ^1J(^{31}P,^{103}Rh) = 154.8 Hz, CHCH$_2$CH$_2$*P*Ph$_2$).

P⌒P = dppe (**8c**). Yield: 375 mg (86%, route A). Found: C, 64.32; H, 5.20; Calcd. for $C_{47}H_{44}P_3SO_2Rh$ (868.76): C, 64.98; H, 5.10. ^{1}H NMR (400 MHz, THF-d_8): δ 1.13–1.25/1.70–1.84 (m/m, 1H/1H, CHC*H*$_2$CH$_2$), 1.95–2.20/2.36–2.51 (m/m, 2H/2H, Ph$_2$PC*H*$_2$C*H*$_2$PPh$_2$), 2.21–2.30/2.99–3.09

(m/m, 1H/1H, $CHCH_2CH_2PPh_2$), 3.53 (s, br, 1H, $CHSO_2Ph$), 6.89–7.88 (m, 35H, H_{Ar}). ^{13}C NMR (100 MHz, THF-d_8): δ 27.0/30.2 (m/m, $CHCH_2CH_2/Ph_2PCH_2CH_2PPh_2$), 29.5 (d, $^2J(^{13}C,^{31}P)$ = 24.0 Hz, $CHCH_2CH_2$), 35.0 (dd, $^1J(^{13}C,^{31}P)$ = 22.2 Hz, $^3J(^{13}C,^{31}P_{trans})$ = 7.0 Hz, $CHCH_2CH_2$), 61.1–63.0 (m, $CHSO_2Ph$), 127.2–145.6 (C_{Ar}). ^{31}P NMR (81 MHz, THF-d_8): δ 55.5 (m, $^2J(^{31}P,^{31}P)$ = 31.7 Hz, $^2J(^{31}P,^{31}P)$ = 321.8 Hz, $^1J(^{31}P,^{103}Rh)$ = 153.1 Hz, $CHCH_2CH_2PPh_2$), 59.3 (m, $^2J(^{31}P,^{31}P)$ = 28.7 Hz, $^2J(^{31}P,^{31}P)$ = 31.7 Hz, $^1J(^{31}P,^{103}Rh)$ = 133.0 Hz, *P* (dppe) *trans* to *C*), 61.1 (m, $^2J(^{31}P,^{31}P)$ = 28.7 Hz, $^2J(^{31}P,^{31}P)$ = 321.8 $^1J(^{31}P,^{103}Rh)$ = 155.5 Hz, *P* (dppe) *trans* to P).

P⌒P = dppp (**8d**). Yield: 401 mg (91%, route A). Found: C, 65.55; H, 5.01; Calcd. for $C_{48}H_{46}P_3SO_2Rh$ (882.78): C, 65.31; H, 5.25. ^1H NMR (400 MHz, THF-d_8): δ 0.74–0.88/1.62–1.76 (m/m 1H/1H, $CHCH_2CH_2$), 1.21–1.42/2.01–2.09 (m/m, 1H/1H, $Ph_2PCH_2CH_2CH_2PPh_2$), 2.01–2.09/2.93 (m/m 1H/1H, $CHCH_2CH_2$), 2.13–2.25/2.70 (m/m 2H/2H, $Ph_2PCH_2CH_2CH_2PPh_2$), 2.81 (s, br, 1H, $CHSO_2Ph$), 6.55–8.08 (m, H_{Ar}). ^{13}C NMR (125 MHz, THF-d_8): δ 21.5 (s, $Ph_2PCH_2CH_2CH_2PPh_2$), 29.5 (d, $^2J(^{13}C,^{31}P)$ = 14.4 Hz, $CHCH_2CH_2$), 30.0/30.9 ("d"/"d", *N* = 23.6/18.5 Hz, $Ph_2PCH_2CH_2CH_2PPh_2$), 37.5 (dd, $^1J(^{13}C,^{31}P)$ = 23.8 Hz, $^3J(^{13}C,^{31}P_{trans})$ = 5.2 Hz, $CHCH_2CH_2$), 66.1–67.0 (m, $CHSO_2Ph$), 126.4–147.1 (m, C_{Ar}). ^{31}P NMR (81 MHz, THF-d_8): δ 16.3 (m, $^2J(^{31}P,^{31}P)$ = 25.8 Hz , $^2J(^{31}P,^{31}P)$ = 52.1 Hz, $^1J(^{31}P,^{103}Rh)$ = 127.1 Hz, *P* (dppp) *trans* to *C*), 19.5 (m, $^2J(^{31}P,^{31}P)$ = 52.1 Hz, $^2J(^{31}P,^{31}P)$ = 310.8 Hz, $^1J(^{31}P,^{103}Rh)$ = 150.1 Hz, *P* (dppp) *trans* to P), 55.6 (m, $^2J(^{31}P,^{31}P)$ = 25.8 Hz, $^2J(^{31}P,^{31}P)$ = 310.8, $^1J(^{31}P,^{103}Rh)$ = 156.0 Hz, $CHCH_2CH_2PPh_2$).

3.3. Preparation of [Rh{CH(SO_2Ph)$CH_2CH_2NMe_2$-κ*C*,κ*N*}(P⌒P)] (9a–d)

Complexes **9a–d** were obtained as described in 3.2 (route A) but using Li[CH(SO_2Ph)$CH_2CH_2NMe_2$] (**4**) (0.50 mmol) instead of **2**.

P⌒P = dmpe (**9a**). Yield: 114 mg (48%). Found: C, 43.01; H, 6.51; N, 2.92; Calcd. for $C_{17}H_{32}NP_2SO_2Rh$ (479.38): C, 42.60; H, 6.73; N, 2.86. ^1H NMR (400 MHz, THF-d_8): δ 1.31/1.44/1.56/1.62 (d/d/d/d, $^2J(^1H,^{31}P)$ = 6.2/6.3/9.3/9.6 Hz, 3H/3H/3H/3H, $P(CH_3)_2$), 1.50–1.66 (m, 4H, $Me_2PCH_2CH_2PMe_2$), 1.77–1.98 (m, 2H, $CHCH_2CH_2$), 2.14 (m, 2H, CH_2NMe_2), 2.61/2.71 (s/s, 3H/3H, $N(CH_3)_2$), 2.84–2.91 (m, 1H, $CHSO_2Ph$), 7.31–7.40 (m, 3H, *m*-, *p*-*H*, SO_2Ph), 7.74–7.83 2H, *o*-*H*, SO_2Ph). ^{13}C NMR (100 MHz, THF-d_8): δ 16.9–17.6 (m, $((CH_3)_2PCH_2CH_2P(CH_3)_2)$, 29.7–30.2/32.3–31.8 (m/m, $Me_2PCH_2CH_2PMe_2$), 30.6 (s, $CHCH_2CH_2$), 51.8/52.5 (s/s, $N(CH_3)_2$), 57.0 (ddd, $^2J(^{13}C,^{31}P_{cis})$ = 9.1 Hz, $^2J(^{13}C,\ ^{31}P_{trans})$ = 69.2 Hz, $^1J(^{13}C,^{103}Rh)$ = 25.5 Hz, $CHSO_2Ph$), 66.3 (s, CH_2NMe_2), 128.1 (s, *m*-*C*, SO_2Ph), 128.5 (s, *o*-*C*, SO_2Ph), 130.4 (s, *p*-*C*, SO_2Ph), 146.9 (s, *i*-*C*, SO_2Ph). ^{31}P NMR (81 MHz, THF-d_8): δ 28.3 (dd, $^2J(^{31}P,^{31}P)$ = 29.6 Hz, $^1J(^{31}P,^{103}Rh)$ = 148.2 Hz, *P trans* to *C*), 47.1 (dd, $^2J(^{31}P,^{31}P)$ = 29.6 Hz, $^1J(^{31}P,^{103}Rh)$ = 175.9 Hz, *P trans* to N).

P⌒P = dppm (**9b**). Yield: 258 mg (72%). Found: C, 60.69; H, 5.11; N, 2.01; Calcd. for $C_{36}H_{38}NP_2SO_2Rh$ (713.62): C, 60.59; H, 5.37; N, 1.96. ^1H NMR (500 MHz, THF-d_8): δ 1.29–1.45 (m, 2H, $CHCH_2CH_2$), 2.12–2.17/2.90–3.01(m/m, 1H/1H, $CHCH_2CH_2$), 2.23/2.78 (s/s, 3H/3H, $N(CH_3)_2$), 3.07 (m, $CHSO_2Ph$), 3.55–3.63/4.00–4.08 (m/m, 1H/1H, $Ph_2PCH_2PPh_2$), 7.07–8.14 (m, 25H, H_{Ar}). ^{13}C NMR (100 MHz, THF-d_8): δ 30.4 (s, $CHCH_2CH_2$), 51.7–52.2 (m, $Ph_2PCH_2PPh_2/N(CH_3)_2$), 57.1 (ddd, $^2J(^{13}C,^{31}P_{cis})$ = 7.0 Hz, $^2J(^{13}C,^{31}P_{trans})$ = 68.8 Hz, $^1J(^{13}C,^{103}Rh)$ = 27.1 Hz $CHSO_2Ph$), 65.8 (s, CH_2NMe_2), 127.3–146.4 (m, C_{Ar}). ^{31}P NMR (81 MHz, THF-d_8): δ –17.2 (dd, $^2J(^{31}P,^{31}P)$ = 83.7 Hz, $^1J(^{31}P,^{103}Rh)$ = 125.0 Hz, *P trans* to *C*),–1.7 (dd, $^2J(^{31}P,^{31}P)$ = 83.7 Hz, $^1J(^{31}P,^{103}Rh)$ = 165.5 Hz, *P trans* to N).

P⌒P = dppe (**9c**). Yield: 277 mg (76%). Found: C, 61.47; H, 5.54; N, 1.79; Calcd. for $C_{37}H_{40}NP_2SO_2Rh$ (727.66): C, 61.08; H, 5.50; N, 1.92. ^1H NMR (500 MHz, THF-d_8): δ 1.11–1.20/1.25–1.34 (m/m, 1H/1H, $CHCH_2CH_2$), 1.45–1.52/1.83–1.89/2.13–2.22/2.23–2.30 (m/m/m/m, 1H/1H/1H/1H, $Ph_2PCH_2CH_2PPh_2$), 2.10/3.23 (m/m, 1H/1H, $CHCH_2CH_2$), 2.17/2.48 (s/s, 3H/3H, $N(CH_3)_2$), 2.66 (s, br, $CHSO_2Ph$), 7.07–8.18 (m, 25H, H_{Ar}). ^{13}C NMR (100 MHz, THF-d_8): δ 30.2–30.6/34.2–34.8 (m/m, $Ph_2PCH_2CH_2PPh_2$), 30.4 (s, $CHCH_2CH_2$), 51.8/52.6 (s/s, $N(CH_3)_2$), 60.9 (ddd, $^2J(^{13}C,^{31}P_{cis})$ = 7.9 Hz, $^2J(^{13}C,^{31}P_{trans})$ = 67.9 Hz, $^1J(^{13}C,^{103}Rh)$ = 25.5 Hz, $CHSO_2Ph$), 66.3 (s, CH_2NMe_2), 126.1–146.2 (m, C_{Ar}). ^{31}P NMR (81 MHz, THF-d_8): δ 58.2 (dd, $^2J(^{31}P,^{31}P)$ = 30.1 Hz, $^1J(^{31}P,^{103}Rh)$ = 150.5 Hz, *P trans* to *C*), 76.0 (dd, $^2J(^{31}P,^{31}P)$ = 30.1 Hz, $^1J(^{31}P,^{103}Rh)$ = 188.1 Hz, *P trans* to N).

P⌒P = dppp (**9d**). Yield: 270 mg (73%). Found: C, 61.00; H, 5.74; N, 1.91; Calcd. for $C_{38}H_{42}NP_2SO_2Rh$ (741.69): C, 61.55; H, 5.71; N, 1.89. ^1H NMR (500 MHz, benzene-d_6): δ 1.34–1.55 (m, 2H/2H, $Ph_2PCH_2CH_2CH_2PPh_2/CHCH_2CH_2$), 1.79–1.83/1.92–2.02/2.20–2.28 (m/m/m, 1H/2H/1H, $Ph_2PCH_2CH_2CH_2PPh_2$), 2.15 (s, br, 6H, $N(CH_3)_2$), 2.31–2.40/2.60 (m/m, 1H/1H, $CHCH_2CH_2$), 3.20 (s, br, $CHSO_2Ph$), 6.86–8.49 (m, 25H, H_{Ar}). ^{13}C NMR (100 MHz, benzene-d_6): δ 19.4 (s, $Ph_2PCH_2CH_2CH_2PPh_2$), 28.2/28.9 (dd/dd, $^1J(^{13}C,^{31}P)$ = 29.7 Hz, $^2J(^{13}C,^{103}Rh)$ = 10.4 Hz/$^1J(^{13}C,^{31}P)$ = 26.3 Hz, $^2J(^{13}C,^{103}Rh)$ = 10.9 Hz $Ph_2PCH_2CH_2CH_2PPh_2$), 29.8 (s, $CHCH_2CH_2$), 53.85/53.89 (s/s, $N(CH_3)_2$), 61.4 (ddd, $^2J(^{13}C,^{31}P_{cis})$ = 8.9 Hz, $^2J(^{13}C,^{31}P_{trans})$ = 67.0 Hz, $^1J(^{13}C,^{103}Rh)$ = 26.4 Hz $CHSO_2Ph$), 66.4 (s, CH_2NMe_2), 127.0–145.8 (m, C_{Ar}). ^{31}P NMR (81 MHz, benzene-d_6): δ 14.2 (dd, $^2J(^{31}P,^{31}P)$ = 54.4 Hz, $^1J(^{31}P,^{103}Rh)$ = 141.3 Hz, *P trans* to *C*), 37.8 (dd, $^2J(^{31}P,^{31}P)$ = 54.4 Hz, $^1J(^{31}P,^{103}Rh)$ = 187.8 Hz, *P trans* to N).

3.4. Preparation of [RhCl(P⌒P)($Ph_2PCH_2CH_2CH_2SO_2Ph$-κ*P*)] (10a–d)

At room temperature to a stirred suspension of the respective rhodium complex [{Rh(P⌒P)}$_2$(μ-Cl)$_2$] (**7a–d**; 0.25 mmol) in toluene (5 mL) $PhSO_2CH_2CH_2CH_2PPh_2$ (**1**) (184.0 mg, 0.50 mmol) dissolved in toluene (3 mL) was added *via* a syringe and the mixture was stirred for 1 h. The solution was concentrated under reduced pressure to half of its volume before *n*-pentane (5 mL) was added. The resulted precipitate was filtered off, washed with *n*-pentane (3 × 5 mL) and dried *in vacuo*.

P⌒P = dmpe (**10a**). Yield: 212 mg (65%). Found: C 50.90, H, 5.76; Calcd. for $C_{27}H_{37}ClP_3SO_2Rh$ (656.95): C, 49.37; H, 5.68. ^1H NMR (400 MHz, THF-d_8): 0.83/1.47 (d/d, $^2J(^1H,^{31}P)$ = 8.7/9.6 Hz, 6H/6H, $P(CH_3)_2$), 1.28–1.62 (m/m, 2H/2H, $Me_2PCH_2CH_2PMe_2$), 2.10–2.20 (m, 2H, $CH_2CH_2CH_2$), 2.58 (m, 2H, CH_2PPh_2), 3.88 ("t", *N* = 15.4 Hz, 2H, CH_2SO_2Ph), 7.06–7.92 (m, 15H, H_{Ar}). ^{13}C NMR (100 MHz, THF-d_8): 14.5/17.1 (d/d, $^1J(^{13}C,^{31}P)$ = 24.0/24.5 Hz, $P(CH_3)_2$), 20.7 (d, $^2J(^{13}C,^{31}P)$ = 5.2 Hz, $CH_2CH_2CH_2$), 26.0–26.5/34.5–35.2 (m/m,

$Me_2PCH_2CH_2PMe_2$), 27.6 (d, $^1J(^{13}C,^{31}P) = 20.9$ Hz, CH_2PPh_2), 58.2 (d, $^3J(^{13}C,^{31}P) = 10.3$ Hz, CH_2SO_2Ph), 125.9–141.6 (m, C_{Ar}). ^{31}P NMR (81 MHz, THF-d_8): δ 23.8 (m, $^2J(^{31}P,^{31}P) = 6.5$ Hz, $^2J(^{31}P,^{31}P) = 355.1$ Hz, $^1J(^{31}P,^{103}Rh) = 118.0$ Hz, PPh_2), 43.4 (m, $^2J(^{31}P,^{31}P) = 39.1$ Hz, $^2J(^{31}P,^{31}P) = 6.5$ Hz, $^1J(^{31}P,^{103}Rh) = 154.1$ Hz, *P* (dmpe) *trans* to *Cl*), 45.8 (m, $^2J(^{31}P,^{31}P) = 39.1$ Hz, $^2J(^{31}P,^{31}P) = 355.1$ Hz, $^1J(^{31}P,^{103}Rh) = 141.4$ Hz, *P* (dmpe) *trans* to P).

P⌒P = dppm (**10b**). Yield: 336 mg (75%). Found: C, 61.55; H, 4.83; Calcd. for $C_{46}H_{42}ClO_2P_3SRh$ (890.19): C, 62.07; H, 4.76. ^1H NMR (400 MHz, THF-d_8): δ 2.10 (m, 2H, $CH_2CH_2CH_2$), 2.37 (m, 2H, $CH_2CH_2CH_2PPh_2$), 3.36 ("t", $N = 15.0$ Hz, 2H, CH_2SO_2Ph), 3.93 ("t", $N = 19.4$ Hz, 2H, $PPh_2CH_2PPh_2$), 6.99–8.03 (m, 35H, H_{Ar}). ^{13}C NMR (100 MHz, THF-d_8): δ 19.7 (d, $^2J(^{13}C,^{31}P) = 5.2$ Hz, $CH_2CH_2CH_2$), 26.3 (d, $^1J(^{13}C,^{31}P) = 22.3$ Hz, $CH_2CH_2CH_2PPh_2$), 49.4 ("t", $N = 42.6$ Hz, $PPh_2CH_2PPh_2$), 56.8 (d, $^3J(^{13}C,^{31}P) = 12.7$ Hz, CH_2SO_2Ph), 127.9 (s, *m*-*C*, SO_2Ph), 128.0 (s, *p*-*C*, SO_2Ph), 128.8 (s, *o*-*C*, SO_2Ph), 140.5 (s, *i*-*C*, SO_2Ph), 127.3–136.5 (C_{Ar}). ^{31}P NMR (81 MHz, THF-d_8): δ –41.5 (ddd, $^2J(^{31}P,^{31}P) = 98.4$ Hz, $^2J(^{31}P,^{31}P) = 386.0$ Hz, $^1J(^{31}P,^{103}Rh) = 118.5$ Hz, *P* (dppm) *trans* to P), –15.5 (ddd, $^2J(^{31}P,^{31}P) = 32.1$ Hz, $^2J(^{31}P,^{31}P) = 98.4$ Hz, $^1J(^{31}P,^{103}Rh) = 156.0$ Hz, *P* (dppm) *trans* to *Cl*), 23.3 (ddd, $^2J(^{31}P,^{31}P) = 32.1$ Hz, $^2J(^{31}P,^{31}P) = 386.0$ Hz, $^1J(^{31}P,^{103}Rh) = 134.2$ Hz, $CH_2CH_2CH_2PPh_2$).

P⌒P = dppe (**10c**). Yield: 396 mg (88%). Found: C, 61.66; H, 5.11; Calcd. for $C_{47}H_{44}ClO_2P_3SRh$ (904.21): C, 62.43; H, 4.90. ^1H NMR (400 MHz, CD_2Cl_2): δ 1.77–1.89 (m, 2H, $CH_2CH_2CH_2$), 1.97–2.13 (m/m, 2H/2H, $PPh_2CH_2CH_2PPh_2$), 2.16–2.22 (m, 2H, $CH_2CH_2CH_2PPh_2$), 3.16 ("t", $N = 14.8$ Hz, 2H, CH_2SO_2Ph), 6.88–8.01 (m, 35H, H_{Ar})

^{13}C NMR (100 MHz, CD_2Cl_2): δ 20.1 (d, $^2J(^{13}C,^{31}P) = 5.1$ Hz, $CH_2CH_2CH_2$), 26.3/35.4 (m/m, $Ph_2PCH_2CH_2PPh_2$), 26.9 (d, $^1J(^{13}C,^{31}P) = 22.5$ Hz, $CH_2CH_2CH_2PPh_2$), 57.6 (d, $^3J(^{13}C,^{31}P) = 13.6$ Hz, CH_2SO_2Ph), 128.2 (s, *m*-*C*, SO_2Ph), 129.5 (s, *p*-*C*, SO_2Ph), 133.7 (s, *o*-*C*, SO_2Ph), 139.9 (s, *i*-*C*, SO_2Ph), 127.9–136.1 (C_{Ar}). ^{31}P NMR (81 MHz, THF-d_8): δ 23.7 (ddd, $^2J(^{31}P,^{31}P) = 35.6$ Hz, $^2J(^{31}P,^{31}P) = 351.5$ Hz, $^1J(^{31}P,^{103}Rh) = 131.6$ Hz, $CH_2CH_2CH_2PPh_2$), 58.9 (ddd, $^2J(^{31}P,^{31}P) = 33.4$ Hz, $^2J(^{31}P,^{31}P) = 351.5$ Hz, $^1J(^{31}P,^{103}Rh) = 140.2$ Hz, *P* (dppe) *trans* to P), 73.9 (ddd, $^2J(^{31}P,^{31}P) = 33.4$ Hz, $^2J(^{31}P,^{31}P) = 35.6$ Hz, $^1J(^{31}P,^{103}Rh) = 184.7$ Hz, *P* (dppe) *trans* to *Cl*).

P⌒P = dppp (**10d**). Yield: 382 mg (83%). Found: C, 61.77; H, 5.15; Calcd. for $C_{48}H_{47}ClO_2P_3SRh$ (919.25): C, 62.72; H, 5.15. ^1H NMR (400 MHz, THF-d_8): δ 1.64–1.79 (m, 2H, $PhSO_2CH_2CH_2CH_2PPh_2$), 2.11 (s, br, 2H/2H, $PhSO_2CH_2CH_2CH_2PPh_2/Ph_2PCH_2CH_2CH_2PPh_2$), 2.24 (s, br, 2H/2H, $Ph_2PCH_2CH_2CH_2PPh_2$), 3.49 ("t", $N = 14.2$ Hz, 2H, CH_2SO_2Ph), 6.82–7.94 (m, 35H, H_{Ar}). ^{13}C NMR (125 MHz, THF-d_8): δ 20.4 (s, $Ph_2PCH_2CH_2CH_2PPh_2$), 21.3 (d, $^2J(^{13}C,^{31}P) = 7.1$ Hz, $PhSO_2CH_2CH_2CH_2PPh_2$), 27.6–27.97/32.7 (m/m, $Ph_2PCH_2CH_2CH_2PPh_2$), 27.98 (d, $^1J(^{13}C,^{31}P) = 24.0$ Hz, $PhSO_2CH_2CH_2CH_2PPh_2$), 58.2 (d, $^3J(^{13}C,^{31}P) = 13.0$ Hz, CH_2SO_2Ph), 127.8–141.7 (C_{Ar}). ^{31}P NMR (81 MHz, THF-d_8): δ 12.9 (ddd, $^2J(^{31}P,^{31}P) = 56.4$ Hz, $^2J(^{31}P,^{31}P) = 349.0$ Hz, $^1J(^{31}P,^{103}Rh) = 132.5$ Hz, *P* (dppp) *trans* to P), 25.6 (ddd, $^2J(^{31}P,^{31}P) = 35.7$ Hz, $^2J(^{31}P,^{31}P) = 349.0$ Hz, $^1J(^{31}P,^{103}Rh) = 132.9$ Hz, 1P, $PhSO_2CH_2CH_2CH_2PPh_2$), 34.0 (ddd, $^2J(^{31}P,^{31}P) = 56.4$ Hz, $^2J(^{31}P,^{31}P) = 35.7$ Hz, $^1J(^{31}P,^{103}Rh) = 174.9$ Hz, *P* (dppp) *trans* to *Cl*).

3.5. Preparation of [Rh{CH(SO$_2$Ph)CH$_2$CH$_2$PPh$_2$-κ*C*,κ*P*}(cod)]·LiCl (11·LiCl)

Complex **11**·LiCl was obtained as described in 3.2 (route A) but using [{Rh(cod)}$_2$(μ-Cl)$_2$] (**5**) (123.3 mg, 0.25 mmol) instead of **7a–d**. Yield: 245 mg (79%).

Found: C, 56.72; H, 5.42; Calcd. for $C_{29}H_{32}PLiClSO_2Rh$ (620.91): C, 56.10; H, 5.19. ^1H NMR (400 MHz, THF-d_8): δ 1.87–2.60 (m, 8H/2H/2H, 4 × CH_2 (cod)/$CHCH_2CH_2/CH_2PPh_2$), 3.08/4.00/5.93/6.24 (m/m/m/m, 1H/1H/1H/1H, 4 × *C*H (cod)), 3.51 (m, 1H, $CHSO_2Ph$), 7.35–7.77 (m, 15H, H_{Ar}). ^{13}C NMR (100 MHz, THF-d_8): δ 29.4/29.9/32.6/33.4 (s/s/s/s, 4 × CH_2 (cod)), 29.7 (d, $^2J(^{13}C,^{31}P) = 13.3$ Hz, $CHCH_2CH_2$), 33.0 (d, $^1J(^{13}C,^{31}P) = 26.9$ Hz, CH_2PPh_2), 63.0 (dd, $^2J(^{13}C,^{31}P) = 4.6$ Hz, $^1J(^{13}C,^{103}Rh) = 29.1$ Hz, $CHSO_2Ph$), 80.1/80.9/100.3/100.8 (d/d/"t"/dd, $^1J(^{13}C,^{103}Rh) = 9.2$ Hz/$^1J(^{13}C,^{103}Rh) = 8.3$ Hz/$N = 16.6$ Hz/$^1J(^{13}C,^{103}Rh) = 12.0$ Hz, $^2J(^{13}C,^{31}P) = 6.7$ Hz, 4 × *C*H (cod)), 128.1–135.5 (C_{Ar}). ^{31}P NMR (80 MHz, THF-d_8): δ 52.0 (d, $^1J(^{31}P,^{103}Rh) = 172.0$ Hz, PPh_2). ^7Li NMR (194 MHz, THF-d_8): δ 0.23 (s, *Li*Cl).

3.6. Preparation of [Rh{CH(SO$_2$Ph)CH$_2$CH$_2$NMe$_2$-κ*C*,κ*N*}(cod)]·LiCl (12·LiCl)

Complex **12**·LiCl was obtained as described in 3.2 (route A) but using Li[CH(SO$_2$Ph)CH$_2$CH$_2$NMe$_2$] (**4**) (0.50 mmol) and [{Rh(cod)}$_2$(μ-Cl)$_2$] (**5**) (123.3 mg, 0.25 mmol) instead of **2** and **7a–d**, respectively. Yield: 159 mg (66%).

Found: C, 47.83; H, 6.00; N, 2.96. Calcd. for $C_{19}H_{28}NSO_2LiClRh$ (479.80): C, 47.56; H, 5.88; N, 2.92. ^1H NMR (400 MHz, THF-d_8): δ 1.01–1.09/1.39–1.50/1.98–2.63 (m/m/m, 1H/1H/6H/2H, 4×CH_2 (cod)/CH_2PPh_2), 1.55–1.65 (m, 2H, $CHCH_2CH_2$), 2.74 (d"t", $^2J(^1H,^{103}Rh) = 2.5$ Hz/$N = 5.4$ Hz, 1H, $CHSO_2Ph$), 3.81/3.90/4.64/5.21 (m/m/m/m, 1H/1H/1H/1H, 4 × *C*H (cod)), 7.35–7.77 (m, 15H, H_{Ar}). ^{13}C NMR (100 MHz, THF-d_8): δ 28.74/29.7/31.6/34.1 (s/s/s/s, 4 × CH_2 (cod)), 30.6 (s, $CHCH_2CH_2$), 45.5/49.8 (s/s, $N(CH_3)_2$), 54.9 (d, $^1J(^{13}C,^{103}Rh) = 30.4$ Hz, $CHSO_2Ph$), 66.5 (s, CH_2NMe_2), 76.5/76.6/85.3/86.4 (d/d/d/dd, $^1J(^{13}C,^{103}Rh) = 7.9$ Hz/$^1J(^{13}C,^{103}Rh) = 7.8$ Hz/$^1J(^{13}C,^{103}Rh) = 10.1$ Hz/$^1J(^{13}C,^{103}Rh) = 9.2$ Hz, 4 × *C*H (cod)), 128.1 (s, *m*-*C*, SO_2Ph), 128.7 (s, *o*-*C*, SO_2Ph), 131.0 (s, *p*-*C*, SO_2Ph), 146.0 (s, *i*-*C*, SO_2Ph). ^7Li NMR (194 MHz, THF-d_8): δ 0.23 (s, *Li*Cl).

3.7. Preaparation of [RhCl(cod)(Ph$_2$PCH$_2$CH$_2$CH$_2$SO$_2$Ph-κ*P*)] (13)

Complex **13** was obtained as described in 3.4 but using [{Rh(cod)}$_2$(μ-Cl)$_2$] (**5**) (246.5 mg, 0.50 mmol) instead of **7a–d**. Yield: 511 mg (83%).

Found: C, 56.41; H, 5.97; Calcd. for $C_{29}H_{33}PClSO_2Rh$ (614.98): C, 56.65; H, 5.41. ^1H NMR (400 MHz, $CDCl_3$): δ 1.86/2.01/2.23–2.44 (m/m/m, 2H/2H/6H, $CH_2CH_2CH_2$ + 4 × CH_2 (cod)), 2.57 (m, 2H, CH_2PPh_2), 2.96/5.40 (s/s, br/br, 2H/2H, 4 × *C*H (cod)), 3.33 (m, 2H, CH_2SO_2Ph), 7.33–7.89 (m, 15H, H_{Ar}). ^{13}C NMR (100 MHz, $CDCl_3$): δ 20.0 (d, $^2J(^{13}C,^{31}P) = 2.7$ Hz, $CH_2CH_2CH_2$), 26.6 (d, $^1J(^{13}C,^{31}P) = 25.2$ Hz, CH_2PPh_2), 28.72/28.73/32.9/33.0 (s/s/s/s, 4 × CH_2 (cod)), 57.1 (d, $^3J(^{13}C,^{31}P) = 13.8$ Hz, CH_2SO_2Ph), 70.6/105.3 (d/dd, $^1J(^{13}C,^{103}Rh) = 13.8$ Hz/$^1J(^{13}C,^{103}Rh) = 12.2$ Hz,

Table 3 Crystallographic data, data collection parameters, and refinement parameters for **9c**·THF, **10c**, **11**, and **12**

	9c·THF	**10c**	**11**	**12**
Empirical formula	$C_{37}H_{40}NO_2P_2RhS{\cdot}C_4H_8O$	$C_{47}H_{45}ClO_2P_3RhS$	$C_{29}H_{32}O_2PRhS$	$C_{19}H_{28}NO_2RhS$
M_r	799.71	905.16	578.49	437.39
Crystal System	Orthorhombic	Monoclinic	Triclinic	Orthorhombic
Space group	*Fdd*2	$P2_1/c$	$P\bar{1}$	*Pbca*
a/Å	30.109(3)	21.349(5)	9.3705(9)	12.2943(9)
b/Å	41.095(4)	16.099(5)	12.1565(11)	17.1678(16)
c/Å	12.580(3)	12.008(5)	12.6514(13)	17.2075(14)
α/°			63.954(7)	
β/°		94.237(5)	78.562(8)	
γ/°			77.146(7)	
V/Å^3	15565(4)	4116(2)	1254.0(2)	3631.9(5)
Z	16	4	2	8
D_c/g cm^{-1}	1.365	1.461	1.532	1.600
μ(Mo-Kα)/mm^{-1}	0.613	0.686	0.853	1.067
F(000)	6656	1864	596	1808
θ range/°	1.5–30.0	2.71–25.19	2.61–29.17	2.36–27.50
Rfln. collected	33 320	65 301	17 184	32 256
Refln. observed [$I > 2\sigma(I)$]	7229	3462	6075	3330
Rfln. independent	7652 ($R_{int} = 0.0665$)	7399 ($R_{int} = 0.1424$)	6724 ($R_{int} = 0.0322$)	4144 ($R_{int} = 0.0593$)
Data/restraints/parameters	7652/1/444	7399/0/496	6724/0/436	4144/0/330
Goodness-of-fit on F^2	1.126	0.7	1.110	1.025
R_1	0.0390	0.0325	0.0443	0.0392
wR_2 [$I > 2\sigma(I)$]	0.0837	0.0353	0.1188	0.0939
R_1	0.0428	0.1089	0.0488	0.0524
wR_2 (all data)	0.0854	0.0403	0.1215	0.1000
Largest diff. peak and hole/e Å^{-3}	0.597 and –0.431	0.409 and –0.563	0.825 and –1.112	0.709 and –0.830

$^2J(^{13}C,^{31}P) = 7.0$ Hz, 4 × *C*H (cod)), 127.9–137.2 (C_{Ar}). ^{31}P NMR (80 MHz, $CDCl_3$): *δ* 27.8 (d, $^1J(^{31}P, ^{103}Rh) = 149.2$ Hz, *P*Ph_2).

3.8. Preparation of [RhCl(C_2H_4)$_2$($Ph_2PCH_2CH_2CH_2SO_2Ph$-κ*P*)] (14)

Complex **14** was obtained as described in 3.4 but using [{Rh(C_2H_4)$_2$}$_2$(μ-Cl)$_2$] (**6**) (194.5 mg, 0.50 mmol) instead of **7a–d** and using thf instead of toluene as solvent. Yield: 405 mg (72%). Found: C, 53.08; H, 5.25; Calcd. for $C_{25}H_{29}PClSO_2Rh$ (562.90): C, 53.34; H, 5.19. ^1H NMR (400 MHz, THF-d_8): *δ* 2.05/2.90 (s/s, br/br 4H/4H, 4 × =C*H*$_2$), 2.57 (m, 2H, C*H*$_2$PPh_2), 2.27 (s, br, 2H, $CH_2CH_2CH_2$), 2.42 (s, br, 2H, C*H*$_2$PPh_2), 3.27 (s, br, 2H, C*H*$_2$$SO_2Ph$), 7.35–7.87 (m, 15H, H_{Ar}). ^{13}C NMR (100 MHz, THF-d_8): *δ* 20.9 (s, br, $CH_2CH_2CH_2$), 28.2 (d, $^1J(^{13}C,^{31}P) = 29.4$ Hz, *C*H$_2$PPh_2), 48.2 (s, br, 4 × =*C*H$_2$), 57.3 (d, $^3J(^{13}C,^{31}P) = 14.2$ Hz, *C*H$_2$$SO_2Ph$), 128.8–414.2 ($C_{Ar}$). ^{31}P NMR (80 MHz, THF-d_8): *δ* 48.7 (d, br, $^1J(^{31}P, ^{103}Rh) = 186.1$ Hz, *P*Ph_2).

3.9. X-Ray crystallography

Data for X-ray diffraction analyses of single crystals of **9c**·THF, **11** and **12** were collected on a Stoe-IPDS 2T diffractometer at 200(2) K and of **10c** at 130(2) K on a CCD Oxford Xcalibur S diffractometer using Mo-Kα radiation (*λ* = 0.7103 Å, graphite monochromator). A summary of the crystallographic data, the data collection parameters, and the refinement parameters is given in Table 3. Absorption corrections were applied numerically with X-RED32[70] (T_{min}/T_{max} 0.90/0.93, **11**; 0.84/0.95, **12**) and multi-scanning with SCALE3 ABSPACK[71] (T_{min}/T_{max} 0.90/1.00, **10c**), respectively. The structures were solved with direct methods using SHELXS-97[72] and refined using full-matrix least-square routines against F^2 with SHELXL-97.[73] All non-hydrogen atoms were refined with anisotropic displacement parameters and hydrogen atoms with isotropic ones. The positions of H atoms in **11** and **12** were found in the difference Fourier map and refined freely. H atoms in **9c** and **10c** were placed in calculated positions according to the riding model.

References

1 C. Elschenbroich and A. Salzer, *Organometallics*, 2nd edn, Wiley-VCH, Weinheim, 2003.
2 D. Steinborn, *Grundlagen der metallorganischen Komplexkatalyse*, 2nd edn, Vieweg + Teubner, Wiesbaden 2010.
3 T. Satoh, K. Ueura and M. Miura, *Pure Appl. Chem.*, 2008, **80**, 1127.
4 K. V. L. Crépy and T. Imamoto, *Org. Synth.*, 2005, **82**, 22.
5 L. Li, W. W. Brennessel and W. D. Jones, *Organometallics*, 2009, **28**, 3492.
6 A. S. Tsai, R. M. Wilson, H. Harada, R. G. Bergman and J. A. Ellman, *Chem. Commun.*, 2009, 3910.
7 H. Harada, R. K. Thalji, R. G. Bergman and J. A. Ellman, *J. Org. Chem.*, 2008, **73**, 6772.
8 S. S. Stahl, J. A. Labinger and J. E. Bercaw, *Angew. Chem., Int. Ed.*, 1998, **37**, 2180.
9 R. R. Schrock, J. H. Freudenberger, M. L. Listemann and L. G. McCullough, *J. Mol. Catal.*, 1985, **28**, 1.
10 A. H. Hoveyda and R. R. Schrock, *Chem.–Eur. J.*, 2001, **7**, 945.
11 G. Bähr and G. E. Müller, *Chem. Ber.*, 1955, **88**, 251.
12 S. Matsuda, S. Kikkawa and I. Omae, *Kogyo Kagaku Zasshi*, 1966, **69**, 646.
13 A. D. Ryabov, *Chem. Rev.*, 1990, **90**, 403.
14 J. P. Kleiman and M. Dubeck, *J. Am. Chem. Soc.*, 1963, **85**, 1544.
15 I. Omae, *J. Organomet. Chem.*, 2007, **692**, 2608.
16 J. M. Thompson and R. F. Heck, *J. Org. Chem.*, 1975, **40**, 2667.
17 R. A. Holton, *Tetrahedron Lett.*, 1977, **18**, 355.
18 R. A. Holton and K. J. Natalie, Jr., *Tetrahedron Lett.*, 1981, **22**, 267.
19 W.-C. Yeo, J. J. Vittal, L. L. Koh, G.-K. Tan and P.-H. Leung, *Organometallics*, 2004, **23**, 3474.

20 H.-F. Klein, M. Helwig, U. Koch, U. Flörke and H.-J. Haupt, *Z. Naturforsch.*, 1993, **48b**, 778.
21 F. Kakiuchi, M. Matsumoto, K. Tsuchiya, K. Igi, T. Hayamizu, N. Chatani and S. Murai, *J. Organomet. Chem.*, 2003, **686**, 134.
22 R. F. Jordan and D. F. Taylor, *J. Am. Chem. Soc.*, 1989, **111**, 778.
23 K.-J. Chang, D. K. Rayabarapu and C.-H. Cheng, *Org. Lett.*, 2003, **5**, 3963.
24 J. K. Stille, *Angew. Chem., Int. Ed. Engl.*, 1986, **25**, 508.
25 N. Miyaura and A. Suzuki, *Chem. Rev.*, 1995, **95**, 2457.
26 W. A. Herrmann, V. P. W. Böhm and C.-P. Reisinger, *J. Organomet. Chem.*, 1999, **576**, 23.
27 T. K. Hollis and L. E. Overman, *J. Organomet. Chem.*, 1999, **576**, 290.
28 Q. Yao and Y. Zhang, *Angew. Chem., Int. Ed.*, 2003, **42**, 3395.
29 H. Clavier, N. Audic, J.-C. Guillemin and M. Mauduit, *J. Organomet. Chem.*, 2005, **690**, 3585.
30 M. Arisawa, Y. Terada, C. Theeraladanon, K. Takahashi, M. Nakagawa and A. Nishida, *J. Organomet. Chem.*, 2005, **690**, 5398.
31 W. Baratta, P. Da Ros, A. Del Zotto, A. Sechi, E. Zangrando and P. Rigo, *Angew. Chem., Int. Ed.*, 2004, **43**, 3584.
32 M. Linnert, C. Bruhn, C. Wagner, M. Block, T. Rüffer, H. Schmidt and D. Steinborn, *Advances in Coordination, Bioinorganic and Inorganic Chemistry*, ed. M. Melnik, J. Sima and M. Tatarko, STU Press, Bratislava, 2005, 170.
33 M. Block, M. Linnert, S. Gómez-Ruiz and D. Steinborn, *J. Organomet. Chem.*, 2009, **694**, 3353.
34 H. J. Gais, G. Hellmann, H. Günther, F. Lopez, H. J. Lindner and S. Braun, *Angew. Chem., Int. Ed. Engl.*, 1989, **28**, 1025.
35 W. Hollstein, K. Harms, M. Marsch and G. Boche, *Angew. Chem., Int. Ed. Engl.*, 1988, **27**, 846.
36 M. Linnert, C. Bruhn, C. Wagner and D. Steinborn, *J. Organomet. Chem.*, 2006, **691**, 2358.
37 M. Linnert, C. Wagner, K. Merzweiler and D. Steinborn, *Z. Anorg. Allg. Chem.*, 2008, **634**, 43.
38 B. R. James and D. Mahajan, *Can. J. Chem.*, 1979, **57**, 180.
39 D. A. Slack and M. C. Baird, *J. Organomet. Chem.*, 1977, **142**, C69.
40 *PERCH NMR Software*, Version 1/2000, University of Kuopio, Finland, 2000.
41 M. L. Clarke, G. L. Holliday, A. M. Z. Slawin and J. D. Woollins, *J. Chem. Soc., Dalton Trans.*, 2002, 1093.
42 C. Pettinari, F. Marchetti, R. Pettinari, A. Pizzabiocca, A. Drozdov, S. I. Troyanov and V. Vertlib, *J. Organomet. Chem.*, 2003, **688**, 216.
43 E. Arpac and L. Dahlenburg, *J. Organomet. Chem.*, 1983, **241**, 27.
44 D. A. Slack, I. Greveling and M. C. Baird, *Inorg. Chem.*, 1979, **18**, 3125.
45 D. P. Fairlie and B. Bosnich, *Organometallics*, 1988, **7**, 936.
46 H. Werner, A. Hampp and B. Windmüller, *J. Organomet. Chem.*, 1992, **435**, 169.
47 H.-C. Wu, S. Abd Hamid, J.-Q. Yu and J. B. Spencer, *J. Am. Chem. Soc.*, 2009, **131**, 9604.
48 M. Aresta, A. Dibenedetto, I. Papai and G. Schubert, *Inorg. Chim. Acta*, 2002, **334**, 294.
49 G. Canepa, C. D. Brandt and H. Werner, *Organometallics*, 2001, **20**, 604.
50 T. G. Appleton, H. C. Clark and L. E. Manzer, *Coord. Chem. Rev.*, 1973, **10**, 335.
51 B. J. Coe and S. J. Glenwright, *Coord. Chem. Rev.*, 2000, **203**, 5.
52 J. G. Verkade, *Coord. Chem. Rev.*, 1972, **9**, 1.
53 A. R. Sanger, *J. Chem. Soc., Dalton Trans.*, 1977, 120.
54 F. Dahan and R. Choukroun, *Acta Crystallogr., Sect. C: Cryst. Struct. Commun.*, 1985, **41**, 704.
55 A. L. Balch, L. A. Fossett, R. R. Guimerans and M. M. Olmstead, *Organometallics*, 1985, **4**, 781.
56 T. E. Nappier, Jr., D. W. Meek, R. M. Kirchner and J. A. Ibers, *J. Am. Chem. Soc.*, 1973, **95**, 4194.
57 D. P. Allen, C. M. Crudden, L. A. Calhoun, R. Wang and A. Decken, *J. Organomet. Chem.*, 2005, **690**, 5736.
58 V. V. Grushin and W. J. Marshall, *J. Am. Chem. Soc.*, 2004, **126**, 3068.
59 S. S. Oster and W. D. Jones, *Polyhedron*, 2004, **23**, 2959.
60 *Cambridge Structural Database (ConQuest)*, Version 1.11, Crystallographic Data Centre, University Chemical Laboratory, Cambridge, UK, 2009.
61 C. Krug and J. F. Hartwig, *J. Am. Chem. Soc.*, 2004, **126**, 2694.
62 R. Cohen, M. E. van der Boom, L. J. W. Shimon, H. Rozenberg and D. Milstein, *J. Am. Chem. Soc.*, 2000, **122**, 7723.
63 A. C. Chen, D. P. Allen, C. M. Crudden, R. Wang and A. Decken, *Can. J. Chem.*, 2005, **83**, 943.
64 R. P. Hughes, in *Comprehensive Organometallic Chemistry*, ed. G. Wilkinson, F. G. A. Stone and E. W. Abel, Vol. 5, Pergamon, Oxford 1982, p. 277.
65 M. P. Li and R. S. Drago, *J. Am. Chem. Soc.*, 1976, **98**, 5129.
66 P. Imhoff, S. C. A. Nefkens, C. J. Elsevier, K. Goubitz and C. H. Stam, *Organometallics*, 1991, **10**, 1421.
67 P. Imhoff, C. J. Elsevier and C. H. Stam, *Inorg. Chim. Acta*, 1990, **175**, 209.
68 R. Cramer, *Inorg. Synth.*, 1990, **28**, 86.
69 P. Cao, B. Wang and X. Zhang, *J. Am. Chem. Soc.*, 2000, **122**, 6490.
70 *X-RED32 (version 1.03): Stoe Data Reduction Program*, Stoe & Cie GmbH, Darmstadt 2002.
71 *SCALE3 ABSPACK, Empirical Absorption Correction, CrysAlis–Software package*, Oxford Diffraction Ltd. 2006.
72 G. M. Sheldrick, *SHELXS-97, Program for solution of crystal structures*, University of Göttingen, Germany, 1997.
73 G. M. Sheldrick, *SHELXL-97, Program for refinement of crystal structures*, University of Göttingen, Germany, 1997.

ORGANOMETALLICS
Article

Organometallics **2010,** *29,* 6749–6762 6749
DOI: 10.1021/om100878n

On the Reactivity of Rhodium(I) Complexes with κ*P*-Coordinated γ-Phosphino-Functionalized Propyl Phenyl Sulfide Ligands: Routes to Cyclic Rhodium Complexes with κ*C*,κ*P*- and κ*P*,κ*S*-Coordinated Ligands as Well as Bis(diphenylphosphino)methanide Ligands

Michael Block,[†] Tim Kluge,[†] Martin Bette,[†] Jürgen Schmidt,[‡] and Dirk Steinborn*,[†]

[†]*Institute of Chemistry, Martin Luther University Halle-Wittenberg, Kurt-Mothes-Strasse 2, D-06120 Halle, Germany, and* [‡]*Department of Bioorganic Chemistry, Leibniz Institute of Plant Biochemistry, Weinberg 3, D-06120 Halle, Germany*

Received September 10, 2010

Reactions of dinuclear μ-chlorido rhodium(I) complexes $[(RhL_2)_2(\mu\text{-}Cl)_2]$ (L_2 = cycloocta-1,5-diene, cod, **3**; L_2 = P^P: $Ph_2PCH_2PPh_2$, dppm, **4a**; $Ph_2P(CH_2)_2PPh_2$, dppe, **4b**; $Ph_2P(CH_2)_3PPh_2$, dppp, **4c**; $Me_2P(CH_2)_2PMe_2$, dmpe, **4d**) with γ-phosphino-functionalized propyl phenyl sulfides $PhSCH_2CH_2CH_2PR_2$ (R = Ph, **1**; Cy, **2**) afforded mononuclear rhodium(I) complexes of the type $[RhCl(R_2PCH_2CH_2CH_2SPh\text{-}\kappa P)L_2]$ (R = Ph/L_2 = P^P, **5a**−**c**; R = Ph/L_2 = cod, **6**; R = Cy/L_2 = P^P, **7a**−**d**; R = Cy/L_2 = cod, **8**). Single-crystal X-ray diffraction analysis of **7b**·C_6H_6 exhibited the expected square-planar coordination of the rhodium atom having coordinated dppe-κ^2P,P', $Cy_2PCH_2CH_2CH_2SPh\text{-}\kappa P$, and a chlorido ligand. Deprotonation of complexes **5b/c**, **6**, **7b/c**, and **8** with lithium diisopropyl amide (LDA) yielded, with a selective deprotonation of the CH_2 group next to the sulfur atom (α-CH_2 group), complexes of the type $[Rh\{CH(SPh)CH_2CH_2PR_2\text{-}\kappa C,\kappa P\}L_2]$ (**13b/c**, **14**, **15b/c**, **16**), thus being organorhodium intramolecular coordination compounds. Unexpectedly, reactions of the dppm complexes **5a** and **7a** with LDA led to deprotonation of the CH_2 group of the dppm ligand, resulting in formation of mononuclear rhodium complexes with a bis(diphenylphosphino)methanide-κ^2P,P' ligand and a R_2P^SPh-κ*P*,κ*S* ligand, as well (**17**, **18**). Single-crystal X-ray diffraction analysis of $[Rh(dppm_{-H}\text{-}\kappa^2P,P')(Cy_2PCH_2CH_2CH_2SPh\text{-}\kappa P,\kappa S)]\cdot THF$ (**18**·THF) shows the rhodium atom located in the center of a distorted square-planar environment having bound the P^S-κ*P*,κ*S* ligand and the anionic $dppm_{-H}$-κ^2P,P' ligand with a very small P2−Rh−P3 angle (68.8(2)°) reflecting the small bite of that ligand. Addition of $Tl[PF_6]$ to complexes **5**−**8** afforded cationic rhodium(I) complexes of the type $[Rh(R_2PCH_2CH_2CH_2SPh\text{-}\kappa P,\kappa S)L_2][PF_6]$ (**9**−**12**) bearing bidentately coordinated neutral co-ligands (P^P: **9**, **11**; cod, **10**, **12**) and κ*P*,κ*S*-coordinated γ-phosphino-functionalized propyl phenyl sulfide ligands, as well. Single-crystal X-ray diffraction analysis of **10** reveals that the rhodium atom adopts a slightly distorted square-planar conformation. Complexes **9a**−**c** and **11a**−**d** were found to react with carbon monoxide, yielding cationic rhodium carbonyl complexes $[Rh(CO)(R_2PCH_2CH_2CH_2SPh\text{-}\kappa P,\kappa S)(P^P\text{-}\kappa^2P,P')]^+$ (**19**, **20**), being in a dynamic equilibrium between two diastereomers each at room temperature, which was additionally verified by DFT calculations.

1. Introduction

Since the synthesis and characterization of the organoaluminum compounds **Ia**/**Ib** (Chart 1), in which an alkyl ligand is additionally coordinated to aluminum through a Lewis-basic group (κ*O*/κ*N*), by Bähr and Müller in 1955[1] and the report on the cyclometalation of azobenzene resulting in an *o*-(phenylazo)phenyl nickel complex in 1963 by Kleimann and Dubeck,[2] the syntheses of organometallic intramolecular coordination compounds (also named "organometallic inner complexes"[1]) were the subject of a large number of studies.[3−8] Hence, from almost all metals of the periodic table organometallic intramolecular coordination compounds are known, and they are widely used in organic syntheses. Applications are carbonylations[9] and Diels−Alder reactions;[10] see **II** and **III** (Chart 1) as examples. Furthermore, they are used in

*To whom correspondence should be addressed. E-mail: steinborn@chemie.uni-halle.de.

(1) Bähr, G.; Müller, G. E. *Chem. Ber.* **1955**, *88*, 251.
(2) Kleiman, J. P.; Dubeck, M. *J. Am. Chem. Soc.* **1963**, *85*, 1544.
(3) Nolte, M.; Singleton, E.; van der Stok, E. *J. Organomet. Chem.* **1977**, *142*, 387.
(4) Klei, E.; Teuben, J. H. *J. Organomet. Chem.* **1981**, *214*, 53.
(5) Al-Allaf, T. A. K. *Asian J. Chem.* **2000**, *12*, 869.
(6) Omae, I. *J. Organomet. Chem.* **2007**, *692*, 2608.
(7) Beck, R.; Frey, M.; Camadanli, S.; Klein, H.-F. *Dalton Trans.* **2008**, 4981.
(8) Campos, J.; Esqueda, A. C.; Carmona, E. *Chem. Eur. J.* **2010**, *16*, 419.
(9) Thompson, J. M.; Heck, R. F. *J. Org. Chem.* **1975**, *40*, 2667.
(10) Leung, P.-H.; He, G.; Lang, H.; Liu, A.; Loh, S.-K.; Selvaratnam, S.; Mok, K. F.; White, A. J. P.; Williams, D. J. *Tetrahedron* **2000**, *56*, 7.

Published on Web 12/01/2010

Chart 1

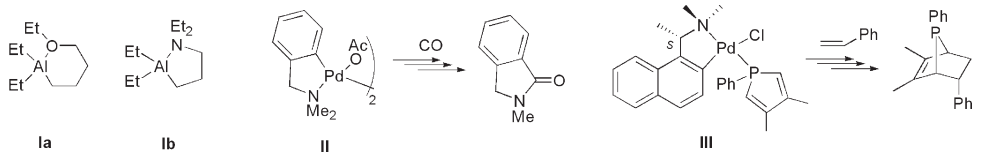

alkenylations[11] and metal-catalyzed reactions such as metathesis[12,13] or cross-coupling reactions.[14,15] In general, in cyclometalations a precoordination of the ligand via a Lewis basic heteroatom YR_n (YR_n = OR, SR, NR_2, PR_2, ...) was found followed by a deprotonation of a C−H bond in a chelating-favorable position to the metal center under formation of an M−C σ-bond. Among organometallic intramolecular coordination compounds those complexes having five-membered ring structures are of particular stability compared to four- and six-membered metallacycles.[16]

Apart from complexes of the type described above, complexes having bidentately coordinated ligands with different donor sites, among those of the type $R_2P-(CH_2)_n-SR'$ (R, R′ = alkyl, aryl), are also of interest for various reasons.[17] For example, they may act as hemilabile ligands permitting temporary generation of a vacant coordination site at the metal center; thus reactions such as oxidative additions[18,19] and substitutions[20,21] may proceed more easily. Moreover, they may facilitate the activation of small molecules such as CO or O_2, thus playing an important role in homogeneously catalyzed reactions.[22−24]

We are interested in metal complexes with α-sulfur-functionalized alkyl ligands of the type $^{-}CH\{PhS(O)_x\}CH_2CH_2-YR_n$ (x = 0−2) bearing in the γ-position an additional donor site YR_n = NR_2, PR_2, OR (R = alkyl, aryl). α-Lithiated thioethers (x = 0) without this donor functionality YR_n tend to yield oligonuclear compounds in the solid state,[25,26] whereas those having a donor functionality YR_n (NR_2, OR) were found to be mononuclear organolithium intramolecular coordination compounds in the solid state.[27,28] Moreover, the corresponding α-sulfonyl-functionlized ligands (x = 2) were also found to yield organorhodium intramolecular coordination compounds, thus forming a Rh−C σ-bond.[29] This is in contrast to the majority of the lithiated compounds, which are mostly higher aggregated and have the sulfone ligand κO-coordinated to the Li atom, thus bearing a "free" carbanionic center.[30,31]

Here we report on the synthesis, characterization, and reactivity of rhodium(I) complexes of the type [RhCl($R_2PCH_2CH_2CH_2SPh$-κP)L_2] (R = Ph, Cy; L = diphosphanes, cycloocta-1,5-diene), which were found to yield organorhodium intramolecular coordination compounds having anionic C^P-κC,κP ligands upon deprotonation and cationic rhodium(I) complexes bearing hemilabile P^S-κP,κS ligands upon Cl^- abstraction, and their reactions with carbon monoxide.

2. Results and Discussion

2.1. Syntheses. The reactions of dinuclear chlorido-bridged rhodium complexes bearing cycloocta-1,5-diene and diphosphanes as ligands (**3**, **4a**−**d**) with γ-phosphino-functionalized propyl phenyl sulfides **1** and **2** led to the formation of mononuclear rhodium complexes of the type [RhCl($R_2PCH_2CH_2CH_2SPh$-κP)L_2] (**5**−**8**) (Scheme 1, routes a/c). Only the reaction of the diphenylphosphino-functionalized thioether ligand **1** with the dmpe complex **4d** resulted in decomposition. The reactions were performed in either THF or CH_2Cl_2. Using methylene chloride as solvent, the reactions with complexes **4** have to be performed at −78 °C to avoid the oxidative addition of dichloromethane to **4**, which results in the formation of μ-methylene rhodium(III) complexes.[32] The yellow to orange air-sensitive complexes **5**−**8** were obtained in yields between 48% and 90% and were characterized NMR spectroscopically (^1H, ^{13}C, ^{31}P), by elemental analysis, and by a single-crystal X-ray measurement (**7b**·C_6H_6). All compounds were soluble in THF and dichloromethane but showed decomposition in chloroform within a few hours at room temperature. The complexes with the dicyclohexylphosphino-functionalized ligand (**7**, **8**) were even slightly soluble in *n*-pentane, explaining the lower yields compared to complexes **5** and **6**. Furthermore, it has been shown that the reaction of the cyclooctadiene rhodium complexes [RhCl($R_2PCH_2CH_2CH_2SPh$-κP)(cod)] (**6**, **8**) with diphosphanes (P^P) resulted in a ligand substitution reaction (cod → P^P) forming the respective diphosphane complexes **5** and **7** (Scheme 1, route a → e).

Addition of Tl[PF_6] to complexes **5**−**8** in THF or CH_2Cl_2 afforded, with precipitation of TlCl, cationic rhodium

(11) Cravotto, G.; Demartin, F.; Palmisano, G.; Penoni, A.; Radice, T.; Tollari, S. *J. Organomet. Chem.* **2005**, *690*, 2017.
(12) Garber, S. B.; Kingsbury, J. S.; Gray, B. L.; Hoveyda, A. H. *J. Am. Chem. Soc.* **2000**, *122*, 8168.
(13) Yao, Q.; Zhang, Y. *Angew. Chem., Int. Ed.* **2003**, *42*, 3395.
(14) Herrmann, W. A.; Brossmer, C.; Reisinger, C.-P.; Riermeier, T. H.; Öfele, K.; Beller, M. *Chem. Eur. J.* **1997**, *3*, 1357.
(15) Ogo, S.; Takebe, Y.; Uehara, K.; Yamazaki, T.; Nakai, H.; Watanabe, Y.; Fukuzumi, S. *Organometallics* **2006**, *25*, 331.
(16) (a) Omae, I. *Coord. Chem. Rev.* **1979**, *28*, 97. (b) Omae, I. *Coord. Chem. Rev.* **1980**, *32*, 235. (c) Omae, I. *Coord. Chem. Rev.* **1982**, *42*, 245. (d) Omae, I. *Coord. Chem. Rev.* **1988**, *83*, 137.
(17) Sanger, A. R. *Can. J. Chem.* **1983**, *61*, 2214.
(18) Bassetti, M.; Capone, A.; Salamone, M. *Organometallics* **2004**, *23*, 247.
(19) Gonsalvi, L.; Adams, H.; Sunley, G. J.; Ditzel, E.; Haynes, A. *J. Am. Chem. Soc.* **2002**, *124*, 13597.
(20) Ulmann, P. A.; Mirkin, C. A.; DiPasquale, A. G.; Liable-Sands, L. M.; Rheingold, A. L. *Organometallics* **2009**, *28*, 1068.
(21) Pàmies, O.; Diéguez, M.; Net, G.; Ruiz, A.; Claver, C. *Organometallics* **2000**, *19*, 1488.
(22) Bressan, M.; Morandini, F.; Rigo, P. *J. Organomet. Chem.* **1983**, *247*, C8.
(23) Bressan, M.; Morandini, F.; Morvillo, A.; Rigo, P. *J. Organomet. Chem.* **1985**, *280*, 139.
(24) Dilworth, J. R.; Miller, J. R.; Wheatley, N.; Baker, M. J.; Sunley, J. G. *J. Chem. Soc., Chem. Commun.* **1995**, 1579.
(25) Amstutz, R.; Laube, T.; Schweizer, W. B.; Seebach, D.; Dunitz, J. D. *Helv. Chim. Acta* **1984**, *67*, 224.
(26) Becke, F.; Heinemann, F. W.; Steinborn, D. *Organometallics* **1997**, *16*, 2736.
(27) Linnert, M.; Bruhn, C.; Wagner, C.; Block, M.; Rüffer, T.; Schmidt, H.; Steinborn, D. In *Advances in Coordination, Bioinorganic and Inorganic Chemistry*; Melnik, M.; Sima, J.; Tatarko, M., Eds.; STU Press: Bratislava, 2005; p 170.
(28) Block, M.; Linnert, M.; Gómez-Ruiz, S.; Steinborn, D. *J. Organomet. Chem.* **2009**, *694*, 3353.
(29) Block, M.; Wagner, C.; Gómez-Ruiz, S.; Steinborn, D. *Dalton Trans.* **2010**, *39*, 4636.
(30) Gais, H.-J.; Hellmann, G.; Günther, H.; Lopez, F.; Lindner, H. J.; Braun, S. *Angew. Chem., Int. Ed. Engl.* **1989**, *28*, 1025.
(31) Boche, G. *Angew. Chem., Int. Ed. Engl.* **1989**, *28*, 277.
(32) Ball, G. E.; Cullen, W. R.; Fryzuk, M. D; James, B. R.; Rettig, S. J. *Organometallics* **1991**, *10*, 3767.

Scheme 1. Routes to Rhodium Complexes Bearing κP (5−8) and $\kappa P,\kappa S$ (9−12) Coordinated $R_2PCH_2CH_2CH_2SPh$ Ligands

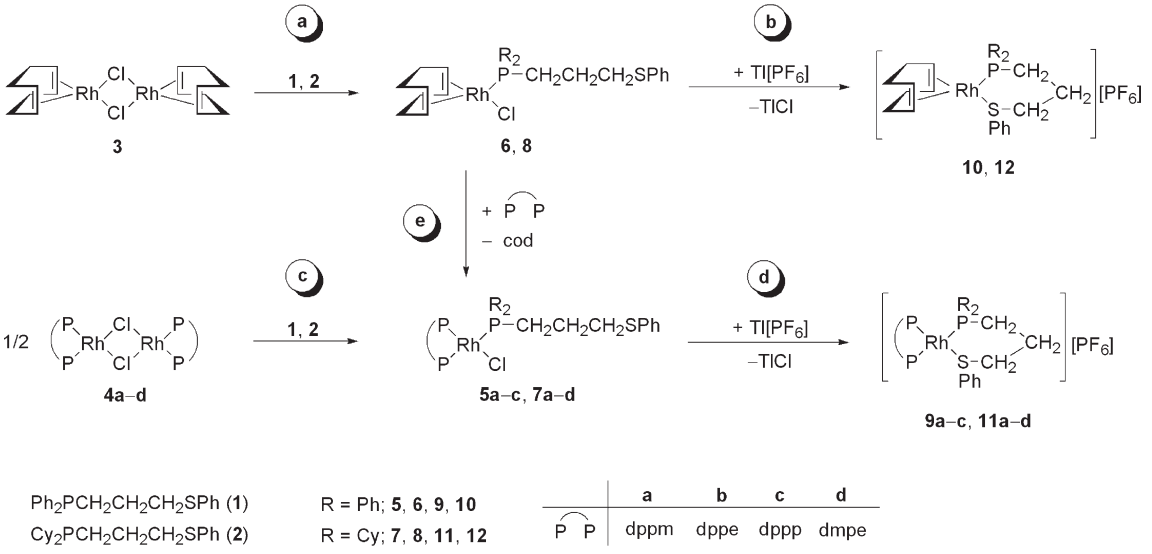

complexes with $\kappa P,\kappa S$-coordinated phosphino-functionalized propyl phenyl suldfides (**9**−**12**) (Scheme 1, routes b/d). The complexes formed were found to be air-sensitive, yellow microcrystalline solids, which were islolated in yields between 71% and 88%, and they were characterized by ^{1}H, ^{13}C, and ^{31}P NMR spectroscopy, high-resolution mass spectrometric (HRMS-ESI) investigations, and a single-crystal X-ray diffraction (**10**). To simplify the syntheses, it has been shown that complexes **9**−**12** can also be obtained according to route a → b or c → d without isolation of the neutral rhodium complexes **5**−**8**. Furthermore, the cationic complexes bearing a P^P ligand (**9**, **11**) were easily accessible via route a → e → d starting from the commerically available cod complex **3** without isolation of any intermediate complex (Scheme 1).

Reactions of complexes [RhCl($R_2PCH_2CH_2CH_2SPh$-κP)L_2] (L_2 = dppe, **5b**/**7b**; dppp, **5c**/**7c**; L_2 = cod, **6**/**8**) with lithium diisopropylamide (LDA) in toluene at −78 °C led selectively to deprotonation of the carbon atom neighboring the sulfur center (α-C) and its coordination to rhodium, thus forming organorhodium intramolecular coordination compounds of the type [Rh{CH(SPh)$CH_2CH_2PPh_2$-$\kappa C,\kappa P$}L_2] (**13b**/**c**, **14**, **15b**/**c**, **16**; Scheme 2). In contrast, the reaction of the dmpe complex [RhCl($R_2PCH_2CH_2CH_2SPh$-κP)(dmpe)] (**7d**) with LDA did not lead to a type **15** complex but to decomposition with cleavage of the P^S ligand. In general, attempts to use MeLi or *n*-BuLi as deprotonating agent led to decomposition, which might be attributed to the stronger nucleophilicity of these bases. Complexes **13**−**16** were soluble in toluene, benzene, and THF but showed decomposition in chloroform. Moreover, the complexes with the dicyclohexylphosphino-functionalized ligand (**15b**/**c**, **16**) exhibited a pronounced solubility in *n*-pentane, even at −78 °C, which made it impossible to remove residual amounts of diisopropylamine. Thus, the yields for the dark orange to brown air-sensitive complexes were low for **15b**/**c** and **16** (31−35%) but good for complexes **13b**/**c** and **14** (ca. 85%). The organorhodium complexes were characterized by ^{1}H, ^{13}C, and ^{31}P NMR spectroscopy as well as by elemental analysis (**13b**/**c**, **14**). By analogy to the synthesis of the cationic rhodium complexes **9**−**12** the intermediate compounds **5**−**8** do not need to be isolated; thus **13**−**16** can be obtained in a one-pot reaction directly from the dinuclear starting complexes **3** and **4**.

Scheme 2. Routes to Organorhodium Intramolecular Coordination Compounds

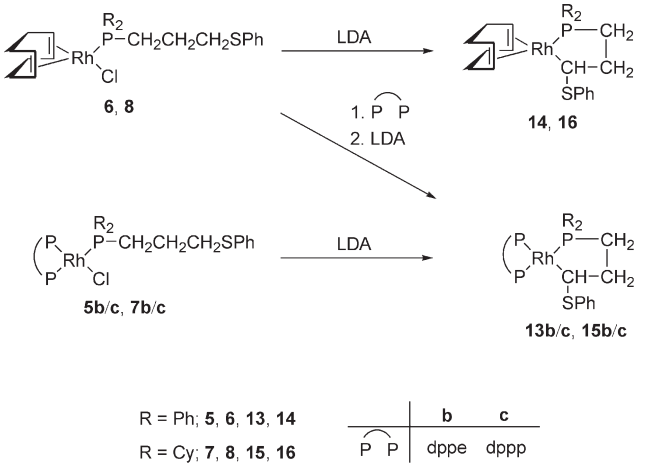

Unexpectedly, the reactions of the dppm complexes [RhCl($R_2PCH_2CH_2CH_2SPh$-κP)(dppm)] (**5a**, **7a**) with LDA led to a deprotonation of the CH_2 group of the dppm ligand, resulting in the formation of mononuclear rhodium complexes having bound an anionic bis(diphenylphosphino)methanide-κ^2P,P' ligand and a R_2P^SPh-$\kappa P,\kappa S$ ligand (**17**, **18**) (Scheme 3). Complexes **17** and **18** were obtained in yields of about 72% as orange to brown air- and moisture-sensitive solids, which were characterized by NMR spectroscopy (^{1}H, ^{13}C, ^{31}P), HRMS-ESI investigations, and a single-crystal X-ray diffraction analysis (**18**·THF).

2.2. Structures. 2.2.1. Structure of [RhCl($Cy_2PCH_2CH_2CH_2SPh$-κP)(dppe)] (7b). Crystals of **7b**·C_6H_6 suitable for X-ray diffraction analysis were obtained from benzene solution at room temperature. The compound crystallized in isolated molecules without unusual intermolecular interactions (shortest distance between non-hydrogen atoms: 3.410(3) Å, C23···C37′). The molecular structure is shown in Figure 1, and selected structural parameters are given in the figure caption. The rhodium atom adopts a square-planar geometry and is coordinated by a chlorido ligand, a κ^2P,P'-bound dppe ligand, and a γ-phosphino-functionalized propyl phenyl sulfide with a κP-coordination mode. The angles between neighboring

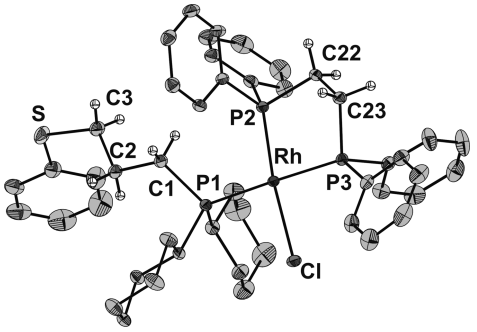

Figure 1. Molecular structure of [RhCl($Cy_2PCH_2CH_2CH_2SPh$-κP)(dppe)] in crystals of **7b**·C_6H_6. The ellipsoids are shown with a probability of 30%. H atoms of phenyl and cyclohexyl rings have been omitted for clarity. Selected structural parameters (distances in Å, angles in deg): Rh−P1 2.3476(7), Rh−P2 2.2024(7), Rh−P3 2.2987(7), Rh−Cl 2.4114(8), Cl−Rh−P1 88.35(2), P1−Rh−P2 97.06(2), P2−Rh−P3 83.77(3), P3−Rh−Cl 90.69(2), Cl−Rh−P2 174.02(2), P1−Rh−P3 176.84(2).

Scheme 3. Synthesis of Zwitterionic Rhodium Complexes

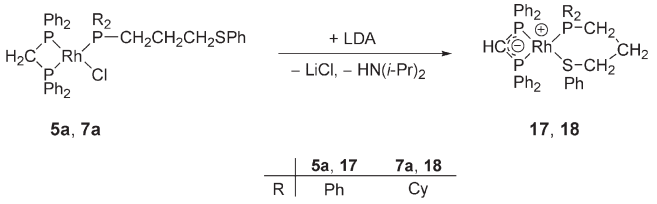

ligands are all close to 90° (83.77(3)−97.06(2)°). The five-membered RhP_2C_2 rhodacycle has a half-chair conformation twisted on C22 and C23. Noteworthy, the Rh−P1 bond (2.3476(7) Å) is significantly longer than the Rh−P3 bond (2.2987(7) Å), which is in accordance with other rhodium(I) complexes having a PPh_2R and a PCy_2R (R = alkyl) group in mutual *trans* position.[33,34] Both the Rh−P2 (2.2024(7) Å) and the Rh−Cl (2.4114(8) Å) bond lengths are quite standard for square-planar rhodium complexes bearing a phosphane and a chlorido ligand *trans* to each other.[35−38]

2.2.2. Rhodium Complexes Bearing Bidentately Coordinated *P,S* Ligands. Crystals of [Rh($Ph_2PCH_2CH_2CH_2SPh$-$\kappa P,\kappa S$)(cod)][PF_6] (**10**) and [Rh($dppm_{-H}$-$\kappa^2 P,P'$)($Cy_2PCH_2CH_2CH_2SPh$-$\kappa P,\kappa S$)]·THF (**18**·THF) suitable for X-ray diffraction analyses were obtained from THF solutions at room temperature. Complex **10** crystallized as discrete cations and anions without unusual intermolecular interactions (shortest distance between non-hydrogen atoms: 3.082(8) Å, C2···F4′). Complex **18**·THF crystallized in isolated molecules (shortest distance between non-hydrogen atoms: 3.510(3) Å, C8···C43′). The molecular structures are shown in Figures 2 and 3. Selected structural parameters are given in the figure captions.

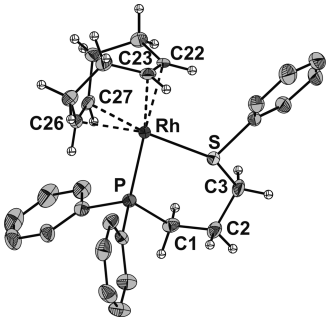

Figure 2. Molecular structure of the cation in crystals of [Rh($Ph_2PCH_2CH_2CH_2SPh$-$\kappa P,\kappa S$)(cod)][PF_6] (**10**). The ellipsoids are shown with a probability of 30%. H atoms of phenyl rings have been omitted for clarity. Selected structural parameters (distances in Å, angles in deg): Rh−P 2.299(2), Rh−C22/23_{cg} (cg = center of gravity) 2.0602(2), Rh−C26/27_{cg} 2.1388(5), Rh−S 2.353(2), C22−C23 1.378(9), C26−C27 1.362(9), P1−Rh−S 86.96(5), P−Rh−C22/23_{cg} 92.25(4), C22/23_{cg}−Rh−C26/27_{cg} 85.32(2), C26/27_{cg}−Rh−S 95.32(4), C26/27_{cg}−Rh−P 177.23(4), C22/23_{cg}−Rh−S 173.70(4).

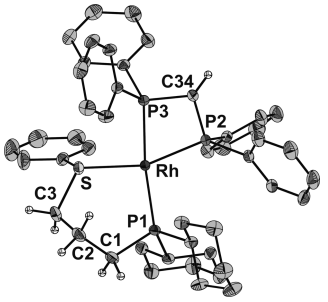

Figure 3. Molecular structure of [Rh($dppm_{-H}$-$\kappa^2 P,P'$)($Cy_2PCH_2CH_2CH_2SPh$-$\kappa P,\kappa S$)] in crystals of **18**·THF. The ellipsoids are shown with a probability of 30%. H atoms of phenyl and cyclohexyl rings have been omitted for clarity. Selected structural parameters (distances in Å, angles in deg): Rh−P1 2.2965(5), Rh−P2 2.2963(4), Rh−P3 2.3130(4), Rh−S 2.3123(4), P2−C34 1.725(2), P3−C34 1.728(2), P2−Rh−P3 68.82(2), P3−Rh−S 91.41(2), S−Rh−P1 96.37(2), P1−Rh−P2 104.31(2), P2−C34−P3 97.92(9), P2−Rh−S 159.31(2), P1−Rh−P3 163.55(2).

In both complexes the rhodium atom exhibits a distorted square-planar conformation where the primary donor sets are built up by the bidentately $\kappa P,\kappa S$-coordinated phosphino-functionalized sulfides as well as by a bidentately bound cycloocta-1,5-diene ligand (**10**) and a bis(diphenylphosphino)methanide-$\kappa^2 P,P'$ ($dppm_{-H}$) ligand (**18**·THF), respectively. The six-membered $RhPC_3S$ metallacycles adopt a chair form (**10**) and a screw-boat form (**18**·THF), respectively. In complex **10** all angles between neighboring ligands are close to 90° (85.32(5)−95.32(5)°), and those between *trans*-standing ligands are 173.70(4)° and 177.23(4)°, close to 180°. Contrary to this, due to the small bite of the chelating $dppm_{-H}$ ligand (P2−Rh−P3 68.82(2)°) in complex **18**·THF, greater deviations were found. Thus, the angles between *trans*-standing ligands amount to 159.31(2)° (S−Rh−P2) and 163.55(2)° (P1−Rh−P3).

The Rh−P bond length in **10** (2.299(2) Å) is in the expected range for Rh(I) complexes containing a phosphane and a cod ligand in mutual *trans* position (median: 2.307 Å, lower/higher quartile: 2.285/2.327 Å, $n = 189$).[39] However, the Rh−P1 bond in **18**·THF (2.2965(5) Å) was found to be relatively short

(33) Lamač, M.; Císařová, I.; Stěpnička, P. *J. Organomet. Chem.* **2005**, *690*, 4285.
(34) Lamač, M.; Císařová, I.; Stěpnička, P. *Eur. J. Inorg. Chem.* **2007**, 2274.
(35) Brown, A. M.; Ovchinnikov, M. V.; Stern, C. L.; Mirkin, C. A. *J. Am. Chem. Soc.* **2004**, *126*, 14316.
(36) Rios-Moreno, G.; Toscano, R. A.; Redón, R.; Nakano, H.; Okuyama, Y.; Morales-Morales, D. *Inorg. Chim. Acta* **2005**, *358*, 303.
(37) Le Gall, I.; Laurent, P.; Soulier, E.; Salaün, J.-Y.; des Abbayes, H. *J. Organomet. Chem.* **1998**, *567*, 13.
(38) Andrieu, J.; Richard, P.; Camus, J.-M.; Poli, R. *Inorg. Chem.* **2002**, *41*, 3876.

compared to four-coordinated rhodium complexes bearing two *trans*-standing phosphane ligands (median: 2.318 Å, lower/higher quartile: 2.298/2.333 Å, $n = 432$).[39] The higher *trans* influence of phosphanes compared to thioethers[40] is reflected in the longer bond of Rh−P3 (2.3130(4) Å, P3 is *trans* to P1) compared to Rh−P2 (2.2963(4) Å, P2 is *trans* to S). Noteworthy, the Rh−S bond in **10** (2.353(2) Å) is considerably longer than that in **18**·THF (2.3123(4) Å).

The structure of the deprotonated dppm ligand is of particular interest. The four-membered RhP_2C cycle is slightly more hinged (torsion angle Rh−P2···P3−C34 166.0(1)°) than in other metal complexes bearing a dppm$_{-H}$-κ^2P,P' ligand (median: 176.0°, lower/higher quartile: 170.6/177.9°, $n = 18$; absolute values of the torsion angles are given).[39] The Rh−P3 bond in **18**·THF (2.3130(4) Å, P3 is *trans* to P1) is of a similar length as the Rh−P bonds of the dppm$_{-H}$-κ^2P,P' ligand (2.342(3)/2.324(3) Å) in complex [Rh(dppm$_{-H}$-κ^2P,P')(dppm-κ^2P,P')];[41] thus the deprotonation of the dppm ligand is accompanied by a Rh−P bond elongation (dppm: Rh−P 2.293(3)/2.237(4) Å).[41] On the other hand, the P−C bond lengths in **18**·THF (1.725(2)/1.728(2) Å) are clearly shortened compared to those of (nondeprotonated) dppm ligands (1.839(2)−1.853(4) Å),[41−43] which can be explained in terms of an ylidic bonding model with some charge delocalization within the PCP moiety.[44] Additionally, the transannular Rh···C34 distance of 3.014(2) Å clearly demonstrates that there is no bond between these two atoms.

To get insight into the unexpected deprotonation of the dppm ligand, quantum chemical calculations on the DFT level of theory were performed. With the intention to limit the computational expense, the calculations were performed by replacing the PCy_2 groups in **18**·THF by PPh_2 groups, thus representing complex **17**. Two isomers were calculated, namely, a complex bearing an anionic dppm$_{-H}$ ligand (**17**$_{calc}$) and a type **13** complex with an anionic $^-CH(SPh)CH_2$-CH_2PPh_2-$\kappa C,\kappa P$ ligand (**13a**$_{calc}$), which are shown in Figure 4. As found in the structure of **18**·THF, the deprotonation of the dppm ligand gives rise to a marked shortening of the P2−C34/P3−C34 bonds (1.786/1.784 Å in **17**$_{calc}$ versus 1.921/1.913 Å in **13a**$_{calc}$) and a concomitant lengthening of the Rh−P3 bond (2.419 Å in **17**$_{calc}$ versus 2.392 Å in **13a**$_{calc}$).

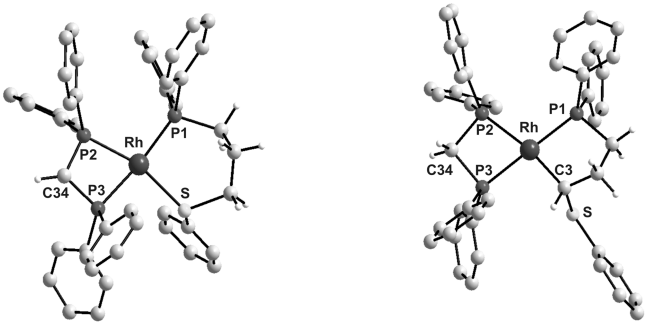

Figure 4. Calculated structures of [Rh(dppm$_{-H}$-κ^2P,P')(Ph_2-$PCH_2CH_2CH_2SPh$-$\kappa P,\kappa S$)] (**17**$_{calc}$, left) and [Rh{$CH(SPh)CH_2$-CH_2PPh_2-$\kappa C,\kappa P$}(dppm-κ^2P,P')] (**13a**$_{calc}$, right). H atoms of the phenyl rings have been omitted for clarity.

Noteworthy, the intramolecular coordination compound **13a**$_{calc}$ was found to be more stable by 21.6 kcal/mol (Gibbs free energy at 298 K). This clearly demonstrates that the experimentally observed formation of complex **17** and also—in analogy—of complex **18** is under kinetic control.

2.3. Spectroscopic Investigations. 2.3.1. Rhodium Complexes with $PhSCH_2CH_2CH_2PR_2$-κP Ligands. Selected NMR spectroscopic parameters of complexes **5**−**8** are given in Table 1. All ^{31}P NMR spectra are of first order, exhibiting an AEMX spin system (A, E, M = ^{31}P; X = ^{103}Rh; **5**, **7**) and an AX spin system (**6**, **8**), respectively. Due to the smaller *trans* influence of olefin ligands compared to phosphane ligands, the $^1J_{Rh,P}$ coupling constants of the P atoms of the P^S ligands in **6** (147.1 Hz) and **8** (144.5 Hz) are larger than those in **5** and **7** (127.5−133.3 Hz). The two P atoms of the P′^P″ ligands (P′ is *trans* to P; P″ is *trans* to Cl) in complexes **5** and **7** could be unambiguously assigned on the basis of the difference in the $^1J_{Rh,P'}/^1J_{Rh,P''}$ coupling constants (ΔJ = 37.3−57.3 Hz), which reflects the *trans* influence order PR_3 > Cl, being also found in numerous structurally similar complexes.[45−48] Furthermore, the assignement was confirmed by the magnitudes of the two $^2J_{P,P}$ coupling constants: While P″ exhibits two *cis* couplings (31.5−98.8 Hz), P′ has one *cis* (32.6−98.8 Hz) and one *trans* coupling (338.6−388.5 Hz). The coordination-induced shifts (CISs) of the aliphatic carbon atoms of the propanediyl chains of the P^S ligands were found to be up to 4.2 ppm; those of the H atoms, up to 0.70 ppm. The absolute values of the $^2J_{P,C}$ couplings in complexes **5** were found to be decreased by about 13 Hz upon coordination (in complexes **6**, **7**, and **8** the signals of the β-carbon atoms appeared as broader singlets; thus the $^2J_{P,C}$ coupling constants were estimated to be <2 Hz). However, the $^1J_{P,C}$ couplings were found to be increased by about 10 Hz in **5** and **6** but decreased (ca. 5 Hz) in **7** and **8** compared to the "free" ligands **1** and **2**.

2.3.2. Cationic Rhodium Complexes Containing *P,S* Chelate Ligands. Selected NMR spectroscopic data of the cationic

Table 1. Selected NMR Sepctroscopic Data (δ in ppm, J in Hz) of [RhCl($PhSCH_2CH_2CH_2PR_2$-κP)L_2] (5−8)

			$PhS-C_\alpha H_2-C_\beta H_2-C_\gamma H_2-PR_2$				co-ligand L_2	
	R	L_2	$\delta_{\alpha\text{-C}}$ ($^3J_{P,C}$)	$\delta_{\beta\text{-C}}$ ($^2J_{P,C}$)	$\delta_{\gamma\text{-C}}$ ($^1J_{P,C}$)	δ_P ($^1J_{Rh,P}$)	$\delta_{P'}$ ($^1J_{Rh,P'}$)[a]	$\delta_{P''}$ ($^1J_{Rh,P''}$)[a]
5a	Ph	dppm	35.3 (15.0)	26.6 (3.9)	28.0 (21.5)	23.1 (133.3)	−42.1 (118.9)	−15.8 (156.2)
5b	Ph	dppe	35.4 (15.8)	27.2 (4.8)	28.4 (22.7)	23.8 (131.6)	56.8 (141.6)	73.9 (183.2)
5c	Ph	dppp	35.4 (16.1)	27.6 (5.5)	29.0 (24.2)	25.5 (133.3)	12.3 (133.3)	34.5 (176.4)
6	Ph	cod	35.4 (15.0)	25.9 (s)	26.9 (25.2)	26.2 (147.1)		
7a	Cy	dppm	35.5 (11.9)	26.4 (s)	22.7 (13.9)	25.6 (131.4)	−42.0 (115.5)	−14.7 (161.1)
7b	Cy	dppe	34.4 (17.7)	25.8 (s)	21.0 (15.2)	24.0 (127.5)	58.9 (135.4)	71.2 (192.7)
7c	Cy	dppp	34.9 (13.9)	25.9 (s)	20.2 (15.7)	24.6 (128.4)	12.4 (129.1)	32.3 (184.4)
7d	Cy	dmpe	35.7 (12.4)	27.0 (s)	22.4 (14.6)	27.2 (128.1)	46.8 (131.7)	40.5 (182.4)
8	Cy	cod	35.0 (11.3)	24.9 (s)	17.2 (17.0)	23.7 (144.5)		
1[b]	Ph		34.7 (14.0)	25.7 (17.6)	27.2 (13.2)	−16.2		
2[b]	Cy		35.3 (13.7)	28.9 (21.6)	21.4 (19.4)	−5.6		

[a] P′ and P″ are *trans* to P of the $PhSCH_2CH_2CH_2PR_2$ ligand and Cl, respectively. [b] The values for $PhSCH_2CH_2CH_2PR_2$ (R = Ph, **1**; Cy, **2**) are given for comparison.

Table 2. Selected NMR Spectroscopic Data (δ in ppm, J in Hz) of $[Rh(R_2PCH_2CH_2CH_2SPh\text{-}\kappa P,\kappa S)L_2][PF_6]$ (9−12)

			PhS−$C_\alpha H_2$−$C_\beta H_2$−$C_\gamma H_2$−PR_2				co-ligand L_2	
	R	L_2	$\delta_{\alpha\text{-C}}$ ($^3J_{P,C}/^3J_{P'',C}$)[a]	$\delta_{\beta\text{-C}}$[b]	$\delta_{\gamma\text{-C}}$ ($^1J_{P,C}$)	δ_P ($^1J_{Rh,P}$)	$\delta_{P'}$ ($^1J_{Rh,P'}$)[c]	$\delta_{P''}$ ($^1J_{Rh,P''}$)[c]
9a	Ph	dppm	40.3 (4.8/2.0)	22.8	27.2 (21.9)	10.3 (131.4)	−30.8 (113.8)	−18.3 (140.8)
9b	Ph	dppe	36.3 (8.7/3.7)	21.5	26.0 (24.1)	7.2 (130.0)	59.9 (128.7)	66.8 (167.2)
9c	Ph	dppp	35.2 (8.2/3.6)	21.0	27.0 (23.1)	8.9 (130.7)	11.2 (134.1)	21.3 (160.4)
10	Ph	cod	39.4 (3.5/−)	22.7	25.7 (26.3)	12.3 (140.0)		
11a	Cy	dppm	40.0 (5.5/4.1)	25.1	17.3 (17.6)	17.9 (127.3)	−28.3 (111.2)	−14.1 (144.7)
11b	Cy	dppe	39.0 (6.4/5.1)	23.1	15.5 (17.6)	13.1 (124.5)	56.3 (126.4)	71.2 (170.2)
11c	Cy	dppp	35.4 (7.9/3.9)	22.2	12.7 (18.3)	16.3 (125.4)	6.5 (120.8)	19.0 (161.7)
11d	Cy	dmpe	36.7 (6.7/−)	23.1	16.0 (17.3)	18.2 (125.1)	37.4 (124.1)	36.9 (159.9)
12	Cy	cod	39.3 (2.5/−)	24.8	16.6 (22.2)	14.4 (134.4)		

[a] May be reversed. [b] The $^2J_{P,C}$ coupling constants were estimated to be <2 Hz. [c] P′ and P″ are *trans* to P and S, respectively, of the $PhSCH_2CH_2CH_2PR_2$ ligand.

rhodium complexes $[Rh(PhSCH_2CH_2CH_2PR_2\text{-}\kappa P,\kappa S)L_2][PF_6]$ (**9**−**12**) are given in Table 2. The ^{31}P NMR spectra were found to be of first-order AEMX (A, E, M = ^{31}P; X = ^{103}Rh; **9**, **11**) and AX spin systems (**10**, **12**), respectively. The formation of the $RhPC_3S$ rhodacycles go along with a decrease of the $^1J_{Rh,P''}$ coupling constants (P″ is *trans* to S) by up to about 20 Hz in **9** and **11** (Table 2) compared to the analogous neutral complexes **5** and **7** (Table 1), in accord with the *trans* influence order R_2S > Cl.[49] A comparison of the ^{13}C NMR data of the propanediyl group in complexes **9**−**12** to those in complexes **5**−**8** reveals that the C_β and C_γ resonances are highfield shifted up to 7.5 ppm. Unexpectedly, the shift differences of the α-C atoms were noticeable ($\Delta\delta_C$ = 4−5 ppm) only for the dppm (**9a**, **11a**), the cod complexes (**10**, **12**), and the dppe complex **11b**. Noteworthy, in complexes **9** and **11** the additional κS coordination of the P^S ligands gives rise to a further splitting of the doublet patterns of the C_α resonances into a doublet of doublets ($^3J_{P,C}/^3J_{P'',C}$). Both coupling constants were found to be in a similar range; thus they cannot clearly be assigned. Since the doublet pattern of the α-C atoms in the cod complexes remains unchanged (**10**/**12** versus **6**/**8**), it can be excluded that the additional coupling is a $^2J_{Rh,C}$ coupling constant. Surprisingly, in complexes **9a**−**c** and **11a**−**c** the signals of the γ-carbon atoms appeared as dd patterns, too, exhibiting $^1J_{P,C}$ (17.6−24.1 Hz) and $^3J_{P',C}$ (2.1−3.2 Hz; P′ is *trans* to P) couplings, whereas the C_γ resonances in the analogous neutral complexes **5** and **7** were found to be doublets due to too small $^3J_{P',C}$ constants.

2.3.3. Organorhodium Intramolecular Coordination Compounds and Bis(diphenylphosphino)methanide Rhodium Complexes. The ^{31}P NMR spectra of the intramolecular coordination compounds (Table 3) appeared as higher order ABCX spin systems in the case of the dppe derivatives **13b**/**15b** and ABMX spin systems in the case of the dppp derivatives **13c**/**15c** (A, B, C, M = ^{31}P; X = ^{103}Rh), which were analyzed by using the PERCH NMR software package;[50] see Figure 5 for an example. In the complexes **13**−**16**, having $\kappa C,\kappa P$-coordianted *P*,*S*-functionalized organyl ligands, lowfield shifts of the ^{31}P resonances (up to 43.5 ppm) and larger $^1J_{Rh,P}$ coupling constants by up to 31.3 Hz were found compared to the respective complexes **5b/c**, **6**, **7b/c**, and **8** with the corresponding κP-coordinated neutral ligands (see Tables 3 and 1). In the case of the diphosphane complexes **13** and **15** the considerably higher *trans* influence of alkyl ligands compared to the chlorido ligand is attested by a marked decrease of the $^1J_{Rh,P''}$ coupling constants (P″ is *trans* to C or Cl, respectively) by up to 68.1 Hz. Furthermore, the formation of the organorhodium intramolecular coordination compounds gives rise to lowfield shifts of the γ-C atoms (about 6 ppm) as well as of the α-carbon atoms by ca. 10 ppm. The latter appeared as dd patterns in the cod complexes (**14**, **16**) showing $^1J_{Rh,C}$ and $^2J_{P,C}$ couplings, whereas the signals of the C_α atoms in the complexes having coordinated diphosphanes (**13**, **15**) proved to be of too high multiplicity to be resolved. In the ^1H NMR spectra the most pronounced differences of **13**−**16** compared to **5**−**8** were found for the α-H signals, which were lowfield shifted by up to 0.7 ppm.

A comparison of the NMR spectra of the zwitterionic complexes **17** and **18**, bearing a $dppm_{-H}$ ligand, to those of the corresponding cationic complexes **9a** and **11a**, bearing a dppm ligand, exhibits marked highfield shifts of the P−C−P carbon atoms by 19.2 (**17**) and 16.8 ppm (**18**) as well as of the corresponding proton by 1.7 ppm in complex **17**. The ^1H resonance of the CH^- group in **18** could not be unambiguously located due to signal overlapping.

Both the $^1J_{Rh,P''}$ coupling constants (P″ is *trans* to S) and the $^1J_{Rh,P'}$ couplings (P′ is *trans* to P) were found to be diminished by, respectively, about 16 and 20 Hz compared to those of the dppm ligands in complexes **9a**/**11a** (Table 2). The only differences in the NMR parameters of the P^S ligands worth mentioning are the larger $^1J_{Rh,P}$ couplings (ca. 8 Hz) in complexes **17** and **18** compared to **9a** and **11a**.

2.4. Reactions with Carbon Monoxide. Reaction of the cationic rhodium complexes $[Rh(R_2PCH_2CH_2CH_2SPh\text{-}\kappa P,\kappa S)(P\text{^}P)][PF_6]$ (**9**, **11**) with carbon monoxide in CH_2Cl_2 at −78 °C led to the immediate formation of cationic monocarbonyl

(39) Cambridge Structural Database (ConQuest). Version 5.31; Crystallographic Data Centre, University Chemical Laboratory, Cambridge (UK), 2009.
(40) Appleton, T. G.; Clark, H. C.; Manzer, L. E. *Coord. Chem. Rev.* **1973**, *10*, 335.
(41) Chebi, D. E.; Fanwick, P. E.; Rothwell, I. P. *Organometallics* **1990**, *9*, 2948.
(42) Ohta, K.; Hashimoto, M.; Takahashi, Y.; Hikichi, S.; Akita, M.; Moro-oka, Y. *Organometallics* **1999**, *18*, 3234.
(43) Dai, C.; Robins, E. G.; Scott, A. J.; Clegg, W.; Yufit, D. S.; Howard, J. A. K.; Marder, T. B. *Chem. Commun.* **1998**, 1983.
(44) Karsch, H. H.; Reisky, M. *Eur. J. Inorg. Chem.* **1998**, 905.
(45) Mézailles, N.; Avarvari, N.; Ricard, L.; Mathey, F.; Le Floch, P. *Inorg. Chem.* **1998**, *37*, 5313.
(46) Hofmann, P.; Meier, C.; Englert, U.; Schmidt, M. U. *Chem. Ber.* **1992**, *125*, 353.
(47) Westcott, S. A.; Stringer, G.; Anderson, S.; Taylor, N. J.; Marder, T. B. *Inorg. Chem.* **1994**, *33*, 4589.
(48) Brunner, H.; Zettler, C.; Zabel, M. *Z. Anorg. Allg. Chem.* **2003**, *629*, 1131.
(49) Graham, D. E.; Lamprecht, G. J.; Potgieter, I. M.; Roodt, A.; Leipoldt, J. G. *Transition Met. Chem.* **1991**, *16*, 193.
(50) *PERCH NMR Software*, Version 1/2000; University of Kuopio, Finland, 2000.

Table 3. Selected NMR Spectroscopic Data (δ in ppm, J in Hz) of [Rh{CH(SPh)$CH_2CH_2PPh_2$-$\kappa C,\kappa P$}L_2] (13−16) and [Rh(dppm$_{-H}$-κ^2P,P')($R_2PCH_2CH_2CH_2SPh$-$\kappa P,\kappa S$)] (R = Ph, 17; R = Cy, 18)

			PhS−$C_\alpha H_n$−$C_\beta H_2$−$C_\gamma H_2$−PR_2				co-ligand L_2	
	R	L_2	$\delta_{\alpha\text{-}C}$	$\delta_{\beta\text{-}C}$[a]	$\delta_{\gamma\text{-}C}$ ($^1J_{P,C}$)	δ_P ($^1J_{Rh,P}$)	$\delta_{P'}$ ($^1J_{Rh,P'}$)[b]	$\delta_{P''}$ ($^1J_{Rh,P''}$)[c]
13b[d]	Ph	dppe	41.9−42.8	28.1	33.6 (17.1)	58.6 (162.3)	63.1 (165.9)	60.2 (123.6)
13c[d]	Ph	dppp	45.9−46.7	30.3	34.8 (24.4)	57.7 (164.6)	21.0 (162.1)	18.2 (119.1)
14[d]	Ph	cod	35.5 (16.4/4.5)[f]	28.8	31.9 (22.4)	58.6 (168.3)		
15b[d]	Cy	dppe	41.2−43.3	27.1	22.3 (18.9)	67.5 (155.2)	61.9 (159.5)	61.2 (124.6)
15c[d]	Cy	dppp	44.5−46.1	26.3	22.2 (19.6)	66.3 (156.5)	17.2 (154.5)	18.3 (120.9)
16[d]	Cy	cod	38.4 (20.6/4.0)[f]	24.0	22.5 (15.9)	63.5 (170.2)		
17[e]	Ph	dppm$_{-H}$	38.6 (7.5/3.3)[g]	22.3	28.7 (18.6)	12.8 (144.1)	−35.0 (93.6)	−24.2 (124.2)
18[e]	Cy	dppm$_{-H}$	38.2 (8.1/5.3)[g]	26.3	19.2 (13.0)	19.4 (137.7)	−33.1 (93.0)	−21.9 (129.0)

[a] The $^2J_{P,C}$ coupling constants were estimated to be <2 Hz. [b] P′ is *trans* to P of the PhSCH$_n$CH$_2$CH$_2$PR$_2$ ligand. [c] P″ is *trans* to C and S of the PhSCH$_n$CH$_2$CH$_2$PR$_2$ ligand, respectively. [d] $C_\alpha H_n$ with $n = 1$. [e] $C_\alpha H_n$ with $n = 2$. [f] $^1J_{Rh,C}/^2J_{P,C}$. [g] $^3J_{P,C}/^3J_{P'',C}$; may be reversed.

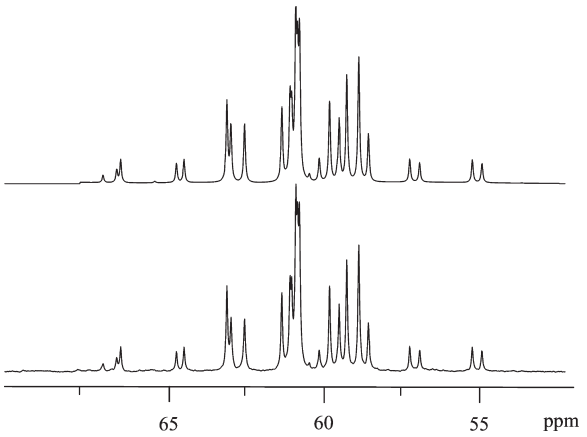

Figure 5. Simulated (above) and measured (81 MHz, below) ^{31}P NMR spectra of [Rh{CH(SPh)$CH_2CH_2PPh_2$-$\kappa C,\kappa P$}(dppe)] (**13a**). The ABC part of the ABCX spin system is shown (A, B, C = ^{31}P; X = ^{103}Rh).

rhodium complexes **19** and **20**, as revealed by NMR spectroscopic investigations (Table 4). In contrast, the analogous cod complexes **10** and **12** did not react with CO, even at room temperature. ^{13}C and ^{31}P NMR spectroscopic measurements of the reaction solutions of **19** and **20** indicated the formation of complexes of the type $[Rh(CO)(P\wedge S)(P\wedge P)]^+$. The ^{31}P NMR spectra at room temperature showed broad signals indicating molecular dynamics in solution (Table 4). All of these reactions proceed quantitatively; no other signals were found, especially none of the "free" P^P and P^S ligands. Only in the case of the dppm complexes do additional doublets at −21.1/−21.2 ppm (**19a**/**20a**) in the ^{31}P NMR spectra point to the formation of [Rh(dppm-κ^2P,P')$_2$]$^{+}$[51] as a side product. Furthermore, in the case of **19a** a doublet at 18.3 ppm is likely caused by the formation of the dinuclear rhodium(I) carbonyl complex [Rh_2(μ-Cl)(μ-CO)(dppm-1κP:2$\kappa P'$)$_2$(CO)$_2$]$^+$ as side product. This was further confirmed by a single-crystal X-ray diffraction measurement of colorless crystals obtained from the respective reaction solution, which proved to be of the same molecular structure as described in ref 52.

For **19b** it was shown that at −80 °C the above-mentioned equilibrium is frozen, showing two rhodium complexes at an intensity ratio of 3:1. Each of these complexes has coordinated three chemically inequivalent phosphorus atoms, in accord with an AEMX spin system (A, E, M = ^{31}P, X = ^{103}Rh). Thus,

Table 4. Selected NMR (δ in ppm) and IR (ν in cm^{-1}) Spectroscopic Data of Cations [Rh(CO)($R_2PCH_2CH_2CH_2SPh$)(P^P)]$^+$ (19, 20)

	R	P^P	δ_P (P^P)[a]	δ_P (P^S)[a]	δ_C (CO)	ν (CO)
19a	Ph	dppm	−25.3	29.9	190.7	1989, 2024
19b	Ph	dppe	55.9	27.3	190.1	1988, 2022
19c	Ph	dppp	6.4	24.8	190.7	1994, 2024
20a	Cy	dppm	−20.6	37.6	190.0	1994, 2025
20b	Cy	dppe	55.3	34.5	189.8	1994, 2019
20c	Cy	dppp	6.8	39.9	192.8	1994, 2022
20d	Cy	dmpe	28.4	42.1	192.2	1994, 2024

[a] Broad signals in an intensity ratio of 2:1.

for the major component three ddd coupling patterns were found, and for the minor component only one ddd resonance, whereas the other two resonances remained broad as nonresolved signals. The coordination of CO was exhibited ^{13}C NMR spectroscopically by broad signals in the typical range for a carbonyl ligands (δ_C 189.8−192.8 ppm, Table 4). Furthermore, IR spectra of reaction solutions showed two ν(CO) bands in the region of terminally bound carbonyl ligands at about 1990 and 2022 cm^{-1}, in the typical range for cationic pentacoordianted rhodium(I) phosphane carbonyl complexes.[53−55] HRMS-ESI measurements in the cationic mode did not show the molecular peaks $[M]^+$ but only the mass peaks of the decarbonylated cations $[M - CO]^+$ as the most intensive peaks (base peaks) in all cases with the exception of **20a** and **20c**. Only in the case of **20c** was the CO-containing molecular peak detected being even the base peak. In almost all spectra peaks of the bis(diphosphane)-rhodium cations $[Rh(P\wedge P)_2]^+$ were found; in the case of **20a** it is even the base peak. The NMR investigations showed these species are not present in the original solutions (with the exception of **19a**/**20a**), thus being formed during the ionization process of the HRMS-ESI experiments. All attempts to isolate complexes of type **19** and **20** failed. Evaporation of the solvent (CH_2Cl_2) in vacuo or precipitation of the complexes with nonpolar solvents such as *n*-pentane followed by filtration and drying led to decomposition with a partial reformation of the starting complexes **9** and **11**.

In order to get insight into the formation of such rhodium carbonyl complexes, quantum chemical calculations at the DFT level of theory were performed. To reduce the computational

(51) Ernsting, J. M.; Elsevier, C. J.; de Lange, W. G. J.; Timmer, K. *Magn. Reson. Chem.* **1991**, *29*, S118.
(52) Cowie, M. *Inorg. Chem.* **1979**, *18*, 286.
(53) Pignolet, L. H.; Doughty, D. H.; Nowicki, S. C.; Anderson, M. P.; Casalnuovo, A. L. *J. Organomet. Chem.* **1980**, *202*, 211.
(54) Turculet, L.; Feldman, J. D.; Tilley, T. D. *Organometallics* **2004**, *23*, 2488.
(55) Tejel, C.; Shi, Y.-M.; Ciriano, M. A.; Edwards, A. J.; Lahoz, F. J.; Modrego, J.; Oro, L. A. *J. Am. Chem. Soc.* **1997**, *119*, 6678.

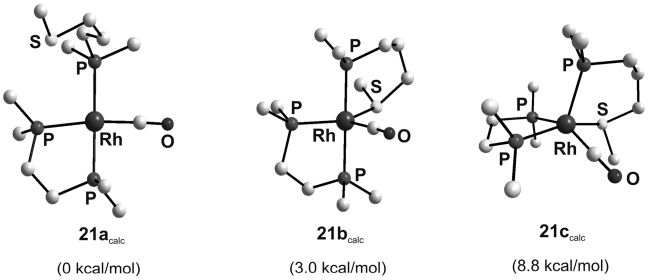

Figure 6. Calculated structures of $[Rh(CO)(Me_2PCH_2CH_2CH_2SMe)(dmpe)]^+$ having the $Me_2PCH_2CH_2CH_2SMe$ ligand bound κP (**21a**$_{calc}$) and $\kappa P,\kappa S$ (**21b**$_{calc}$, **21c**$_{calc}$). H atoms have been omitted for clarity. Energies are relative to the most stable isomer (**21a**$_{calc}$).

expense, the calculations were done by substituting the phenyl and cyclohexyl groups by methyl groups, thus calculating complexes of the type $[Rh(CO)(Me_2PCH_2CH_2CH_2SMe)(dmpe)]^+$ (**21**$_{calc}$). Three isomeric equilibrium structures could be located (Figure 6); using other starting geometries resulted in the formation of one of these equilibrium structures. In the thermodynamically most stable isomer, **21a**$_{calc}$, the rhodium atom is located in the center of a slightly distorted square-planar environment, coordinated by the dmpe-κ^2P,P', the $Me_2PCH_2CH_2CH_2SMe$-κP, and the carbonyl ligand. On the basis of the structural index τ[56] the other two isomers, **21b**$_{calc}$ and **21c**$_{calc}$, can be described as, respectively, strongly distorted trigonal-bipyramidal and square-pyramidal complexes. In these two complexes the rhodium atom has the carbonyl ligand coordinated equatorially, whereas the P^S ligand adopts an equatorial-apical (e-a) coordination, with the posphorus atoms in the apical position. While in **21b**$_{calc}$ the dmpe ligand is coordinated e-a, too, in **21c**$_{calc}$ the dmpe ligand occupies the remaining equatorial positions. Complex **21b**$_{calc}$ was found to be of a similar energy (3.0 kcal/mol) to **21a**$_{calc}$. However, complex **21c**$_{calc}$ is the thermodynamically least favorable (8.8 kcal/mol) isomer.

The carbonyl complex formation

$$[Rh(Me_2PCH_2CH_2CH_2SMe)(dmpe)]^+ (\mathbf{11d}_{calc}) + CO \rightarrow [Rh(CO)(Me_2PCH_2CH_2CH_2SMe)(dmpe)]^+ (\mathbf{21}_{calc})$$

was found to be exothermic ($\Delta E = -16.1$ kcal/mol, 0 K). Calculation of the standard Gibbs free energy considering solvent effects (CH_2Cl_2) using the polarized continuum model[57] was performed and revealed that the reaction is exergonic ($\Delta G^{\ominus} = -7.7$ kcal/mol). If the results of the DFT calculations are conveyed to the experimental findings, the dynamic equilibrium found in complexes **19** and **20** is based on an equilibrium between a four- and a five-coordinated Rh(I) complex having the P^S ligands, respectively, κP and $\kappa P,\kappa S$ coordinated (Scheme 4). Thus, the ligand is hemilabile, which might be an explanation for the—at least partial—re-formation of the starting complexes **9** and **11** when complexes **19** and **20** were attempted to be isolated.

Scheme 4. Synthesis of Cationic Rhodium Carbonyl Complexes

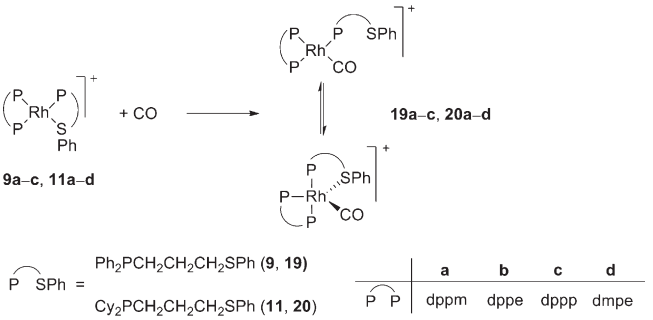

Furthermore, the corresponding calculations for the cod complex were performed. Here, five equilibrium structures of **22**$_{calc}$ were found (Figure S1, Supporting Information). The thermodynamically most stable isomer **22a**$_{calc}$ showed a square-planar geometry where the primary donor set of the rhodium atom is built up by the $Me_2PCH_2CH_2CH_2SMe$-$\kappa P,\kappa S$ ligand, the carbonyl ligand (CO is *trans* to S), and the cod ligand, which is coordinated in a monodentate fashion only. Slightly less stable (1.4 kcal/mol) is the isomer **22b**$_{calc}$, where the cod ligand is coordinated in a bidentate fashion; thus the rhodium atom exhibits a distorted square-pyramidal geometry having the sulfur atom in the apical position. The carbonyl complex formation of **22a**$_{calc}$ according to the equation

$$[Rh(Me_2PCH_2CH_2CH_2SMe\text{-}\kappa P,\kappa S)(cod)]^+ (\mathbf{10}_{calc}) + CO \rightarrow [Rh(CO)(Me_2PCH_2CH_2CH_2SMe\text{-}\kappa P,\kappa S)(cod)]^+ (\mathbf{22a}_{calc})$$

was calculated to be exothermic ($\Delta E = -10.4$ kcal/mol, 0 K) but only slightly exergonic ($\Delta G^{\ominus} = -1.4$ kcal/mol) under standard conditions considering solvent effects (CH_2Cl_2). This value lies within the margin of error of DFT calculations and must not be exaggerated; experimentally the cod complexes **10** and **12**, which differ from **10**$_{calc}$ in that the P^S ligand has Ph_2P/Cy_2P and SPh substituents, were not found to react with CO.

2.5. Conclusions. Reactions of dinuclear chlorido-bridged rhodium(I) complexes $[(RhL_2)_2(\mu\text{-}Cl)_2]$ with phosphino-functionalized sulfides $PhSCH_2CH_2CH_2PR_2$ afford mononuclear complexes of type **I** (Scheme 5) bearing κP-coordinated P^S ligands. These reactions go along with a cleavage of the Rh−Cl−Rh bridges and formation of Rh−P bonds, as demonstrated in numerous reactions described in the literature.[58] Reactions of these complexes with LDA (**I** → **II**) lead to a regioselective deprotonation of the α-carbon atom under formation of organorhodium intramolecular coordination compounds. This is noteworthy since the deprotonation of the "free" ligands proceeds nonregioselectively (α- versus *ortho*-metalation).[28,59] The intramolecular coordination compounds **II** are much more stable than rhodium complexes bearing nonfunctionalized alkyl ligands[60,61] because decomposition reactions such as hydride eliminations are hampered for stereoelectronic reasons. Reactions of LDA with **I** bearing dppm as a ligand result in formation of type **III** complexes

(56) Addison, A. W.; Rao, T. N.; Reedijk, J.; van Rijn, J.; Verschoor, G. C. *J. Chem. Soc., Dalton Trans.* **1984**, 1349.
(57) (a) Cancès, E.; Mennucci, B.; Tomasi, J. *J. Chem. Phys.* **1997**, *107*, 3032. (b) Cossi, M.; Barone, V.; Mennucci, B.; Tomasi, J. *Chem. Phys. Lett.* **1998**, *286*, 253. (c) Mennucci, B.; Tomasi, J. *J. Chem. Phys.* **1997**, *106*, 5151.
(58) Hughes, R. P. In *Comprehensive Organometallic Chemistry*; Wilkinson, G.; Stone, F. G. A.; Abel, E. W., Eds.; Pergamon: Oxford, 1982; Vol. 5, p 277.
(59) Linnert, M.; Bruhn, C.; Rüffer, T.; Schmidt, H.; Steinborn, D. *Organometallics* **2004**, *23*, 3668.

Scheme 5. Reactivity of Rhodium Complexes with P^S Ligands toward Bases, Chloride Acceptors, and Carbon Monoxide

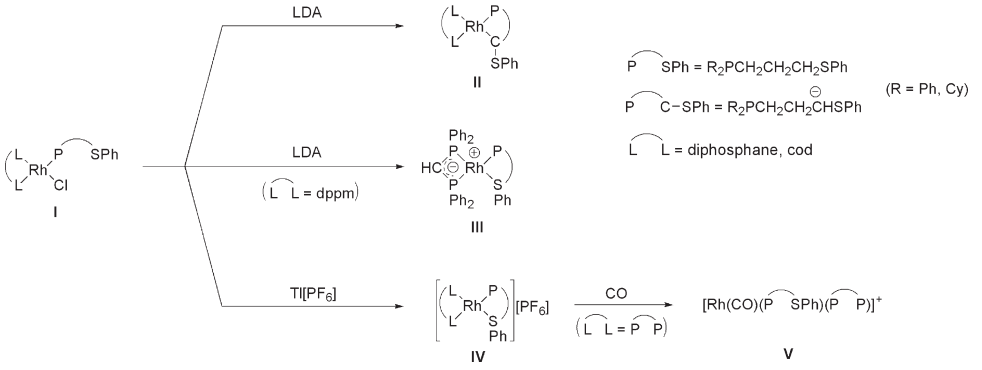

having bound an anionic dppm$_{-H}$-κ^2P,P' ligand and a γ-phosphino-functionalized thioether ligand ($\kappa P,\kappa S$ coordinated), as well. These neutral complexes have a formal charge separation between a cationic metal center and a negatively charged ligand; thus they are zwitterionic (betaine-like) complexes,[62] which might make them attractive in homogeneous catalysis.[63−65] The formation of these dppm$_{-H}$ complexes (type **III**) proceeds under kinetic control because the respective (calculated) organorhodium intramolecular coordination compound bearing a (nondeprotonated) dppm ligand of type **II** was found to be more stable by more than 20 kcal/mol. Apart from [Rh(dppm$_{-H}$-κ^2P,P')(dppm-κ^2P,P')],[41] complex **18**·THF is the only one structurally characterized rhodium type **III** complex. Reactions of the neutral rhodium(I) complexes with Tl[PF$_6$] (**I** → **IV**) afford cationic Rh(I) complexes having the phoshino-functionalized propyl phenyl sulfide ligands bound in $\kappa P,\kappa S$ mode.

Rhodium complexes bearing P^S ligands were often found to react with CO under formation of rhodium carbonyl complexes.[66] Here, the complexes with a cod ligand show no reaction, and those having diphosphanes as ligands (P^P) are found to react with CO (**IV** → **V**), yielding monocarbonyl complexes that are in a dynamic equilibrium at room temperature. DFT calculations indicated that this equilibrium is between two constitutional isomers having the P^S ligand bound monodentately κP and bidentately $\kappa P,\kappa S$, respectively. This reflects a hemilabile behavior of such P^S ligand, as also found in other transition metal complexes.[67,68] On the basis of all these findings, the reactivity of rhodium(I) complexes bearing κP-coordinated phosphino-functionalized propyl phenyl sulfide ligands toward deprotonation and reaction with Tl[PF$_6$] can be understood. Moreover, an easy access to organorhodium intramolecular coordination compounds, zwitterionic rhodium complexes, and rhodium complexes bearing hemilabile $\kappa P,\kappa S$-coordinated ligands was found.

3. Experimental Part

3.1. General Comments. All reactions and manipulations were carried out under argon using standard Schlenk techniques. Diethyl ether, toluene, *n*-pentane, and THF were dried over Na/benzophenone and freshly distilled prior to use. NMR spectra (^{1}H, ^{13}C, ^{31}P) were recorded at 27 °C on Varian Gemini 200, VXR 400, and Unity 500 spectrometers. Chemical shifts are relative to solvent signals ($CDCl_3$, δ_H 7.24, δ_C 77.0; CD_2Cl_2, δ_H 5.32, δ_C 53.8; C_6D_6, δ_H 7.15, δ_C 128.0; THF-d_8, δ_H 1.73/3.58, δ_C 25.4/67.6) as internal references; $\delta(^{19}F)$ is relative to external CCl_3F; $\delta(^{31}P)$ is relative to external H_3PO_4 (85%). Multiplets in NMR spectra of higher order resulting in pseudodoublets and pseudotriplets are denoted by "d" and "t", respectively; the distance between the outer lines is given as *N*. Coupling constants $J_{P,P}$ and $J_{P,Rh}$ from higher order multiplets ("m") were obtained by using the PERCH NMR software package.[50] For couplings in ring systems only the shortest coupling path is given. Microanalyses (C, H, N) were performed in the Microanalytical Laboratory of the University of Halle using a CHNS-932 (LECO) elemental analyzer. The high-resolution ESI mass spectra were obtained from a Bruker Apex III Fourier transform ion cyclotron resonance (FT-ICR) mass spectrometer (Bruker Daltonics) equipped with an Infinity cell, a 7.0 T superconducting magnet (Bruker), a rf-only hexapole ion guide, and an external APOLLO electrospray ion source (Agilent, off-axis spray). The sample solutions were introduced continuously via a syringe pump with a flow rate of 120 μL h^{-1}. [{Rh(cod)}$_2$(μ-Cl)$_2$] (**3**) and [{Rh(P^P)}$_2$(μ-Cl)$_2$] (**4a**−**d**) were prepared according to literature procedures.[29,69−71] Details of the preparation of starting compounds **1** and **2** and a complete set of their NMR spectroscopic data are given in the Supporting Information.

3.2. Preparation of [RhCl($R_2PCH_2CH_2CH_2SPh$-κP)L$_2$] (5−8). Route A. To a stirred suspension of the respective rhodium complex [(RhL$_2$)(μ-Cl)$_2$)] (**3**, **4**; 0.25 mmol) in THF (3 mL) was added a solution of $R_2PCH_2CH_2CH_2SPh$ (**1**, **2**; 0.50 mmol) in THF (2 mL), and the mixture was stirred for 1 h. The solution was concentrated under reduced pressure almost to dryness before *n*-pentane (5 mL) was added. The resulting precipitate was filtered off, washed with *n*-pentane (3 × 2 mL), and dried in vacuo.

Route B. To a stirred solution of [{Rh(cod)}$_2$(μ-Cl)$_2$] (123.3 mg, 0.25 mmol) in THF (3 mL) was added a solution of $R_2PCH_2CH_2CH_2SPh$ (**1**, **2**; 0.50 mmol) in THF (2 mL), and the mixture was stirred for 1 h. The respective diphosphane (0.50 mmol) in

(60) Cundy, C. S.; Lappert, M. F.; Pearce, R. *J. Organomet. Chem.* **1973**, *59*, 161.
(61) Keim, W. *J. Organomet. Chem.* **1968**, *14*, 179.
(62) Stradiotto, M.; Hesp, K. D.; Lundgren, R. J. *Angew. Chem., Int. Ed.* **2010**, *49*, 494.
(63) Stradiotto, M.; Cipot, J.; McDonald, R. *J. Am. Chem. Soc.* **2003**, *125*, 5618.
(64) Cipot, J.; McDonald, R.; Stradiotto, M. *Chem. Commun.* **2005**, 4932.
(65) Cipot, J.; Vogels, C. M.; McDonald, R.; Westcott, S. A.; Stradiotto, M. *Organometallics* **2006**, *25*, 5965.
(66) Yoo, H.; Mirkin, C. A.; DiPasquale, A. G.; Rheingold, A. L.; Stern, C. L. *Inorg. Chem.* **2008**, *47*, 9727.
(67) Ulmann, P. A.; Mirkin, C. A.; DiPasquale, A. G.; Liable-Sands, L. M.; Rheingold, A. L. *Organometallics* **2009**, *28*, 1068.
(68) Brown, A. M.; Ovchinnikov, M. V.; Mirkin, C. A. *Angew. Chem., Int. Ed.* **2005**, *44*, 4207.
(69) Cramer, R. *Inorg. Synth.* **1990**, *28*, 86.
(70) Cao, P.; Wang, B.; Zhang, X. *J. Am. Chem. Soc.* **2000**, *122*, 6490.
(71) Fairlie, D. P.; Bosnich, B. *Organometallics* **1988**, *7*, 936.

THF (3 mL) was added, and the reaction mixture was stirred for 5 h. The solution was concentrated under reduced pressure almost to dryness before *n*-pentane (5 mL) was added. The resulting precipitate was filtered off, washed with *n*-pentane (5 × 1 mL), and dried in vacuo.

R = Ph, L$_2$ = P^P = dppm (5a). Yield: 213 mg (50%, route A). Anal. Found: C, 64.68; H, 5.04. Calcd for $C_{46}H_{42}ClP_3SRh$ (858.19): C, 64.39; H, 4.93. ^{1}H NMR (400 MHz, THF-d_8): δ 2.03 (m, 2H, $CH_2CH_2CH_2$), 2.41 (m, 2H, $CH_2CH_2CH_2PPh_2$), 2.98 ("t", N = 14.3 Hz, 2H, CH_2SPh), 3.93 ("t", N = 19.2 Hz, 2H, $PPh_2CH_2PPh_2$), 7.00−7.48 (m, 35H, H_{Ph}). ^{13}C NMR (100 MHz, THF-d_8): δ 26.6 (d, $^2J(^{13}C, ^{31}P)$ = 3.9 Hz, $CH_2CH_2CH_2$), 28.0 (d, $^1J(^{13}C, ^{31}P)$ = 21.5 Hz, $CH_2CH_2CH_2PPh_2$), 35.3 (d, $^3J(^{13}C, ^{31}P)$ = 15.0 Hz, CH_2SPh), 50.4 ("t", N = 43.9 Hz, $PPh_2CH_2PPh_2$), 125.9−138.3 (C_{Ph}). ^{31}P NMR (81 MHz, THF-d_8): δ −42.1 (m, $^2J(^{31}P, ^{31}P)$ = 98.8 Hz, $^2J(^{31}P, ^{31}P)$ = 388.5 Hz, $^1J(^{31}P, ^{103}Rh)$ = 118.9 Hz, *P* (dppm) *trans* to *P*), −15.8 (m, $^2J(^{31}P, ^{31}P)$ = 31.5 Hz, $^2J(^{31}P, ^{31}P)$ = 98.8 Hz, $^1J(^{31}P, ^{103}Rh)$ = 156.2 Hz, *P* (dppm) *trans* to *Cl*), 23.1 (m, $^2J(^{31}P, ^{31}P)$ = 31.5 Hz, $^2J(^{31}P, ^{31}P)$ = 388.5 Hz, $^1J(^{31}P, ^{103}Rh)$ = 133.3 Hz, PPh_2).

R = Ph, L$_2$ = P^P = dppe (5b). Yield: 393 mg (90%, route B). Anal. Found: C, 64.40; H, 5.15. Calcd for $C_{47}H_{44}ClP_3SRh$ (872.22): C, 64.73; H, 5.09. ^{1}H NMR (400 MHz, THF-d_8): δ 1.77−1.89/2.36−2.10 (m/m, 4H, $PPh_2CH_2CH_2PPh_2$), 2.05−2.07 (m, $CH_2CH_2CH_2$), 2.42 (m, 2H, $CH_2CH_2CH_2PPh_2$), 2.96 ("t", N = 14.5 Hz, 2H, CH_2SPh), 6.94−8.07 (m, 35H, H_{Ph}). ^{13}C NMR (100 MHz, THF-d_8): δ 26.5/35.8 (m/m, $Ph_2PCH_2CH_2PPh_2$), 27.2 (d, $^2J(^{13}C, ^{31}P)$ = 4.8 Hz, $CH_2CH_2CH_2$), 28.4 (d, $^1J(^{13}C, ^{31}P)$ = 22.7 Hz, $CH_2CH_2CH_2PPh_2$), 35.4 (d, $^3J(^{13}C, ^{31}P)$ = 15.8 Hz, CH_2SPh), 126.0−138.4 (C_{Ph}). ^{31}P NMR (81 MHz, THF-d_8): δ 23.8 (ddd, $^2J(^{31}P, ^{31}P)$ = 357.2 Hz, $^2J(^{31}P, ^{31}P)$ = 35.6 Hz, $^1J(^{31}P, ^{103}Rh)$ = 131.6 Hz, PPh_2), 56.8 (ddd, $^2J(^{31}P, ^{31}P)$ = 357.2 Hz, $^2J(^{31}P, ^{31}P)$ = 33.6 Hz, $^1J(^{31}P, ^{103}Rh)$ = 141.6 Hz, *P* (dppe) *trans* to *P*), 73.9 (ddd, $^2J(^{31}P, ^{31}P)$ = 33.6 Hz, $^2J(^{31}P, ^{31}P)$ = 35.6 Hz, $^1J(^{31}P, ^{103}Rh)$ = 183.2 Hz, *P* (dppe) *trans* to *Cl*).

R = Ph, L$_2$ = P^P = dppp (5c). Yield: 355 mg (80%, route B). Anal. Found: C, 64.64; H, 5.16. Calcd for $C_{48}H_{46}ClP_3SRh$ (886.25): C, 65.06; H, 5.23. ^{1}H NMR (400 MHz, THF-d_8): δ 1.63−1.78 (m, 2H, $PPh_2CH_2CH_2CH_2PPh_2$), 2.08 (m, 6H, $PhSCH_2CH_2CH_2PPh_2$, $PhSCH_2CH_2$), 2.24 (m, 2H, $PhSCH_2CH_2CH_2$), 2.95 ("t", N = 14.4 Hz, 2H, CH_2SPh), 6.82−7.90 (m, 35H, H_{Ph}). ^{13}C NMR (100 MHz, THF-d_8): δ 20.5 (s, br, $PPh_2CH_2CH_2CH_2PPh_2$), 27.6 (d, $^2J(^{13}C, ^{31}P)$ = 5.5 Hz, $PhSCH_2CH_2$), 27.8/32.7 (m/m, $PPh_2CH_2CH_2CH_2PPh_2$), 29.0 (d, $^1J(^{13}C, ^{31}P)$ = 24.2 Hz, $PhSCH_2CH_2CH_2$), 35.4 (d, $^3J(^{13}C, ^{31}P)$ = 16.1 Hz, CH_2SPh), 125.9−138.7 (C_{Ph}). ^{31}P NMR (81 MHz, THF-d_8): δ 12.3 (ddd, $^2J(^{31}P, ^{31}P)$ = 351.5 Hz, $^2J(^{31}P, ^{31}P)$ = 55.5 Hz, $^1J(^{31}P, ^{103}Rh)$ = 133.3 Hz, *P* (dppp) *trans* to *P*), 25.5 (ddd, $^2J(^{31}P, ^{31}P)$ = 351.5 Hz, $^2J(^{31}P, ^{31}P)$ = 53.9 Hz, $^1J(^{31}P, ^{103}Rh)$ = 133.3 Hz, PPh_2), 34.5 (ddd, $^2J(^{31}P, ^{31}P)$ = 55.5 Hz, $^2J(^{31}P, ^{31}P)$ = 53.9 Hz, $^1J(^{31}P, ^{103}Rh)$ = 176.4 Hz, *P* (dppp) *trans* to *Cl*).

R = Ph, L$_2$ = cod (6). Yield: 248 mg (85%, route A). Anal. Found: C, 58.32; H, 5.51. Calcd for $C_{29}H_{33}PClSRh$ (582.98): C, 58.75; H, 5.71. ^{1}H NMR (400 MHz, $CDCl_3$): δ 1.87−1.93/2.28−2.35 (m/m, 4H/4H, 4 × CH_2, cod), 2.15−2.25 (m, 2H, $CH_2CH_2CH_2$), 2.61−2.67 (m, 2H, CH_2PPh_2), 3.10 (m, 2H, CH_2SPh), 4.15 (s, br, 4H, 4 × CH, cod), 7.14−7.59 (m, 15H, H_{Ph}). ^{13}C NMR (100 MHz, $CDCl_3$): δ 25.9 (s, $CH_2CH_2CH_2$), 26.9 (d, $^1J(^{13}C, ^{31}P)$ = 25.2 Hz, CH_2PPh_2), 31.0 (s, br, 4 × CH_2, cod), 35.4 (d, $^3J(^{13}C, ^{31}P)$ = 15.0 Hz, CH_2SPh), 78.6−78.9 (m, 4 × CH, cod), 126.2−133.5 (C_{Ph}). ^{31}P NMR (81 MHz, $CDCl_3$): δ 26.2 (d, $^1J(^{31}P, ^{103}Rh)$ = 147.1 Hz, PPh_2).

R = Cy, L$_2$ = P^P = dppm (7a). Yield: 369 mg (85%, route A). Anal. Found: C, 63.22 H, 6.29. Calcd for $C_{51}H_{60}ClP_3SRh$ (871.29): C, 63.41; H, 6.36. ^{1}H NMR (400 MHz, THF-d_8): δ 0.97−2.04 (m, 26H, $PCy_2/CH_2CH_2CH_2PCy_2$), 2.73 ("t", 2H, CH_2SPh), 3.92 ("t", 2H, $Ph_2PCH_2PPh_2$), 7.06−7.99 (m, 25H, H_{Ph}). ^{13}C NMR (100 MHz, THF-d_8): δ 22.7 (d, $^1J(^{13}C, ^{31}P)$ = 13.9 Hz, CH_2PCy_2), 26.4 (s, $CH_2CH_2CH_2$), 27.4 (s, *C4*, PCy_2), 30.1/30.8 (s/d, $J(^{13}C, ^{31}P)$ = 3.4 Hz, *C2*/*C3*, PCy_2), 34.5 (d, $^1J(^{13}C, ^{31}P)$ = 17.5 Hz, *C1*, PCy_2), 35.5 (d, $^3J(^{13}C, ^{31}P)$ = 11.9 Hz, CH_2SPh), 51.3 ("t", $Ph_2PCH_2PPh_2$), 126.0−137.9 (C_{Ph}). ^{31}P NMR (81 MHz, THF-d_8): δ −42.0 (ddd, $^2J(^{31}P, ^{31}P)$ = 98.1 Hz, $^2J(^{31}P, ^{31}P)$ = 374.6 Hz, $^1J(^{31}P, ^{103}Rh)$ = 115.5 Hz, *P* (dppm) *trans* to *P*), −14.7 (ddd, $^2J(^{31}P, ^{31}P)$ = 32.7 Hz, $^2J(^{31}P, ^{31}P)$ = 98.1 Hz, $^1J(^{31}P, ^{103}Rh)$ = 161.1 Hz, *P* (dppm) *trans* to *Cl*), 25.6 (ddd, $^2J(^{31}P, ^{31}P)$ = 32.7 Hz, $^2J(^{31}P, ^{31}P)$ = 374.6 Hz, $^1J(^{31}P, ^{103}Rh)$ = 131.4 Hz, PCy_2).

R = Cy, L$_2$ = P^P = dppe (7b). Yield: 213 mg (48%, route B). Anal. Found: C, 63.34 H, 6.55. Calcd for $C_{47}H_{57}ClP_3SRh$ (885.33): C, 63.77; H, 6.49. ^{1}H NMR (400 MHz, THF-d_8): δ 0.97−2.21 (m, 30H, $PCy_2/Py_2PCH_2CH_2CH_2/Ph_2PCH_2CH_2PPh_2$), 2.58 ("t", 2H, CH_2SPh), 7.84−8.06 (m, 25H, H_{Ph}). ^{13}C NMR (100 MHz, THF-d_8): δ 21.0 (d, $^1J(^{13}C, ^{31}P)$ = 15.2 Hz, CH_2PCy_2), 25.1/35.4 (m/m, $Ph_2PCH_2CH_2PPh_2$), 25.8 (s, $CH_2CH_2CH_2$), 26.6 (s, *C4*, PCy_2), 29.5/30.6 (s/d, $J(^{13}C, ^{31}P)$ = 2.7 Hz *C3*/*C2*, PCy_2), 34.4 (d, $^1J(^{13}C, ^{31}P)$ = 17.7 Hz, *C1*, PCy_2), 34.8 (d, $^3J(^{13}C, ^{31}P)$ = 12.6 Hz, CH_2SPh), 125.3−137.1 (C_{Ph}). ^{31}P NMR (81 MHz, THF-d_8): δ 24.0 (ddd, $^2J(^{31}P, ^{31}P)$ = 35.5 Hz, $^2J(^{31}P, ^{31}P)$ = 342.9 Hz, $^1J(^{31}P, ^{103}Rh)$ = 127.5 Hz, PCy_2), 58.9 (ddd, $^2J(^{31}P, ^{31}P)$ = 32.6 Hz, $^2J(^{31}P, ^{31}P)$ = 342.9 Hz, $^1J(^{31}P, ^{103}Rh)$ = 135.4 Hz, *P* (dppe) *trans* to *P*), 71.2 (ddd, $^2J(^{31}P, ^{31}P)$ = 32.6 Hz, $^2J(^{31}P, ^{31}P)$ = 35.5 Hz, $^1J(^{31}P, ^{103}Rh)$ = 192.7 Hz, *P* (dppm) *trans* to *Cl*).

R = Cy, L$_2$ = P^P = dppp (7c). Yield: 216 mg (48%, route A). Anal. Found: C, 64.33 H, 6.52. Calcd for $C_{48}H_{59}ClP_3SRh$ (899.34): C, 64.11; H, 6.61. ^{1}H NMR (400 MHz, benzene-d_6): δ 0.95−2.28 (m, 32H, $Cy_2PCH_2CH_2/Ph_2PCH_2CH_2CH_2PPh_2$), 2.65 ("t", 2H, CH_2SPh), 7.87−7.98 (m, 25H, H_{Ph}). ^{13}C NMR (100 MHz, benzene-d_6): δ 19.2 (s, $Ph_2PCH_2CH_2CH_2PPh_2$), 20.2 (d, $^1J(^{13}C, ^{31}P)$ = 15.7 Hz, CH_2PCy_2), 25.9 (s, CH_2CH_2SPh), 26.1/31.5 (m/m, $Ph_2PCH_2CH_2CH_2PPh_2$), 26.6 (s, *C4*, PCy_2), 29.8/31.1 (s/s, *C2*/*C3*, PCy_2), 34.9 (d, $^3J(^{13}C, ^{31}P)$ = 13.9 Hz, CH_2SPh), 35.0 (d, $^1J(^{13}C, ^{31}P)$ = 16.7 Hz *C1*, PCy_2), 125.3−138.2 (C_{Ph}). ^{31}P NMR (81 MHz, benzene-d_6): δ 12.4 (ddd, $^2J(^{31}P, ^{31}P)$ = 56.2 Hz, $^2J(^{31}P, ^{31}P)$ = 338.6 Hz, $^1J(^{31}P, ^{103}Rh)$ = 129.1 Hz, *P* (dppp) *trans* to *P*), 24.6 (ddd, $^2J(^{31}P, ^{31}P)$ = 35.7 Hz, $^2J(^{31}P, ^{31}P)$ = 338.7 Hz, $^1J(^{31}P, ^{103}Rh)$ = 128.4 Hz, PCy_2), 32.3 (ddd, $^2J(^{31}P, ^{31}P)$ = 35.7 Hz, $^2J(^{31}P, ^{31}P)$ = 56.2 Hz, $^1J(^{31}P, ^{103}Rh)$ = 184.4 Hz, *P* (dppp) *trans* to *Cl*).

R = Cy, L$_2$ = P^P = dmpe (7d). Yield: 251 mg (79%, route A). Anal. Found: C, 50.43 H, 7.76. Calcd for $C_{27}H_{49}ClP_3SRh$ (637.04): C, 50.91; H, 7.75. ^{1}H NMR (400 MHz, THF-d_8): δ 1.10−2.05 (m, 22H, PCy_2), 1.37/1.43 (d/d, $^2J(^1H, ^{31}P)$ = 8.1/9.3 Hz, 12H, PCH_3), 1.66 (m, 2H, CH_2PCy_2), 1.73 (m, 4H, $Me_2PCH_2CH_2PMe_2$), 1.86 (m, 2H, $CH_2CH_2CH_2$), 3.07 (m, 2H, CH_2SPh), 7.09 (m, 1H, *p-H*, SPh), 7.23 (m, 2H, *m-H*, SPh), 7.34 (m, 2H, *o-H*, SPh). ^{13}C NMR (100 MHz, THF-d_8): δ 14.7/19.8 (d/d, $^1J(^{13}C, ^{31}P)$ = 24.3 Hz/$^1J(^{13}C, ^{31}P)$ = 22.9 Hz, PCH_3), 22.4 (d, $^1J(^{13}C, ^{31}P)$ = 14.6 Hz, CH_2PCy_2), 26.1/35.6 (m/m, $Me_2PCH_2CH_2PMe_2$), 27.0 (s, $CH_2CH_2CH_2$), 27.6 (s, *C4*, PCy_2), 30.4/31.4 (s/d, $J(^{13}C, ^{31}P)$ = 3.6 Hz, *C3*/*C2*, PCy_2), 35.7 (d, $^3J(^{13}C, ^{31}P)$ = 12.4 Hz, CH_2SPh), 36.2 (d, $^1J(^{13}C, ^{31}P)$ = 16.8 Hz, *C1*, PCy_2), 126.0 (s, *p-C*, SPh), 129.4 (s, *m-C*, SPh), 129.5 (s, *o-C*, SPh), 138.1 (s, *i-C*, SPh). ^{31}P NMR (81 MHz, THF-d_8): δ 27.2 (ddd, $^2J(^{31}P, ^{31}P)$ = 351.6 Hz, $^2J(^{31}P, ^{31}P)$ = 34.1 Hz, $^1J(^{31}P, ^{103}Rh)$ = 128.1 Hz, PCy_2), 40.5 (ddd, $^2J(^{31}P, ^{31}P)$ = 34.1 Hz, $^2J(^{31}P, ^{31}P)$ = 34.2 Hz, $^1J(^{31}P, ^{103}Rh)$ = 182.4 Hz, *P* (dmpe) *trans* to *Cl*), 46.8 (ddd, $^2J(^{31}P, ^{31}P)$ = 34.2 Hz, $^2J(^{31}P, ^{31}P)$ = 351.6 Hz, $^1J(^{31}P, ^{103}Rh)$ = 131.7 Hz, *P* (dmpe) *trans* to *P*).

R = Cy, L$_2$ = cod (8). Yield: 154 mg (52%, route A). Anal. Found: C, 58.66 H, 7.57. Calcd for $C_{29}H_{45}ClPSRh$ (595.07): C, 58.53; H, 7.62. ^{1}H NMR (200 MHz, THF-d_8): δ 0.98−1.22/1.36−1.75/2.05−2.18 (m/m/m, 34H, $CH_2CH_2CH_2PCy_2$/4 × CH_2, cod), 2.64 (m, 2H, CH_2SPh), 3.46/5.58 (s/s, br/br, 2H/2H, 4 × CH (cod)), 6.83−6.87 (m, 1H, *p-H*, SPh), 6.95−7.00 (m, 2H, *m-H*, SPh), 7.20−7.22 (m, 2H, *o-H*, SPh). ^{13}C NMR (100 MHz, THF-d_8): δ 17.2 (d, $^1J(^{13}C, ^{31}P)$=17.0 Hz, CH_2PCy_2), 24.9 (s, $CH_2CH_2CH_2$), 26.5 (s, br, 4 × CH_2, cod), 27.4 (s, *C4*,

PCy_2), 27.5 (d, $^2J(^{13}C, ^{31}P) = 4.7$ Hz, *C2*, PCy_2), 29.8 (d, $^3J(^{13}C, ^{31}P) = 19.4$ Hz, *C3*, PCy_2), 33.9 (d, $^1J(^{13}C, ^{31}P) = 21.0$ Hz, *C1*, PCy_2), 35.0 (d, $^3J(^{13}C, ^{31}P) = 11.3$ Hz, CH_2SPh), 67.3/103.1 (m/m, $4 \times CH$, cod), 126.0 (s, *p-C*, SPh), 129.1 (s, *m-C*, SPh), 129.3 (s, *o-C*, SPh), 136.4 (s, *i-C*, SPh). ^{31}P NMR (81 MHz, THF-d_8): δ 23.7 (d, $^1J(^{31}P, ^{103}Rh) = 144.5$ Hz, PCy_2).

3.3. Preparation of [Rh($R_2PCH_2CH_2CH_2SPh$-$\kappa P,\kappa S$)L_2][PF_6] (9−12). Route A. To the respective rhodium complex [(RhL_2)-(μ-Cl)$_2$)] (**3**, **4**; 0.25 mmol) in THF (3 mL) was added a solution of $R_2PCH_2CH_2CH_2SPh$ (**1**, **2**; 0.50 mmol) in THF (2 mL), and the mixture was stirred for 1 h. Then Tl[PF_6] (174.68 mg, 0.5 mmol) suspended in THF (3 mL) was added. The mixture was stirred for 30 min, and the precipitated TlCl was filtered off. The filtrate was reduced almost to dryness, and *n*-pentane (3 mL) was added. The precipitated solid was filtered off, washed with *n*-pentane (3 × 3 mL), and dried in vacuo.

Route B. To a stirred solution of [{Rh(cod)}$_2$(μ-Cl)$_2$] (123.3 mg, 0.25 mmol) in THF (5 mL) was added a solution of $R_2PCH_2CH_2CH_2SPh$ (**1**, **2**; 0.50 mmol) in THF (2 mL), and the mixture was stirred for 1 h before the respective diphosphane (0.50 mmol) dissolved in THF (3 mL) was added slowly. After 5 h Tl[PF_6] (174.68 mg, 0.5 mmol) suspended in THF (3 mL) was added, and the mixture was stirred for 30 min. The precipitated TlCl was filtered off, the filtrate was reduced almost to dryness, and *n*-pentane (3 mL) was added. The precipitated solid was filtered off, washed with *n*-pentane (3 × 5 mL), and dried in vacuo.

R = Ph, L_2 = P^P = dppm (9a). Yield: 411 mg (85%, route A). HRMS (ESI): *m*/*z* calcd for $[C_{46}H_{43}P_3RhS]^+$ 823.1348; found for $[M]^+$ 823.1359. ^1H NMR (500 MHz, CD_2Cl_2): δ 2.00−2.09 (m, 2H, $CH_2CH_2CH_2$), 2.53 (s, br, 2H, $Ph_2PCH_2CH_2$), 3.21 (m, 2H, $PhSCH_2$), 4.01 ("t", $N = 19.8$ Hz, 2H, $Ph_2PCH_2PPh_2$), 6.76−7.49 (m, 35H, H_{Ph}). ^{13}C NMR (125 MHz, CD_2Cl_2): δ 22.8 (s, br, $CH_2CH_2CH_2$), 27.2 (dd, $^1J(^{13}C, ^{31}P) = 21.9$ Hz, $^3J(^{13}C, ^{31}P_{trans}) = 2.1$ Hz, $Ph_2PCH_2CH_2$), 40.3 (dd, $^3J(^{13}C, ^{31}P)/^3J(^{13}C, ^{31}P_{trans}) = 4.8/2.0$ Hz (the two coupling constants given may be reversed here and also in complexes **9b**/**c** and **11b**/**c**), $PhSCH_2$), 50.8 ("t", $N = 45.0$ Hz, $Ph_2PCH_2PPh_2$), 128.3−135.2 (C_{Ph}). ^{31}P NMR (81 MHz, CD_2Cl_2): δ −142.7 (sept, $^1J(^{31}P, ^{19}F) = 709.5$ Hz, PF_6^-), −30.8 (ddd, $^2J(^{31}P, ^{31}P) = 87.6$ Hz, $^2J(^{31}P, ^{31}P) = 290.5$ Hz, $^1J(^{31}P, ^{103}Rh) = 113.8$ Hz, *P* (dppm) *trans* to *P*), −18.3 (ddd, $^2J(^{31}P, ^{31}P) = 32.0$ Hz, $^2J(^{31}P, ^{31}P) = 87.6$ Hz, $^1J(^{31}P, ^{103}Rh) = 140.8$ Hz, *P* (dppm) *trans* to *S*), 10.3 (ddd, $^2J(^{31}P, ^{31}P) = 32.0$ Hz, $^2J(^{31}P, ^{31}P) = 290.5$, $^1J(^{31}P, ^{103}Rh) = 131.4$ Hz, PPh_2). ^{19}F NMR (188 MHz, CD_2Cl_2): δ −73.4 (d, $^1J(^{19}F, ^{31}P) = 709.5$ Hz, PF_6^-).

R = Ph, L_2 = P^P = dppe (9b). Yield: 432 mg (88%, route B). HRMS (ESI): *m*/*z* calcd for $[C_{47}H_{45}P_3RhS]^+$ 837.1504, found for $[M]^+$ 837.1490. ^1H NMR (500 MHz, CD_2Cl_2): δ 1.89−2.00/2.09−2.32 (m 4H, $PH_2PCH_2CH_2PPh_2$), 1.98−2.05 (m, 2H, $CH_2CH_2CH_2$), 2.32 (m, 2H, $Ph_2PCH_2CH_2CH_2$), 2.91 (m, 2H, $PhSCH_2$), 6.85−7.63 (m, 35H, H_{Ph}). ^{13}C NMR (125 MHz, CD_2Cl_2): δ 21.5 (s, $CH_2CH_2CH_2$), 26.0 (dd, $^1J(^{13}C, ^{31}P) = 24.1$ Hz, $^3J(^{13}C, ^{31}P_{trans}) = 2.1$ Hz, $Ph_2PCH_2CH_2$), 27.6−27.9/32.9−33.3 (m/m, $Ph_2PCH_2CH_2PPh_2$), 36.3 (dd, $^3J(^{13}C, ^{31}P)/^3J(^{13}C, ^{31}P_{trans}) = 8.7/3.7$ Hz, $PhSCH_2$), 128.3−133.4 (C_{Ph}). ^{31}P NMR (81 MHz, CD_2Cl_2): δ −142.3 (sept, $^1J(^{31}P, ^{19}F) = 710.3$ Hz, PF_6^-), 7.2 (ddd, $^2J(^{31}P, ^{31}P) = 33.4$ Hz, $^2J(^{31}P, ^{31}P) = 286.2$ Hz, $^1J(^{31}P, ^{103}Rh) = 130.0$ Hz, PPh_2), 59.9 (ddd, $^2J(^{31}P, ^{31}P) = 31.5$ Hz, $^2J(^{31}P, ^{31}P) = 286.2$ Hz, $^1J(^{31}P, ^{103}Rh) = 128.7$ Hz, *P* (dppe) *trans* to *P*), 66.8 (ddd, $^2J(^{31}P, ^{31}P) = 31.5$ Hz, $^2J(^{31}P, ^{31}P) = 33.4$, $^1J(^{31}P, ^{103}Rh) = 167.2$ Hz, *P* (dppe) *trans* to *S*). ^{19}F NMR (188 MHz, THF-d_8): δ −73.4 (d, $^1J(^{19}F, ^{31}P) = 710.3$ Hz, PF_6^-).

R = Ph, L_2 = P^P = dppp (9c). Yield: 388 mg (78%, route A). HRMS (ESI): *m*/*z* calcd for $[C_{48}H_{47}P_3RhS]^+$ 851.1661, found for $[M]^+$ 851.1661. ^1H NMR (500 MHz, CD_2Cl_2): δ 1.81 (m 4H, $PhSCH_2CH_2CH_2$, $Ph_2CH_2PCH_2CH_2PPh_2$), 2.20 (s, br, 2H, $PhSCH_2CH_2CH_2$), 2.25−2.33 (m, 4H, $Ph_2CH_2PCH_2CH_2PPh_2$), 2.71 (s, br, 2H, $PhSCH_2$), 6.98−7.59 (m, 35H, H_{Ph}). ^{13}C NMR (125 MHz, CD_2Cl_2): δ 18.6 (s, $Ph_2CH_2PCH_2CH_2PPh_2$), 21.0 (s, $PhSCH_2CH_2CH_2$), 27.0 (dd, $^1J(^{13}C, ^{31}P) = 23.1$ Hz, $^3J(^{13}C, ^{31}P_{trans}) = 3.2$ Hz, $PhSCH_2CH_2CH_2$), 25.6/28.8 (m/m, $Ph_2PCH_2CH_2CH_2PPh_2$), 35.2 (dd, $^3J(^{13}C, ^{31}P)/^3J(^{13}C, ^{31}P_{trans}) = 8.2/3.6$ Hz $PhSCH_2$), 128.1−133.1 (C_{Ph}). ^{31}P NMR (81 MHz, THF-d_8): δ −142.9 (sept, $^1J(^{31}P, ^{19}F) = 709.6$ Hz, PF_6^-), 8.9 (m, $^2J(^{31}P, ^{31}P) = 38.5$ Hz, $^2J(^{31}P, ^{31}P) = 338.5$ Hz, $^1J(^{31}P, ^{103}Rh) = 130.7$ Hz, PPh_2), 11.2 (m, $^2J(^{31}P, ^{31}P) = 53.3$ Hz, $^2J(^{31}P, ^{31}P) = 338.5$ Hz, $^1J(^{31}P, ^{103}Rh) = 134.1$ Hz, *P* (dppp) *trans* to *P*), 21.3 (ddd, $^2J(^{31}P, ^{31}P) = 53.3$ Hz, $^2J(^{31}P, ^{31}P) = 38.5$, $^1J(^{31}P, ^{103}Rh) = 160.5$ Hz, *P* (dppp) *trans* to *S*). ^{19}F NMR (188 MHz, THF-d_8): δ −73.4 (d, $^1J(^{19}F, ^{31}P) = 709.6$ Hz, PF_6^-).

R = Ph, L_2 = cod (10). Yield: 256.1 mg (86%, route A). HRMS (ESI): *m*/*z* calcd for $[C_{29}H_{33}PRhS]^+$ 547.5166, found for $[M]^+$ 547.5155. ^1H NMR (400 MHz, CD_2Cl_2): δ 2.05−2.22/2.35−2.46 (m/m, 6H/4H, $CH_2CH_2CH_2/4 \times CH_2$, cod), 2.75 (m, 2H, CH_2PPh_2), 3.48 (m, 2H, CH_2SPh), 3.83/4.65 (s/s, br/br, 2H/2H, $4 \times CH$, cod), 7.46−7.70 (m, 15H, H_{Ph}). ^{13}C NMR (125 MHz, CD_2Cl_2): δ 22.7 (s, br, $CH_2CH_2CH_2$), 25.7 (d, $^1J(^{13}C, ^{31}P) = 26.3$ Hz, CH_2PPh_2), 29.28/29.29/32.19/32.22 (s/s/s/s, $4 \times CH_2$ (cod)), 39.4 (d, $^3J(^{13}C, ^{31}P) = 3.5$ Hz, CH_2SPh), 86.3/105.0 (d/dd, $^1J(^{13}C, ^{103}Rh) = 11.0/10.1$ Hz, $^2J(^{13}C, ^{31}P_{trans}) = 7.1$ Hz, $4 \times CH$, cod), 129.6−134.0 (C_{Ph}). ^{31}P NMR (80 MHz, CD_2Cl_2): δ −142.8 (sept, $^1J(^{31}P, ^{19}F) = 709.6$ Hz, PF_6^-), 12.3 (d, $^1J(^{31}P, ^{103}Rh) = 140.0$ Hz, PPh_2). ^{19}F NMR (188 MHz, CD_2Cl_2): δ −73.4 (d, $^1J(^{19}F, ^{31}P) = 709.6$ Hz, PF_6^-).

R = Cy, L_2 = P^P = dppm (11a). Yield: 431 mg (88%, route A). HRMS (ESI): *m*/*z* calcd for $[C_{46}H_{55}P_3RhS]^+$ 835.2287, found for $[M]^+$ 835.2299. ^1H NMR (400 MHz, CD_2Cl_2): δ 0.94−2.18 (m, 26H, $CH_2CH_2CH_2PCy_2$), 2.87 (m, 2H, CH_2SPh), 4.03 ("t", $N = 9.8$ Hz, 2H, $Ph_2PCH_2PPh_2$), 7.04−7.80 (m, 25H, H_{Ph}). ^{13}C NMR (100 MHz, CD_2Cl_2): δ 17.3 (dd, $^1J(^{13}C, ^{31}P) = 17.6$ Hz, $^3J(^{13}C, ^{31}P_{trans}) = 2.9$ Hz, CH_2PCy_2), 25.1 (s, $CH_2CH_2CH_2$), 26.3 (s, *C4*, PCy_2), 28.6/30.6 (s/d, $J(^{13}C, ^{31}P) = 3.1$ Hz, *C3*/*C2*, PCy_2), 37.4 (d, $^1J(^{13}C, ^{31}P) = 23.1$ Hz, *C1*, PCy_2), 40.0 (dd, $^3J(^{13}C, ^{31}P)/^3J(^{13}C, ^{31}P_{trans}) = 5.5/4.1$ Hz, CH_2SPh), 49.8 ("t", $N = 23.1$ Hz, $Ph_2PCH_2PPh_2$), 129.0−135.8 (C_{Ph}). ^{31}P NMR (80 MHz, CD_2Cl_2): δ −143.0 (sept, $^1J(^{31}P, ^{19}F) = 708.6$ Hz, PF_6^-), −28.3 (ddd, $^2J(^{31}P, ^{31}P) = 85.2$ Hz, $^2J(^{31}P, ^{31}P) = 275.1$ Hz, $^1J(^{31}P, ^{103}Rh) = 111.2$ Hz, *P* (dppm) *trans* to *P*), −14.1 (ddd, $^2J(^{31}P, ^{31}P) = 85.2$ Hz, $^2J(^{31}P, ^{31}P) = 32.3$ Hz, $^1J(^{31}P, ^{103}Rh) = 144.7$ Hz, *P* (dppm) *trans* to *S*), 17.9 (ddd, $^2J(^{31}P, ^{31}P) = 32.3$ Hz, $^2J(^{31}P, ^{31}P) = 275.1$, $^1J(^{31}P, ^{103}Rh) = 127.3$ Hz, PCy_2). ^{19}F NMR (188 MHz, CD_2Cl_2): δ −73.7 (d, $^1J(^{19}F, ^{31}P) = 708.6$ Hz, PF_6^-).

R = Cy, L_2 = P^P = dppe (11b). Yield: 413 mg (82%, route A). HRMS (ESI): *m*/*z* calcd for $[C_{47}H_{57}P_3RhS]^+$ 849.2443; found for $[M]^+$ 849.2439. ^1H NMR (500 MHz, THF-d_8): δ 0.95 −2.26 (m, 30H, $CH_2CH_2CH_2PCy_2/Ph_2PCH_2CH_2PPh_2$), 3.01 (s, br, 2H, CH_2SPh), 7.10−8.33 (m, 25H, H_{Ph}). ^{13}C NMR (125 MHz, CD_2Cl_2): δ 15.0 (dd $^1J(^{13}C, ^{31}P) = 17.7$ Hz, $^3J(^{13}C, ^{31}P_{trans}) = 2.7$ Hz CH_2PCy_2), 23.3 (s, $CH_2CH_2CH_2$), 25.3−25.7/32.2−32.9 (m/m, $Ph_2PCH_2CH_2PPh_2$), 26.2 (s, *C4*, PCy_2), 29.0/31.5 (d/d, $J(^{13}C, ^{31}P) = 4.7/4.8$ Hz, *C3*/*C2*, PCy_2), 37.8 (d, $^1J(^{13}C, ^{31}P) = 21.2$ Hz, *C1*, PCy_2), 39.0 (dd, $^3J(^{13}C, ^{31}P)/^3J(^{13}C, ^{31}P_{trans}) = 6.4/5.1$ Hz, CH_2SPh), 128.8−134.5 (C_{Ph}). ^{31}P NMR (80 MHz, THF-d_8): δ −142.7 (sept, $^1J(^{31}P, ^{19}F) = 708.8$ Hz, PF_6^-), 13.1 (ddd, $^2J(^{31}P, ^{31}P) = 34.3$ Hz, $^2J(^{31}P, ^{31}P) = 264.4$ Hz, $^1J(^{31}P, ^{103}Rh) = 124.5$ Hz, PCy_2), 56.3 (ddd, $^2J(^{31}P, ^{31}P) = 31.9$ Hz, $^2J(^{31}P, ^{31}P) = 264.4$ Hz, $^1J(^{31}P, ^{103}Rh) = 126.4$ Hz, *P* (dppe) *trans* to *P*), 71.2 (d"t", $^2J(^{31}P, ^{31}P) = 34.3$ Hz, $^2J(^{31}P, ^{31}P) = 31.9$ Hz, $^1J(^{31}P, ^{103}Rh) = 170.2$ Hz, *P* (dppe) *trans* to *S*). ^{19}F NMR (188 MHz, THF-d_8): δ −74.0 (d, $^1J(^{19}F, ^{31}P) = 708.8$ Hz, PF_6^-).

R = Cy, L_2 = P^P = dppp (11c). Yield: 393 mg (78%, route A). HRMS (ESI): *m*/*z* calcd for $[C_{48}H_{59}P_3RhS]^+$ 863.2600, found for $[M]^+$ 863.2600. ^1H NMR (500 MHz, CD_2Cl_2): δ 1.00−2.13/2.23/2.45/2.56 (m/m/m/m, 32H, $CH_2CH_2PCy_2$, $Ph_2PCH_2CH_2CH_2PPh_2$), 2.94 (m, 2H, CH_2SPh), 7.17−7.75 (m, 25H, H_{Ph}). ^{13}C NMR (100 MHz, CD_2Cl_2): δ 12.7 (dd, $^1J(^{13}C, ^{31}P) = 18.3$ Hz, $^3J(^{13}C, ^{31}P_{trans}) = 2.6$ Hz, CH_2PCy_2), 19.0 (s, $Ph_2PCH_2CH_2CH_2PPh_2$), 22.2 (s, $PhSCH_2CH_2$), 24.9/28.3 (m/m, $Ph_2PCH_2CH_2CH_2PPh_2$), 26.3 (s, *C4*, PCy_2), 29.5/33.1 (d/d, $J(^{13}C,$

^{31}P) = 6.1 Hz/J(^{13}C, ^{31}P) = 5.4 Hz, *C2*/*C3*, P*Cy*$_2$), 35.4 (dd, ^3J(^{13}C, ^{31}P)/^3J(^{13}C, ^{31}P$_{trans}$) = 7.9/3.9 Hz, *C*H$_2$SPh), 36.9 (d, ^1J(^{13}C, ^{31}P) = 19.4 Hz, *C1*, P*Cy*$_2$), 128.6−136.1 (*C*$_{Ph}$). ^{31}P NMR (80 MHz, CD_2Cl_2): δ −142.9 (sept, ^1J(^{31}P, ^{19}F) = 710.1 Hz, *P*F$_6^-$), 6.5 (ddd, ^2J(^{31}P, ^{31}P) = 55.3 Hz, ^2J(^{31}P, ^{31}P) = 267.2 Hz, ^1J(^{31}P, ^{103}Rh) = 120.8 Hz, *P* (dppp) *trans* to *P*), 19.0 (ddd, ^2J(^{31}P, ^{31}P) = 55.3 Hz, ^2J(^{31}P, ^{31}P) = 32.8 Hz, ^1J(^{31}P, ^{103}Rh) = 161.7 Hz, *P* (dppp) *trans* to *S*), 16.3 (ddd, ^2J(^{31}P, ^{31}P) = 32.8 Hz, ^2J(^{31}P, ^{31}P) = 267.2, ^1J(^{31}P, ^{103}Rh) = 125.4 Hz, *P*Cy$_2$). ^{19}F NMR (188 MHz, CD_2Cl_2): δ −73.4 (d, ^1J(^{19}F, ^{31}P) = 710.1 Hz, P*F*$_6^-$).

R = Cy, L$_2$ = P^P = dmpe (11d). Yield: 265 mg (71%, route A). HRMS (ESI): *m*/*z* calcd for $[C_{27}H_{49}P_3RhS]^+$ 601.1817, found for $[M]^+$ 601.1819. ^{1}H NMR (400 MHz, CD_2Cl_2): δ 1.08/1.58 (d/d, ^2J(^{1}H, ^{31}P) = 8.7/8.4 Hz, 12H, PC*H*$_3$), 1.15−2.09/2.28 (m/s, −/br, 30H, CH$_2$C*H*$_2$C*H*$_2$P*Cy*$_2$/Me$_2$PC*H*$_2$C*H*$_2$PMe$_2$), 2.90 (m, 2H, C*H*$_2$SPh), 7.43 (m, 2H, *m*-*H*, SPh), 7.52 (m, 1H, *p*-*H*, SPh), 7.86 (m, 2H, *o*-*H*, SPh). ^{13}C NMR (100 MHz, CD_2Cl_2): δ 13.6/17.6 (d/d, ^1J(^{13}C, ^{31}P) = 22.9/25.4 Hz, P*C*H$_3$), 16.0 (d, ^1J(^{13}C, ^{31}P) = 17.3 Hz, *C*H$_2$PCy$_2$), 23.1 (s, CH$_2$*C*H$_2$CH$_2$), 25.1−25.6/35.0−36.0 (m/m, Me$_2$P*C*H$_2$*C*H$_2$PMe$_2$), 26.3 (s, *C4*, PCy$_2$), 29.4/32.3 (d/d, J(^{13}C, ^{31}P) = 3.8/6.1 Hz, *C3*/*C2*, PCy$_2$), 36.7 (d, ^3J(^{13}C, ^{31}P) = 6.7 Hz, *C*H$_2$SPh), 39.2 (d, ^3J(^{13}C, ^{31}P) = 22.5 Hz, *C1*, PCy$_2$), 129.6 (s, *m*-*C*, SPh), 130.2 (s, *p*-*C*, SPh), 134.2 (s, *o*-*C*, SPh), 136.0 (s, *i*-*C*, SPh). ^{31}P NMR (80 MHz, THF-d_8): δ −142.8 (sept, ^1J(^{31}P, ^{19}F) = 708.5 Hz, *P*F$_6^-$), 18.2 (ddd, ^2J(^{31}P, ^{31}P) = 37.0 Hz, ^2J(^{31}P, ^{31}P) = 272.3 Hz, ^1J(^{31}P, ^{103}Rh) = 125.1 Hz, *P*Cy$_2$), 36.9 (ddd, ^2J(^{31}P, ^{31}P) = 37.0 Hz, ^2J(^{31}P, ^{31}P) = 32.8 Hz, ^1J(^{31}P, ^{103}Rh) = 159.9 Hz, *P* (dmpe) *trans* to *S*), 37.4 (ddd, ^2J(^{31}P, ^{31}P) = 272.3 Hz, ^2J(^{31}P, ^{31}P) = 32.8 Hz, ^1J(^{31}P, ^{103}Rh) = 124.1 Hz, *P* (dmpe) *trans* to *P*). ^{19}F NMR (188 MHz, THF-d_8): δ −73.8 (d, ^1J(^{19}F, ^{31}P) = 708.5 Hz, P*F*$_6^-$).

R = Cy, L$_2$ = cod (12). Yield: 250 mg (71%, route A). HRMS (ESI): *m*/*z* calcd for $[C_{29}H_{45}PRhS]^+$ 559.2029, found for $[M]^+$ 559.2021. ^{1}H NMR (200 MHz, CD_2Cl_2): δ 1.24−2.56 (m, 34H, CH$_2$C*H*$_2$C*H*$_2$P*Cy*$_2$/4 × C*H*$_2$, cod), 3.22 (m, 2H, C*H*$_2$SPh), 4.44/4.58 (m/m, 2H/2H, 4 × C*H*, cod), 7.45−7.52 (m, 3H, *o*-*H*/*p*-*H*, SPh), 6.57−6.64 (m, 2H, *m*-*H*, SPh). ^{13}C NMR (100 MHz, CD_2Cl_2): δ 16.6 (d, ^1J(^{13}C, ^{31}P) = 22.2 Hz, *C*H$_2$PCy$_2$), 24.8 (s, CH$_2$*C*H$_2$CH$_2$), 26.3 (s, *C4*, PCy$_2$) 27.1/27.3/27.4/27.6 (s/s/s/s, 4 × *C*H$_2$, cod), 31.1/32.4 (s/d, J(^{13}C, ^{31}P) = 2.6 Hz, *C2*/*C3*PCy$_2$), 36.2 (d, ^1J(^{13}C, ^{31}P) = 21.9 Hz, *C1*, PCy$_2$), 39.3 (d, ^3J(^{13}C, ^{31}P) = 2.5 Hz, *C*H$_2$SPh), 84.2/103.1 (d/dd, ^1J(^{13}C, ^{103}Rh) = 11.1/10.6 Hz, ^2J(^{13}C, ^{31}P$_{trans}$) = 7.3 Hz, 4 × *C*H, cod), 130.2/132.4 (s/s, *m*-*C*/*o*-*C* SPh), 130.4 (s, *i*-*C*, SPh), 130.9 (s, *p*-*C*, SPh). ^{31}P NMR (81 MHz, CD_2Cl_2): δ −143.0 (sept, ^1J(^{31}P, ^{19}F) = 708.6 Hz, *P*F$_6^-$), 14.4 (d, ^1J(^{31}P, ^{103}Rh) = 134.4 Hz, *P*Cy$_2$). ^{19}F NMR (188 MHz, CD_2Cl_2): δ −73.0 (d, ^1J(^{19}F, ^{31}P) = 708.6 Hz, P*F*$_6^-$).

3.4. Preparation of [Rh{CH(SPh)CH$_2$CH$_2$PPh$_2$-κ*C*,κ*P*}L$_2$] (13b/c, 14, 15b/c, 16). Route A. To a stirred suspension of the respective rhodium complex [(RhL$_2$)(μ-Cl)$_2$)] (**3**, **4**; 0.25 mmol) in toluene (3 mL) was added a solution of R$_2$PCH$_2$CH$_2$CH$_2$SPh (**1**, **2**; 0.50 mmol) in toluene (2 mL), and the mixture was stirred for 1 h before LDA (0.5 mmol, 0.91 M in THF) was added slowly at −78 °C. The mixture was allowed to warm to room temperature, and the precipitated LiCl was filtered off. The filtrate was reduced to half of its volume, and *n*-pentane (3 mL) was added. The precipitated solid was filtered off, washed with *n*-pentane (3 × 1 mL), and dried in vacuo.

Route B. To a stirred solution of [{Rh(cod)}$_2$(μ-Cl)$_2$] (123.3 mg, 0.25 mmol) in toluene (3 mL) was added a solution of R$_2$PCH$_2$-CH$_2$CH$_2$SPh (0.50 mmol) in toluene (2 mL), followed by the addition of the respective diphosphane (0.50 mmol) dissolved in toluene (2 mL). After 5 h LDA (**1**, **2**; 0.55 mL, 0.5 mmol, 0.91 M in THF) was added slowly at −78 °C. The mixture was allowed to warm to room temperature, and the precipitated LiCl was filtered off. The filtrate was reduced to half of its volume, and *n*-pentane (3 mL) was added. The precipitated solid was filtered off, washed with *n*-pentane (3 × 1 mL), and dried in vacuo.

R = Ph, L$_2$ = P^P = dppe (13b). Yield: 352 mg (84%, route B). Anal. Found: C, 67.72; H, 5.55. Calcd for $C_{47}H_{44}P_3SRh$ (836.76): C, 67.46; H, 5.30. ^{1}H NMR (500 MHz, benzene-d_6): δ 1.74−2.66 (m, 8H, Ph$_2$PC*H*$_2$C*H*$_2$PPh$_2$, CHC*H*$_2$C*H*$_2$), 3.07 (m, 1H, C*H*SPh), 6.77−8.00 (m, 35H, *H*$_{Ph}$). ^{13}C NMR (100 MHz, benzene-d_6): δ 28.1 (s, CH*C*H$_2$CH$_2$), 28.7−29.2/33.1−33.4 (m/m, Ph$_2$P*C*H$_2$*C*H$_2$PPh$_2$), 33.6 (dd, ^1J(^{13}C, ^{31}P) = 17.1 Hz, ^3J(^{13}C, ^{31}P$_{trans}$) = 2.7 Hz, CHCH$_2$C*H*$_2$), 41.9−42.8 (m, *C*HSPh), 123.4−143.2 (*C*$_{Ph}$). ^{31}P NMR (81 MHz, benzene-d_6): δ 58.6 (m, ^2J(^{31}P, ^{31}P) = 27.9 Hz, ^2J(^{31}P, ^{31}P) = 304.0 Hz, ^1J(^{31}P, ^{103}Rh) = 162.3 Hz, *P*Ph$_2$), 60.2 (m, ^2J(^{31}P, ^{31}P) = 27.9 Hz, ^2J(^{31}P, ^{31}P) = 25.0 Hz, ^1J(^{31}P, ^{103}Rh) = 123.6 Hz, *P* (dppe) *trans* to *C*), 63.1 (m, ^2J(^{31}P, ^{31}P) = 304.0 Hz, ^2J(^{31}P, ^{31}P) = 25.0, ^1J(^{31}P, ^{103}Rh) = 165.9 Hz, *P* (dppe) *trans* to *P*).

R = Ph, L$_2$ = P^P = dppp (13c). Yield: 352 mg (84%, route A). Anal. Found: C, 66.84; H, 5.79. Calcd for $C_{48}H_{46}P_3SRh$ (850.79): C, 67.76; H, 5.45. ^{1}H NMR (400 MHz, THF-d_8): δ 1.11−1.22/1.55−1.79 (m/m, 1H/1H, CHC*H*$_2$CH$_2$), 1.55−1.79/1.86−1.94 (m/m, 1H/1H, Ph$_2$PCH$_2$C*H*$_2$CH$_2$PPh$_2$), 1.94−2.07/2.40−2.55 (m/m, 2H/2H, Ph$_2$PC*H*$_2$CH$_2$C*H*$_2$PPh$_2$), 2.17−2.25/2.58−2.68 (m/m, 1H/1H, CHCH$_2$C*H*$_2$), 3.33 (m, 1H, C*H*SPh), 6.68−7.89 (m, 35H, *H*$_{Ph}$). ^{13}C NMR (100 MHz, THF-d_8): δ 20.7 (s, Ph$_2$PCH$_2$*C*H$_2$CH$_2$PPh$_2$), 30.3 (s, CH*C*H$_2$CH$_2$) 31.5−31.7/34.9−35.3 (m/m, Ph$_2$P*C*H$_2$CH$_2$*C*H$_2$PPh$_2$), 34.8 (dd, ^1J(^{13}C, ^{31}P) = 24.4 Hz, ^1J(^{13}C, ^{31}P$_{trans}$) = 5.7 Hz, CHCH$_2$*C*H$_2$), 45.9−46.7 (m, *C*HSPh), 123.4−143.5 (*C*$_{Ph}$). ^{31}P NMR (81 MHz, THF-d_8): δ 18.2 (m, ^2J(^{31}P, ^{31}P) = 21.9 Hz, ^2J(^{31}P, ^{31}P) = 47.9 Hz, ^1J(^{31}P, ^{103}Rh) = 119.1 Hz, *P* (dppm) *trans* to *C*), 21.0 (m, ^2J(^{31}P, ^{31}P) = 293.1 Hz, ^2J(^{31}P, ^{31}P) = 47.9 Hz, ^1J(^{31}P, ^{103}Rh) = 162.1 Hz, *P* (dppm) *trans* to *P*), 57.7 (ddd, ^2J(^{31}P, ^{31}P) = 293.1 Hz, ^2J(^{31}P, ^{31}P) = 21.9, ^1J(^{31}P, ^{103}Rh) = 164.6 Hz, *P*Ph$_2$).

R = Ph, L$_2$ = cod (14). Yield: 248 mg (85%, route A). Anal. Found: C, 62.02; H, 8.33. Calcd for $C_{28}H_{44}PSRh$ (546.60): C, 61.53; H, 8.11. ^{1}H NMR (200 MHz, THF-d_8): δ 1.25−2.51 (m, 12H, Ph$_2$PC*H*$_2$C*H*$_2$CH, 4 × C*H*$_2$, cod), 2.78 (s, br, 1H, C*H*SPh), 3.88−4.54 (m, 4H, 4 × C*H*, cod), 6.83−7.63 (m, 15H, *H*$_{Ph}$). ^{13}C NMR (50 MHz, THF-d_8): δ 28.8 (s, CH$_2$*C*H$_2$CH), 31.9 (d, ^1J(^{13}C, ^{31}P) = 22.4, *C*H$_2$PPh$_2$), 31.6/31.8/32.0/33.3 (s/s/s/s, 4 × *C*H$_2$, cod), 35.5 (dd, ^2J(^{13}C, ^{31}P) = 4.5 Hz, ^1J(^{13}C, ^{103}Rh) = 16.4 Hz, *C*HSPh), 70.1/73.4/76.1/79.6 (d/d/d/d, ^1J(^{13}C, ^{103}Rh) = 13.4/13.4/10.5/10.6 Hz, 4 × *C*H, cod), 126.4−147.2 (*C*$_{Ph}$). ^{31}P NMR (80 MHz, THF-d_8): δ 58.6 (d, ^1J(^{31}P, ^{103}Rh) = 168.3 Hz, *P*Ph$_2$).

R = Cy, L$_2$ = P^P = dppe (15b). Yield: 146 mg (35%, route A). ^{1}H NMR (400 MHz, benzene-d_6): δ 1.04−2.32 (m, 30H, *Cy*$_2$PC*H*$_2$C*H*$_2$/Ph$_2$PC*H*$_2$C*H*$_2$PPh$_2$), 3.01 (m, 1H, C*H*SPh), 6.78−8.07 (m, 25H, *H*$_{Ph}$). ^{13}C NMR (50 MHz, THF-d_8): δ 22.3 (dd, ^1J(^{13}C, ^{31}P) = 18.9 Hz, ^1J(^{13}C, ^{31}P$_{trans}$) = 6.8 Hz *C*H$_2$PCy$_2$), 27.1 (s, CH$_2$*C*H$_2$CH$_2$), 27.2−36.6 (Ph$_2$P*C*H$_2$*C*H$_2$-PPh$_2$/*C4*/*C3*/*C2*/*C1*, PCy$_2$), 41.2−43.3 (m, *C*HSPh), 123.2−144.5 (*C*$_{Ph}$). ^{31}P NMR (81 MHz, THF-d_8): δ 61.2 (m, ^2J(^{31}P, ^{31}P) = 27.4 Hz, ^2J(^{31}P, ^{31}P) = 25.6 Hz, ^1J(^{31}P, ^{103}Rh) = 124.6 Hz, *P* (dppe) *trans* to *C*), 61.9 (m, ^2J(^{31}P, ^{31}P) = 25.6 Hz, ^2J(^{31}P, ^{31}P) = 300.3 Hz, ^1J(^{31}P, ^{103}Rh) = 159.5 Hz, *P* (dppe) *trans* to *P*), 67.5 (ddd, ^2J(^{31}P, ^{31}P) = 27.4 Hz, ^2J(^{31}P, ^{31}P) = 300.3 Hz, ^1J(^{31}P, ^{103}Rh) = 155.2 Hz, *P*Cy$_2$).

R = Cy, L$_2$ = P^P = dppp (15c). Yield: 140 mg (33%, route A). ^{1}H NMR (400 MHz, THF-d_8): δ 1.04−2.55 (m, 32H, *Cy*$_2$PC*H*$_2$-C*H*$_2$/Ph$_2$PC*H*$_2$C*H*$_2$C*H*$_2$PPh$_2$), 3.32 (m, 1H, C*H*SPh), 6.65−7.89 (m, 25H, *H*$_{Ph}$). ^{13}C NMR (50 MHz, THF-d_8): δ 20.0 (s, Ph$_2$PCH$_2$CH$_2$CH$_2$PPh$_2$), 22.2 (dd, ^1J(^{13}C, ^{31}P) = 19.6 Hz, ^1J(^{13}C, ^{31}P$_{trans}$) = 7.6 Hz, *C*H$_2$PCy$_2$), 26.3 (s, CH*C*H$_2$CH$_2$), 26.6−30.8 (*C4*/*C3*/*C2*, PCy$_2$), 27.2−27.7/31.7−32.3 (m/m, Ph$_2$-P*C*H$_2$CH$_2$*C*H$_2$PPh$_2$), 37.9 (d, ^1J(^{13}C, ^{31}P) = 18.3 Hz, *C1*, PCy$_2$), 44.5−46.1 (m, *C*HSPh), 122.2−143.4 (*C*$_{Ph}$). ^{31}P NMR (81 MHz, THF-d_8): δ 17.2 (m, ^2J(^{31}P, ^{31}P) = 289.9 Hz, ^2J(^{31}P, ^{31}P) = 46.3 Hz, ^1J(^{31}P, ^{103}Rh) = 154.5 Hz, *P* (dppp) *trans* to *P*), 18.3 (m, ^2J(^{31}P, ^{31}P) = 32.4 Hz, ^2J(^{31}P, ^{31}P) = 46.3 Hz, ^1J(^{31}P, ^{103}Rh) = 120.9 Hz, *P* (dppp) *trans* to *C*), 66.3 (ddd, ^2J(^{31}P, ^{31}P) = 32.4 Hz, ^2J(^{31}P, ^{31}P) = 289.9 Hz, ^1J(^{31}P, ^{103}Rh) = 156.5 Hz, *P*Cy$_2$).

R = Cy, L$_2$ = cod (16). Yield: 87 mg (31%, route A). ^{1}H NMR (400 MHz, THF-d_8): δ 1.17−3.00 (m, 37H, $Cy_2PCH_2CH_2CH$ /4 × CH_2/4 × CH, cod), 7.09−7.48 (m, 5H, H_{Ph}). ^{13}C NMR (50 MHz, THF-d_8): δ 22.5 (d, $^1J(^{13}C, ^{31}P) = 15.9$ Hz, CH_2PCy_2), 24.0 (s, $CHCH_2CH_2$), 26.5−30.0 (*C4*/*C3*/*C2*, PCy_2, 4 × CH_2, cod), 38.0 (d, $^1J(^{13}C, ^{31}P) = 21.6$ Hz, *C1*, PCy_2), 38.4 (dd, $^2J(^{13}C, ^{31}P) = 4.0$ Hz, $^1J(^{13}C, ^{103}Rh) = 20.6$ Hz, $CHSPh$), 72.7/80.0 (m/m, 4 × CH, cod), 126.2 (s, *m-C*, SPh), 128.9 (s, *o-C*, SPh), 130.9 (s, *p-C*, SPh), 145.7 (s, *i-C*, SPh). ^{31}P NMR (202 MHz, THF-d_8): δ 62.9 (d, $^1J(^{31}P, ^{103}Rh) = 170.0$ Hz, PCy_2).

3.5. Preparation of [Rh(dppm$_{-H}$-κ^2P,P')(R$_2$PCH$_2$CH$_2$CH$_2$-SPh-$\kappa P,\kappa S$)] (17, 18). To a stirred suspension of [{Rh(dppm)}$_2$-(μ-Cl)$_2$] (261.39 mg, 0.25 mmol) in toluene (3 mL) was added a solution of $R_2PCH_2CH_2CH_2SPh$ (**1**, **2**; 0.50 mmol) in toluene (2 mL), and the mixture was stirred for 1 h before LDA (0.5 mmol, 0.91 M in THF) was added slowly at −78 °C. The mixture was alowed to warm to room temperature, and the precipitated LiCl was filtered off. The filtrate was reduced to half of its volume, and *n*-pentane (3 mL) was added. The precipitated compound was filtered off, washed with *n*-pentane (3 × 1 mL), and dried in vacuo.

R = Ph (17). Yield: 292 mg (71%) HRMS (ESI): *m*/*z* calcd for [$C_{46}H_{42}P_3RhS$] 822.7175, found for [M] 822.7168. ^{1}H NMR (500 MHz, THF-d_8): δ 1.80−1.91 (m, 2H, $CH_2CH_2CH_2$), 2.25 (m, 3H, $CH_2CH_2Ph_2$, $Ph_2PCHPPh_2$), 2.98 (s, br, 2H, CH_2SPh), 6.78−7.81 (m, 35H, H_{Ph}). ^{13}C NMR (125 MHz, benzene-d_6): δ 22.3 (s, br, $CH_2CH_2CH_2PPh_2$), 28.7 (d, $^1J(^{13}C, ^{31}P) = 18.6$ Hz, $CH_2CH_2PPh_2$), 31.2 ("t", N = 102.3 Hz, $Ph_2PCHPPh_2$), 38.6 (dd, $^3J(^{13}C, ^{31}P)/^3J(^{13}C, ^{31}P_{trans}) = 7.5/3.3$ Hz (the two coupling constants may be reversed), CH_2SPh), 127.4−144.7 (C_{Ph}). ^{31}P NMR (81 MHz, benzene-d_6): δ −35.0 (ddd, $^2J(^{31}P, ^{31}P) = 60.3$ Hz, $^2J(^{31}P, ^{31}P) = 301.0$ Hz, $^1J(^{31}P, ^{103}Rh) = 93.6$ Hz, *P* (dppm) *trans* to *P*), −24.2 (ddd, $^2J(^{31}P, ^{31}P) = 23.3$ Hz, $^2J(^{31}P, ^{31}P) = 60.3$ Hz, $^1J(^{31}P, ^{103}Rh) = 124.2$ Hz, *P* (dppm) *trans* to *S*), 12.8 (ddd, $^2J(^{31}P, ^{31}P) = 23.3$ Hz, $^2J(^{31}P, ^{31}P) = 301.0$, $^1J(^{31}P, ^{103}Rh) = 144.1$ Hz, 1P, PPh_2). The complex contained residual amounts of diisopropylamine.

R = Cy (18). Yield: 305 mg (73%). HRMS (ESI): *m*/*z* calcd for [$C_{46}H_{55}P_3RhS$] 835.2287, found for [M] 835.2250. ^{1}H NMR (400 MHz, THF-d_8): δ 0.60−2.23 (m, 27H, $CH_2CH_2PCy_2$, $Ph_2PCHPPh_2$), 2.71 (s, br, 2H, CH_2SPh), 6.95−8.03 (m, 25H, H_{Ph}). ^{13}C NMR (100 MHz, THF-d_8): δ 19.2 (dd, $^1J(^{13}C, ^{31}P) = 13.0$ Hz, $^3J(^{13}C, ^{31}P_{trans}) = 2.0$ Hz, CH_2PCy_2), 26.3 (s, $CH_2CH_2CH_2$), 27.0 (s, *C4*, PCy_2), 29.2/30.8 (s/d, $J(^{13}C, ^{31}P) = 5.6$ Hz, *C2*/*C3*, PCy_2), 34.5 ('t', N=99.2 Hz, $Ph_2PCHPPh_2$), 38.2 (d, $^1J(^{13}C, ^{31}P) = 19.4$ Hz, *C1*, PCy_2), 39.8 (dd, $^3J(^{13}C, ^{31}P)/^3J(^{13}C, ^{31}P_{trans}) = 8.1/5.3$ Hz (the two coupling constants may be reversed), CH_2SPh), 127.4−146.4 (C_{Ph}). ^{31}P NMR (81 MHz, THF-d_8): δ −33.1 (ddd, $^2J(^{31}P, ^{31}P) = 57.4$ Hz, $^2J(^{31}P, ^{31}P) = 281.8$ Hz, $^1J(^{31}P, ^{103}Rh) = 93.1$ Hz, *P* (dppm) *trans* to *P*), −22.0 (ddd, $^2J(^{31}P, ^{31}P) = 26.6$ Hz, $^2J(^{31}P, ^{31}P) = 57.4$ Hz, $^1J(^{31}P, ^{103}Rh) = 129.1$ Hz, *P* (dppp) *trans* to *S*), 19.4 (ddd, $^2J(^{31}P, ^{31}P) = 26.6$ Hz, $^2J(^{31}P, ^{31}P) = 281.8$ Hz, $^1J(^{31}P, ^{103}Rh) = 137.7$ Hz, PCy_2).

3.6. Reaction of [Rh(R$_2$PCH$_2$CH$_2$CH$_2$SPh-$\kappa P,\kappa S$)(P^P)]-[PF$_6$] with Carbon Monoxide. At −78 °C carbon monoxide is bubbled through a solution of [Rh($R_2PCH_2CH_2CH_2SPh$-$\kappa P,\kappa S$)(P^P)][PF_6] (**9**, **11**; 0.03 mmol) in CD_2Cl_2 (1 mL) for two minutes. Spectroscopic investigations were performed directly from the solutions obtained.

R/P^P: Ph/dppm (19a). HRMS (ESI): *m*/*z* calcd for [$C_{46}H_{43}P_3RhS$]$^+$ 823.1348, found for [M − CO]$^+$ 823.1350. IR: ν = 1989 (CO), 2024 (CO) cm^{-1}. ^{13}C NMR (100 MHz, CD_2Cl_2): δ 190.7 (*C*O). ^{31}P NMR (27 °C, 81 MHz, CD_2Cl_2): δ −25.3 ("t", br, *P* (dppm)), 29.9 ("q", br, PPh_2), −21.1 (d, $^1J(^{31}P, ^{103}Rh) = 97.3$ Hz, [Rh(dppm-κ^2P,P')$_2$]$^+$), 18.3 (d, $^1J(^{31}P, ^{103}Rh) = 104.8$ Hz, [Rh_2(μ-Cl)(μ-CO)(dppm-1κP:2$\kappa P'$)$_2$(CO)$_2$]$^+$).

Ph/dppe (19b). HRMS (ESI): *m*/*z* calcd for [$C_{47}H_{45}P_3RhS$]$^+$ 837.1504, found for [M − CO]$^+$ 837.1513. IR: ν = 1988 (CO), 2022 (CO) cm^{-1}. ^{13}C NMR (100 MHz, CD_2Cl_2): δ 190.1 (*C*O). ^{31}P NMR (27 °C, 81 MHz, CD_2Cl_2): δ 27.3 ("q", br, PPh_2), 55.9 ("t", br, *P* (dppe)). ^{31}P NMR (−80 °C, 202 MHz, CD_2Cl_2): major isomer δ 30.6 (ddd, $^2J(^{31}P, ^{31}P) = 30.3$ Hz, $^2J(^{31}P, ^{31}P) = 250.2$ Hz, $^1J(^{31}P, ^{103}Rh) = 80.1$ Hz, PPh_2), 49.5 (ddd, $^2J(^{31}P, ^{1}P) = 30.3$ Hz, $^2J(^{31}P, ^{31}P) = 15.2$ Hz, $^1J(^{31}P, ^{103}Rh) = 121.2$ Hz, *P* (dppe)), 60.8 (ddd, $^2J(^{31}P, ^{31}P) = 15.2$ Hz, $^2J(^{31}P, ^{31}P) = 250.2$ Hz, $^1J(^{31}P, ^{103}Rh) = 76.3$ Hz, *P* (dppe)); minor isomer δ 18.1 (ddd, $^2J(^{31}P, ^{31}P) = 30.2$ Hz, $^2J(^{31}P, ^{31}P) = 263.9$ Hz, $^1J(^{31}P, ^{103}Rh) = 98.5$ Hz, PPh_2), 42.8−46.2 (m, br, *P* (dppe)), 67.6−70.2 (m, br, *P* (dppe)).

Ph/dppp (19c). HRMS (ESI): *m*/*z* calcd for [$C_{48}H_{47}P_3RhS$]$^+$ 851.1661, found for [M − CO]$^+$ 851.1651. IR: ν = 1994 (CO), 2024 (CO) cm^{-1}. ^{13}C NMR (100 MHz, CD_2Cl_2): δ 190.7 (*C*O). ^{31}P NMR (27 °C, 81 MHz, CD_2Cl_2): δ 6.4 ("t", br, *P* (dppp)), 24.8 ("q", br, PPh_2).

Cy/dppm (20a). HRMS (ESI): *m*/*z* calcd for [$C_{46}H_{55}P_3RhS$]$^+$ 835.2287, found for [M − CO]$^+$ 835.2276. IR: ν = 1994 (CO), 2025 (CO) cm^{-1}. ^{13}C NMR (100 MHz, CD_2Cl_2): δ 190.0 (*C*O). ^{31}P NMR (27 °C, 81 MHz, CD_2Cl_2): δ −20.6 ("t", br, *P* (dppm)), 37.6 ("q", br, PCy_2), −21.2 (d, $^1J(^{31}P, ^{103}Rh) = 97.3$ Hz, [Rh(dppm-κ^2P,P')$_2$]$^+$).

Cy/dppe (20b). HRMS (ESI): *m*/*z* calcd for [$C_{47}H_{57}P_3RhS$]$^+$ 849.2443, found for [M − CO]$^+$ 849.2433. IR: ν = 1994 (CO) cm^{-1}, 2019 (CO). ^{13}C NMR (100 MHz, CD_2Cl_2): δ 189.8 (*C*O). ^{31}P NMR (27 °C, 81 MHz, CD_2Cl_2): δ 34.5 ("q", br, PCy_2), 55.3 ("t", br, *P* (dppe)).

Cy/dppp (20c). HRMS (ESI): *m*/*z* calcd for [$C_{49}H_{59}OP_3RhS$]$^+$ 891.2549, found for [M]$^+$ 891.2547. IR: ν = 1994 (CO), 2022 (CO) cm^{-1}. ^{13}C NMR (100 MHz, CD_2Cl_2): δ 192.8 (*C*O). ^{31}P NMR (27 °C, 81 MHz, CD_2Cl_2): δ 6.8 ("t", br, *P* (dppp)), 39.9 ("q", br, PCy_2).

Cy/dmpe (20d). HRMS (ESI): *m*/*z* calcd for [$C_{27}H_{49}P_3RhS$]$^+$ 601.1817, found for [M − CO]$^+$ 601.1823. IR: ν = 1994 (CO), 2024 (CO) cm^{-1}. ^{13}C NMR (100 MHz, CD_2Cl_2): δ 192.2 (*C*O). ^{31}P NMR (27 °C, 81 MHz, CD_2Cl_2): δ 28.4 ("t", br, *P* (dmpe)), 42.1 ("q", br, PCy_2).

3.7. X-ray Crystallography. Data for X-ray diffraction analyses of single crystals of **7b**·C_6H_6 and **18**·THF were collected on a Stoe-IPDS 2T diffractometer at 200(2) K and of **10** at 220(2) K on a Stoe-IPDS diffractometer using Mo Kα radiation (λ = 0.7103 Å, graphite monochromator). A summary of the crystallographic data, the data collection parameters, and the refinement parameters is given in Table S1 (see Supporting Information). Absorption corrections were applied numerically with X-RED32[72] (T_{min}/T_{max} 0.63/0.96, **7b**·C_6H_6; 0.92/0.97, **10**; 0.79/0.87, **18**·THF). The structures were solved with direct methods using SHELXS-97[73] and refined using full-matrix least-squares routines against F^2 with SHELXL-97.[74] All non-hydrogen atoms were refined with anisotropic displacement parameters and hydrogen atoms with isotropic ones. H atoms were placed in calculated positions according to the riding model.

3.8. Computational Details. DFT calculations were carried out by the Gaussian 03 program[75] package using the hybrid functional B3LYP,[76] and the 6-311++G(3df,3pd) (P, S) and 6-31+G* (O, C, H) basis sets as implemented in Gaussian 03 were employed for main group atoms. The valence shell of rhodium has been approximated by a split valence basis set too (Def2-TZVPP); for its core orbitals an effective core potential

(72) *X-RED32* (*version 1.03*)*: Stoe Data Reduction Program*; Stoe & Cie GmbH: Darmstadt, 2002.

(73) Sheldrick, G. M. *SHELXS-97, Program for Crystal Structure Solution*; University of Göttingen: Göttingen, 1998.

(74) Sheldrick, G. M. *SHELXL-97, Program for the Refinement of Crystal Structures*; University of Göttingen: Göttingen, 1997.

(75) Frisch, M. J.; et al. *Gaussian 03*, revision B.04; Gaussian, Inc.: Pittsburgh, PA, 2004.

(76) (a) Becke, A. D. *Phys. Rev. A* **1988**, *38*, 3098. (b) Becke, A. D. *J. Chem. Phys.* **1993**, *98*, 5648. (c) Lee, C.; Yang, W.; Parr, R. G. *Phys. Rev. B* **1988**, *37*, 785. (d) Stephens, P. J.; Devlin, F. J.; Chabalowski, C. F.; Frisch, M. J. *J. Phys. Chem.* **1994**, *98*, 11623.

in combination with consideration of relativistic effects has been used.[77] For complexes **13a**$_{calc}$ and **17**$_{calc}$ the SDD basis set as implemented in Gaussian 03 was used. All systems were fully optimized without any symmetry restrictions. The resulting geometries were characterized as equilibrium structures by the analysis of the force constants of normal vibrations. Solvent effects were considered according to the polarized continuum model as implemented in Gaussian 03.[57]

(77) (a) Weigend, F.; Ahlrichs, R. *Phys. Chem. Chem. Phys.* **2005**, *7*, 3297. (b) Andrae, D.; Häussermann, U.; Dolg, M.; Stoll, H.; Preuss, H. *Theor. Chim. Acta* **1990**, *77*, 123.

Supporting Information Available: Synthesis and NMR spectroscopic data of starting materials, molecular structures, energies, and Cartesian coordinates of calculated molecules and X-ray crystallographic files (CIF) are available free of charge via the Internet at http://pubs.acs.org.

Journal of Organometallic Chemistry xxx (2011) 1–14

Contents lists available at ScienceDirect

Journal of Organometallic Chemistry

journal homepage: www.elsevier.com/locate/jorganchem

Rhodium(I) complexes with κ*P* coordinated ω-phosphinofunctionalized alkyl phenyl sulfide, sulfoxide and sulfone ligands and their reactions with sodium bis(trimethylsilyl)amide and Ag[BF_4]

Michael Block [a], Martin Bette [a], Christoph Wagner [a], Jürgen Schmidt [b], Dirk Steinborn [a,*]

[a] *Institute of Chemistry – Inorganic Chemistry, Martin Luther University Halle-Wittenberg, Kurt-Mothes-Straße 2, 06120 Halle, Germany*
[b] *Department of Bioorganic Chemistry, Leibniz Institute of Plant Biochemistry, Weinberg 3, 06120 Halle, Germany*

ARTICLE INFO

Article history:
Received 27 October 2010
Received in revised form
30 November 2010
Accepted 14 December 2010

Keywords:
P,S ligands
P,O ligands
Organorhodium intramolecular coordination compounds
Zwitterionic complexes

ABSTRACT

Reactions of ω-diphenylphosphinofunctionalized alkyl phenyl sulfides $Ph_2P(CH_2)_nSPh$ ($n = 1$, **1a**; 2, **2a**; 3, **3a**), sulfoxides $Ph_2P(CH_2)_nS(O)Ph$ ($n = 1$, **1b**; 2, **2b**; 3, **3b**) and sulfones $Ph_2P(CH_2)_nS(O)_2Ph$ ($n = 1$, **1c**; 2, **2c**; 3, **3c**) with dinuclear chlorido bridged rhodium(I) complexes $[(RhL_2)_2(\mu\text{-}Cl)_2]$ (L_2 = cycloocta-1.5-diene, cod, **4**; bis(diphenylphosphino)ethane, dppe, **5**) afforded mononuclear Rh(I) complexes of the type $[RhCl\{Ph_2P(CH_2)_nS(O)_x Ph\text{-}\kappa P\}(cod)]$[1] ($n/x = 1/0$, **6a**; 1/1, **6b**; 1/2, **6c**; 2/0, **8a**; 2/1, **8b**; 2/2, **8c**; 3/0, **10a**; 3/1, **10b**; 3/2, **10c**) and $[RhCl\{Ph_2P(CH_2)_nS(O)_xPh\text{-}\kappa P\}(dppe)]$ ($n/x = 1/0$, **7a**; 1/1, **7b**; 1/2, **7c**; 2/0, **9a**; 2/1, **9b**; 2/2, **9c**; 3/0, **11a**; 3/1, **11b**; 3/2, **11c**) having the P^S(O)$_x$ ligands κ*P* coordinated. Addition of Ag[BF_4] to complexes **6**–**11** in CH_2Cl_2 led with precipitation of AgCl to cationic rhodium complexes of the type $[Rh\{Ph_2P(CH_2)_nS(O)_xPh\text{-}\kappa P,\kappa S/O\}L_2][BF_4]$ having bound the P^S(O)$_x$ ligands bidentately in a κ*P*,κ*S* (**13a**–**18a**, **15b**–**18b**) or a κ*P*,κ*O* (**13b**, **14b**, **13c**–**18c**) coordination mode. Unexpectedly, the addition of Ag[BF_4] to **6a** in THF afforded the trinuclear cationic rhodium(I) complex $[Rh_3(\mu\text{-}Cl)(\mu\text{-}Ph_2PCH_2SPh\text{-}\kappa P{:}\kappa S)_4][BF_4]_2 \cdot 4THF$ (**12**·4THF) with a four-membered Rh_3Cl ring as basic framework. Addition of sodium bis(trimethylsilyl)amide to complexes **6**–**11** led to a selective deprotonation of the carbon atom neighbored to the S(O)$_x$ group (α-C) yielding three different types of organorhodium complexes: a) Organorhodium intramolecular coordination compounds of the type $[Rh\{CH\{S(O)_xPh\}CH_2CH_2PPh_2\text{-}\kappa C,\kappa P\}L_2]$ (**22a**–**c**, **23a**–**c**), b) zwitterionic complexes $[Rh\{Ph_2PCHS(O)_xPh\text{-}\kappa P,\kappa S/O\}L_2]$ having κ*P*,κ*S* (**21a**, **21b**) and κ*P*,κ*O* (**20b**/**c**, **21c**) coordinated anionic $[Ph_2PCHS(O)_xPh]$ ligands, and c) the dinuclear rhodium(I) complex $[\{Rh\{\mu\text{-}CH(SPh)PPh_2\text{-}\kappa C{:}\kappa P\}(cod)\}_2]$ (**19**). All complexes were fully characterized spectroscopically and complexes **15b**, **15c**, **12**·4THF and **19**·THF additionally by X-ray diffraction analysis. DFT calculations of zwitterionic complexes gave insight into the coordination mode of the $[Ph_2PCHS(O)Ph]$ ligand (κ*P*,κ*S* versus κ*P*,κ*O*).

1. Introduction

Sterical and electronical effects of bidentate ligands on the structure and reactivity of metal complexes are a substantial subject of research in organometallic chemistry as well as in homogeneous catalysis. While many investigations were done with homobidentate ligands such as diphosphanes [1–3], heterobidentate ligands offer the possibility to introduce two completely different donor centers having different electronic (e.g. trans influence, trans effect) and sterical effects. In this way, stability and reactivity of intermediates in a reaction may be influenced in a targetted manner [4,5]. As an example, bidentate P^S and P^O type ligands are equipped with a strong and a weak donor group; thus, they might offer a hemilabile character which permits a temporary generation of a vacant coordination site at the metal center [6]. Moreover, complexes bearing ligands of that type can play an important role in various homogeneously catalyzed reactions [7–10] or as chemosensors [11].

Furthermore, deprotonation of such ligands may lead to the formation of zwitterionic (betaine-like) complexes. They are characterized by a formal charge separation between a cationic metal center and a negatively charged ancillary ligand moiety within an overall neutral molecular framework [12]. Hence, they combine the reactivity of related cationic complexes with the solubility properties of neutral species which makes them useful in some homogeneously catalyzed reactions [13–15]. If the deprotonation of the P^S and P^O ligands leads to a κ*C*,κ*P* coordination, organometallic intramolecular coordination compounds (also named "organometallic inner complexes")

* Corresponding author. Tel.: +49 345 55 25620; fax: +49 345 55 27028.
E-mail address: dirk.steinborn@chemie.uni-halle.de (D. Steinborn).

[1] Here and in the following the letters **a**, **b**, and **c** in the numbering schemes refer to a sulfanyl ($x = 0$), sulfinyl ($x = 1$) and sulfonyl ($x = 2$) functionality, respectively.

0022-328X/$ – see front matter © 2010 Published by Elsevier B.V.
doi:10.1016/j.jorganchem.2010.12.019

are formed. In general, they are characterized as metallacyclic compounds with an M–C bond and a bond of the metal to a neutral Lewis-basic heteroatom group like NR_2, PR_2, OR or SR being also part of the cycle. Over the past years, they were subject of a large number of researches [16–19], thus, from almost all metals of the periodic table organometallic intramolecular coordination compounds are known and they are widely used in various ways in organic syntheses.

We are interested in α,ω-functionalized ligands of the type $R_mY(CH_2)_nS(O)_xR$ bearing a Lewis-basic heteroatom group YR_m ($YR_m = PR_2$, NR_2, OR; R = alkyl, aryl) as well as, respectively, a sulfanyl ($x = 0$), sulfinyl ($x = 1$) and sulfonyl group ($x = 2$). While the functionalized sulfides and sulfones can act as κ*S*,κ*Y* and κ*O*,κ*Y* donors, respectively, in case of the analogous flexidentate sulfoxides both coordination modes are possible [20–22]. Structure and reactivity of metal complexes with the requisite deprotonated ligands depend on the nature of sulfur functionalization neighbored to the carbanionic atom (α-C). Ligands with a Lewis-basic sulfide group ($x = 0$) next to the α-carbon atom are found to be κ*C*,κ*Y* coordinated in most cases, thereby organometallic intramolecular coordination compounds are formed, irrespective of the nature of the metal [23–26]. However, in the analogous complexes with a functionalized sulfone ligand ($x = 2$) the dipole stabilization of the SO_2 group gives rise to the formation of a less basic carbanion [27]. While in solid state the majority of the respective lithiated compounds are higher aggregated having the sulfonyl group κ*O* coordinated to the Li atom resulting in a "free" carbanionic center [28] the corresponding transition metal complexes were generally found to be mononuclear organometallic intramolecular coordination compounds exhibiting a κ*C*,κ*Y* coordination [29,30]. On the other hand, the sulfinyl functionalization ($x = 1$) can be regarded both as a Lewis-basic and a dipole-stabilized heteroatom group. Yet there have been only few studies on these ligands; even for non-functionalized ligands of the type $^{\ominus}$CHR–S(O)R only few structural data are presented in the literature. They seem to resemble more the sulfones: lithiated sulfoxides exhibit a κ*O* coordination with a "free" carbanionic center [31] whereas in transition metal complexes a κ*C* coordination is observed [32].

Here we present a systematic study on reactions of rhodium(I) complexes of the type [RhCl{$Ph_2P(CH_2)_nS(O)_x$Ph-κ*P*}L_2] (L_2 = cod, dppe) with sodium bis(trimethylsilyl)amide and Ag[BF_4], respectively, in dependence on the type of the sulfur functionalization ($x = 0–2$) and on the spacer length ($n = 1–3$). Thus, it is reported on the formation and characterization of organorhodium intramolecular coordination compounds and zwitterionic complexes having the deprotonated P^S(O)$_x$ ligands κ*C*,κ*P*, κ*P*,κ*S* and κ*P*,κ*O* coordinated as well as of cationic complexes with non-deprotonated P^S(O)$_x$-κ*P*,κ*S*/*O* ligands.

2. Results and discussion

2.1. Syntheses

Chlorido bridged Rh(I) complexes [$(RhL_2)_2(\mu\text{-}Cl)_2$] ($L_2$ = cod, **4**; dppe, **5**) were reacted with compounds of the type $Ph_2P(CH_2)_nS(O)_xPh$ that include ω-diphenylphosphinofunctionalized alkyl phenyl sulfides ($x = 0$), sulfoxides ($x = 1$) and sulfones ($x = 2$). As spacers between the two donor sites the methylene ($n = 1$), dimethylene ($n = 2$) and trimethylene ($n = 3$) groups were used. As shown in Scheme 1 (routes **a**/**b**/**c**) the reactions afforded neutral rhodium(I) complexes (**6a**/**b**/**c**–**11a**/**b**/**c**) having bound the $Ph_2P(CH_2)_nS(O)_xPh$ ligands in a κ*P* coordination mode as it was shown for complexes **10a**/**11a** [24] and **10c**/**11c** [29] before. The reactions were conducted in THF at room temperature. Using methylene chloride as solvent, the reactions with the dppe complex **5** have to be performed at −78 °C to avoid the oxidative addition of methylene chloride to **5** which results in the formation of a methylene-bridged rhodium(III) complex [33]. Complexes **6**–**11** were obtained as yellow to orange moderately air and moisture sensitive solids in good to excellent yields (72–91%) and they were characterized NMR spectroscopically (^{1}H, ^{13}C, ^{31}P) as well as by high-resolution mass spectrometric (HRMS-ESI) investigations. All complexes were soluble in THF and CH_2Cl_2. Solutions were found to be stable at room temperature, except for complexes **8a** and **8b** that showed a decomposition within several hours. In chloroform all complexes (except of **6**, **8c** and **10**) decomposed within several minutes.

Addition of Ag[BF_4] to complexes **6a**/**b**/**c**–**11a**/**b**/**c** led with precipitation of AgCl to cationic rhodium complexes of the type [Rh{$Ph_2P(CH_2)_nS(O)_x$Ph-κ*P*,κ*S*/*O*}L_2][BF_4] (**13a**/**b**/**c**–**18a**/**b**/**c**) bearing chelating P^S(O)$_x$ ligands with a κ*P*,κ*S* and a κ*P*,κ*O* coordination mode, respectively (Scheme 1, routes **d**/**e**/**f**). To simplify these

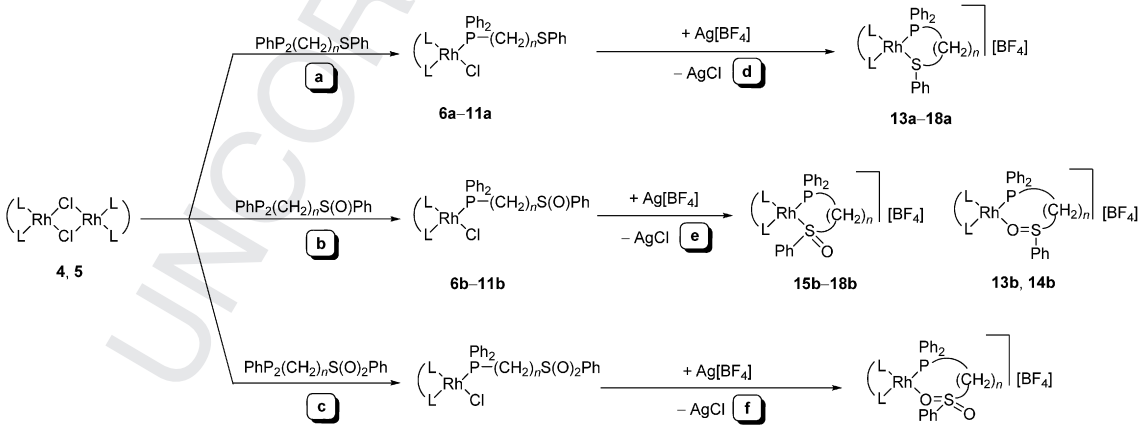

	4	5	6	7	8	9	10	11	13	14	15	16	17	18
n	–	–	1	1	2	2	3	3	1	1	2	2	3	3
L L	cod	dppe	cod	dppe	cod	dppe	cod	dppe	cod	dppe	cod	dppe	cod	dppe

Scheme 1. Synthesis of rhodium complexes bearing monodentately coordinated P^S(O)$_x$-κ*P* ligands (**6**–**11**) and chelating P^S(O)$_x$-κ*P*,κ*S*/*O* ligands (**13**–**18**).

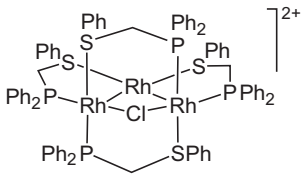

Chart 1. Structural formula of the cation in $[Rh_3(\mu\text{-}Cl)(\mu\text{-}Ph_2PCH_2SPh\text{-}\kappa P{:}\kappa S)_4][BF_4]_2\cdot 4THF$ (**12**·4THF).

syntheses, the neutral complexes **6**–**11** obtained via routes **a**/**b**/**c** do not have to be isolated. In such a way complexes **13**–**18** were isolated in yields of 78–92% as yellow moderate air and moisture sensitive solids. While **16c** showed only a limited stability in CH_2Cl_2 (ca 1 h at room temperature) all other complexes were soluble in methylene chloride without decomposition.

Complexes **13**–**18** were characterized by ^1H, ^{13}C, ^{31}P NMR spectroscopy as well as by HRMS-ESI measurements. The phosphinofunctionalized sulfides ($x = 0$) and sulfones ($x = 2$) are $\kappa P,\kappa S$ and $\kappa P,\kappa O$ coordinated, respectively. The corresponding sulfoxides exhibit both a $\kappa P,\kappa S$ ($n = 2, 3$) and a $\kappa P,\kappa O$ ($n = 1$) coordination, thus forming five- and six-membered rhodacycles. ^{31}P NMR spectroscopic measurements of the reaction solutions showed that all reactions were highly selective with the exception of complex **18c** where several by-products (>60%) were found which could not be removed. Furthermore, attempts failed to obtain complex **18c** alternatively by ligand substitution (cod → dppe) from complex **17c**: As shown NMR spectroscopically, adding 1 equivalent dppe to complex **17c** resulted with cleavage of cod in the formation of the two homoleptic cationic complexes $[Rh(dppe)_2]^+$ and $[Rh\{Ph_2PCH_2CH_2CH_2S(O)_2Ph\text{-}\kappa P,\kappa O\}_2]^+$.

While the addition of $Ag[BF_4]$ to complex **6a** in CH_2Cl_2 afforded selectively the cationic rhodium complex **13a** (Scheme 1), the analogous reaction performed in THF led to the immediate formation of a deep red solution which contains three different complexes in a ratio of about 2:1:2 as revealed by ^{31}P NMR spectroscopic measurements. Within 24 h, one of these products precipitated as red crystals which were isolated in a yield of 32%. NMR spectroscopic and structural measurements exhibited that a trinuclear rhodium(I) complex, $[Rh_3(\mu\text{-}Cl)(\mu\text{-}Ph_2PCH_2SPh\text{-}\kappa P{:}\kappa S)_4][BF_4]_2\cdot 4THF$ (**12**·4THF; Chart 1), has been formed.

Reactions of the neutral rhodium complexes **6**–**11** with sodium bis(trimethylsilyl)amide at −78 °C led to a selective deprotonation of the α-carbon atom yielding three different types of organorhodium complexes (Scheme 2, routes **a**/**b**/**c**):

*Route **a***. Starting from the neutral complexes having a trimethylene spacer ($n = 3$; **10**, **11**) organorhodium intramolecular coordination compounds of the type $[Rh\{CH\{S(O)_xPh\}CH_2CH_2PPh_2\text{-}\kappa C,\kappa P\}L_2]$ (**22**, **23**) were obtained. The two complexes bearing the deprotonated sulfinylfunctionalized ligand ($x = 1$; **22b**, **23b**) were isolated in yields of about 75% as yellow highly air and moisture sensitive solids which were found to be soluble in THF and CH_2Cl_2 without decomposition. Moreover, they showed a moderate solubility in *n*-pentane. Complexes **22a**/**c** and **23a**/**c** have been prepared before by using lithium diisopropyl amide as base [24,29]. Hence, in this work the formation of these complexes has been proved by ^{31}P NMR spectroscopic measurements of the reaction solutions only.

*Route **b***. The second class are zwitterionic complexes of the type $[Rh\{Ph_2PCHS(O)_xPh\text{-}\kappa P,\kappa S/O\}L_2]$ (**20**, **21**) which were obtained by starting from the neutral complexes bearing a methylene spacer ($n = 1$; **6**, **7**). These complexes have $\kappa P,\kappa S$ (**21a**, **21b**) and $\kappa P,\kappa O$ (**20b**/**c**, **21c**) coordinated anionic $[Ph_2PCHS(O)_xPh]$ ligands, thus the methine C atom is not coordinated to Rh. The complexes were obtained as brown highly air and moisture sensitive solids showing limited thermal stability only. Due to that, they were isolated without removing the NaCl formed in the course of the reaction. Furthermore, they exhibited a pronounced solubility even in *n*-pentane which made it difficult to remove residual amounts of $HN(SiMe_3)_2$. Complex **21a** was characterized by ^{31}P NMR spectroscopically from the reaction mixture only. All attempts to isolate complex **21a** in substance led to decomposition. Complexes **20c** and **21b** were found to decompose in THF within 1 h at room temperature and immediately in methylene chloride. For complexes **20b** and **21c** the opposite was the case. Complexes **20**–**23** (except of complex **21a**) were characterized by NMR spectroscopy (^1H, ^{13}C, ^{31}P) and HRMS-ESI measurements.

*Route **c***. In contrast, the reaction of the neutral complex [RhCl($Ph_2PCH_2SPh\text{-}\kappa P$)(cod)] (**6a**) with $NaN(SiMe_3)_2$ led to the formation of the dinuclear rhodium complex $[\{Rh\{\mu\text{-}CH(SPh)PPh_2\text{-}\kappa C{:}\kappa P\}(cod)\}_2]$ (**19**). As ^{31}P NMR spectroscopic measurements from the reaction mixture revealed, the reaction proceeded with a high selectivity (>90%), too. Within 24 h, **19** crystallized from the reaction mixture as THF adduct (**19**·THF) in a yield of 81% as orange

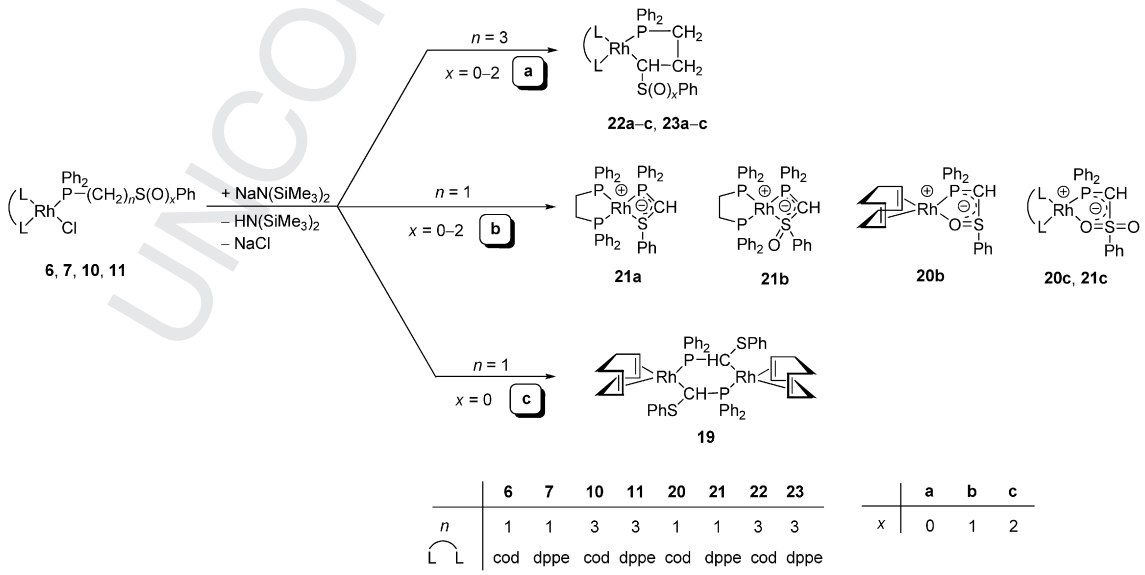

Scheme 2. Synthesis of organorhodium intramolecular coordination compounds (**22**, **23**), zwitterionic complexes (**20**, **21**) and a dinuclear organorhodium complex (**19**).

Table 1
Selected NMR spectroscopic data (δ in ppm, J in Hz) of [RhCl{$Ph_2P(CH_2)_nS(O)_xPh$-κ*P*}L_2] (**6**–**11**).

L (x)	$Ph_2PC_\alpha H_2S(O)_xPh$			$Ph_2PC_\beta H_2C_\alpha H_2S(O)_xPh$				$Ph_2PC_\gamma H_2CH_2C_\alpha H_2S(O)_xPh$			
		$\delta_{\alpha\text{-C}}$ ($^1J_{P,C}$)	δ_P ($^1J_{Rh,P}$)		$\delta_{\alpha\text{-C}}$ ($^2J_{P,C}$)	$\delta_{\beta\text{-C}}$ ($^1J_{P,C}$)	δ_P ($^1J_{Rh,P}$)		$\delta_{\alpha\text{-C}}$ ($^3J_{P,C}$)	$\delta_{\gamma\text{-C}}$ ($^1J_{P,C}$)	δ_P ($^1J_{Rh,P}$)
cod (0)	**6a**	31.4 (17.8)	28.1 (150.1)	**8a**	36.9 (7.2)	31.4 (15.9)	26.1 (150.7)	**10a**[a]	35.4 (15.0)	26.9 (25.2)	26.2 (147.1)
cod (1)	**6b**	62.3 (18.3)	30.8 (151.2)	**8b**	52.9 (s)	20.1 (22.9)	26.8 (151.2)	**10b**	58.0 (12.1)	26.9 (25.3)	26.8 (146.4)
cod (2)	**6c**	54.9 (6.8)	24.0 (154.1)	**8c**	53.5 (2.7)	22.6 (23.6)	24.7 (153.2)	**10c**[b]	57.1 (13.8)	26.6 (25.2)	27.8 (149.2)
dppe (0)	**7a**	32.0 (13.7)	24.4 (132.2)	**9a**	38.4 (9.0)	32.4 (22.8)	60.6 (134.9)	**11a**[a]	35.4 (15.8)	28.4 (22.7)	23.8 (131.6)
dppe (1)	**7b**	63.1 (13.8)	27.9 (142.3)	**9b**	53.6 (6.3)	20.4 (21.6)	23.1 (133.2)	**11b**	58.7 (13.0)	27.1 (21.9)	24.2 (131.5)
dppe (2)	**7c**	53.7 (6.9)	22.0 (135.0)	**9c**	52.7 (5.1)	21.2 (19.6)	22.1 (133.8)	**11c**[b]	57.6 (13.6)	26.9 (22.5)	23.7 (131.6)

[a] Values taken from Ref. [24].
[b] Values taken from Ref. [29].

moderately air and moisture sensitive crystals being suitable for a single-crystal X-ray diffraction analysis. Moreover, the isolated product was found to be insoluble in all common solvents which prevented further NMR spectroscopic characterization.

By analogy to the synthesis of the cationic rhodium complexes **13**–**18**, for the synthesis of all these complexes (**19**–**23**) the intermediate compounds **6**–**11** do not have to be isolated. Hence, complexes **19**–**23** can be obtained in a one-pot procedure directly from the dinuclear starting complexes **4** and **5**. In no case we succeeded to obtain definite complexes starting from rhodium complexes bearing P^S(O)$_x$ ligands with the dimethylene spacer ($n = 2$; **8**, **9**) since all reactions with $NaN(SiMe_3)_2$ led to decomposition, as ^{31}P NMR spectroscopic investigations revealed.

2.2. Spectroscopic investigations

2.2.1. Rhodium complexes with $Ph_2P(CH_2)_nS(O)_xPh$-κ*P* ligands ($n = 1$–3, $x = 0$–2)

Selected NMR spectroscopic parameters of complexes **6**–**11** are given in Table 1. The ^{31}P NMR spectra were of first order where all dppe complexes (**7**, **9**, **11**) exhibited an AEMX spin system and all cod complexes (**6**, **8**, **10**) an AX spin system (A, E, M = ^{31}P; X = ^{103}Rh). The κ*P* coordination of the P^S(O)$_x$ ligands went along with a strong lowfield shift of the ^{31}P resonances ($\Delta\delta_P > 30$ ppm). The $^1J_{P,C}$ couplings for ligands with the same spacer length (**6**/**7**, **8**/**9**, **10**/**11**) were in a narrow range, with the exception of **6c**, **7c** and **8c**. In all dppe complexes (**7**, **9**, **11**) the $^1J_{Rh,P}$ couplings (P is part of the P^S(O)$_x$ ligands) were about 20 Hz smaller than those of the cod complexes (**6**, **8**, **10**) reflecting the higher trans influence of phosphanes compared to olefines [34]. Due to the chiral sulfur center in the rhodium complexes bearing ω-phosphinofunctionalized alkyl phenyl sulfoxide ligands (**6b**–**11b**) the aliphatic and olefinic (**6b**, **8b**, **10b**) hydrogen atoms are diastereotopic. The best it could be seen in case of complexes **6b** and **7b** where each of the aliphatic protons of the $Ph_2PCH_2S(O)Ph$-κ*P* ligand exhibited a doublet of doublet pattern caused by $^2J_{H,H}$ (13.5/13.5 Hz, **6b**; 13.3/13.3 Hz, **7b**) and $^2J_{P,H}$ couplings (9.1/8.0 Hz, **6b**; 7.4/6.4 Hz, **7b**). Due to signal overlapping and/or additional H–H couplings only broad signals or non-resolved multiplets were observed in the other complexes bearing ligands with a sulfinyl functionalization.

2.2.2. Cationic rhodium complexes bearing P,S and P,O chelate ligands and $[Rh_3(\mu\text{-}Cl)(\mu\text{-}Ph_2PCH_2SPh$-κ*P*:κ*S*$)_4][BF_4]_2\cdot 4THF$

Selected NMR spectroscopic parameters of complexes **13**–**18** are given in Table 2. The ^{31}P NMR spectra of the complexes bearing a dppe ligand appeared as first order AEMX spin systems (**14a**, **14c**, **16c**, **18a**, **18b**, **18c**) as well as higher order ABMX (**14b**, **16a**) and ABCX (**16b**) spin systems, respectively (A, B, C, E, M = ^{31}P; X = ^{103}Rh) which were analyzed by using the PERCH NMR software package [35]. The ^{31}P NMR spectra of all cod complexes (**13**, **15**, **17**) were AX spin systems.

As expected, the $^1J_{Rh,P}$ couplings (P is part of the P^S(O)$_x$ ligands) were in a similar range as those of the analogous neutral complexes **6**–**11**. Only in complexes **13a** and **14a** the formation of a four-membered RhPCS cycle led to a decrease of the $^1J_{Rh,P}$ coupling constants by 30.6 Hz (**13a**) and 21.1 Hz (**14a**), respectively. Moreover, in complexes **13a** and **14a** the ^{31}P resonances of the Ph_2PCH_2SPh ligand exhibited a marked highfield shift by 59.2 ppm (**13a**) and 47.2 ppm (**15a**) compared to the respective neutral complexes **6a** and **7a** (Table 1). These pronounced highfield shifts are also found in structurally similar rhodium complexes having bound a dppm-κ^2*P*,*P*′ ligand (four-membered RhP_2C ring) [29,36,37]. Furthermore, the formation of the four-membered rhodacycles led to a, respectively, strong ($\Delta\delta_C$ 76.3 ppm, **13a**) and a reasonable ($\Delta\delta_C$ 28.3 ppm, **14a**) lowfield shift of the α-C resonances whereas the κ*P*,κ*O* and κ*P*,κ*S* coordination of the P^S(O)$_x$ ligands in all other complexes had only little effect on the ^{13}C NMR shifts of the α-carbon atoms ($\Delta\delta \leq 7$ ppm) compared to the neutral rhodium complexes **6**–**11**.

Table 2
Selected NMR spectroscopic data (δ in ppm, J in Hz) for complexes [Rh{$Ph_2P(CH_2)_{n-1}C_\alpha H_2S(O)_xPh$-κ*P*,κ*S*/*O*}$L_2$][$BF_4$] (**13**–**18**).

	L_2 = cod					L_2 = dppe			
	n/x	$\delta_{\alpha\text{-C}}$ ($^mJ_{P,C}$)	δ_P ($^1J_{Rh,P}$)	δ_C=C[a] ($^1J_{Rh,C}$)		n/x	$\delta_{\alpha\text{-C}}$ ($^mJ_{P,C}$)	δ_P ($^1J_{Rh,P}$)	$\delta_{P'}$[b] ($^1J_{Rh,P'}$)
13a	1/0	107.7 (7.3)[c]	−31.1 (119.5)	86.5 (9.3)	**14a**	1/0	60.3 (19.3)[c]	−22.8 (111.1)	69.1 (166.6)
13b	1/1	57.4 (10.2)[c]	53.6 (162.7)	69.4/74.1 (13.9/14.5)	**14b**	1/1	56.6 (s)	55.5 (146.3)	74.0 (182.4)
13c	1/2	57.2 (10.0)[d]	25.3 (149.0)	72.4 (14.3)	**14c**	1/2	56.4 (s)	27.1 (129.7)	76.2 (184.7)
15a	2/0	37.5 (7.2)[d]	59.0 (147.2)	87.7 (10.8)	**16a**	2/0	39.2 (10.9)[d]	59.4 (135.3)	65.5 (151.2)
15b	2/1	52.9 (s)	52.7 (135.8)	78.0/78.3 (8.1/11.3)	**16b**	2/1	60.3 (9.5)[d]	57.8 (136.4)	60.1 (145.1)
15c	2/2	51.9 (s)	18.9 (149.5)	71.1 (15.6)	**16c**	2/2	52.4 (6.4)[d]	16.5 (136.6)	77.4 (204.5)
17a	3/0	39.3 (3.6)[e]	12.4 (140.0)	86.0 (11.2)	**18a**	3/0	35.9 (8.8)[e]	7.1 (131.1)	66.4 (160.0)
17b	3/1	57.7 (4.8)[e]	11.0 (140.0)	94.5/99.0 (10.0/8.4)	**18b**	3/1	58.7 (7.6)[e]	7.7 (132.2)	60.0 (148.2)
17c	3/2	57.0 (3.8)[e]	24.2 (147.8)	71.6 (15.3)	**18c**	3/2	–	21.2 (127.0)	70.5 (182.5)

[a] C=C is part of the cod ligand and *trans* to S and O, respectively.
[b] P′ is part of the dppe ligand and *trans* to S and O, respectively.
[c] $m = 1$.
[d] $m = 2$.
[e] $m = 3$.

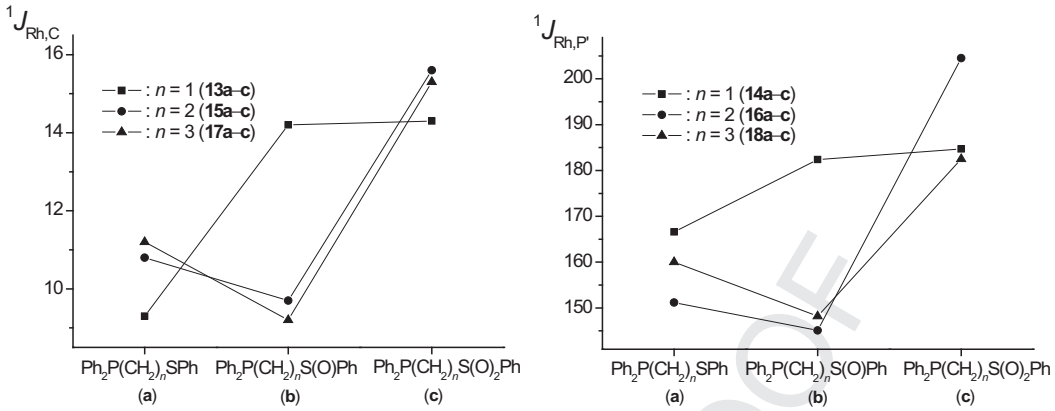

Fig. 1. Graphical representation of $^1J_{Rh,C}$ couplings in complexes **13**, **15**, **17** (left) and $^1J_{Rh,P'}$ couplings in complexes **14**, **16**, **18** (right). In complexes **13b**, **15b** and **17b** the mean value of the two $^1J_{Rh,C}$ couplings are given.

The different trans influences of the R_2S group (*S* donor) and the R_2SO_2 group (*O* donor) allowed an assignment of the coordination mode (κ*P*,κ*S* versus κ*P*,κ*O*) of the ω-phosphinofunctionalized alkyl phenyl sulfoxide ligands in complexes **13b**–**18b**. In Fig. 1, the magnitudes of the $^1J_{Rh,C}$ (C is *trans* to S/O) and $^1J_{Rh,P'}$ (P′ is *trans* to S/O) couplings of the complexes bearing sulfinylfunctionalized ligands ($x = 1$) are compared to those of the analogous complexes having bound functionalized sulfide ($x = 0$) and sulfone ($x = 2$) ligands where the κ*P*,κ*S* and κ*P*,κ*O* coordination, respectively, is obvious (Fig. 1).

As it can be seen, the two rhodium complexes having bound the $Ph_2PCH_2S(O)Ph$ ligand (**13b**, **14b**) most likely adopt a κ*P*,κ*O* coordination thus avoiding a strained four-membered ring whereas the other sulfoxide ligands in complexes **15b**, **16b**, **17b** and **18b** most probably exhibit a κ*P*,κ*S* coordination mode. For **15b** this is in full accordance with the result of the single-crystal X-ray diffraction analysis (vide infra, Fig. 2).

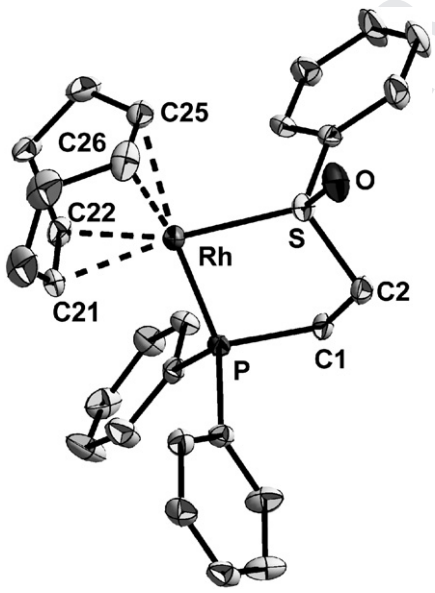

Fig. 2. Molecular structure of the cation in crystals of [Rh{$Ph_2PCH_2CH_2S(O)Ph$-κ*P*,κ*S*}(cod)][BF_4] (**15b**). The ellipsoides are shown with a probability of 30%. H atoms have been omitted for clarity. Selected structural parameters (distances in Å, angles in °): Rh–P 2.269(2), Rh–C21/22_{cg} (cg = center of gravity) 2.0868(5), Rh–C25/26_{cg} 2.1425(5), Rh–S 2.270(2), C21–C22 1.361(9), C25–C26 1.346(1), S–O 1.462(5), P–Rh–S 85.8(5), P–Rh–C21/22_{cg} 94.6(1), C21/22_{cg}–Rh–C25/26_{cg} 85.7(1), C25/26_{cg}–Rh–S 94.1(1), C25/26_{cg}–Rh–P 179.1(1), C21/22_{cg}–Rh–S 173.0(1).

In the ^{31}P NMR spectrum of the trinuclear complex **12**·4THF the resonances of two magnetically inequivalent phosphorus atoms appeared as ddd patterns from which the $^1J_{Rh,P}$ (140.7/180.3 Hz), $^2J_{P,P}$ (35.3/35.3 Hz) and $^2J_{Rh,P}$ (2.5/3.5 Hz) couplings could be obtained. Apart from the THF signals and the resonances in the aromatic region the ^1H NMR spectrum showed one broad singlet at 2.78 ppm whereas in the ^{13}C NMR spectrum two doublet patterns (δ_C 31.6/42.5 ppm) appeared showing $^1J_{P,C}$ couplings (27.8/26.7 Hz). The solid-state structure of this complex (vide infra, Fig. 4) let expect the AA′EE′ part of an AA′EE′MM′X spin system (A, E = ^{31}P; M, X = ^{103}Rh) in the ^{31}P NMR spectrum. An analysis with the PERCH software revealed that due to small $^3J_{Rh,P}$ and $^4J_{P,P}$ long-range couplings (<2 Hz) the NMR spectrum is simplified, hence two ddd patterns are found only, which is in full accord with the experimental findings.

2.2.3. Organorhodium intramolecular coordination and zwitterionic complexes, [{Rh{μ-CH(SPh)PPh_2-κ*C*:κ*P*}(cod)}$_2$]

While the ^{31}P NMR spectra of the intramolecular coordination compounds bearing a dppe ligand **23** (Table 3) appeared as higher order ABCX spin systems, those of the zwitterionic rhodium complexes [Rh{$Ph_2PCHS(O)_xPh$-κ*P*,κ*S*/*O*}(dppe)] (**21**) were found to be first order AEMX spin systems (A, B, C, E, M = ^{31}P; X = ^{103}Rh). However, all cod complexes (**20**, **22**) proved to be of first order with an AX spin system.

As revealed NMR spectroscopically, the reaction of **10b** and **11b** with $NaN(SiMe_3)_2$ to form the organometallic complexes [Rh{CH{S(O)Ph}$CH_2CH_2PPh_2$-κ*C*,κ*P*}L_2] (L_2 = cod, **22b**; dppe, **23b**) with a deprotonated sulfinyl ligand and thereby having two centers of chirality (sulfur and α-C atom) proceeded diastereoselectively. This was confirmed by the presence of only one set of signals in the NMR spectra (^1H, ^{13}C, ^{31}P). Noteworthy, in the case of **22b** initially two diastereomers in an intensity ratio of about 1:1 were observed in the ^{31}P NMR spectrum of the reaction solution (δ_P 51.6/52.1 ppm; $^1J_{Rh,P}$ = 174.6/176.4 Hz). At room temperature within 2 h an isomerization took place yielding selectively only one diastereomer (δ_P 51.6 ppm). The α-carbon atoms in the cod complex **22b** appeared as dd pattern showing $^1J_{Rh,C}$ and $^2J_{P,C}$ couplings. In contrast, the signal of the C_α atom in the dppe complex (**23b**) proved to be of too high multiplicity to be resolved.

In the zwitterionic complexes **20** and **21** the signals of the α-carbon nuclei appeared as doublet ($^1J_{P,C}$) and broad singlet patterns, respectively, which excluded a coordination of the C_α atom to the rhodium atom due to the missing $^1J_{Rh,C}$ couplings. Furthermore, from the signal pattern in the ^{31}P NMR spectra (d, **20**; 3 × ddd, **21**) it could be seen that the complexes were mononuclear. On the basis

Table 3
Selected NMR spectroscopic data (δ in ppm, J in Hz) for complexes [Rh{$Ph_2PCHS(O)_xPh$-κ*P*,κ*S*/*O*}L_2] (**20**, **21**) and [Rh{$CH\{S(O)_xPh\}CH_2CH_2PPh_2$-κ*C*,κ*P*}$L_2$] (**22**, **23**).

		$Ph_2PC_\alpha HS(O)_xPh$						$Ph_2PC_\gamma H_2CH_2C_\alpha HS(O)_xPh$			
	L	*x*	$\delta_{\alpha\text{-}C}$ ($^1J_{P,C}$)	$\delta_{C=C}$[a] ($^1J_{Rh,C}$)	$\delta_{P'}$[a] ($^1J_{Rh,P'}$)		L	*x*	$\delta_{\alpha\text{-}C}$ ($^2J_{P,C}$)	$\delta_{\gamma\text{-}C}$ ($^1J_{P,C}$)	δ_P ($^1J_{Rh,P}$)
						22a[b]	cod	0	35.5 (4.5)	31.9 (22.4)	58.6 (168.3)
20b	cod	1	70.1 (14.3)	87.0/87.3 (10.1/9.7)	–	**22b**	cod	1	63.0 (4.9)	34.0 (26.9)	51.6 (174.6)
20c	cod	2	69.0 (14.7)	85.5/87.9 (9.9/9.8)	–	**22c**[c]	cod	2	63.0 (4.6)	33.0 (26.9)	52.0 (172.0)
21a[d]	dppe	0	–	–	69.4 (159.1)	**23a**[b]	dppe	0	41.9–42.8 (m)	33.6 (17.1)	58.6 (162.3)
21b	dppe	1	66.6 (s)	–	67.1 (157.3)	**23b**	dppe	1	57.9–59.8 (m)	29.3 (15.9)	58.0 (156.1)
21c	dppe	2	37.4 (s)	–	74.1 (189.0)	**23c**[c]	dppe	2	61.1–63.0 (m)	35.0 (22.2)	55.5 (153.1)

[a] *trans* to S or O, respectively.
[b] Values taken from Ref. [24].
[c] Values taken from Ref. [29].
[d] Not isolated in substance; only characterized ^{31}P NMR spectroscopically.

of these facts it was concluded that complexes **20** and **21** have the anionic [$Ph_2PCHS(O)Ph$] ligand κ*P*,κ*S* (**21a**/**b**) and κ*P*,κ*O* (**20b**/**c**, **21c**) coordinated. Since the central methine carbon atom is not coordinated to Rh, these are zwitterionic complexes as it is found in numerous structurally similar dppm$_{-H}$-κ^2*P*,*P*′ complexes [36,38,39]. Till now, in literature zwitterionic complexes with P^S ligands are described only in which the anionic carbon atom is part of a carboborane [40] or of a ring system [41]. The assignment of the coordination mode of the flexidentate anionic [$Ph_2PCHS(O)Ph$] ligand in **20b** (κ*P*,κ*O*) and **21b** (κ*P*,κ*S*) was performed on the same basis as it was done for the appropriate cationic rhodium complexes **13b** and **14b** (see Section 2.2.2.).

The ^{31}P NMR spectrum of the dinuclear complex **19** which was obtained directly from the reaction solution exhibited a higher order spectrum showing 6 lines. Considering the solid-state structure of [{Rh(μ-Ph_2PCH(SPh)-κ*C*:κ*P*)(cod)}$_2$]·THF (**19**·THF) (vide infra, Fig. 5) the pattern can be interpreted as an AA′XX′ spin system (A = ^{31}P, X = ^{103}Rh) showing only 6 instead of the expected 10 lines caused by a too small (<1 Hz) $^3J_{Rh,Rh}$ coupling constant. Using the PERCH software $^1J_{Rh,P}$ (169.6/167.3 Hz), $^2J_{Rh,P}$ (4.0/1.0 Hz) and $^3J_{P,P}$ (147.4 Hz) coupling constants could be identified. Complex **19**·THF, which crystallized from the reaction mixture within 24 h, could not be re-dissolved in any common solvent which prevented further NMR spectroscopic investigations.

2.3. Structures

2.3.1. Structures of [Rh{$Ph_2PCH_2CH_2S(O)_xPh$}(cod)][BF_4] (*x* = 1, ***15b***; *x* = 2, ***15c***)

Crystals of **15b** and **15c** suitable for X-ray diffraction analyses were obtained from THF solutions at room temperature. The two complexes crystallized as discrete cations and anions without unusual intermolecular interactions (shortest distance between non-hydrogen atoms: 3.323(8) Å, C2···F3′, **15b**; 3.054(5) Å, C2···F3′, **15c**). The structures of the cations are shown in Figs. 2 and 3. Selected structural parameters are given in the figure captions.

In the two complexes the rhodium atoms exhibit a slightly distorted square-planar configuration where the primary donor sets are built up by the bidentately bound cycloocta-1,5-diene ligand and, respectively, a chelating κ*P*,κ*S* coordinated β-phosphino-functionalized ethyl phenyl sulfoxide ligand (**15b**) and a chelating κ*P*,κ*O* coordinated β-phosphinofunctionalized ethyl phenyl sulfone ligand (**15c**). In the two complexes all angles between neighbored ligands are close to 90° (85.7(1)–94.6(1)°, **15b**; 87.0(1)–93.1(1)°, **15c**) and those between *trans* standing ligands are close to 180° (179.1(1)/173.0(1)°, **15b**; 178.0(1)/172.9(1)°, **15c**). The trans influence order $PR_3 > R_2SO$-κ*S* > R_2SO_2-κ*O* is clearly reflected in different Rh–C_{olefin} bond lengths. As expected, the Rh–C25/26$_{cg}$ (C25/26$_{cg}$ is *trans* to P; cg = center of gravity) bonds are of the same length (2.1433(3) Å, **15b**; 2.1425(5) Å, **15c**). However, the Rh–C21/22$_{cg}$ bond in **15b** (2.0868(5) Å, *trans* to S) is markedly longer than the analogous bond in **15c** (1.9877(3) Å, *trans* to O). Furthermore, the olefinic C–C bond *trans* to O in **15c** is considerably longer than the other three C–C double bonds *trans* to P and S in **15b**/**c** (1.413(6) Å versus 1.346(1)–1.361(9) Å), respectively. This might be traced back to the weak trans influence of the R_2SO_2-κ*O* donor which goes along with the above mentioned short Rh–C bond; similar observations were made in other cod rhodium complexes [42–44].

2.3.2. Structure of [Rh_3(μ-Cl)(μ-Ph_2PCH_2SPh-κ*P*:κ*S*)$_4$][BF_4]$_2$·4THF (***12***·4THF)

Crystals of **12**·4THF suitable for an X-ray diffraction analysis were obtained from CH_2Cl_2 solution with a layer of *n*-pentane at room temperature. The complex crystallized as discrete [Rh_3(μ-Cl)(μ-Ph_2PCH_2SPh-κ*P*:κ*S*)$_4$]$^{2+}$ cations and [BF_4]$^-$ anions without unusual intermolecular interactions (shortest distance between non-hydrogen atoms: 3.486(9) Å, C20···O1′). The structure of the cation is

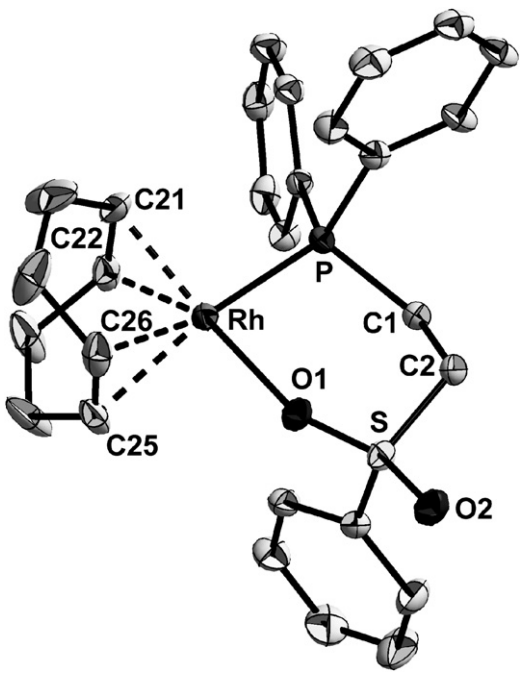

Fig. 3. Molecular structure of the cation in crystals of [Rh{$Ph_2PCH_2CH_2S(O)_2Ph$-κ*P*,κ*O*}(cod)][BF_4] (**15c**). The ellipsoides are shown with a probability of 30%. H atoms have been omitted for clarity. Selected structural parameters (distances in Å, angles in °): Rh–P 2.2859(8), Rh–C21/22$_{cg}$ 1.9877(3), Rh–C25/26$_{cg}$ 2.1433(3), Rh–O1 2.166(2), C21–C22 1.413(6), C25–C26 1.358(6), P–Rh–O1 92.2(1), P–Rh–C21/22$_{cg}$ 93.1(1), C22/23$_{cg}$–Rh–C25/26$_{cg}$ 87.0(1), C25/26$_{cg}$–Rh–O1 87.9(1), C25/26$_{cg}$–Rh–P 178.0(1), C21/22$_{cg}$–Rh–O1 172.9(1).

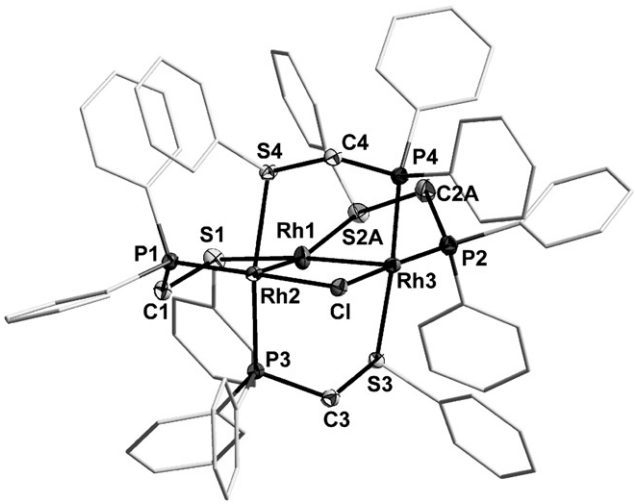

Fig. 4. Molecular structure of the cation in crystals of $[Rh_3(\mu\text{-}Cl)(\mu\text{-}Ph_2PCH_2SPh\text{-}\kappa P{:}\kappa S)_4][BF_4]_2\cdot 4THF$ (**12**·4THF). The ellipsoides are shown with a probability of 30%. For clarity, H atoms have been omitted and phenyl rings are displayed as wire model. One CH_2SPh group (C2A/S2A and C2B/S2B) was found to be disordered over two positions with an occupancy of 58.8(4) and 41.2(4)%; only the major occupied position is shown. Selected structural parameters (distances in Å, angles in °): Rh1–Rh2 2.7357 (5), Rh1–Rh3 2.7606(5), Rh2–Cl 2.406(1), Rh3–Cl 2.415(1), Rh1–S2A 2.637(2), Rh1–S2B 2.458(3), Rh1–S1 2.553(1), Rh2–P1 2.266(1), Rh2–P3 2.276(1), Rh2–S4 2.401(1), Rh3–P2 2.249(1), Rh3–P4 2.288(1), Rh3–S3 2.371(1), Rh2–Rh1–Rh3 74.06 (1), Rh1–Rh2–Cl 99.85(3), Rh1–Rh3–Cl 98.92(3), Rh2–Cl–Rh3 86.72(3), Rh1–Rh2–S1 101.63(3), Rh1–Rh2–P1 84.02(3), P1–Rh2–Cl 176.13(4), S4–Rh2–P3 170.65(5), P2–Rh3–Cl 175.62(4), P4–Rh3–S3 172.85(4), Rh1–Rh2···Rh3–Cl 173.38 (4).

shown in Fig. 4. Selected structural parameters are given in the figure caption.

The cation is built up by a four-membered Rh_3Cl cycle and four μ-Ph_2PCH_2SPh-$\kappa P{:}\kappa S$ ligands. The overall disposition of the ligands is consistent with a C_2 symmetry (axis through Rh1 and Cl) in rough approximation. The central rhodium atom (Rh1) adopts a distorted square-planar configuration where the primary donor set is built up by two *cis* standing sulfur atoms of two μ-Ph_2PCH_2SPh ligands and by the other two rhodium atoms Rh2 and Rh3. In contrast, these two rhodium atoms exhibit a square-pyramidal configuration having Rh1 in the apical position each. The equatorial positions are occupied by the μ-Cl ligand as well as by two *cis* standing phosphorus atoms and one sulfur atom. The torsion angle Rh1–Rh2···Rh3–Cl is 173.38(4)°, thus the four-membered ring is almost planar. Regarding the Rh_3Cl cycle, the Cl–Rh2–Rh1 (99.85(3)°) and the Cl–Rh3–Rh1 (98.92(3)°) angles are of a similar size whereas the Rh2–Rh1–Rh3 (74.06(1)°) and the Rh2–Cl–Rh3 (86.72(3)°) angles are considerably smaller. The two five-membered rhodacycles Rh1–S1–C1–P1–Rh2 and Rh1–S2A–C2A–P2–Rh3/Rh1–S2B–C2B–P2–Rh3 adopt a half-chair conformation twisted on P1 and C1 as well as on P2 and C2A/C2B, respectively. Even though the Rh1–Rh2 bond (2.7357(5) Å) is shorter than the Rh1–Rh3 bond (2.7606(5) Å), both are in the expected range for Rh–Rh bonds (median: 2.760 Å, lower/higher quartile: 2.682/2.822 Å, $n = 4446$; n = number of observations) [45]. The distances between Rh2 and Rh3 (3.3100(5) Å) as well as between Rh1 and Cl (3.940(1) Å) exclude any interactions between these atoms.

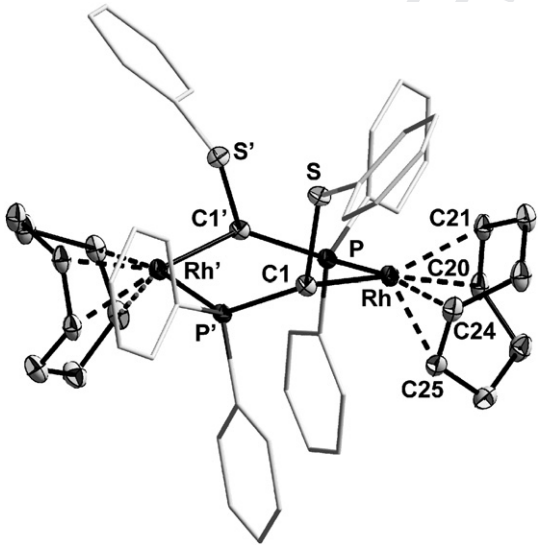

Fig. 5. Molecular structure of $[\{Rh\{\mu\text{-}CH(SPh)PPh_2\text{-}\kappa C{:}\kappa P\}(cod)\}_2]$ (**19**) in crystals of **19**·THF. The ellipsoides are shown with a probability of 30%. For clarity, H atoms have been omitted and phenyl rings are displayed as wire model. Selected structural parameters (distances in Å, angles in °): Rh–P 2.3429(8), Rh–C1 2.077(2), Rh–C20/21_{cg} 2.0979(3), Rh–C24/25_{cg} 2.0625(3), C1–Rh–P 95.42(7), P–Rh–C20/21_{cg} 93.24(2), C20/21_{cg}–Rh–C24/25_{cg} 85.23(1), C24/25_{cg}–Rh–C1 90.42(1), S–C1–Rh 81.5(1), C20/21_{cg}–Rh–C1, 169.05(6); C24/25_{cg}–Rh–P, 150.93(2).

2.3.3. Structure of $[\{Rh\{\mu\text{-}CH(SPh)PPh_2\text{-}\kappa C{:}\kappa P\}(cod)\}_2]\cdot THF$ (**19**·THF)

Crystals of **19**·THF suitable for an X-ray diffraction analysis were obtained from THF solution at room temperature. The complex crystallized as discrete dinuclear entities and between them no unusual intermolecular contacts were found (shortest intermolecular distance between non-hydrogen atoms is 4.09(2) Å, C25···C12″). The dinuclear complex exhibits crystallographically imposed C_2 symmetry. The structure is shown in Fig. 5, selected structural parameters are given in the figure caption. The rhodium atoms are in a distorted square-planar geometry and surrounded by a bidentately bound cycloocta-1,5-diene ligand as well as by a sulfur and a carbon atom of the μ-$CH(SPh)PPh_2$-$\kappa C{:}\kappa P$ ligand. Due to the higher trans influence of the anionic C ligand compared to the neutral P ligand the Rh–C20/21_{cg} bond (2.0979(3) Å, *trans* to C) is markedly longer than the Rh–C24/25_{cg} bond (2.0625(3) Å, *trans* to P). The six-membered $Rh_2C_2P_2$ ring adopts a twist-boat conformation having the SPh groups almost perpendicular to it. Notably, there is a weak interaction between the rhodium and the sulfur atom (Rh···S = 2.5449(8) Å) giving rise to a pseudo-five-coordination [46] which results in a severe distortion from the ideal square-planar geometry (C20/21_{cg}–Rh–C1, 169.05(6)°; C24/25_{cg}–Rh–P, 150.93(2)°).

2.3.4. Structures of calculated zwitterionic complexes

To get insight into the coordination mode of the flexidentate $[Ph_2PCHS(O)Ph]$ ligand ($\kappa P,\kappa S$ versus $\kappa P,\kappa O$), quantum chemical calculations on the DFT level of theory were performed. The calculated structures of the two isomeric zwitterionic complexes with a cod coligand $[Rh\{Ph_2PCHS(O)Ph\text{-}\kappa P,\kappa S/O\}(cod)]$ (**20b**$_{calc}$, **20b′**$_{calc}$) are shown in Fig. 6. The complex with the $\kappa P,\kappa O$ coordination (**20b**$_{calc}$) possessing a five-membered RhPCSO cycle was found to be energetically more stable by 4.4 kcal/mol (Gibbs free energy at 298 K) than the constitutional isomer $[Rh\{Ph_2PCHS(O)Ph\text{-}\kappa P,\kappa S\}(cod)]$ (**20b′**$_{calc}$). This is in full accordance with the experimental findings.

In addition, for structural comparison, the protonated congeners $[Rh\{Ph_2PCH_2S(O)Ph\text{-}\kappa P,\kappa O\}(cod)]^+$ (**13b**$_{calc}$) and $[Rh\{Ph_2PCH_2S(O)Ph\text{-}\kappa P,\kappa S\}(cod)]^+$ (**13b′**$_{calc}$) have been calculated. Thus, complex **13b**$_{calc}$ represents the calculated cation of the isolated complex $[Rh\{Ph_2CH_2S(O)Ph\text{-}\kappa P,\kappa O\}(cod)][BF_4]$ (**13b**). In both complexes the deprotonation of the CH_2 group goes along with a considerable shortening of the P–C bonds (1.758/1.741 Å, **20b**$_{calc}$/**20b′**$_{calc}$) and the S–C bonds (1.674/1.687 Å, **20b**$_{calc}$/**20b′**$_{calc}$) compared to their

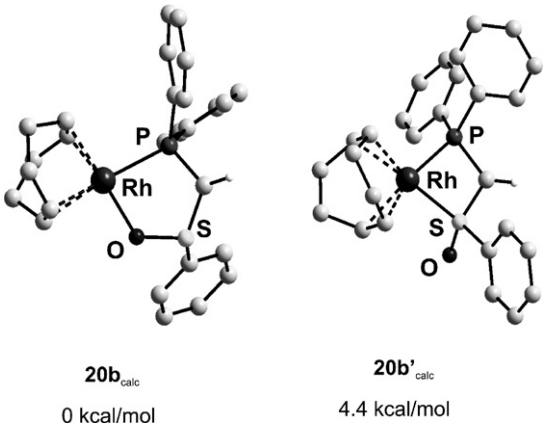

Fig. 6. Calculated structures of [Rh{$Ph_2PCHS(O)Ph$-κ*P*,κ*O*}(cod)] (**20b**$_{calc}$) and [Rh{$Ph_2PCHS(O)Ph$-κ*P*,κ*S*}(cod)] (**20b**′$_{calc}$). For clarity, only the H atoms of the methine carbon atoms are displayed. Gibbs free energy of **20b**′$_{calc}$ is relative to that of **20b**$_{calc}$.

protonated congeners (P–C: 1.880/1.867 Å; S–C: 1.827/1.839 Å; **13b**$_{calc}$/**13b**′$_{calc}$). Such a shortening of the P–C bonds is also found in complexes bearing an anionic dppm$_{-H}$-κ^2*P*,*P*′ ligand which is explained in terms of an ylidic bonding model with some charge delocalization within the PCP moiety [47]. Moreover, the fact that the calculated complex with the κ*P*,κ*O* coordinated ligand (**13b**$_{calc}$) is the thermodynamically favored isomer ($\Delta\Delta G^{\ominus}$ = 10.7 kcal/mol; see Supplemental Material, Figure S 3) is in full accordance with the assignment of the coordination mode of the $Ph_2CH_2S(O)Ph$ ligand in complex [Rh{$Ph_2CH_2S(O)Ph$-κ*P*,κ*O*}(cod)][BF_4] (**13b**) which was done on the basis of the magnitudes of the $^1J_{Rh,C}$ coupling constants (see Section 2.2.2).

For the dppe complex **21b** the two calculated constitutional isomers [Rh{$Ph_2PCHS(O)Ph$-κ*P*,κ*O*}(dppe)] (**21b**$_{calc}$) and [Rh{$Ph_2PCHS(O)Ph$-κ*P*,κ*S*}(dppe)] (**21b**′$_{calc}$; see Supplemental Material, Figure S 1) were found to be of the same energy within the margin of error ($\Delta\Delta G^{\ominus}$ = 0.1 kcal/mol), thus the proposed coordination mode based on NMR spectroscopic investigations (κ*P*,κ*S*) could be neither validated nor invalidated. Additionally, the analogous dmpe complexes ([Rh{$Ph_2PCHS(O)Ph$-κ*P*,κ*O*}(dmpe)], **24**$_{calc}$; [Rh{$Ph_2PCHS(O)Ph$-κ*P*,κ*S*}(dmpe)], **24**′$_{calc}$) were calculated and found to be of the same energy, too ($\Delta\Delta G^{\ominus}$ = 0.2 kcal/mol; see Supplemental Material, Figure S 2).

2.4. Conclusions

From the experimental investigations and quantum chemical calculations performed in this work the following conclusions on the coordination behavior of ω-diphenylphosphinofunctionalized sulfide ($x = 0$), sulfoxide ($x = 1$) and sulfone ($x = 2$) ligands (type **I**, Chart 2) and their deprotonated congeners (type **II**) can be drawn:

1. Reactions of [$(RhL_2)_2(\mu\text{-}Cl)_2$] with type **I** sulfoxide ligands ($x = 1$) followed by the addition of Ag[BF_4] give rise to the formation of cationic complexes of the type [Rh{$Ph_2P(CH_2)_nS(O)Ph$-κ*P*,κ*S*/*O*}L_2][BF_4] (**13**–**18**). While the ligands with the dimethylene ($n = 2$) and the trimethylene ($n = 3$) spacer exhibit a κ*P*,κ*S* coordination, those with the methylene spacer ($n = 1$) afford a κ*P*,κ*O* coordination. In all cases thermodynamically favored five- and six-membered rhodacycles are formed. Thus, phosphinofunctionalized sulfoxides are flexidentate ligands (κ*P*,κ*S* versus κ*P*,κ*O*). Here the coordination mode is dependent on the ring size and not on the Lewis basicity of the coligand (cod, dppe), as it is described for non-functionalized sulfoxides [20] as well as for *N*-phosphino sulfinamide ligands (PNSO-type ligands) [48].
2. In contrast, type **I** sulfide ($x = 0$) and sulfone ligands ($x = 2$) are not flexidentate. Thus, in the respective complexes [Rh{$Ph_2P(CH_2)_n$SPh-κ*P*,κ*S*}L_2][BF_4] (**13a**–**18a**) and [Rh{$Ph_2P(CH_2)_nS(O)_2Ph$-κ*P*,κ*O*}L_2][BF_4] (**13c**–**18c**) also four- (n = 1, **13a**/**14a**) and seven-membered (n = 3, **17c**/**18c**) rhodacycles are yielded. The *O* coordination of the sulfonyl group was unambiguously proved by the solid-state structure in case of **15c**, being one of the few structurally characterized complexes bearing sulfone ligands which is attributed to their low donor capability [49].
3. The weaker coordination capability of the cod ligand compared to the dppe ligand is evident in the reaction of the rhodium complex bearing a κ*P* coordinated type **I** ligand ($x = 0$, $n = 1$, **6a**) with Ag[BF_4] leading, with cleavage of the cod ligand, to the formation of the trinuclear Rh(I) complex [Rh_3(μ-Cl)(μ-Ph_2PCH_2SPh-κ*P*:κ*S*)$_4$][BF_4]$_2$·4THF (**12**·4THF). Noteworthy, **12**·4THF contains the structural motif of an A-frame complex (P1–Rh2–μ-Cl–Rh–P2) which is well known from complexes with dppm ligands [50,51]. The formal addition of Rh1 to that structural unit results in two five-coordinated Rh centers (Rh2, Rh3). The four-membered Rh_3Cl cycle as structural unit in complex **12**·4THF is only found in one further complex, namely in an osmium–rhodium carbonyl cluster [52].
4. Type **II** ligands with a C_3 spacer (n = 3) are found to form organorhodium intramolecular coordination compounds (**22**, **23**) irrespective of the nature of the sulfur functionalization (x = 0–2) [24,29]. In the case of the sulfinylfunctionalized ligands (x = 1) the deprotonation of the prochiral CH_2 group creates a second chiral center; noteworthy, the formation of the respective organorhodium complexes (**22b**, **23b**) proved to be diastereoselective. The diastereoselective synthesis of metallacycles [53–55] and their use as catalysts [56,57] have been described in literature previously.
5. In contrast, the anionic type **II** ligands with a C_1 spacer ($n = 1$) are found to form zwitterionic complexes containing both four- and five-membered rhodacycles. Interestingly, the coordination of the flexidentate sulfinyl group was found to be dependent on the coligand: With the more strongly electron donating dppe coligand a κ*P*,κ*S* coordination of the [$Ph_2PCHS(O)Ph$] ligand was found, whereas the cod coligand causes a κ*P*,κ*O* coordination. Such a coligand-dependency on the coordination mode of sulfoxide ligands has been discussed on the basis of the HSAB theory [58]. A marked influence of the coligand was also found in the complexes bearing the anionic [$Ph_2PCHSPh$] ligand: With dppe a zwitterionic complex (**21a**) was formed as described above, whereas with cod a dinuclear complex (**19**·THF) was yielded having coordinated μ-$Ph_2PCHSPh$-κ*C*:κ*P* ligands. Yet the only structurally similar dinuclear rhodium complex described in literature is the Rh(III) complex [{Rh(Cp^*)Me(μ-PMe_2CH_2-κ*C*:κ*P*)}$_2$] [59].

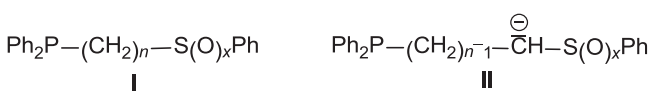

Chart 2. ω-Diphenylphosphinofunctionalized sulfides ($x = 0$), sulfoxides ($x = 1$) and sulfones ($x = 2$) **I** (n = 1–3) and their deprotonated congeners **II** being used as ligands in Rh(I) complexes.

These investigations show the versatile coordination behavior of bidentate neutral P^S(O)$_x$ ligands of type **I** (Chart 2) and their deprotonated congeners (type **II**) which can be understood in terms of the type of the sulfur functionality (sulfanyl versus sulfinyl versus sulfonyl) and the length of the spacer between the two coordination centers (κ*P*,κ*S*; κ*P*,κ*O*; κ*C*,κ*P*). Thus, these ligands offer an easy access to formation of novel cationic rhodium complexes,

organorhodium intramolecular coordination compounds as well as zwitterionic rhodium complexes.

3. Experimental part

3.1. General comments

All reactions and manipulations were carried out under argon using standard Schlenk techniques. Diethyl ether, toluene, *n*-pentane, THF were dried over Na/benzophenone, CH_2Cl_2 over CaH_2 and freshly distilled prior to use. NMR spectra (^1H, ^{13}C, ^{31}P) were recorded at 27 °C on Varian Gemini 200, VXR 400, and Unity 500 spectrometers. Chemical shifts are relative to solvent signals ($CDCl_3$, δ_H 7.24, δ_C 77.0; CD_2Cl_2, δ_H 5.32, δ_C 53.8; C_6D_6, δ_H 7.15, δ_C 128.0; THF-d_8, δ_H 1.73/3.58, δ_C 25.4/67.6) as internal references; δ (^{31}P) is relative to external H_3PO_4 (85%). Multiplets in NMR spectra of higher order resulting in pseudo doublets and triplets are denoted by 'd' and 't', respectively; the distance between the outer lines is given as *N*. Coupling constants $J_{P,P}$ and $J_{P,Rh}$ from higher order multiplets were obtained by using the PERCH NMR software package. For couplings in ring systems only the shortest coupling path is given. Microanalyses were performed in the Microanalytical Laboratory of the University of Halle using a CHNS-932 (LECO) elemental analyzer. The high-resolution ESI mass spectra were obtained from a Bruker Apex III Fourier transform ion cyclotron resonance (FT-ICR) mass spectrometer (Bruker Daltonics) equipped with an Infinity cell, a 7.0 T superconducting magnet (Bruker), a rf-only hexapole ion guide, and an external APOLLO electrospray ion source (Agilent, off-axis spray). The sample solutions were introduced continuously via a syringe pump with a flow rate of 120 μL h^{-1}. Details of the preparation of starting compounds and a complete set of their NMR spectroscopic data are given in the Supplemental Material. [{Rh(cod)}$_2$(μ-Cl)$_2$] (**4**), [{Rh(dppe)}$_2$(μ-Cl)$_2$] (**5**), $Ph_2PCH_2CH_2CH_2SPh$ (**3a**) and $Ph_2PCH_2CH_2CH_2S(O)_2Ph$ (**3c**) were prepared according to literature procedures [24,29,60,61].

3.2. Preparation of [RhCl{$Ph_2P(CH_2)_nS(O)_xPh$-κP}L_2] (**6**–**11**)

At −78 °C to a stirred solution of [$(RhL_2)_2$(μ-Cl)$_2$] (L_2 = cod, **4**; dppe, **5**; 0.25 mmol) in CH_2Cl_2 (5 mL) $Ph_2P(CH_2)_nS(O)_xPh$ (0.50 mmol) dissolved in CH_2Cl_2 (2 mL) was added via a syringe and the mixture was stirred for 1 h at room temperature. The solution was concentrated under reduced pressure to half of its volume before *n*-pentane (5 mL) was added. The resulted precipitate was filtered off, washed with *n*-pentane (3 × 5 mL) and dried in vacuo.

L_2 = cod, n = 1, x = 0 (**6a**). Yield: 228 mg (82%). HRMS (ESI): *m/z* Calcd. for $[C_{27}H_{29}PRhS]^+$: 519.0778; found for $[M-Cl]^+$: 519.0771. ^1H NMR (400 MHz, $CDCl_3$): δ 1.90–2.02/2.35 (m/s, –/br, 4H/4H, 4× CH_2, cod), 3.04/5.54 (s/s, br/br, 2H/2H, 4× *CH*, cod), 4.12 (d, $^2J(^{31}P,^1H)$ = 5.6 Hz, 2H, CH_2SPh), 7.08–7.79 (m, 15H, H_{Ph}). ^{13}C NMR (100 MHz, $CDCl_3$): δ 28.8/33.0 (s/s, br/br, 4× CH_2, cod), 31.4 (d, $^1J(^{13}C,^{31}P)$ = 17.8 Hz, CH_2SPh), 70.7/105.8 (s/s, br/br, 4× *CH*, cod), 126.2–137.1 (C_{Ph}). ^{31}P NMR (81 MHz, $CDCl_3$): δ 28.1 (d, $^1J(^{103}Rh,^{31}P)$ = 150.1 Hz, PPh_2).

L_2 = cod, n = 1, x = 1 (**6b**). Yield: 257 mg (90%). HRMS (ESI): *m/z* Calcd. for $[C_{27}H_{29}OPRhS]^+$: 535.0726; found for $[M-Cl]^+$: 535.0723. ^1H NMR (400 MHz, $CDCl_3$): δ 1.88–2.18/2.46 (m/s, –/br, 4H/4H, 4× CH_2, cod), 3.20/3.29/5.61/5.65 (s/s/s/s, br/br/br/br, 1H/1H/1H/1H, 4× *CH*, cod), 3.86/4.08 (dd/dd, $^2J(^{31}P,^1H)$ = 9.1/8.0 Hz, $^2J(^1H,^1H)$ = 13.5/13.5 Hz, 1H/1H, CH_2SOPh), 7.32–7.87 (m, 15H, H_{Ph}). ^{13}C NMR (100 MHz, $CDCl_3$): δ 28.9/29.2/32.8/33.4 (s/s/s/s, br/br/br/br, 4× CH_2, cod), 62.3 (d, $^1J(^{13}C,^{31}P)$ = 18.3 Hz, CH_2SOPh), 70.4/72.6/106.6/108.0 (m/m/s/s, –/–/br/br, 4× *CH*, cod), 123.9–146.7 (C_{Ph}). ^{31}P NMR (81 MHz, $CDCl_3$): δ 30.8 (d, $^1J(^{103}Rh,^{31}P)$ = 151.2 Hz, PPh_2).

L_2 = cod, n = 1, x = 2 (**6c**). Yield: 258 mg (88%). HRMS (ESI): *m/z* Calcd. for $[C_{27}H_{29}O_2PRhS]^+$: 551.0675; found for $[M-Cl]^+$: 551.0673. ^1H NMR (400 MHz, CD_2Cl_2): δ 1.91–1.95/2.04–2.11/2.41 (m/m/m, 2H/2H/4H, 4× CH_2, cod), 3.16/5.50 (s/s, br/br, 2H/2H, 4× *CH* (cod)), 4.60 (d, $^2J(^{31}P,^1H)$ = 7.4 Hz, CH_2SO_2Ph), 7.41–8.00 (m, 15H, H_{Ph}). ^{13}C NMR (100 MHz, CD_2Cl_2): δ 28.9/32.9 (s/s, br/br, 4× CH_2, cod), 54.9 (d, $^1J(^{13}C,^{31}P)$ = 6.8 Hz, CH_2SO_2Ph), 71.3/105.1 (d/dd, $^1J(^{103}Rh,^{13}C)$ = 13.6/12.2 Hz, $^2J(^{31}P_{trans},^{13}C)$ = 7.4 Hz, 4× *CH*, cod), 127.7–142.1 (C_{Ph}). ^{31}P NMR (81 MHz, CD_2Cl_2): δ 24.0 (d, $^1J(^{103}Rh,^{31}P)$ = 154.1 Hz, PPh_2).

L_2 = cod, n = 2, x = 0 (**8a**). Yield: 211 mg (72%). HRMS (ESI): *m/z* Calcd. for $[C_{28}H_{31}PRhS]^+$: 533.4900; found for $[M-Cl]^+$: 533.4907. ^1H NMR (400 MHz, CD_2Cl_2): δ 1.61–1.82/2.35 (m, 8H, 4× CH_2, cod), 2.53 (s, br, 2H, CH_2PPh_2), 2.74–2.81 (m, CH_2SPh), 4.13 (s, br, 4H, 4× *CH*, cod), 7.26–7.40 (m, 15H, H_{Ph}). ^{13}C NMR (100 MHz, CD_2Cl_2): δ 31.1 (s, 4× CH_2, cod), 31.4 (d, $^1J(^{31}P,^{13}C)$ = 15.9 Hz, CH_2PPh_2), 36.9 (d, $^2J(^{31}P,^{13}C)$ = 7.2 Hz, CH_2SPh), 76.6 (m, 4× *CH*, cod), 128.5–133.4 (C_{Ph}). ^{31}P NMR (202 MHz, CD_2Cl_2): δ 26.1 (d, $^1J(^{103}Rh,^{31}P)$ = 150.7 Hz, PPh_2).

L_2 = cod, n = 2, x = 1 (**8b**). Yield: 252 mg (89%). HRMS (ESI): *m/z* Calcd. for $[C_{28}H_{31}OPRhS]^+$: 549.4894; found for $[M-Cl]^+$: 549.4888. ^1H NMR (400 MHz, CD_2Cl_2): δ 1.60/2.34 (m/m, 4H/4H, 4× CH_2 (cod)), 2.54 (m, 2H, CH_2PPh_2), 2.73–2.83 (m, 2H, CH_2SOPh), 4.12 (s, br, 4H, 4× *CH* (cod)), 7.24–7.40 (m, 15H, H_{Ph}). ^{13}C NMR (125 MHz, CD_2Cl_2): δ 20.1 (d, $^1J(^{31}P,^{13}C)$ = 22.9 Hz, CH_2PPh_2), 31.1/31.3 (s/s, br/br, 4× CH_2, cod), 52.9 (s, br, CH_2SOPh), 71.2/106.4 (d/s, –/br, $^1J(^{103}Rh,^{13}C)$ = 14.2 Hz, 4× *CH*, cod), 106.4–140.5 (C_{Ph}). ^{31}P NMR (202 MHz, CH_2Cl_2): δ 26.8 (d, $^1J(^{103}Rh,^{31}P)$ = 151.2 Hz, PPh_2).

L_2 = cod, n = 2, x = 2 (**8c**). Yield: 252 mg (89%). HRMS (ESI): *m/z* Calcd. for $[C_{28}H_{31}O_2PRhS]^+$: 565.4888; found for $[M-Cl]^+$: 565.4874. ^1H NMR (400 MHz, CD_2Cl_2): δ 1.89/2.02/2.29 (m/m/m, 2H/2H/4H, 4× CH_2, cod), 2.75–2.82 (m, 2H, CH_2PPh_2), 3.73–3.79 (m, CH_2SO_2Ph), 2.95/5.43 (s/s, br/br, 2H/2H, 4× *CH* (cod)), 7.32–7.89 (m, 15H, H_{Ph}). ^{13}C NMR (125 MHz, CD_2Cl_2): δ 22.6 (d, $^1J(^{31}P,^{13}C)$ = 23.6 Hz, CH_2PPh_2), 29.5/33.7 (s/s, 4× CH_2, cod), 53.5 (d, $^2J(^{31}P,^{13}C)$ = 2.7 Hz CH_2SO_2Ph), 71.2/106.4 (d/s, –/br, $^1J(^{103}Rh,^{13}C)$ = 14.2 Hz, 4× *CH*, cod), 106.4–140.5 (C_{Ph}). ^{31}P NMR (202 MHz, THF-d_8): δ 24.7 (d, $^1J(^{103}Rh,^{31}P)$ = 153.2 Hz, PPh_2).

L_2 = cod, n = 3, x = 1 (**10b**). Yield: 270 mg (90%). HRMS (ESI): *m/z* Calcd. for $[C_{29}H_{33}OPRhS]^+$: 563.5160; found for $[M-Cl]^+$: 563.5169. ^1H NMR (400 MHz, CD_2Cl_2): δ 1.92–1.99/2.27–2.40 (m/m, 4H/6H, 4× CH_2 (cod), $CH_2CH_2PPh_2$), 2.44–2.55/2.65–2.74 (m/m, 1H/1H, CH_2PPh_2), 2.89–2.96/3.19–3.27 (m/m, 1H/1H, CH_2SOPh), 4.14 (m, 4H, 4× *CH*, cod), 7.34–7.71 (m, 15H, H_{Ph}). ^{13}C NMR (100 MHz, CD_2Cl_2): δ 19.8 (d, $^2J(^{31}P,^{13}C)$ = 2.9 Hz, $CH_2CH_2PPh_2$), 26.9 (d, $^1J(^{31}P,^{13}C)$ = 25.3 Hz, CH_2PPh_2), 31.1/31.3 (s/s, 4× CH_2 (cod)), 58.0 (d, $^3J(^{13}C,^{31}P)$ = 12.1 Hz, CH_2SOPh), 87.7 (s, br, 4× *CH*, cod), 124.4–144.6 (C_{Ph}). ^{31}P NMR (81 MHz, CD_2Cl_2): δ 26.8 (d, $^1J(^{103}Rh,^{31}P)$ = 146.4 Hz, PPh_2).

L_2 = dppe n = 1, x = 0 (**7a**). Yield: 384 mg (91%). HRMS (ESI): *m/z* Calcd. for $[C_{45}H_{41}P_3RhS]^+$: 809.1191; found for $[M-Cl]^+$: 809.1191. ^1H NMR (400 MHz, CD_2Cl_2): δ 1.81–1.93/2.02–2.15 (m/m, 2H/2H, $Ph_2PCH_2CH_2PPh_2$), 3.81 (d, $^2J(^{31}P,^1H)$ = 4.4 Hz, 2H, CH_2SPh), 7.06–7.96 (m, 35H, H_{Ph}). ^{13}C NMR (100 MHz, CD_2Cl_2): δ 25.8–26.3/34.7–35.2 (m/m, $Ph_2PCH_2CH_2PPh_2$), 32.0 (d, $^1J(^{31}P,^{13}C)$ = 13.7 Hz, CH_2SPh), 125.5–138.1 (C_{Ph}). ^{31}P NMR (81 MHz, THF-d_8): δ 24.4 (ddd, $^2J(^{31}P,^{31}P)$ = 355.0 Hz, $^2J(^{31}P,^{31}P)$ = 35.8 Hz, $^1J(^{103}Rh,^{31}P)$ = 132.2 Hz, PPh_2), 59.0 (ddd, $^2J(^{31}P,^{31}P)$ = 355.0 Hz, $^2J(^{31}P,^{31}P)$ = 33.4 Hz, $^1J(^{103}Rh,^{31}P)$ = 140.9 Hz, *P* of dppe *trans* to *P*), 73.9 (d′t′, $^2J(^{31}P,^{31}P)$ = 35.8 Hz, $^2J(^{31}P,^{31}P)$ = 33.4 Hz, $^1J(^{103}Rh,^{31}P)$ = 183.8 Hz, *P* of dppe *trans* to *Cl*).

L_2 = dppe n = 1, x = 1 (**7b**). Yield: 379 mg (88%). HRMS (ESI): *m/z* Calcd. for $[C_{45}H_{41}OP_3RhS]^+$: 825.1141; found for $[M-Cl]^+$: 825.1140. ^1H NMR (400 MHz, CD_2Cl_2): δ 1.70–1.84/1.98–2.24 (m/m, 2H/2H, $Ph_2PCH_2CH_2PPh_2$), 3.68/4.39 (dd/dd, $^2J(^{31}P,^1H)$ = 7.4/6.4 Hz, $^2J(^1H,^1H)$ = 13.3/13.3 Hz, 1H/1H, CH_2SOPh), 6.75–8.11 (m, 35H, H_{Ph}). ^{13}C NMR (100 MHz, CD_2Cl_2): δ 26.4–26.8/35.3–35.8 (m/m,

$Ph_2PCH_2CH_2PPh_2$), 63.1 (d, $^1J(^{31}P, ^{13}C)$ = 13.8 Hz, CH_2SPh), 124.3–148.2 (C_{Ph}). ^{31}P NMR (81 MHz, CD_2Cl_2): δ 27.9 (ddd, $^2J(^{31}P, ^{31}P)$ = 353.4 Hz, $^2J(^{31}P, ^{31}P)$ = 35.4 Hz, $^1J(^{103}Rh, ^{31}P)$ = 142.3 Hz, PPh_2), 57.9 (ddd, $^2J(^{31}P, ^{31}P)$ = 353.4 Hz, $^2J(^{31}P, ^{31}P)$ = 33.6 Hz, $^1J(^{103}Rh, ^{31}P)$ = 142.1 Hz, *P* of dppe *trans* to *P*), 75.3 (d′t′, $^2J(^{31}P, ^{31}P)$ = 35.4 Hz, $^2J(^{31}P, ^{31}P)$ = 33.6 Hz, $^1J(^{103}Rh, ^{31}P)$ = 183.1 Hz, *P* of dppe *trans* to *Cl*).

L_2 = dppe *n* = 1, *x* = 2 (**7c**). Yield: 351 mg (80%). HRMS (ESI): *m*/*z* Calcd. for $[C_{45}H_{41}O_2P_3RhS]^+$: 841.1088; found for $[M-Cl]^+$: 841.1092. ^1H NMR (400 MHz, CD_2Cl_2): δ 1.80–1.92/2.04–2.16 (m/m, 2H/2H, $Ph_2PCH_2CH_2PPh_2$), 4.66 (d, $^2J(^{31}P, ^1H)$ = 4.6 Hz, 2H, CH_2SO_2Ph), 7.05–7.99 (m, 35H, H_{Ph}). ^{13}C NMR (100 MHz, CD_2Cl_2): δ 25.8–26.2/34.9–35.4 (m/m, $Ph_2PCH_2CH_2PPh_2$), 53.7 (d, $^1J(^{31}P, ^{13}C)$ = 6.9 Hz, CH_2SO_2Ph), 125.5–138.1 (C_{Phr}). ^{31}P NMR (81 MHz, CD_2Cl_2): δ 22.0 (ddd, $^2J(^{31}P, ^{31}P)$ = 361.8 Hz, $^2J(^{31}P, ^{31}P)$ = 35.3 Hz, $^1J(^{103}Rh, ^{31}P)$ = 135.0 Hz, PPh_2), 60.5 (ddd, $^2J(^{31}P, ^{31}P)$ = 361.8 Hz, $^2J(^{31}P, ^{31}P)$ = 34.0 Hz, $^1J(^{103}Rh, ^{31}P)$ = 142.4 Hz, *P* of dppe *trans* to *P*), 73.5 (d′t′, $^2J(^{31}P, ^{31}P)$ = 35.3 Hz, $^2J(^{31}P, ^{31}P)$ = 34.0 Hz, $^1J(^{103}Rh, ^{31}P)$ = 183.7 Hz, *P* of dppe *trans* to *Cl*).

L_2 = dppe *n* = 2, *x* = 0 (**9a**). Yield: 352 mg (82%). HRMS (ESI): *m*/*z* Calcd. for $[C_{46}H_{43}P_3RhS]^+$: 823.1349; found for $[M-Cl]^+$: 823.1364. ^1H NMR (400 MHz, CD_2Cl_2): δ 2.11–2.32 (m, 4H, $Ph_2PCH_2CH_2PPh_2$), 2.40–2.44 (m, 2H, CH_2PPh_2), 2.73–2.82 (m, 2H, CH_2SPh), 7.03–7.49 (m, 35H, H_{Ph}). ^{13}C NMR (100 MHz, CD_2Cl_2): δ 26.2–27.1/30.5–31.6 (m/m, $Ph_2PCH_2CH_2PPh_2$), 32.4 (d, $^1J(^{31}P, ^{13}C)$ = 22.8 Hz, CH_2PPh_2), 38.4 (d, $^2J(^{31}P, ^{13}C)$ = 9.0 Hz, CH_2SPh), 128.4–134.2 (C_{Ph}). ^{31}P NMR (81 MHz, CD_2Cl_2): δ 58.2 (m, $^2J(^{31}P, ^{31}P)$ = 284.7 Hz, $^2J(^{31}P, ^{31}P)$ = 31.3 Hz, $^1J(^{103}Rh, ^{31}P)$ = 131.5 Hz, *P* of dppe *trans* to *P*), 60.6 (m, $^2J(^{31}P, ^{31}P)$ = 284.7 Hz, $^2J(^{31}P, ^{31}P)$ = 32.1 Hz, $^1J(^{103}Rh, ^{31}P)$ = 134.9 Hz, PPh_2), 65.2 (d′t′, $^2J(^{31}P, ^{31}P)$ = 31.3 Hz, $^2J(^{31}P, ^{31}P)$ = 32.1 Hz, $^1J(^{103}Rh, ^{31}P)$ = 161.4 Hz, *P* of dppe *trans* to *Cl*).

L_2 = dppe *n* = 2, *x* = 1 (**9b**). Yield: 357 mg (85%). HRMS (ESI): *m*/*z* Calcd. for $[C_{46}H_{43}OP_3RhS]^+$: 839.1297; found for $[M-Cl]^+$: 839.1305. ^1H NMR (400 MHz, THF-d_8): δ 1.82–2.12 (m, 4H, $Ph_2PCH_2CH_2PPh_2$), 2.38–2.46/2.74–2.82 (m/m, 1H/1H, CH_2PPh_2), 2.90–2.98/3.51–3.58 (m/m, 1H/1H, CH_2SOPh), 6.88–8.18 (m, 35H, H_{Ph}). ^{13}C NMR (125 MHz, THF-d_8): δ 20.4 (d, $^1J(^{31}P, ^{13}C)$ = 21.6 Hz, CH_2PPh_2), 25.2–26.8/33.5–34.6 (m/m, $Ph_2PCH_2CH_2PPh_2$), 53.6 (d, $^2J(^{31}P, ^{13}C)$ = 6.3 Hz, CH_2SOPh), 133.9–145.5 (C_{Ph}). ^{31}P NMR (202 MHz, THF-d_8): δ 23.1 (m, $^2J(^{31}P, ^{31}P)$ = 328.6 Hz, $^2J(^{31}P, ^{31}P)$ = 9.0 Hz, $^1J(^{103}Rh, ^{31}P)$ = 133.2 Hz, PPh_2), 57.0 (m, $^2J(^{31}P, ^{31}P)$ = 328.6 Hz, $^2J(^{31}P, ^{31}P)$ = 48.8 Hz, $^1J(^{103}Rh, ^{31}P)$ = 140.9 Hz, *P* of dppe *trans* to *P*), 74.0 (m, $^2J(^{31}P, ^{31}P)$ = 9.0 Hz, $^2J(^{31}P, ^{31}P)$ = 48.8 Hz, $^1J(^{103}Rh, ^{31}P)$ = 184.3 Hz, *P* of dppe *trans* to *Cl*).

L_2 = dppe *n* = 2, *x* = 2 (**9c**). Yield: 387 mg (87%). HRMS (ESI): *m*/*z* Calcd. for $[C_{46}H_{43}O_2P_3RhS]^+$: 855.1246; found for $[M-Cl]^+$: 855.1263. ^1H NMR (400 MHz, CD_2Cl_2): δ 1.80–1.90/2.00–2.10 (m/m, 2H/2H, $Ph_2PCH_2CH_2PPh_2$), 2.48–2.53 (m, 2H, CH_2PPh_2), 3.41–3.46 (m, 2H, CH_2SO_2Ph), 7.07–7.93 (m, 35H, H_{Ph}). ^{13}C NMR (100 MHz, CD_2Cl_2): δ 21.2 (d, $^1J(^{31}P, ^{13}C)$ = 19.6 Hz, CH_2PPh_2), 25.5–25.9/34.6–35.1 (m/m, $Ph_2PCH_2CH_2PPh_2$), 52.7 (d, $^2J(^{31}P, ^{13}C)$ = 5.1 Hz, CH_2SO_2Ph), 127.7–138.7 (C_{Ph}). ^{31}P NMR (202 MHz, CD_2Cl_2): δ 22.1 (ddd, $^2J(^{31}P, ^{31}P)$ = 357.6 Hz, $^2J(^{31}P, ^{31}P)$ = 35.7 Hz, $^1J(^{103}Rh, ^{31}P)$ = 133.8 Hz, PPh_2), 58.9 (ddd, $^2J(^{31}P, ^{31}P)$ = 357.6 Hz, $^2J(^{31}P, ^{31}P)$ = 33.6 Hz, $^1J(^{103}Rh, ^{31}P)$ = 140.6 Hz, *P* of dppe *trans* to *P*), 74.0 (d′t′, $^2J(^{31}P, ^{31}P)$ = 35.7 Hz, $^2J(^{31}P, ^{31}P)$ = 33.6 Hz, $^1J(^{103}Rh, ^{31}P)$ = 183.1 Hz, *P* of dppe *trans* to *Cl*).

L_2 = dppe *n* = 3, *x* = 1 (**11b**). Yield: 351 mg (79%). HRMS (ESI): *m*/*z* Calcd. for $[C_{47}H_{45}OP_3RhS]^+$: 853.1454; found for $[M-Cl]^+$: 853.1474. ^1H NMR (400 MHz, CD_2Cl_2): δ 1.81–2.36 (m, 8H, $CH_2CH_2CH_2PPh_2$ + $Ph_2PCH_2CH_2PPh_2$), 2.70–2.77/2.82–2.89 (m/m, 1H/1H, CH_2SOPh), 7.07–7.95 (m, 35H, H_{Ph}). ^{13}C NMR (100 MHz, CD_2Cl_2): δ 19.6 (d, $^2J(^{31}P, ^{13}C)$ = 4.5 Hz, $CH_2CH_2CH_2$), 25.8–26.1/34.7–35.3 (m/m, $Ph_2PCH_2CH_2PPh_2$), 27.1 (d, $^1J(^{31}P, ^{13}C)$ = 21.9 Hz, CH_2PPh_2), 58.7 (d, $^3J(^{31}P, ^{13}C)$ = 13.0 Hz, CH_2SOPh), 123.9–144.7 (C_{Ph}). ^{31}P NMR (81 MHz, CD_2Cl_2): δ 24.2 (ddd, $^2J(^{31}P, ^{31}P)$ = 351.2 Hz, $^2J(^{31}P, ^{31}P)$ = 35.7 Hz, $^1J(^{103}Rh, ^{31}P)$ = 131.5 Hz, PPh_2), 58.9 (ddd, $^2J(^{31}P, ^{31}P)$ = 351.2 Hz, $^2J(^{31}P, ^{31}P)$ = 33.4 Hz, $^1J(^{103}Rh, ^{31}P)$ = 140.2 Hz, *P* of dppe *trans* to *P*), 73.9 (d′t′, $^2J(^{31}P, ^{31}P)$ = 35.7 Hz, $^2J(^{31}P, ^{31}P)$ = 33.4 Hz, $^1J(^{103}Rh, ^{31}P)$ = 184.9 Hz, *P* of dppe *trans* to *Cl*).

3.3. Preparation of $[Rh_3(\mu\text{-}Cl)(\mu\text{-}Ph_2PCH_2SPh\text{-}\kappa P{:}\kappa S)_4][BF_4]_2\cdot 4THF$ (**12**·4THF)

At room temperature to a stirred solution of $[(Rh(cod))_2(\mu\text{-}Cl)_2]$ (123.3 mg, 0.25 mmol) in THF (5 mL) Ph_2PCH_2SPh (154.2 mg, 0.50 mmol) dissolved in THF (2 mL) was added and the mixture was stirred for 1 h. Then, at −78 °C $Ag[BF_4]$ (97.3 mg, 0.50 mmol) dissolved in THF (2 mL) was added. The reaction mixture was slowly warmed to room temperature, stirred for 15 min and the precipitated AgCl was filtered off. After 24 h the microcrystals precipitated were filtered off, washed with THF (3 × 3 mL) and dried in vacuo.

Yield: 82 mg (32%). HRMS (ESI): *m*/*z* Calcd. for $[C_{76}H_{68}ClP_4Rh_2S_4]^+$: 1473.0947; found for $[M-Rh]^+$: 1473.0938. ^1H NMR (400 MHz, CD_2Cl_2): δ 1.82 (m, 16H, THF), 2.78 (s, br, 8H, CH_2SPh), 3.67 (m, 16H, THF), 6.99–8.00 (m, 60H, H_{Ph}). ^{13}C NMR (100 MHz, CD_2Cl_2): δ 25.9 (s, THF), 31.6/42.5 (d/d, $^1J(^{31}P, ^{13}C)$ = 27.8/26.7 Hz), 68.0 (s, THF), 128.6–135.8 (C_{Ph}). ^{31}P NMR (81 MHz, CD_2Cl_2): δ 28.4 (ddd, $^2J(^{31}P, ^{31}P)$ = 35.3 Hz, $^1J(^{103}Rh, ^{31}P)$ = 140.7 Hz, $^2J(^{103}Rh, ^{31}P)$ = 2.5 Hz, PPh_2 *trans* to *S*), 45.1 (ddd, $^2J(^{31}P, ^{31}P)$ = 35.3 Hz, $^1J(^{103}Rh, ^{31}P)$ = 180.3 Hz, $^2J(^{103}Rh, ^{31}P)$ = 3.5 Hz, PPh_2 *trans* to *Cl*).

3.4. Preparation of $[Rh\{Ph_2P(CH_2)_nS(O)_xPh\text{-}\kappa P,\kappa S/O\}L_2][BF_4]$ (**13**–**18**)

At room temperature to $[(RhL_2)_2(\mu\text{-}Cl)_2]$ (L_2 = cod, **4**; dppe, **5**; 0.25 mmol) in THF (5 mL) $Ph_2P(CH_2)_nS(O)_xPh$ (0.50 mmol) dissolved in THF (2 mL) was added with stirring. After 1 h $Ag[BF_4]$ (97.3 mg, 0.50 mmol) dissolved in THF (2 mL) was added at −78 °C. The reaction mixture was allowed to warm to room temperature and stirred for 15 min. Then, the precipitated AgCl was filtered off and the filtrate was concentrated under reduced pressure to half of its volume before *n*-pentane (5 mL) was added. The resulted precipitate was filtered off, washed with *n*-pentane (3 × 5 mL) and dried in vacuo.

L_2 = cod, *n* = 1, *x* = 0 (**13a**). Yield: 234 mg (90%). HRMS (ESI): *m*/*z* Calcd. for $[C_{27}H_{29}PRhS]^+$: 519.0777; found for $[M]^+$: 519.0772. ^1H NMR (200 MHz, CD_2Cl_2): δ 2.26/2.53 (m/m, 3H/5H, 4× CH_2, cod), 5.68/5.33 (s/s, br/br, 2H/2H, 4× *CH*, cod), 5.24 (d, $^2J(^{31}P, ^1H)$ = 5.8 Hz, CH_2SPh), 7.25–7.91 (m, 15H, H_{Ph}). ^{13}C NMR (50 MHz, CD_2Cl_2): δ 29.1/31.7 (s/s, br/br, 4× CH_2, cod), 86.5/106.0 (d/s, −/br, $^1J(^{103}Rh, ^{13}C)$ = 9.3 Hz, 4× *CH*, cod), 107.7 (d, $^1J(^{13}C, ^{31}P)$ = 7.3 Hz, CH_2SPh), 127.5–134.3 (C_{Ph}). ^{31}P NMR (81 MHz, CD_2Cl_2): δ −31.1 (d, $^1J(^{103}Rh, ^{31}P)$ = 119.5 Hz, PPh_2).

L_2 = cod, *n* = 1, *x* = 1 (**13b**). Yield: 274 mg (88%). HRMS (ESI): *m*/*z* Calcd. for $[C_{27}H_{29}OPRhS]^+$: 535.0722; found for $[M]^+$: 535.0718. ^1H NMR (400 MHz, CD_2Cl_2): δ 2.04–2.40/2.49–2.67 (m/m, 5H/3H, 4× CH_2, cod), 3.26/3.69/5.71/5.78 (s/s/s/s, br/br/br/br, 1H/1H/1H/1H, 4× *CH*, cod), 4.23/4.48 (dd/dd, $^2J(^{31}P, ^1H)$ = 9.0/2.8 Hz, $^2J(^1H, ^1H)$ = 14.9/14.9 Hz, 1H/1H, CH_2SOPh), 7.23–7.60 (m, 15H, H_{Ph}). ^{13}C NMR (100 MHz, CD_2Cl_2): δ 27.8/27.9/32.3/33.1 (s/s/s/s, 4× CH_2, cod), 57.4 (d, $^1J(^{13}C, ^{31}P)$ = 10.2 Hz, CH_2SOPh), 69.4/74.1/108.1/109.9 (d/d/dd/dd, br/br, $^1J(^{103}Rh, ^{13}C)$ = 13.9/14.5/10.5/9.9 Hz, $^2J(^{31}P_{trans}, ^{13}C)$ = 7.1/7.2 Hz, 4× *CH*, cod), 124.1–136.1 (C_{Ph}). ^{31}P NMR (81 MHz, CD_2Cl_2): δ 53.6 (d, $^1J(^{103}Rh, ^{31}P)$ = 162.7 Hz, PPh_2).

L_2 = cod, *n* = 1, *x* = 2 (**13c**). Yield: 268 mg (84%). HRMS (ESI): *m*/*z* Calcd. for $[C_{27}H_{29}O_2PRhS]^+$: 551.0675; found for $[M]^+$: 551.0675. ^1H NMR (400 MHz, CD_2Cl_2): δ 2.08–2.21/2.45–2.59 (m/m, 3H/5H, 4× CH_2, cod), 3.74/5.71 (s/s, br/br, 2H/2H, 4× *CH*, cod), 4.36 (d, $^2J(^{31}P, ^1H)$ = 8.1 Hz, CH_2SO_2Ph), 7.51–8.31 (m, 15H, H_{Ph}). ^{13}C NMR

(100 MHz, CD_2Cl_2): δ 27.7/32.7 (s/s, br/br, 4× CH_2, cod), 57.2 (d, ^1J (^{13}C, ^{31}P) = 10.0 Hz, CH_2SO_2Ph), 72.4/109.6 (d/s, −/br $^1J(^{103}Rh, ^{13}C)$ = 14.3 Hz, 4× *C*H, cod), 126.0–137.0 (C_{Ph}). ^{31}P NMR (81 MHz, CD_2Cl_2): δ 25.3 (d, $^1J(^{103}Rh, ^{31}P)$ = 149.0 Hz, PPh_2).

L_2 = cod, *n* = 2, *x* = 0 (**15a**). Yield: 267 mg (86%). HRMS (ESI): *m*/*z* Calcd. for $[C_{28}H_{31}PRhS]^+$: 533.4901; found for $[M]^+$: 533.4909. ^1H NMR (400 MHz, CD_2Cl_2): δ 2.30–2.48 (m, 8H, 4× CH_2, cod), 2.60–2.65 (m, 2H, CH_2PPh_2), 2.90–2.99 (m, 2H, CH_2SPh), 4.27/5.16 (s/s, br/br, 2H/2H, 4× *C*H, cod), 7.53–7.72 (m, 15H, H_{Ph}). ^{13}C NMR (100 MHz, CD_2Cl_2): δ 29.1/32.0 (s/s, br/br, 4× CH_2, cod), 30.2 (d, $^1J(^{31}P, ^{13}C)$ = 30.2 Hz, CH_2PPh_2), 37.5 (d, $^2J(^{31}P, ^{13}C)$ = 7.2 Hz, CH_2SPh), 87.7/105.4 (d/dd, $^1J(^{103}Rh, ^{13}C)$ = 10.8/9.2 Hz, $^2J(^{31}P_{trans}, ^{13}C)$ = 6.7 Hz, 4× *C*H, cod), 128.5–133.4 (C_{Ph}). ^{31}P NMR (81 MHz, CD_2Cl_2): δ 59.0 (d, $^1J(^{103}Rh, ^{31}P)$ = 147.2 Hz, PPh_2).

L_2 = cod, *n* = 2, *x* = 1 (**15b**). Yield: 280 mg (88%). HRMS (ESI): *m*/*z* Calcd. for $[C_{28}H_{31}OPRhS]^+$: 549.4890; found for $[M]^+$: 549.4887. ^1H NMR (400 MHz, CD_2Cl_2): δ 1.77–2.49 (m, 8H, 4× CH_2 (cod)), 2.81–3.29 (m, 4H, CH_2CH_2SOPh), 4.09/4.212/4.24 (s/s/s, br, 1H/2H/1H, 4× *C*H (cod)), 7.27–8.00 (m, 15H, H_{Ph}). ^{13}C NMR (100 MHz, CD_2Cl_2): δ 29.1/32.0 (s/s, br/br, 4× CH_2 (cod)), 30.2 (d, $^1J(^{31}P, ^{13}C)$ = 30.2 Hz, CH_2PPh_2), 52.9 (s, CH_2SOPh), 78.0/78.3/79.0 (d/d/m, $^1J(^{103}Rh, ^{13}C)$ = 8.1/11.3 Hz, 4× *C*H, cod), 124.6–134.1 (C_{Ph}). ^{31}P NMR (81 MHz, CD_2Cl_2): δ 52.7 (d, $^1J(^{103}Rh, ^{31}P)$ = 135.8 Hz, PPh_2).

L_2 = cod, *n* = 2, *x* = 2 (**15c**). Yield: 261 mg (80%). HRMS (ESI): *m*/*z* Calcd. for $[C_{28}H_{31}O_2PRhS]^+$: 565.4881; found for $[M]^+$: 565.4875. ^1H NMR (400 MHz, CD_2Cl_2): δ 2.01/2.12/2.46–2.62 (m/m/m, 2H/2H/4H, 4× CH_2, cod), 3.10–3.15 (m, 2H, CH_2PPh_2), 3.39–3.46 (m, CH_2SO_2Ph), 3.25/5.38 (s/s, br/br, 2H/2H, 4× *C*H, cod), 7.54–7.89 (m, 15H, H_{Ph}). ^{13}C NMR (125 MHz, CD_2Cl_2): δ 20.1 (d, $^1J(^{31}P, ^{13}C)$ = 23.3 Hz, CH_2PPh_2), 28.4/31.1/31.3 (s/s/s, −/−/br, 4× CH_2, cod), 51.9 (s, CH_2SO_2Ph), 71.1/110.4 (d/dd, $^1J(^{103}Rh, ^{13}C)$ = 15.6/10.1 Hz, $^2J(^{31}P_{trans}, ^{13}C)$ = 6.7 Hz, 4× *C*H, cod), 127.6–135.8 (C_{Ph}). ^{31}P NMR (202 MHz, CD_2Cl_2): δ 18.9 (d, $^1J(^{103}Rh, ^{31}P)$ = 149.5 Hz, PPh_2).

L = cod, *n* = 3, *x* = 0 (**17a**). Yield: 285 mg (90%). HRMS (ESI): *m*/*z* Calcd. for $[C_{29}H_{33}PRhS]^+$: 547.5166; found for $[M]^+$: 547.5168. ^1H NMR (400 MHz, CD_2Cl_2): δ 2.02–2.21/2.34–2.42 (m/m, 6H/4H, $CH_2CH_2CH_2$/4× CH_2, cod), 2.78 (m, 2H, CH_2PPh_2), 3.52 (m, 2H, CH_2SPh), 3.82/4.64 (s/s, br/br, 2H/2H, 4× *C*H, cod), 7.15–7.61 (m, 15H, H_{Ar}). ^{13}C NMR (125 MHz, CD_2Cl_2): δ 22.7 (s, br, $CH_2CH_2CH_2$), 25.6 (d, $^1J(^{13}C, ^{31}P)$ = 26.3 Hz, CH_2PPh_2), 29.26/29.27/32.16/32.19 (s/s/s/s, 4× CH_2, cod), 39.3 (d, $^3J(^{13}C, ^{31}P)$ = 3.6 Hz, CH_2SPh), 86.0/104.8 (d/dd, $^1J(^{13}C, ^{103}Rh)$ = 11.2/10.0 Hz, $^2J(^{13}C, ^{31}P_{trans})$ = 7.1 Hz, 4× *C*H, cod), 126.6–134.0 (C_{Ar}). ^{31}P NMR (80 MHz, CD_2Cl_2): 12.4 (d, $^1J(^{31}P, ^{103}Rh)$ = 140.0 Hz, PPh_2).

L_2 = cod, *n* = 3, *x* = 1 (**17b**). Yield: 288 mg (87%). HRMS (ESI): *m*/*z* Calcd. for $[C_{29}H_{33}OPRhS]^+$: 563.5157; found for $[M]^+$: 563.5165. ^1H NMR (400 MHz, CD_2Cl_2): δ 2.02–2.44/2.50–2.61 (m/m, 8H/3H, $CH_2CHHPPh_2$, 4× CH_2, cod), 3.06 (m, 1H, $CHHPPh_2$), 3.18/3.99 (m/m, 1H/1H, CH_2SOPh), 4.15/4.37/4.54/5.17 (s/s/s/s, br/br/br/br, 4H, 4× *C*H, cod), 7.47–8.11 (m, 15H, H_{Ph}). ^{13}C NMR (100 MHz, CD_2Cl_2): δ 17.3 (s, br, $CH_2CH_2PPh_2$), 24.2 (d, $^1J(^{31}P, ^{13}C)$ = 24.2 Hz, CH_2PPh_2), 28.7/30.7/30.9/31.8 (s/s/s/s, 4× CH_2 (cod)), 57.7 (d, $^3J(^{31}P, ^{13}C)$ = 4.8 Hz, CH_2SOPh), 94.5/99.0/104.3–104.7 (d/d/m, $^1J(^{103}Rh, ^{13}C)$ = 10.0/8.4 Hz, 4× *C*H, cod), 125.5–141.3 (C_{Ph}). ^{31}P NMR (81 MHz, CD_2Cl_2): δ 11.0 (d, $^1J(^{103}Rh, ^{31}P)$ = 140.0 Hz, PPh_2).

L_2 = cod, *n* = 3, *x* = 2 (**17c**). Yield: 277 mg (83%). HRMS (ESI): *m*/*z* Calcd. for $[C_{29}H_{33}O_2PRhS]^+$: 579.5154; found for $[M]^+$: 579.5155. ^1H NMR (400 MHz, CD_2Cl_2): δ 1.74–2.45 (m, 10H, $CH_2CH_2CH_2$, 4× CH_2, cod), 2.61 (m, 2H, CH_2PPh_2), 3.17/5.32 (s/s, br/br, 2H/2H, 4× *C*H (cod)), 3.57 (m, 2H, CH_2SO_2Ph), 7.44–7.82 (m, 15H, H_{Ph}). ^{13}C NMR (100 MHz, CD_2Cl_2): δ 17.5 (s, br, $CH_2CH_2CH_2$), 27.4 (d, $^1J(^{13}C, ^{31}P)$ = 17.3 Hz, CH_2PPh_2), 28.3/33.2 (s/s, 4× CH_2, cod), 57.0 (d, $^3J(^{13}C, ^{31}P)$ = 3.8 Hz, CH_2SO_2Ph), 71.6/108.3 (d/s, −/br, $^1J(^{103}Rh, ^{13}C)$ = 15.3 Hz, 4× *C*H, cod), 128.2–136.4 (C_{Ph}). ^{31}P NMR (81 MHz, CD_2Cl_2): δ 24.2 (d, $^1J(^{103}Rh, ^{31}P)$ = 147.8 Hz, PPh_2).

L_2 = dppe, *n* = 1, *x* = 0 (**14a**). Yield: 394 mg (88%). HRMS (ESI): *m*/*z* Calcd. for $[C_{45}H_{41}P_3RhS]^+$: 809.1180; found for $[M]^+$: 809.1181. ^1H NMR (400 MHz, CD_2Cl_2): δ 2.20–2.33/2.44–2.57 (m/m, 2H/2H, $Ph_2PCH_2CH_2PPh_2$), 5.58 (d, $^2J(^{31}P, ^1H)$ = 5.7 Hz, 2H, CH_2SPh), 6.94–7.93 (m, 35H, H_{Ph}). ^{13}C NMR (100 MHz, CD_2Cl_2): δ 26.8–27.2/30.7–31.2 (m/m, $Ph_2PCH_2CH_2PPh_2$), 60.3 (d, $^1J(^{31}P, ^{13}C)$ = 19.3 Hz, CH_2SPh), 128.7–135.2 (C_{Ph}). ^{31}P NMR (81 MHz, CD_2Cl_2): δ −22.8 (ddd, $^2J(^{31}P, ^{31}P)$ = 305.2 Hz, $^2J(^{31}P, ^{31}P)$ = 22.8 Hz, $^1J(^{103}Rh, ^{31}P)$ = 111.1 Hz, PPh_2), 61.6 (ddd, $^2J(^{31}P, ^{31}P)$ = 305.2 Hz, $^2J(^{31}P, ^{31}P)$ = 29.4 Hz, $^1J(^{103}Rh, ^{31}P)$ = 139.3 Hz, *P* of dppe *trans* to *P*), 69.1 (ddd, $^2J(^{31}P, ^{31}P)$ = 22.8 Hz, $^2J(^{31}P, ^{31}P)$ = 29.4 Hz, $^1J(^{103}Rh, ^{31}P)$ = 166.6 Hz, *P* of dppe *trans* to *S*).

L_2 = dppe, *n* = 1, *x* = 1 (**14b**). Yield: 392 mg (86%). HRMS (ESI): *m*/*z* Calcd. for $[C_{45}H_{41}OP_3RhS]^+$: 825.1136; found for $[M]^+$: 825.1131. ^1H NMR (500 MHz, CD_2Cl_2): δ 1.93–2.78 (m, 4H, $Ph_2PCH_2CH_2PPh_2$), 4.39–4.47 (m, 2H, CH_2SOPh), 6.76–8.14 (m, 35H, H_{Ph}). ^{13}C NMR (100 MHz, CD_2Cl_2): δ 22.6–23.0/32.4–32.9 (m/m, $Ph_2PCH_2CH_2PPh_2$), 56.6 (s, br, CH_2SOPh), 124.4–137.5 (C_{Ph}). ^{31}P NMR (202 MHz, CD_2Cl_2): δ 55.5 (ddd, $^2J(^{31}P, ^{31}P)$ = 308.6 Hz, $^2J(^{31}P, ^{31}P)$ = 31.6 Hz, $^1J(^{103}Rh, ^{31}P)$ = 146.3 Hz, PPh_2), 58.9 (ddd, $^2J(^{31}P, ^{31}P)$ = 308.6 Hz, $^2J(^{31}P, ^{31}P)$ = 34.3 Hz, $^1J(^{103}Rh, ^{31}P)$ = 143.6 Hz, *P* of dppe *trans* to *P*), 74.0 (d′t′, $^2J(^{31}P, ^{31}P)$ = 31.6 Hz, $^2J(^{31}P, ^{31}P)$ = 34.3 Hz, $^1J(^{103}Rh, ^{31}P)$ = 182.4 Hz, *P* of dppe *trans* to *O*).

L_2 = dppe, *n* = 1, *x* = 2 (**14c**). Yield: 367 mg (79%). HRMS (ESI): *m*/*z* Calcd. for $[C_{45}H_{41}O_2P_3RhS]^+$: 841.1080; found for $[M]^+$: 841.1090. ^1H NMR (500 MHz, CD_2Cl_2): δ 2.06–2.14/2.47–2.56 (m/m, 2H/2H, $Ph_2PCH_2CH_2PPh_2$), 4.67 (d, $^2J(^{31}P, ^1H)$ = 6.9 Hz, 2H, CH_2SO_2Ph), 7.16–8.03 (m, 35H, H_{Ph}). ^{13}C NMR (100 MHz, CD_2Cl_2): δ 23.9–24.4/33.5–34.2 (m/m, $Ph_2PCH_2CH_2PPh_2$), 56.4 (s, br, CH_2SO_2Ph), 126.0–139.7 (C_{Ph}). ^{31}P NMR (202 MHz, CD_2Cl_2): δ 27.1 (ddd, $^2J(^{31}P, ^{31}P)$ = 307.0 Hz, $^2J(^{31}P, ^{31}P)$ 29.5 Hz, $^1J(^{103}Rh, ^{31}P)$ = 129.7 Hz, PPh_2), 60.1 (ddd, $^2J(^{31}P, ^{31}P)$ = 307.0 Hz, $^2J(^{31}P, ^{31}P)$ = 34.4 Hz, $^1J(^{103}Rh, ^{31}P)$ = 145.6 Hz, *P* of dppe *trans* to *P*), 76.2 (d′t′, $^2J(^{31}P, ^{31}P)$ = 29.5 Hz, $^2J(^{31}P, ^{31}P)$ = 34.4 Hz, $^1J(^{103}Rh, ^{31}P)$ = 184.7 Hz, *P* of dppe *trans* to *O*).

L_2 = dppe, *n* = 2, *x* = 0 (**16a**). Yield: 414 mg (91%). HRMS (ESI): *m*/*z* Calcd. for $[C_{46}H_{43}P_3RhS]^+$: 823.1348; found for $[M]^+$: 823.1354. ^1H NMR (500 MHz, CD_2Cl_2): δ 2.18–2.28/2.37–2.44 (m/m, 2H/2H, $Ph_2PCH_2CH_2PPh_2$), 2.54–2.58 (m, 2H, CH_2PPh_2), 2.78–2.83 (m, 2H, CH_2SPh), 7.14–7.57 (m, 35H, H_{Ph}). ^{13}C NMR (125 MHz, CD_2Cl_2): δ 27.4–27.8/31.6–32.1 (m/m, $Ph_2PCH_2CH_2PPh_2$), 33.0 (d, $^1J(^{31}P, ^{13}C)$ = 23.6 Hz, CH_2PPh_2), 39.2 (d, $^2J(^{31}P, ^{13}C)$ = 10.9 Hz, CH_2SPh), 129.3–134.9 (C_{Ph}). ^{31}P NMR (202 MHz, CD_2Cl_2): δ 59.4 (m, $^2J(^{31}P, ^{31}P)$ = 285.2 Hz, $^2J(^{31}P, ^{31}P)$ = 31.6 Hz, $^1J(^{103}Rh, ^{31}P)$ = 135.3 Hz, PPh_2), 60.6 (m, $^2J(^{31}P, ^{31}P)$ = 285.2 Hz, $^2J(^{31}P, ^{31}P)$ = 31.7 Hz, $^1J(^{103}Rh, ^{31}P)$ = 132.1 Hz, *P* of dppe *trans* to *P*), 65.5 (d′t′, $^2J(^{31}P, ^{31}P)$ = 31.7 Hz, $^2J(^{31}P, ^{31}P)$ = 31.6 Hz, $^1J(^{103}Rh, ^{31}P)$ = 151.2 Hz, *P* of dppe *trans* to *S*).

L_2 = dppe, *n* = 2, *x* = 1 (**16b**). Yield: 361 mg (78%). HRMS (ESI): *m*/*z* Calcd. for $[C_{46}H_{43}OP_3RhS]^+$: 839.1290; found for $[M]^+$: 839.1284. ^1H NMR (400 MHz, CD_2Cl_2): δ 1.89–3.39 (m, 8H, $Ph_2PCH_2CH_2PPh_2$ + CH_2CH_2SOPh), 6.99–8.23 (m, 35H, H_{Ph}). ^{13}C NMR (125 MHz, CD_2Cl_2): δ 21.6 (d, $^1J(^{31}P, ^{13}C)$ = 21.0 Hz, CH_2PPh_2), 26.4–27.6/35.1–35.8 (m/m, $Ph_2PCH_2CH_2PPh_2$), 60.3 (d, $^2J(^{31}P, ^{13}C)$ = 9.5 Hz, CH_2SOPh), 124.4–143.4 (C_{Ph}). ^{31}P NMR (202 MHz, CD_2Cl_2): δ 57.8 (m, $^2J(^{31}P, ^{31}P)$ = 263.2 Hz, $^2J(^{31}P, ^{31}P)$ = 33.1 Hz, $^1J(^{103}Rh, ^{31}P)$ = 136.4 Hz, PPh_2), 59.0 (m, $^2J(^{31}P, ^{31}P)$ = 263.2 Hz, $^2J(^{31}P, ^{31}P)$ = 29.4 Hz, $^1J(^{103}Rh, ^{31}P)$ = 133.1 Hz, *P* of dppe *trans* to *P*), 60.1 (m, $^2J(^{31}P, ^{31}P)$ = 29.4 Hz, $^2J(^{31}P, ^{31}P)$ = 33.1 Hz, $^1J(^{103}Rh, ^{31}P)$ = 145.1 Hz, *P* of dppe *trans* to *S*).

L_2 = dppe, *n* = 2, *x* = 2 (**16c**). Yield: 361 mg (78%). HRMS (ESI): *m*/*z* Calcd. for $[C_{46}H_{43}O_2P_3RhS]^+$: 855.1239; found for $[M]^+$: 855.1246. ^1H NMR (400 MHz, CD_2Cl_2): δ 1.98–2.33 (m, 4H, $Ph_2PCH_2CH_2PPh_2$), 2.91 (m, 2H, CH_2PPh_2), 3.31 (m, 2H, CH_2SO_2Ph), 7.05–7.89 (m, 35H, H_{Ph}). ^{13}C NMR (50 MHz, CD_2Cl_2): δ 22.5 (d, $^1J(^{31}P, ^{13}C)$ = 1.9 Hz, CH_2PPh_2), 24.5–25.2/34.0–35.4 (m/m, $Ph_2PCH_2CH_2PPh_2$), 52.4 (d, $^2J(^{31}P, ^{13}C)$ = 6.4 Hz, CH_2SO_2Ph), 127.9–135.8 (C_{Ph}). ^{31}P NMR (81 MHz,

CD_2Cl_2): δ 16.5 (ddd, $^2J(^{31}P, ^{31}P)$ = 304.9 Hz, $^2J(^{31}P, ^{31}P)$ = 34.4 Hz, $^1J(^{103}Rh, ^{31}P)$ = 136.6 Hz, PPh_2), 60.5 (ddd, $^2J(^{31}P, ^{31}P)$ = 304.9 Hz, $^2J(^{31}P, ^{31}P)$ = 33.1 Hz, $^1J(^{103}Rh, ^{31}P)$ = 139.0 Hz, *P* of dppe *trans* to *P*), 77.4 (d′t′, $^2J(^{31}P, ^{31}P)$ = 34.4 Hz, $^2J(^{31}P, ^{31}P)$ = 33.1 Hz, $^1J(^{103}Rh, ^{31}P)$ = 204.5 Hz, *P* of dppe *trans* to *O*).

L = dppe, *n* = 3, *x* = 0 (**18a**). Yield: 425 mg (92%). HRMS (ESI): *m/z* Calcd. for $[C_{47}H_{45}P_3RhS]^+$: 837.1504; found for $[M]^+$: 837.1493. ^1H NMR (500 MHz, CD_2Cl_2): δ 1.87–2.02/2.04–2.37 (m, 4H, $PH_2PCH_2CH_2PPh_2$), 1.92–2.01 (m, 2H, $CH_2CH_2CH_2$), 2.30 (m, 2H, $Ph_2PCH_2CH_2CH_2$), 2.96 (m, 2H, $PhSCH_2$), 6.80–7.74 (m, 35H, H_{Ar}). ^{13}C NMR (125 MHz, CD_2Cl_2): δ 21.3 (s, $CH_2CH_2CH_2$), 26.4 (dd, $^1J(^{13}C, ^{31}P)$ = 24.7 Hz, $^3J(^{13}C, ^{31}P_{trans})$ = 1.8 Hz, $Ph_2PCH_2CH_2$), 27.7–27.9/32.5–33.1 (m/m, $Ph_2PCH_2CH_2PPh_2$), 35.9 (dd, $^3J(^{13}C, ^{31}P)/^3J(^{13}C, ^{31}P_{trans})$ = 8.8 Hz/3.4 Hz, $PhSCH_2$), 126.1–135.9 (C_{Ar}). ^{31}P NMR (81 MHz, CD_2Cl_2): δ 7.1 (ddd, $^2J(^{31}P, ^{31}P)$ = 33.2 Hz, $^2J(^{31}P, ^{31}P)$ = 287.8 Hz, $^1J(^{31}P, ^{103}Rh)$ = 131.1 Hz, PPh_2), 59.6 (ddd, $^2J(^{31}P, ^{31}P)$ = 31.4 Hz, $^2J(^{31}P, ^{31}P)$ = 287.8 Hz, $^1J(^{31}P, ^{103}Rh)$ = 128.2 Hz, *P* (dppe) *trans* to *P*), 66.4 (ddd, $^2J(^{31}P, ^{31}P)$ = 31.4 Hz, $^2J(^{31}P, ^{31}P)$ = 33.2, $^1J(^{31}P, ^{103}Rh)$ = 160.0 Hz, *P* (dppe) *trans* to *S*).

L_2 = dppe, *n* = 3, *x* = 1 (**18b**). Yield: 423 mg (90%). HRMS (ESI): *m/z* Calcd. for $[C_{47}H_{45}P_3ORhS]^+$: 853.1448; found for $[M]^+$: 853.1456. ^1H NMR (400 MHz, CD_2Cl_2): δ 1.71–2.47 (m, 8H, $CH_2CH_2CH_2PPh_2$ + $Ph_2PCH_2CH_2PPh_2$), 3.16–3.20/3.24–3.29 (m/m, 1H/1H, CH_2SOPh), 6.95–8.14 (m, 35H, H_{Ph}). ^{13}C NMR (100 MHz, CD_2Cl_2): δ 18.5 (s, $CH_2CH_2CH_2$), 27.1–27.5/31.4–31.8 (m/m, $Ph_2PCH_2CH_2PPh_2$), 27.3 (d, $^1J(^{31}P, ^{13}C)$ = 25.4 Hz CH_2PPh_2), 58.7 (dd, $^3J(^{13}C, ^{31}P)$ = 7.6 Hz, $^3J(^{13}C, ^{31}P_{trans})$ = 3.3 Hz, CH_2SOPh), 124.2–143.7 (C_{Ph}). ^{31}P NMR (202 MHz, THF-d_8): δ 7.7 (ddd, $^2J(^{31}P, ^{31}P)$ = 38.2 Hz, $^2J(^{31}P, ^{31}P)$ = 257.4 Hz, $^1J(^{31}P, ^{103}Rh)$ = 132.2 Hz, PPh_2), 56.4 (ddd, $^2J(^{31}P, ^{31}P)$ = 29.3 Hz, $^2J(^{31}P, ^{31}P)$ = 257.4 Hz, $^1J(^{31}P, ^{103}Rh)$ = 134.2 Hz, *P* of dppe *trans* to *P*), 60.0 (ddd, $^2J(^{31}P, ^{31}P)$ = 38.2 Hz, $^2J(^{31}P, ^{31}P)$ = 29.3, $^1J(^{31}P, ^{103}Rh)$ = 148.2 Hz, *P* of dppe *trans* to *S*).

L_2 = dppe, *n* = 3, *x* = 2 (**18c**). ^{31}P NMR (81 MHz, THF-d_8): δ 21.2 (ddd, $^2J(^{31}P, ^{31}P)$ = 30.6 Hz, $^2J(^{31}P, ^{31}P)$ = 329.5 Hz, $^1J(^{31}P, ^{103}Rh)$ = 127.0 Hz, PPh_2), 57.3 (ddd, $^2J(^{31}P, ^{31}P)$ = 28.4 Hz, $^2J(^{31}P, ^{31}P)$ = 329.5 Hz, $^1J(^{31}P, ^{103}Rh)$ = 121.6 Hz, *P* of dppe *trans* to *P*), 70.5 (d′t′, $^2J(^{31}P, ^{31}P)$ = 30.6 Hz, $^2J(^{31}P, ^{31}P)$ = 28.4, $^1J(^{31}P, ^{103}Rh)$ = 182.5 Hz, *P* of dppe *trans* to *O*).

3.5. Preparation of [{Rh(μ-$Ph_2PCH(SPh)$-κC:κP)(cod)}$_2$]·THF (**19**·THF)

At room temperature to a stirred solution of $[(Rh(cod))_2(\mu\text{-}Cl)_2]$ (123.3 mg, 0.25 mmol) in THF (5 mL) Ph_2PCH_2SPh (154.2 mg, 0.50 mmol) dissolved in THF (2 mL) was added and the mixture was stirred for 1 h. The solution was reduced to half of its volume and sodium bis(trimethylsilyl)amide (0.50 mmol, 2 M in THF) was added at −78 °C. After 24 h the crystals formed were filtered off, washed with THF (3 × 3 mL) and dried in vacuo.

Yield: 210 mg (81%). Found: C, 62.48; H, 5.35; Calcd. for $C_{58}H_{64}OP_2S_2Rh_2$ (1109.02): C, 62.81; H, 5.82. ^{31}P NMR (81 MHz, THF): δ 20.8 (m, $^1J(^{103}Rh, ^{31}P)$ = 169.6 Hz, $^2J(^{103}Rh, ^{31}P)$ = 4.0 Hz, $^3J(^{31}P, ^{31}P)$ = 147.4 Hz, PPh_2), 20.9 (m, $^1J(^{103}Rh, ^{31}P)$ = 167.3 Hz, $^2J(^{103}Rh, ^{31}P)$ = 1.0 Hz, $^3J(^{31}P, ^{31}P)$ = 147.4 Hz, PPh_2).

3.6. Preparation of [Rh{$Ph_2PCHS(O)_xPh$-κP,κS/O}L_2] (**20**, **21**) and [Rh{CH{S(O)Ph}$CH_2CH_2PPh_2$-κC,κP}L_2] (**22b**, **23b**)

To $[(RhL_2)_2(\mu\text{-}Cl)_2]$ (L_2 = cod, **4**; dppe, **5**; 0.25 mmol) in THF (5 mL) $Ph_2P(CH_2)_nS(O)_xPh$ (0.50 mmol) dissolved in THF (2 mL) was added with stirring. After 30 min the solution was reduced to half of its volume, cooled to −78 °C and sodium bis(trimethylsilyl)amide (0.50 mmol, 2 M in THF) was added. In case of **20** and **21** *n*-pentane (5 mL) was added, the precipitate filtered off, which was washed with *n*-pentane (3 × 1 mL) and dried in vacuo. In case of **22b** and **23b** the reaction mixtures were allowed to warm to room temperature. The precipitated NaCl was filtered off and *n*-pentane (5 mL) was added to the filtrate. The precipitate obtained was filtered off, washed with *n*-pentane (3 × 1 mL) and dried in vacuo.

L_2 = cod, *n* = 1, *x* = 1 (**20b**).[2] HRMS (ESI): *m/z* Calcd. for $[C_{27}H_{29}OPRhS]^+$: 535.0726; found for $[M + H]^+$: 535.0733. ^1H NMR (500 MHz, THF-d_8): δ 1.91–2.41 (m, 8H, 4× CH_2, cod), 2.88 (d, $^2J(^{31}P, ^1H)$ = 10.1 Hz, 1H, $CHSOPh$), 3.81/4.08/5.02/5.14 (s/s/s/s, br/br/br/br, 1H/1H/1H/1H, 4× *CH*, cod), 6.98–8.35 (m, 15H, H_{Ph}). ^{13}C NMR (100 MHz, THF-d_8): δ 27.7/30.0/31.9/32.4 (s/s/s/s, 4× CH_2 (cod)), 70.1 (d, $^1J(^{13}C, ^{31}P)$ = 14.3 Hz, CHSOPh), 87.0/87.3/99.4/101.4 (d/d/m/m, $^1J(^{103}Rh, ^{13}C)$ = 10.1/9.7 Hz, 4× CH, cod), 124.4–140.2 (C_{Ph}). ^{31}P NMR (81 MHz, THF-d_8): δ 32.2 (d, $^1J(^{103}Rh, ^{31}P)$ = 149.6 Hz, PPh_2).

L_2 = cod, *n* = 1, *x* = 2 (**20c**).[1] HRMS (ESI): *m/z* Calcd. for $[C_{27}H_{29}O_2PRhS]^+$: 551.0675; found for $[M + H]^+$: 551.0669. ^1H NMR (500 MHz, CD_2Cl_2): δ 1.91–2.54 (m, 8H, 4× CH_2, cod), 2.71 (d, $^2J(^{31}P, ^1H)$ = 12.8 Hz, 1H, $CHSO_2Ph$), 3.39/4.79/4.84 (s/s/s, br/br/br, 2H/1H/1H, 4× *CH*, cod), 6.86–8.44 (m, 15H, H_{Ph}). ^{13}C NMR (100 MHz, CD_2Cl_2): δ 27.6/28.3/31.2/31.7 (s/s/s/s, 4× CH_2, cod), 69.0 (d, $^1J(^{13}C, ^{31}P)$ = 14.7 Hz, $CHSO_2Ph$), 85.5/87.9/97.8/99.2 (d/d/m/m, $^1J(^{103}Rh, ^{13}C)$ = 9.9/9.8 Hz, 4× *CH*, cod), 124.4–140.2 (C_{Ph}). ^{31}P NMR (81 MHz, CD_2Cl_2): δ 26.6 (d, $^1J(^{103}Rh, ^{31}P)$ = 159.1 Hz, PPh_2).

L_2 = dppe, *n* = 1, *x* = 0 (**21a**).[3] ^{31}P NMR (81 MHz, THF): δ 9.4 (ddd, $^2J(^{31}P, ^{31}P)$ = 8.2 Hz, $^2J(^{31}P, ^{31}P)$ = 248.7 Hz, $^1J(^{31}P, ^{103}Rh)$ = 112.3 Hz, PPh_2), 62.0 (ddd, $^2J(^{31}P, ^{31}P)$ = 10.0 Hz, $^2J(^{31}P, ^{31}P)$ = 248.7 Hz, $^1J(^{31}P, ^{103}Rh)$ = 148.9 Hz, *P* of dppe *trans* to *P*), 69.4 (ddd, $^2J(^{31}P, ^{31}P)$ = 8.2 Hz, $^2J(^{31}P, ^{31}P)$ = 10.0, $^1J(^{31}P, ^{103}Rh)$ = 159.1 Hz, *P* of dppe *trans* to *S*).

L_2 = dppe, *n* = 1, *x* = 1 (**21b**).[1] HRMS (ESI): *m/z* Calcd. for $[C_{45}H_{41}OP_3RhS]^+$: 825.1147; found for $[M + H]^+$: 825.1141. ^1H NMR (500 MHz, CD_2Cl_2): δ 1.93–2.29 (m, 4H, $Ph_2PCH_2CH_2PPh_2$), 4.12 (s, br, 1H, $CHSOPh$), 6.97–8.05 (m, 35H, H_{Ph}). ^{13}C NMR (125 MHz, CD_2Cl_2): δ 27.5–28.0/30.0–30.4 (m/m, $Ph_2PCH_2CH_2PPh_2$), 66.6 (s, br, CHSOPh), 124.2–143.7 (C_{Ph}). ^{31}P NMR (81 MHz, CD_2Cl_2): δ −25.1 (ddd, $^2J(^{31}P, ^{31}P)$ = 29.0 Hz, $^2J(^{31}P, ^{31}P)$ = 276.7 Hz, $^1J(^{31}P, ^{103}Rh)$ = 106.2 Hz, PPh_2), 60.0 (ddd, $^2J(^{31}P, ^{31}P)$ = 30.4 Hz, $^2J(^{31}P, ^{31}P)$ = 276.7 Hz, $^1J(^{31}P, ^{103}Rh)$ = 145.7 Hz, *P* of dppe *trans* to *P*), 67.1 (ddd, $^2J(^{31}P, ^{31}P)$ = 29.0 Hz, $^2J(^{31}P, ^{31}P)$ = 30.4, $^1J(^{31}P, ^{103}Rh)$ = 157.3 Hz, *P* of dppe *trans* to *S*).

L_2 = dppe, *n* = 1, *x* = 2 (**21c**).[1] HRMS (ESI): *m/z* Calcd. for $[C_{45}H_{41}O_2P_3RhS]^+$: 841.1090; found for $[M + H]^+$: 841.1089. ^1H NMR (500 MHz, CD_2Cl_2): δ 1.93–2.51 (m, 4H, $Ph_2PCH_2CH_2PPh_2$), 2.78 (s, 1H, $CHSOPh$) 7.11–7.99 (m, 35H, H_{Ph}). ^{13}C NMR (100 MHz, CD_2Cl_2): δ 25.3–25.8/31.5–31.8 (m/m, $Ph_2PCH_2CH_2PPh_2$), 37.4 (s, br, $CHSO_2Ph$), 125.9–149.7 (C_{Ph}). ^{31}P NMR (81 MHz, CD_2Cl_2): δ 8.7 (ddd, $^2J(^{31}P, ^{31}P)$ = 27.1 Hz, $^2J(^{31}P, ^{31}P)$ = 286.7 Hz, $^1J(^{31}P, ^{103}Rh)$ = 116.4 Hz, PPh_2), 60.4 (ddd, $^2J(^{31}P, ^{31}P)$ = 30.4 Hz, $^2J(^{31}P, ^{31}P)$ = 286.7 Hz, $^1J(^{31}P, ^{103}Rh)$ = 158.1 Hz, *P* of dppe *trans* to *P*), 74.1 (d′t′, $^2J(^{31}P, ^{31}P)$ = 27.1 Hz, $^2J(^{31}P, ^{31}P)$ = 30.4, $^1J(^{31}P, ^{103}Rh)$ = 189.0 Hz, *P* of dppe *trans* to *O*).

L_2 = cod, (**22b**). Yield: 209 mg (74%). HRMS (ESI): *m/z* Calcd. for $[C_{29}H_{32}NaOPRhS]$: 585.0859; found for $[M + Na]^+$: 585.0856. ^1H NMR (400 MHz, CD_2Cl_2): δ 1.28–3.03 (m, 12H, $CH_2CH_2PPh_2$ + 4× CH_2, cod), 3.45 (s, br, 1H, $CHSOPh$), 3.94/4.05/5.56 (m/m/s, −/−/br, 1H/1H/2H, 4× *CH*, cod), 6.99–8.26 (m, 15H, H_{Ph}). ^{13}C NMR (100 MHz, CD_2Cl_2): δ 20.8 (d, $^2J(^{31}P, ^{13}C)$ = 13.9 Hz, $CH_2CH_2PPh_2$), 34.0 (d, $^1J(^{31}P, ^{13}C)$ = 26.9 Hz, CH_2PPh_2), 28.4/28.9/29.3/32.5 (s/s/s/s, 4× CH_2, cod), 63.0 (dd, $^2J(^{31}P, ^{13}C)$ = 4.9 Hz, $^1J(^{103}Rh, ^{13}C)$ = 28.7 Hz, CHSOPh), 81.1/82.7/93.6/100.4 (d/d/dd/dd, $^1J(^{103}Rh, ^{13}C)$ = 8.6/8.2/11.9/9.8 Hz, $^2J(^{31}P_{trans}, ^{13}C)$ = 7.2/7.8 Hz, 4× *CH* (cod)), 124.3–147.4 (C_{Ph}). ^{31}P NMR (81 MHz, THF-d_8): δ 51.6 (d, $^1J(^{103}Rh, ^{31}P)$ = 174.6 Hz, PPh_2).

[2] Includes NaCl which was not separated.
[3] Not isolated in substance; only characterized by ^{31}P NMR spectroscopy.

Table 4
Crystallographic data, data collection parameters and refinement parameters for **15b**, **15c**, **12**·4THF and **19**·THF.

	15b	**15c**	**12**·4THF	**19**·THF
Empirical formula	$C_{28}H_{31}BF_4OPRhS$	$C_{28}H_{31}BF_4O_2PRhS$	$C_{92}H_{100}B_2ClF_8O_4\ P_4Rh_3S_4$	$C_{58}H_{64}OP_2Rh_2S_2$
M_r	636.28	652.28	2039.64	1108.97
Crystal System	Orthorhombic	Orthorhombic	Monoclinic	Monoclinic
Space group	$Pca2_1$	$Pca2_1$	$P2_1/n$	$P2/n$
a/Å	16.738(1)	17.432(3)	20.6888(5)	13.103(2)
b/Å	9.334(1)	9.376(1)	19.4795(4)	10.1480(9)
c/Å	17.413(1)	16.759(2)	23.0532(6)	18.569(2)
β/°			107.593(2)	94.67(1)
V/Å^3	2720.6(4)	2739.0(6)	8856.1(4)	2460.8(5)
Z	4	4	4	2
D_{calc}/g cm^{-1}	1.553	1.582	1.530	1.497
μ(Mo-K$_\alpha$)/mm^{-1}	0.811	0.811	0.817	0.862
F(000)	1296	1328	4168	1144
θ range/°	2.18–25.98	2.34–26.00	2.09–25.00	1.98–25.00
Rfln. collected	20426	9223	45711	11854
Refln. observed [$I > 2\sigma(I)$]	3964	4682	11941	3227
Rfln. independent	5307 ($R_{int} = 0.0912$)	4935 ($R_{int} = 0.0199$)	15572 ($R_{int} = 0.0477$)	4311 ($R_{int} = 0.0384$)
Data/restraints/parameters	5307/1/334	4935/1/343	15572/28/1082	4311/5/316
Goodness-of-fit on F^2	0.928	1.052	1.043	0.836
$R1$, $wR2$ [$I > 2\sigma(I)$]	0.0415, 0.0652	0.0260, 0.0693	0.0451, 0.0938	0.0240, 0.0470
$R1$, $wR2$ (all data)	0.0705, 0.0712	0.0277, 0.0700	0.0678, 0.1018	0.0404, 0.0489
Largest diff. peak and hole/e Å^{-3}	0.624 and −0.351	0.380 and −0.497	0.987 and −0.479	0.380 and −0.299

L_2 = dppe, (**23b**). Yield: 324 mg (76%). HRMS (ESI): *m*/*z* Calcd. for [$C_{47}H_{45}OP_3RhS$]: 853.7514; found for [M + H]: 853.7511. ^{1}H NMR (500 MHz, THF-d_8): δ 1.12/1.78 (m/m, 1H/1H, CHC*H*$_2$CH$_2$PPh$_2$), 1.93/2.13–2.27/2.58–2.66/3.09 (m/m/m/m, 2H/2H/2H/1H, C*H*CH$_2$C*H*$_2$PPh + Ph$_2$PC*H*$_2$C*H*$_2$PPh$_2$), 6.83–8.29 (m, 35H, H_{Ph}). ^{13}C NMR (50 MHz, THF-d_8): δ 28.6 (s, CHCH$_2$CH$_2$), 28.8–29.0/37.0–37.4 (m/m, /Ph$_2$PCH$_2$CH$_2$PPh$_2$), 29.3 (dd, ^1J(^{13}C, ^{31}P) = 15.9 Hz, ^3J(^{13}C, $^{31}P_{trans}$) = 5.3 Hz, CHCH$_2$CH$_2$), 57.9–59.8 (m, CHSOPh), 123.9–149.6 (C_{Ph}). ^{31}P NMR (81 MHz, THF-d_8): δ 58.0 (m, ^2J(^{31}P, ^{31}P) = 31.1 Hz, ^2J(^{31}P, ^{31}P) = 307.2 Hz, ^1J(^{31}P, ^{103}Rh) = 156.1 Hz, *P*Ph$_2$), 59.1 (m, ^2J(^{31}P, ^{31}P) = 27.2 Hz, ^2J(^{31}P, ^{31}P) = 31.1 Hz, ^1J(^{31}P, ^{103}Rh) = 128.0 Hz, *P* of dppe *trans* to *C*), 65.2 (m, ^2J(^{31}P, ^{31}P) = 27.2 Hz, ^2J(^{31}P, ^{31}P) = 307.2, ^1J Q5 (^{31}P, ^{103}Rh) = 159.8 Hz, *P* of dppe *trans* to *P*).

3.7. X-ray crystallography

Data for X-ray diffraction analyses of single crystals of **15c**, **12**·4THF and **19**·THF were collected on a Stoe-IPDS 2T diffractometer at 200(2) K and of **15b** on a Stoe-IPDS diffractometer at 223 (2) K using Mo-Kα radiation (λ = 0.7103 Å, graphite monochromator). A summary of the crystallographic data, the data collection parameters and the refinement parameters is given in Table 4. Absorption corrections were applied numerically with X-RED32 [62] (T_{min}/T_{max} 0.86/0.96, **12**·4THF; 0.86/0.92, **15b**; 0.92/0.96, **19**·THF). The structures were solved with direct methods using SHELXS-97 [63] and refined using full-matrix least-square routines against F^2 with SHELXL-97 [64]. All non-hydrogen atoms were refined with anisotropic displacement parameters and hydrogen atoms with isotropic ones. H atoms were placed in calculated positions according to the riding model. In complex **12**·4THF a part of one of the Ph$_2$PCH$_2$SPh ligands has been refined disordered over two positions with a site occupancy of 58.8(4)% (C2A, S2A, C23A–C28A) and 41.2(4)% (C2B, S2B, C23B–C28B). The phenyl rings of these disordered units have been refined constraint. In addition, for the refinement of the THF molecules as packing solvents DFIX and DANG restraints have been used, explaining the comparatively large number of restraints. In complex **19**·THF the THF molecule has been refined disordered over two positions with equal occupancy using 5 DFIX restraints.

3.8. Computational details

DFT calculations were carried out by the Gaussian 03 program package [65] using the hybrid functional B3LYP [66]. 6-311++G (3df,3pd) (P, S) and 6-31+G* (O, C, H) basis sets were employed for main group atoms [65,67]. The valence shell of rhodium has been approximated by a split valence basis set too (Def2-TZVPP); for its core orbitals an effective core potential in combination with consideration of relativistic effects has been used [68]. All systems were fully optimized without any symmetry restrictions. The resulting geometries were characterized as equilibrium structures by the analysis of the force constants of normal vibrations. To limit the computational expense, in the case of complexes with the dppe ligand (**21b**$_{calc}$, **21b**′$_{calc}$) 6-31G* basis sets for O, C and H were used only. Then, after characterizing the structures as equilibrium structures by the analysis of the force constants of normal vibrations, in a second step the molecules were re-optimized with a small step-size (IOP(1/8 = 3)) using the basis sets 6-31+G* for O, C and H as given above.

Appendix A. Supplementary material

Crystallographic data (excluding structure factors) have been deposited at the Cambridge Crystallographic Data Centre as supplementary publication nos. CCDC 797346 (**15b**), CCDC 797347(**15c**), CCDC 797348 (**12**·4THF), CCDC 797349 (**19**·THF). These data can be obtained free of charge via http://www.ccdc.cam.ac.uk/cgi-bin/catreq.cgi or from the Business & Administration, Cambridge Crystallographic Data Centre, 12 Union Road, Cambridge, CB2 1EZ, UK; fax: (+44) 1223 336033; or email: admin@ccdc.cam.ac.uk.

Appendix. Supplementary material

Supplementary data related to this article can be found online at doi:10.1016/j.jorganchem.2010.12.019.

References

[1] A. Börner, Eur. J. Inorg. Chem. (2001) 327.
[2] E.J. Garcia Suarez, C. Godard, A. Ruiz, C. Claver, Eur. J. Inorg. Chem. (2007) 2582.

[3] S. Daly, M.F. Haddow, A.G. Orpen, G.T.A. Rolls, D.F. Wass, R.L. Wingad, Organometallics 27 (2008) 3196.
[4] J.W. Faller, N.J. Zhang, K.J. Chase, W.K. Musker, A.R. Amaro, C.M. Semko, J. Organomet. Chem. 468 (1994) 175.
[5] H. Pellisier, Tetrahedron 63 (2007) 1297.
[6] M. Bassetti, Eur. J. Inorg. Chem. (2006) 4473.
[7] J.W. Faller, B.J. Grimmond, D.G. D'Alliessi, J. Am. Chem. Soc. 123 (2001) 2525.
[8] J.W. Faller, B.J. Grimmond, M. Curtis, Organometallics 19 (2000) 5174.
[9] J.W. Faller, J.C. Wilt, Tetrahedron Lett. 45 (2005) 7613.
[10] E. Guimet, M. Diéguez, A. Ruiz, C. Claver, J. Chem. Soc., Dalton Trans. (2005) 2557.
[11] S.E. Angell, C.W. Rogers, Y. Zhang, M.O. Wolf, W.E. Jones, Coord. Chem. Rev. 250 (2006) 1829.
[12] M. Stradiotto, K.D. Hesp, R.J. Lundgren, Angew. Chem. Int. Ed. 49 (2010) 494.
[13] J. Cipot, R. McDonald, M. Stradiotto, Chem. Commun. (2005) 4932.
[14] R.J. Lundgren, M. Stradiotto, Chem. Eur. J. 14 (2008) 10388.
[15] J. Cipot, C.M. Vogels, R. McDonald, S.A. Westcott, M. Stradiotto, Organometallics 25 (2006) 5965.
[16] T.A.K. Al-Allaf, Asian J. Chem. 12 (2000) 869.
[17] I. Omae, J. Organomet. Chem. 692 (2007) 2608.
[18] R. Beck, M. Frey, S. Camadanli, H.-F. Klein, Dalton Trans. 37 (2008) 4981.
[19] J. Campos, A.C. Esqueda, E. Carmona, Chem. Eur. J. 16 (2010) 419.
Q7 [20] R. Dorta, H. Rozenberg, L.J.W. Shimon, D. Milstein, Chem. Eur. J. 9 (2003) 5237.
[21] R. Dorta, H. Rozenberg, D. Milstein, Chem. Commun. (2002) 710.
[22] T. Schaub, Y. Diskin-Posner, U. Radius, D. Milstein, Inorg. Chem. 47 (2008) 6502.
[23] M. Block, M. Linnert, S. Gómez-Ruiz, D. Steinborn, J. Organomet. Chem. 694 (2009) 3353.
[24] M. Block, T. Kluge, M. Bette, J. Schmidt, D. Steinborn, Organometallics, submitted
Q8 for publication.
[25] D. Seebach, T. Maetzke, R.K. Haynes, M.N. Paddon-Row, S.S. Wong, Helv. Chim. Acta 71 (1988) 299.
[26] J. Vicente, M.-T. Chicote, C. Rubio, M.C. Ramirez de Arellano, P.G. Jones, Organometallics 18 (1999) 2750.
[27] A. Krief, Tetrahedron 36 (1980) 2531.
[28] H.J. Gais, J. Vollhardt, G. Hellmann, H. Paulus, H.J. Lindner, Tetrahedron Lett. 29 (1988) 1259.
[29] M. Block, C. Wagner, S. Gómez-Ruiz, D. Steinborn, Dalton Trans. 39 (2010) 4336.
[30] P. DeShong, D.R. Sidler, P.J. Rybczynski, G.A. Slough, A.L. Rheingold, J. Am. Chem. Soc. 110 (1988) 2575.
[31] M. Marsch, W. Massa, K. Harms, G. Baum, G. Boche, Angew. Chem. Int. Ed. 25 (1986) 1011.
[32] W. Henderson, R.D.W. Kemmitt, L.J.S. Prouse, D.R. Russell, J.Chem. Soc., Dalton Trans. (1990) 1853.
[33] G.E. Ball, W.R. Cullen, M.D. Fryzuk, B.R. James, S.J. Rettig, Organometallics 10 (1991) 3767.
[34] T.G. Appleton, H.C. Clark, L.E. Manzer, Coord. Chem. Rev. 10 (1973) 335.
[35] PERCH NMR Software, Version 1/2000. University of Kuopio, Finland, 2000.
[36] D.E. Chebi, P.E. Fanwick, I.P. Rothwell, Organometallics 9 (1990) 2948.
[37] R. Fornika, C. Six, H. Görls, M. Kessler, C. Krüger, W. Leitner, Can. J. Chem. 79 (2001) 642.
[38] J. Browning, G.W. Bushnell, K.R. Dixon, J. Organomet. Chem. 198 (1980) 11.
[39] S. Okeya, H. Shimomura, Y. Kushi, Chem. Lett. 21 (1992) 2019.
[40] X.-K. Huo, G. Su, G.-X. Jin, Dalton Trans. 39 (2010) 1954.
[41] K.D. Hesp, R. McDonald, M.J. Ferguson, M. Stradiotto, J. Am. Chem. Soc. 130 (2008) 16394.
[42] G. Canepa, C.D. Brandt, K. Ilg, J. Wolf, H. Werner, Chem. Eur. J. 9 (2003) 2502.
[43] C.J. Cobley, R.D.J. Froese, J. Klosin, C. Qin, G.T. Whiteker, K.A. Abboud, Organometallics 26 (2007) 2986.
[44] J. Cipot, M.J. Ferguson, M. Stradiotto, Inorg. Chim. Acta 359 (2006) 2780.
[45] Cambridge Structural Database (ConQuest). Version 5.31. Crystallographic Data Centre, University Chemical Laboratory, Cambridge (UK), 2009.
[46] G. Kemp, A. Roodt, W. Purcell, K.R. Koch, J. Chem. Soc., Dalton Trans. (1997) 4481.
[47] H.H. Karsch, M. Reisky, Eur. J. Inorg. Chem. (1998) 905.
[48] T. Achard, J. Benet-Buchholz, A. Riera, X. Verdaguer, Organometallics 28 (2009) 480.
[49] E.V. Dikarev, R.Y. Becker, E. Block, Z. Shan, R.C. Haltiwanger, M.A. Petrukhina, Inorg. Chem. 42 (2003) 7098.
[50] T.A. Ryan, Coord. Chem. Rev. 57 (1984) 75.
[51] F. Shafiq, K.W. Kramarz, R. Eisenberg, Inorg. Chim. Acta 213 (1993) 111.
[52] J. Po-Kwan Lau, W.-T. Wong, Dalton Trans. (2005) 2579.
[53] C. Schaffner-Hamann, A. von Zelewsky, A. Barbieri, F. Barigelletti, G. Muller, J.P. Riehl, A. Neels, J. Am. Chem. Soc. 126 (2004) 9339.
[54] M.-C.P. Yeh, L.-W. Chuang, C.-C. Hwu, J.-M. Sheu, L.-C. Row, Organometallics 14 (1995) 3396.
[55] P. Alvarez, E. Lastra, J. Gimeno, P. Bran, J.A. Sordo, J. Gomez, L.R. Falvello, M. Bassetti, Organometallics 23 (2004) 2956.
[56] S.B. Han, X. Gao, M.J. Krische, J. Am. Chem. Soc. 132 (2010) 9153.
[57] I.S. Kim, S.B. Han, M.J. Krische, J. Am. Chem. Soc. 131 (2009) 2514.
[58] M. Calligaris, O. Carugo, Coord. Chem. Rev. 153 (1996) 83.
[59] M.-H. Thibault, J. Boudreau, S. Mathiotte, F. Drouin, O. Sigouin, A. Michaud, F.-G. Fontaine, Organometallics 26 (2007) 3807.
[60] R. Cramer, Inorg. Synth. 28 (1990) 86.
[61] D.P. Fairlie, B. Bosnich, Organometallics 7 (1988) 936.
[62] X-RED32 (version 1.07), Stoe Data Reduction Program. Stoe & Cie GmbH, Darmstadt, 2002.
[63] G.M. Sheldrick, SHELXS-97, Program for Crystal Structure Solution. University of Göttingen, Göttingen, 1998.
[64] G.M. Sheldrick, SHELXL-97, Program for the Refinement of Crystal Structures. University of Göttingen, Göttingen, 1997.
[65] M.J. Frisch, et al., Gaussian 03, Revision B.04. Gaussian, Inc., Pittsburgh, PA, 2004.
[66] (a) A.D. Becke, Phys. Rev. A 38 (1988) 3098;
(b) A.D. Becke, J. Chem. Phys. 98 (1993) 5648;
(c) C. Lee, W. Yang, R.G. Parr, Phys. Rev. B 37 (1988) 785;
(d) P.J. Stephens, F.J. Devlin, C.F. Chabalowski, M.J. Frisch, J. Phys. Chem. 98 (1994) 11623.
[67] K.L. Schuchardt, B.T. Didier, T. Elsethagen, L. Sun, V. Gurumoorthi, J. Chase, J. Li, T.L. Windus, J. Chem. Inf. Model. 47 (2007) 1045. https://bse.pnl.gov/bse/portal.
[68] (a) F. Weigend, R. Ahlrichs, Phys. Chem. Chem. Phys. 7 (2005) 3297;
(b) A.U. Haeussermann, M. Dolg, H. Stoll, H. Preuss, Theor. Chim. Acta 77 (1990) 123.

ARTICLE

DOI: 10.1002/zaac.201000344

On the Reactivity of the Platina-β-diketone $[Pt_2\{(COMe)_2H\}_2(\mu\text{-}Cl)_2]$ Towards $Ph_2PCH_2CH_2CH_2SO_xPh$ (x = 0, 2)

Michael Block,[a] Martin Bette,[a] Christoph Wagner,[a] and Dirk Steinborn*[a]

Keywords: Platinum; Platinum complexes; Functionalized phosphane ligands; Decarbonylation; NMR sprectroscopy

Abstract. The reaction of the electronically unsaturated platina-β-diketone $[Pt_2\{(COMe)_2H\}_2(\mu\text{-}Cl)_2]$ (**1**) with $Ph_2PCH_2CH_2CH_2SPh$ (**2**) leads selectively to the formation of the acetyl(chlorido) platinum(II) complex (*SP*-4-3)-[Pt(COMe)Cl($Ph_2PCH_2CH_2CH_2SPh$-κ*P*,κ*S*)] (**4**) having the γ-phosphinofunctionalized propyl phenyl sulfide coordinated in a bidentate fashion (κ*P*,κ*S*). In boiling benzene complex **4** undergoes decarbonylation yielding the methyl(chlorido) platinum(II) complex (*SP*-4-3)-[PtMeCl($Ph_2PCH_2CH_2CH_2SPh$-κ*P*,κ*S*)] (**6**). However, the reaction of **1** with the analogous γ-diphenylphosphinofunctionalized propyl phenyl sulfone $Ph_2PCH_2CH_2CH_2SO_2Ph$ (**3**) affords the acetyl(chlorido) platinum(II) complex (*SP*-4-4)-[Pt(COMe)-Cl($Ph_2PCH_2CH_2CH_2SO_2Ph$-κ*P*)$_2$] (**5**). In boiling benzene complex **5** undergoes a CO extrusion yielding (*SP*-4-4)-[PtMeCl(Ph_2PCH_2-$CH_2CH_2SO_2Ph$-κ*P*)$_2$] (**8**) whereas in presence of **1** the formation of the carbonyl complex (*SP*-4-3)-[PtMeCl(CO)($Ph_2PCH_2CH_2$-CH_2SO_2Ph-κ*P*)] (**7**) is observed. Addition of $Ag[BF_4]$ to complex **5** leads to the formation of the cationic methyl(carbonyl) platinum(II) complex (*SP*-4-1)-[PtMe(CO)($Ph_2PCH_2CH_2CH_2SO_2Ph$-κ*P*)$_2$][BF_4] (**9**). All complexes were characterized by microanalysis and NMR spectroscopy (^{1}H, ^{13}C, ^{31}P) and complexes **4** and **6** additionally by single-crystal X-ray diffraction analyses.

1 Introduction

Reactions of hexachloridoplatinic acid with *n*-butyl alcohol and trimethylsilyl-substituted alkynes lead to the formation of platina-β-diketones $[Pt_2\{(COR)_2H\}_2(\mu\text{-}Cl)_2]$ (R = alkyl) which may be described as hydroxycarbene complexes stabilized by strong intramolecular hydrogen bonds to acyl ligands, as shown in Scheme 1 for the formation of the parent complex **1** (R = Me) [1]. In contrast to *Lukehart*'s metalla-β-diketones $[L_xM\{(COR)_2H\}]$ (L = CO, Cp; M = Mo, Re, Fe,..; R = alkyl, aryl) [2], platina-β-diketones exhibit a unique reactivity due to their electronic unsaturation (16 valence electron complexes) and their kinetically labile ligand sphere [3]. Thus, the platina-β-diketone $[Pt_2\{(COMe)_2H\}_2(\mu\text{-}Cl)_2]$ (**1**) is found to react with numerous monodentate and chelating donors L and L^L yielding, respectively, diacetyl(hydrido) platinum(IV) complexes of type **A** and acetyl platinum(II) complexes of type **B** (Scheme 1). In the case of hard/hard N^N donors, the platinum(IV) complexes of type **A** proved to be thermally extraordinarily stable [4, 5], whereas with soft donors (P, P^P, S^S) type **A** complexes could be detected NMR spectroscopically only or remained unseen at all, thus only type **B** complexes could be isolated [6–8]. The formation of the diacetyl platinum(II) complexes of type **C** can be induced by addition of bases to complexes **A** [9, 10].

Here we report on reactions of the dinuclear platina-β-diketone $[Pt_2\{(COMe)_2H\}_2(\mu\text{-}Cl)_2]$ (**1**) with P^SO_x (x = 0, 2) type ligands $Ph_2PCH_2CH_2CH_2SPh$ (**2**) and $Ph_2PCH_2CH_2CH_2SO_2Ph$ (**3**) yielding mononuclear acetyl(chlorido) platinum(II) complexes of type **B** as well as on their decarbonylation.

2 Results and Discussion

2.1 Syntheses

The dinuclear platina-β-diketone $[Pt_2\{(COMe)_2H\}_2(\mu\text{-}Cl)_2]$ (**1**) was found to react in dichloromethane with $Ph_2PCH_2CH_2CH_2SPh$ (**2**) and $Ph_2PCH_2CH_2CH_2SO_2Ph$ (**3**) to yield mononuclear acetyl(chlorido) platinum(II) complexes (**4**, **5**, routes **a**/**c**, Scheme 2). In these reactions as well as in the reactions described in the following, as a side product traces of a black solid, most likely platinum black, were formed. Complexes **4** and **5** were isolated in yields of > 70 % as colorless air-stable products, which were characterized by NMR (^{1}H, ^{13}C, ^{31}P) and IR spectroscopy as well as by microanalyses and single-crystal X-ray diffraction analysis (**4**).

The platinum complexes **4** and **5** were found to undergo a decarbonylation reaction in boiling benzene within 2 hours, thus yielding the methyl(chlorido) platinum(II) complexes **6** and **8** (routes **b**/**d**). The addition of $Ag[BF_4]$ to complex **5** (route **e**) led with precipitation of AgCl to the formation of the methyl(carbonyl)platinum(II) complex **9**. Complexes **6**, **8** and **9** were isolated as colorless air-stable solids in yields between 70 and 78 % and fully characterized by microanalysis, ^{1}H, ^{13}C, and ^{31}P NMR spectroscopy as well as by single-crystal X-ray diffraction analysis (**6**).

* Prof. Dr. D. Steinborn
E-Mail: dirk.steinborn@chemie.uni-halle.de
[a] Institut für Chemie
Martin-Luther-Universität Halle-Wittenberg
Kurt-Mothes-Straße 2
06120 Halle, Germany

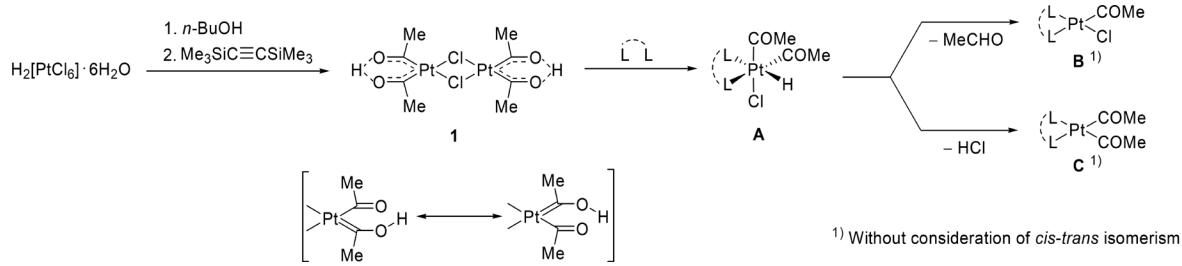

Scheme 1. Synthesis of the platina-β-diketone **1** and its reactivity towards monodentate and chelating ligands L and L^L, respectively.

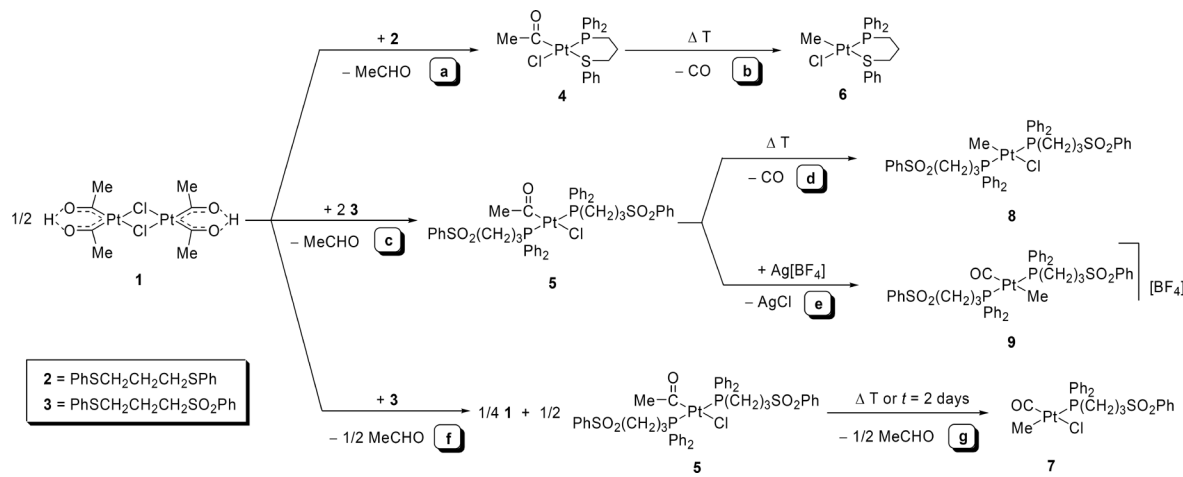

Scheme 2. Reactions of the platina-β-diketone **1** with γ-phosphinofunctionalized propyl phenyl sulfides and sulfones.

The reaction of the platina-β-diketone **1** with a deficiency of the phosphinofunctionalized sulfone **3** (molar ratio 1:2) led – in a fast reaction – to the formation of **5**, whereas the half of complex **1** remained unreacted (route **f**). This obtained mixture was found to undergo – in a slow reaction within two days – a decarbonylation reaction yielding the methyl(chlorido)carbonyl platinum(II) complex **7** (route **g**). In boiling benzene this reaction proceeded within two hours. Complex **7** was isolated (yield 82 %) as colorless air-stable solid and fully characterized analytically and spectroscopically. Noteworthy, the pure complex **5**, prepared according to route **c**, proved to be stable in dichloromethane solution at room temperature and reacted only in boiling benzene according to route **d**.

2.2 Spectroscopic Investigations

Selected NMR spectroscopic parameters of complexes **4**–**9** are given in Table 1. The magnitudes of the $^{1}J_{Pt,P}$ couplings in complexes **4**–**9** are fully consistent with the trans influence order Cl < PR_3 < Me because they were found to decrease from about 4500 Hz (**4**, **6**) over 2500–3400 Hz (**5**, **8**, **9**) to ca 1450 Hz (**7**). In the two acetyl(chlorido) platinum(II) complexes the ^{13}C resonances of the methyl groups exhibited d+dd (**4**) and t+dt (**5**) patterns showing $^{3}J_{P,C}$ and $^{2}J_{Pt,C}$ couplings of about 5/6 Hz and 165/215 Hz, respectively. However, in the ^{1}H NMR spectra the protons of the methyl groups appeared as singlet signals (δ_H = 1.84/1.16) only. The carbonyl carbon atoms showed shifts in the

Table 1. Selected NMR spectroscopic data (δ in ppm, J in Hz) of complexes **4**–**9** bearing the ligands L1 ($Ph_2PCH_2CH_2CH_2SPh$) and L2 ($Ph_2PCH_2CH_2CH_2SO_2Ph$), respectively.

Complex		δ_C (*C*OMe) ($^{2}J_{P,C}$)	δ_C (CO*C*H$_3$) ($^{2}J_{Pt,C}/^{3}J_{P,C}$)	δ_C (*C*O) ($^{2}J_{P,C}$)	δ_C (*C*H$_3$) ($^{1}J_{Pt,C}/^{2}J_{P,C}$)	δ_P ($^{1}J_{Pt,P}$)
[Pt(COMe)Cl(L1-κ*P*,κ*S*)]	(**4**)	213.5 (6.8)	40.7 (167.0/4.7)	–	–	–4.1 (4765)
[Pt(COMe)Cl(L2-κ*P*)$_2$]	(**5**)	215.3 (5.6)	44.2 (216.1/6.2)	–	–	15.7 (3366)
[PtMeCl(L1-κ*P*,κ*S*)]	(**6**)	–	–	–	–1.7 (616.0/5.9)	4.0 (4407)
[PtMeCl(CO)(L2-κ*P*)]	(**7**)	–	–	165.1 (7.4)	2.4 (479.7/87.4)	22.1 (1442)
[PtMeCl(L2-κ*P*)$_2$]	(**8**)	–	–	–	–13.0 (661.8/5.6)	23.2 (3056)
[PtMe(CO)(L2-κ*P*)$_2$][BF_4]	(**9**)	–	–	178.3 (5.3)	2.4 ([a])/6.5)	17.3 (2538)

a) Not detected.

expected range (213.5/215.3 ppm, **4**/**5**), but only $^2J_{P,C}$ couplings (ca 6 Hz) due to weak intensity. The ^1H and ^{13}C resonances of the methyl ligands in complexes **6** and **8** exhibited strong highfield shifts by, respectively, 1.2 and more than 40 ppm compared to the resonances of the methyl group of the acetyl ligand in complexes **4** and **5**. Besides the expected coupling patterns in complexes **6** (d+dd) and **8** (t+dt) the magnitudes of the $^2J_{Pt,H}$ couplings in the region of 70–80 Hz and of the $^1J_{Pt,C}$ coupling constants (600–700 Hz) unambiguously prove that the methyl groups are directly bound to the platinum atom.

As expected, the shifts of the methyl ligands (^1H, ^{13}C) in complexes **7** and **9** were also found in the highfield region (δ_H = 1.10/0.50; δ_C = 2.4/2.4). Whereas the $^1J_{Pt,C}$ coupling constant of **7** (480 Hz) is decreased by, respectively, 136 and 182 Hz compared to the couplings in **6** and **8**, it could not be detected in **9** due to bad signal-to-noise ratio. Noteworthy, the $^2J_{P,C}$ coupling in the methyl(chlorido) carbonyl platinum(II) complex **7** is with 87.4 Hz very large but in the same region as reported for other platinum(II) complexes bearing a methyl and a phosphane ligand in mutual *trans* position [11–13]. The resonances of the carbonyl carbon atoms in **7** and **9** are in the expected region (δ_C ca. 170) showing $^2J_{P,C}$ couplings of 7.4 and 5.3 Hz, respectively.

2.3 Structures

Crystals of **4** and **6** suitable for X-ray diffraction analyses were obtained from dichloromethane solutions with a layer of *n*-pentane at room temperature. In crystals monomeric complexes without unusual intermolecular contacts (shortest intermolecular distance between non-hydrogen atoms: 3.46(2) Å, C4···C14', **4**; 3.44(2) Å, C20···C20', **6**) were found. The molecular structures are shown in Figure 1 and Figure 2. Selected structural parameters are given in the Figure captions.

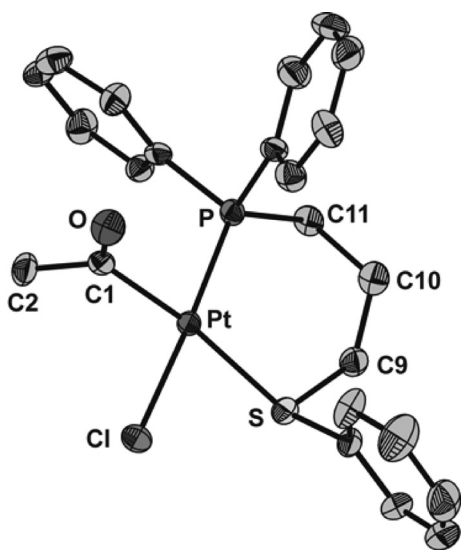

Figure 1. Molecular structure of (*SP*-4-3)-[Pt(COMe)Cl($Ph_2PCH_2CH_2CH_2SPh$-κ*P*,κ*S*)] (**4**). The ellipsoids are shown with a probability of 50 %. Hydrogen atoms were omitted for clarity. Selected structural parameters (distances in Å, angles in °): Pt–Cl 2.378(3), Pt–S 2.435(3), Pt–P 2.217(3), Pt–C1 2.02(1), C1–C2 1.50(2), C1–O 1.226(1), Cl–Pt–S 84.58(9), Cl–Pt–C1 88.5(3), S–Pt–P 98.90(9), P–Pt–C1 88.1(3), Cl–Pt–P 176.5 (1), S–Pt–C1 172.9(3).

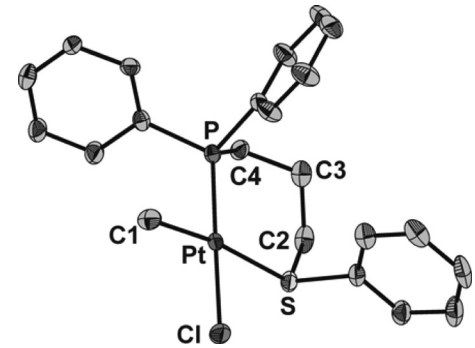

Figure 2. Molecular structure of (*SP*-4-3)-[PtMeCl($Ph_2PCH_2CH_2CH_2SPh$-κ*P*,κ*S*)] (**6**). The ellipsoids are shown with a probability of 50 %. Hydrogen atoms were omitted for clarity. Selected structural parameters (distances in Å, angles in °): Pt–Cl 2.379(2), Pt–S 2.377(2), Pt–P 2.204(2), Pt–C1 2.056(9), Cl–Pt–S 84.36(8), S–Pt–P 97.50(7), P–Pt–C1 90.4(3), C1–Pt–Cl 87.8(3), Cl–Pt–P 176.52(8), S–Pt–C1 171.9(3).

In the two complexes the platinum atoms adopt an almost ideal square-planar configuration; only the S–Pt–P angles are somewhat enlarged (98.90(9)°/97.50(7)°) due to the bite of the chelating P^S ligand. As expected, the Pt–Cl bonds (2.378(3)/2.379(2) Å) are of the same length. The *trans* influence order COMe > Me is reflected in a markedly longer Pt–S bond in **4** (2.435(3) Å) compared to that in **6** (2.377(2) Å). The Pt–C bond lengths in **4** (2.02(1) Å) and **6** (2.056(9) Å) are analogous to those in other platinum(II) complexes bearing a thioether ligand in *trans* position to an acyl ligand [7, 14, 15] and a methyl ligand [16–18], respectively.

2.4 Conclusion

Reactions of the dinuclear platina-β-diketone $[Pt_2\{(COMe)_2H\}_2(\mu\text{-}Cl)_2]$ (**1**) with the γ-phosphinofunctionalized propyl phenyl sulfide ($Ph_2PCH_2CH_2CH_2SPh$, **2**) and sulfone ($Ph_2PCH_2CH_2CH_2SO_2Ph$, **3**) lead via an unseen platinum(IV) intermediate of type **A** with reductive elimination of acetaldehyde [4, 19] (detected ^1H NMR spectroscopically) to the formation of type **B** acetyl(chlorido) platinum(II) complexes (**4**, **5**) (Scheme 1). In complex **4**, ligand **2** acts as a chelating P^S donor; analogous reactions were found with other bidentate P^P [4] or N^S [7] donors. In contrast, in complex **5** the phosphinofunctionalized sulfone **3** acts only as monodentate ligand (κ*P*), obviously due to a too low donor capability of the sulfonyl group. Its reactivity against **1** is analogous to that of non-functionalized phosphanes PR_3 [10].

In boiling benzene complexes **4** and **5** underwent an extrusion of CO yielding the respective methyl(chlorido) platinum(II) complexes **6** and **8**, respectively. This decarbonylation proceeds already at room temperature, if a "vacant" coordination site is generated by reaction of **5** either with $Ag[BF_4]$ or with the (unreacted) platina-β-diketone **1** (routes **e**/**g**, Scheme 2). Here, the latter reaction was found to be diastereoselective yielding the (*SP*-4-3) isomer whereas the analogous

reaction using PPh_3 instead of **3** proceeded non-diastereoselective since the (*SP*-4-3) and the (*SP*-4-2) isomers of complex [PtClMe(CO)(PPh_3)] were isolated in a ratio of 7:3 [6]. On the other hand, in an analogous reaction using a phosphane with a low donor capability ($P(C_6F_5)_3$) only the decarbonylated product was formed [11]. Analogous decarbonylation reactions have also been reported on α-ketoacyl [20] and formyl platinum(II) complexes [21]. The results presented here give further insight into the reactivity of platina-β-diketones towards mono- and bidentate ligands and readily access to novel acetyl, methyl and carbonyl platinum(II) complexes.

3 Experimental Section

3.1 General Remarks

All reactions were performed in an argon atmosphere using the standard Schlenk techniques. Solvents were dried (Et_2O, benzene and *n*-pentane over Na/benzophenone, CH_2Cl_2 over CaH_2) and distilled prior to use. NMR spectra were recorded at 27 °C with Varian Gemini 200, VXR 400 and Unity 500 spectrometers. Solvent signals (^1H, ^{13}C) were used as internal references; $\delta(^{31}P)$ is relative to external H_3PO_4 (85 %). Multiplet signals in NMR spectra of higher order resulting in pseudo triplets are denoted by 't'. IR spectra were recorded with a Bruker Tensor 28 spectrometer with a Platinum ATR unit. Microanalyses were performed by the University of Halle microanalytical laboratory using CHNS-932 (LECO) elemental analyzer. The complex $[Pt_2\{(COMe)_2H\}_2(\mu\text{-}Cl)_2]$ (**1**) as well as the γ-phosphinofunctionalized sulfide (**2**) and sulfone (**3**) were prepared according to literature methods [1, 22, 23].

3.2 Synthesis of [Pt(COMe)Cl(Ph$_2$PCH$_2$CH$_2$CH$_2$SPh-κP,κS)] (4) and [Pt(COMe)Cl(Ph$_2$PCH$_2$CH$_2$CH$_2$SO$_2$Ph-κP)$_2$] (5)

To a stirred suspension of **1** (100 mg, 0.16 mmol) in CH_2Cl_2 (5 mL) a solution of, respectively, **2** (108 mg, 0.32 mmol) and **3** (236 mg, 0.64 mmol) in CH_2Cl_2 (3 mL) was added at –78 °C and allowed to warm to room temperature. After the addition of *n*-pentane (5 mL), the precipitated solid was filtered off, washed with *n*-pentane (3 × 3 mL) and dried in vacuo.

(**4**) Yield: 150 mg (77 %). Anal. $C_{23}H_{24}ClOPPtS$ (610.01 g·mol^{-1}): C, 45.29; H, 3.97; Found: C, 44.61; H, 4.01. **IR**: ν = 1648 (s, CO) cm^{-1}. **^{1}H NMR** (400 MHz, $CDCl_3$): δ = 1.84 (s, 3 H, CH_3), 1.93–2.04 (m, 2 H, CH_2CH$_2$SPh), 2.55 (m, 2 H, CH_2PPh$_2$), 3.15 (m, 2 H, CH_2SPh), 7.23–7.73 (m, 15 H, H_{Ph}). **^{13}C NMR** (100 MHz, $CDCl_3$): δ = 21.8 (s, CH_2CH$_2$SPh), 25.2 (d, $^1J_{P,C}$ = 32.7 Hz, CH_2PPh$_2$), 36.0 (d, $^3J_{P,C}$ = 2.9 Hz, CH_2SPh), 40.7 (d+dd, $^3J_{P,C}$ = 4.7, $^2J_{Pt,C}$ = 167.0 Hz, CH_3), 128.5–133.2 (C_{Ph}), 213.5 (d, $^2J_{P,C}$ = 6.8 Hz, Pt–C). **^{31}P NMR** (81 MHz, $CDCl_3$): δ = –4.1 (s+d, $^1J_{Pt,P}$ = 4765 Hz, *P*Ph$_2$).

(**5**) Yield: 232 mg (72 %). Anal. $C_{44}H_{45}ClO_5P_2PtS_2$ (1010.44 g·mol^{-1}): C, 52.30; H, 4.49; Found: C, 52.01; H, 4.65. **IR**: ν = 1625 (s, CO) cm^{-1}. **^{1}H NMR** (400 MHz, $CDCl_3$): δ = 1.16 (s, 3 H, CH_3), 2.22 (m, 4 H, CH_2CH$_2$SO$_2$Ph), 2.73 (m, 4 H, CH_2PPh$_2$), 3.28 (m, 4 H, CH_2SO$_2$Ph), 7.36–7.82 (m, 30 H, H_{Ph}). **^{13}C NMR** (100 MHz, $CDCl_3$): δ = 18.7 (s, CH_2CH$_2$SO$_2$Ph), 25.1 ('t', *N* = 35.0 Hz, CH_2PPh$_2$), 44.2 (t+dt, $^3J_{P,C}$ = 6.2, $^2J_{Pt,C}$ = 216.1 Hz CH_3), 56.5 ('t', *N* = 14.8 Hz, CH_2SO$_2$Ph), 128.0–139.1 (C_{Ph}), 215.3 (t, $^2J_{P,C}$ = 5.6 Hz, Pt–C). **^{31}P NMR** (81 MHz, $CDCl_3$): δ = 15.7 (s+d, $^1J_{Pt,P}$ = 3366 Hz, *P*Ph$_2$).

3.3 Synthesis of [PtMeCl(Ph$_2$PCH$_2$CH$_2$CH$_2$SPh-κP,κS)] (6), [PtMeCl(CO)(Ph$_2$PCH$_2$CH$_2$CH$_2$SO$_2$Ph-κP)] (7) and [PtMeCl(Ph$_2$PCH$_2$CH$_2$CH$_2$SO$_2$Ph-κP)$_2$] (8)

To a stirred suspension of **1** (100 mg, 0.16 mmol) in CH_2Cl_2 (5 mL) a solution of, respectively, **2** (108 mg, 0.32 mmol) and **3** (0.32 mmol for the preparation of **7**; 0.64 mmol for the preparation of **8**) in CH_2Cl_2 (2 mL) was added at –78 °C, allowed to warm to room temperature and stirred for further 30 minutes. After the solvent was evaporated in vacuo, the residue was dissolved in benzene (2 mL) and the reaction mixture was heated under reflux for two hours. After cooling to room temperature the reaction mixture was filtered, *n*-pentane (5 mL) was added to the filtrate, the precipitated solid was filtered off and washed with *n*-pentane (3 × 3 mL). The crude products were re-precipitated from chloroform/*n*-pentane (1:2), filtered off and dried in vacuo.

(**6**) Yield: 136 mg (73 %). Anal. $C_{22}H_{24}ClPPtS$ (582.00 g·mol^{-1}): C, 45.40; H, 4.16; Found: C, 45.29; H, 4.28. **^{1}H NMR** (400 MHz, CD_2Cl_2): δ = 0.59 (d+dd, $^3J_{P,H}$ = 4.15, $^2J_{Pt,H}$ = 71.81 Hz, 3 H, CH_3), 1.95–2.04 (m, 2 H, CH_2CH$_2$SPh), 2.49 (m, 2 H, CH_2PPh$_2$), 3.19 (m, 2 H, CH_2SPh), 7.06–7.88 (m, 15 H, H_{Ph}). **^{13}C NMR** (100 MHz, CD_2Cl_2): δ = –1.7 (d+dd, $^2J_{P,C}$ = 5.9, $^1J_{Pt,C}$ = 616.0 Hz, CH_3), 22.0 (s, CH_2CH$_2$SPh), 25.4 (d, $^1J_{P,C}$ = 39.5 Hz, CH_2PPh$_2$), 36.9 (d, $^3J_{P,C}$ = 2.7 Hz, CH_2SPh), 128.5–133.5 (C_{Ph}). **^{31}P NMR** (81 MHz, CD_2Cl_2): δ = 4.0 (s+d, $^1J_{Pt,P}$ = 4407 Hz, *P*Ph$_2$).

(**7**) Yield: 168 mg (82 %). Anal. $C_{23}H2_4ClO_3PPtS$ (642.01 g·mol^{-1}): C, 43.03; H, 3.77; Found: C, 42.87; H, 3.71. **IR**: ν = 2075 (s, CO) cm^{-1}. **^{1}H NMR** (400 MHz, CD_2Cl_2): δ = 1.10 (d+dd, $^3J_{P,H}$ = 7.65, $^2J_{Pt,H}$ = 56.88 Hz, 3 H, CH_3), 1.91–2.02 (m, 2 H, CH_2CH$_2$SO$_2$Ph), 2.76–2.82 (m, 2 H, CH_2PPh$_2$), 3.19 (m, 2 H, C*H*2SO$_2$Ph), 7.42–7.84 (m, 15 H, H_{Ph}). **^{13}C NMR** (100 MHz, CD_2Cl_2): δ = 2.4 (d+dd, $^2J_{P,C}$ = 87.4, $^1J_{Pt,C}$ = 479.7 Hz, CH_3), 18.5 (d, $^2J_{P,C}$ = 2.7 Hz, CH_2CH$_2$SO$_2$Ph), 24.3 (d, $^1J_{P,C}$ = 29.0 Hz, CH_2PPh$_2$), 56.7 (d, $^3J_{P,C}$ = 14.8 Hz, CH_2SO$_2$Ph), 128.3–139.3 (C_{Ph}), 165.1 (d, $^2J_{P,C}$ = 7.4 Hz, *C*O). **^{31}P NMR** (81 MHz, CD_2Cl_2): δ = 22.1 (s+d, $^1J_{Pt,P}$ = 1442 Hz, *P*Ph$_2$).

(**8**) Yield: 123 mg (78 %). Anal. $C_{43}H_{45}ClO_4P_2PtS_2$ (982.43 g·mol^{-1}): C, 52.57; H, 4.62; Found: C, 52.42; H, 4.77. **^{1}H NMR** (400 MHz, $CDCl_3$): δ = –0.08 (t+dt, $^3J_{P,H}$ = 6.45, $^2J_{Pt,H}$ = 80.64 Hz, 3 H, CH_3), 2.08 (m, 4 H, CH_2CH$_2$SO$_2$Ph), 2.74 (m, 4 H, CH_2PPh$_2$), 3.27 (m, 4 H, CH_2SO$_2$Ph), 7.36–7.77 (m, 30 H, H_{Ph}). **^{13}C NMR** (100 MHz, $CDCl_3$): δ = –13.0 (t+dt, $^2J_{P,C}$ = 5.6, $^1J_{Pt,C}$ = 661.8 Hz, CH_3), 18.4 (s, CH_2CH$_2$SO$_2$Ph), 24.7 ('t', *N* = 35.2 Hz, CH_2PPh$_2$), 56.5 ('t', *N* = 14.6 Hz, CH_2SO$_2$Ph), 127.9–139.2 (C_{Ph}). **^{31}P NMR** (81 MHz, $CDCl_3$): δ = 23.2 (s+d, $^1J_{Pt,P}$ = 3056 Hz, *P*Ph$_2$).

3.4 Synthesis of [PtMe(CO)(Ph$_2$PCH$_2$CH$_2$CH$_2$SO$_2$Ph-κP)$_2$][BF$_4$] (9)

To a stirred suspension of **1** (100 mg, 0.16 mmol) in CH_2Cl_2 (5 mL) a solution of **3** (236 mg, 0.64 mmol) in CH_2Cl_2 (3 mL) was added at –78 °C and allowed to warm to room temperature. Afterwards, the solution was cooled to –78 °C again before a suspension of $Ag[BF_4]$ (31 mg, 0.16 mmol) in CH_2Cl_2 (1 mL) was added. After warming to room temperature and stirring for 30 minutes, the precipitated AgCl was filtered off and the filtrate was stirred for 12 hours. The volume was reduced to its half under reduced pressure, diethyl ether (5 mL) was added, the precipitated solid was filtered off, washed with diethyl ether (3 × 3 mL) and dried in vacuo.

Yield: 119 mg (70 %). Anal. $C_{44}H_{45}O_5P_2PtS_2BF_4$ (1061.79 g·mol^{-1}): C, 49.77; H, 4.27; Found: C, 49.66; H, 4.33. **IR**: ν = 2077 (s, CO)

cm^{-1}. **^{1}H NMR** (400 MHz, CD_2Cl_2): δ = 0.50 (t+dt, $^2J_{P,H}$ = 8.71, $^1J_{Pt,H}$ = 61.97 Hz, 3 H, CH_3), 2.06–2.15 (m, 4 H, $CH_2CH_2SO_2Ph$), 2.98–3.04 (m, 4 H, CH_2PPh_2), 3.27 (m, 2 H, CH_2SO_2Ph), 7.52–7.83 (m, 30 H, H_{Ph}). **^{13}C NMR** (50 MHz, CD_2Cl_2): δ = 2.4 (t, $^2J_{P,C}$ = 6.5 Hz, CH_3), 18.7 ('t', N = 25.7 Hz, $CH_2CH_2SO_2Ph$), 25.5 ('t', N = 35.7 Hz, CH_2PPh_2), 55.8 ('t', N = 15.9 Hz, CH_2SO_2Ph), 126.7–139.2 (C_{Ph}), 178.3 (t, $^2J_{P,C}$ = 5.3 Hz, CO). **^{31}P NMR** (81 MHz, CD_2Cl_2): δ = 17.3 (s+d, $^1J_{Pt,P}$ = 2538 Hz, PPh_2).

3.5 X-ray Crystallography

Single-crystals suitable for X-ray diffraction measurements of **4** and **6** were obtained from CH_2Cl_2 solutions with a layer of *n*-pentane. Intensity data were collected with STOE diffractometers STADI-4 at 293(2) K (**4**) and IPDS 2T at 200(2) K (**6**) using Mo-K_α radiation (λ = 0.7103 Å, graphite monochromator). A summary of the crystallographic data, the data collection parameters and the refinement parameters is given in Table 2. Absorption corrections were applied numerically with X-RED32 [24] (T_{min}/T_{max} 0.57/0.63, **4**; 0.18/0.51, **6**). The structures were solved with direct methods using SHELXS-97 [25] and refined using full-matrix least-square routines against F^2 with SHELXL-97 [26]. All non-hydrogen atoms were refined with anisotropic displacement parameters and hydrogen atoms with isotropic ones. Hydrogen atoms were placed in calculated positions according to the riding model.

Crystallographic data (excluding structure factors) have been deposited at the Cambridge Crystallographic Data Centre as supplementary publication nos. CCDC-793818 (**4**), CCDC-793819 (**6**). Copies of the data can be obtained free of charge on application to http://www.ccdc.cam.ac.uk/cgi-bin/catreq.cgi or from the Business & Administration, Cambridge Crystallographic Data Centre, 12 Union Road, Cambridge, CB2 1EZ, UK; Fax: +44-1223-336033; or E-Mail: admin@ccdc.cam.ac.uk.

Table 2. Crystallographic data, data collection parameters and refinement parameters for **4** and **6**.

	4	**6**
Empirical formula	$C_{23}H_{24}ClOPPtS$	$C_{22}H_{24}ClPPtS$
M_r	609.99	581.98
Crystal system	monoclinic	triclinic
Space group	$C2/c$	$P\bar{1}$
a /Å	24.687(3)	9.2840(7)
b /Å	8.5402(8)	9.7000(8)
c /Å	21.348(2)	12.844(1)
α /°		75.047(6)
β /°	91.460(9)	86.022(6)
γ /°		70.351(6)
V /Å^3	4499.5(8)	1052.3(1)
Z	8	2
D_{calc} /g·cm^{-3}	1.801	1.837
μ(Mo-K_α) /mm^{-1}	6.531	6.973
F(000)	2368	564
θ range /°	1.65–25.05	2.82–29.22
Rfln. collected	4648	18522
Rfln. observed [$I > 2\sigma(I)$]	3006	4625
Rfln. independent	3978 (R_{int} = 0.0373)	5650 (R_{int} = 0.0620)
Data/restraints/parameters	3978/0/253	5650/0/237
Goodness-of-fit on F^2	1.099	1.190
$R1$, $wR2$ [$I > 2\sigma(I)$]	0.0483, 0.1031	0.0415, 0.0975
$R1$, $wR2$ (all data)	0.0762, 0.1220	0.0546, 0.0994
Largest diff. peak and hole / e·Å^{-3}	1.852 and –2.014	1.998 and –2.802

References

[1] D. Steinborn, M. Gerisch, K. Merzweiler, K. Schenzel, K. Pelz, H. Bögel, J. Magull, *Organometallics* **1996**, *15*, 2454.
[2] C. M. Lukehart, J. V. Zeile, *J. Am. Chem. Soc.* **1976**, *98*, 2365.
[3] D. Steinborn, *Dalton Trans.* **2005**, 2664.
[4] M. Gerisch, C. Bruhn, A. Vyater, J. A. Davies, D. Steinborn, *Organometallics* **1998**, *17*, 3101.
[5] A. Vyater, C. Wagner, K. Merzweiler, D. Steinborn, *Organometallics* **2002**, *21*, 4369.
[6] M. Gerisch, F. W. Heinemann, C. Bruhn, J. Scholz, D. Steinborn, *Organometallics* **1999**, *18*, 564.
[7] T. Gosavi, E. Rusanov, H. Schmidt, D. Steinborn, *Inorg. Chim. Acta* **2004**, *357*, 1781.
[8] T. Gosavi, C. Wagner, H. Schmidt, D. Steinborn, *J. Organomet. Chem.* **2005**, *690*, 3229.
[9] M. Werner, C. Bruhn, D. Steinborn, *J. Organomet. Chem.* **2008**, *693*, 2369.
[10] C. Albrecht, C. Wagner, D. Steinborn, *Z. Anorg. Allg. Chem.* **2008**, *334*, 2858.
[11] C. Albrecht, C. Wagner, K. Merzweiler, T. Lis, D. Steinborn, *Appl. Organomet. Chem.* **2005**, *19*, 1155.
[12] S. Basu, N. Arulsamy, D. M. Roddick, *Organometallics* **2008**, *27*, 3659.
[13] E. M. Pelczar, E. A. Nytko, M. A. Zhuravel, J. M. Smith, D. S. Glueck, R. Sommer, C. D. Incarvito, A. L. Rheingold, *Polyhedron* **2002**, *21*, 2409.
[14] Y. Minami, T. Kato, H. Kuniyasu, J. Terao, N. Kambe, *Organometallics* **2006**, *25*, 2949.
[15] T. Kato, H. Kuniyasu, T. Kajiura, Y. Minami, A. Ohtaka, M. Kinomoto, J. Terao, H. Kurosawa, N. Kambe, *Chem. Commun.* **2006**, 868.
[16] J. R. Dilworth, C. A. Maresca von Beckh W, S. I. Pascu, *Dalton Trans.* **2005**, 2151.
[17] M. Rashidi, M. C. Jennings, R. J. Puddephatt, *Organometallics* **2003**, *22*, 2612.
[18] S. Ye, W. Kaim, M. Niemeyer, N. S. Hosmane, *Organometallics* **2005**, *24*, 794.
[19] D. Steinborn, T. Hoffmann, M. Gerisch, C. Bruhn, H. Schmidt, K. Nordhoff, J. A. Davies, K. Kirschbaum, I. Jolk, *Z. Anorg. Allg. Chem.* **2000**, *626*, 661.
[20] J.-T. Chen, Y.-S. Yeh, C.-S. Yang, F.-Y. Tsai, G.-L. Huang, B.-C. Shu, T.-M. Huang, Y.-S. Chen, G.-H. Lee, M.-C. Cheng, C.-C. Wang, Y. Wang, *Organometallics* **1994**, *13*, 4804.
[21] D. Vuzman, E. Poverenov, Y. Diskin-Posner, G. Leitus, L. J. W. Shimon, D. Milstein, *Dalton Trans.* **2007**, 5692.
[22] M. Block, C. Wagner, S. Gómez-Ruiz, D. Steinborn, *Dalton Trans.* **2010**, *39*, 4636.
[23] M. Block, T. Kluge, M. Bette, J. Schmidt, D. Steinborn, *Organometallics* in press.
[24] *X-RED32* (version 1.07), Stoe Data Reduction Program, Stoe & Cie GmbH, Darmstadt **2002**.
[25] G. M. Sheldrick, *SHELXS-97*, Program for Crystal Structure Solution, University of Göttingen, Göttingen **1998**.
[26] G. M. Sheldrick, *SHELXL-97*, Program for the Refinement of Crystal Structures, University of Göttingen, Göttingen **1997**.

Received: September 16, 2010
Published Online: ■

